FACTORS SHAPING EXCITATORY SYNAPTIC CURRENTS IN CEREBELLAR PURKINJE CELLS

MICHIKO TAKAHASHI

A thesis submitted for the degree of
Doctor of Philosophy
in the
University of London

Department of Physiology
University College London
October 1996

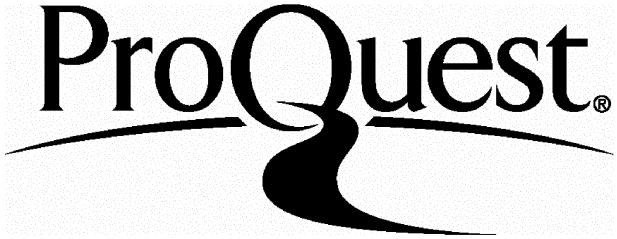

Abstract

Glutamate is a major excitatory neurotransmitter in the central nervous system. Purkinje cells in the cerebellum receive two excitatory synaptic inputs, from climbing fibres and parallel fibres, at which excitatory postsynaptic currents (EPSCs) are mediated by amino-3-hydroxy-5-methyl-4-isoxazolepropinic acid (AMPA) receptors. The determinants of the EPSC magnitude and duration at the parallel fibre and climbing fibre to Purkinje cell synapses were studied.

Adenosine and γ-aminobutyric acid (GABA) act on presynaptic receptors to inhibit neurotransmitter release from presynaptic terminals. They were found to decrease the EPSC amplitude more at the parallel than at the climbing fibre synapses. Adenosine and GABA also speeded the decay of the EPSCs. Applying an extracellular blocker of glutamate uptake prolonged the parallel and climbing fibre EPSCs. Blocking AMPA receptor desensitization also prolonged the decay time course of the EPSCs at both synapses.

Purkinje cells, although postsynaptic neurons, are thought to express EAAC1 glutamate uptake carriers. The pharmacology, voltage-dependence and ion-dependence of a current attributable to this carrier was examined electrophysiologically. Altering the internal solution to block uptake specifically in Purkinje cells produced a prolongation of the climbing fibre EPSC.

These data show that the AMPA-mediated postsynaptic current is shaped by presynaptic factors (the amount of glutamate released), by postsynaptic factors (receptor properties), and by the rate of glutamate removal from the synaptic cleft by uptake. When less glutamate is released into the cleft, it may be cleared from the cleft more quickly.

Contents

List of figures

List of Tables

Acknowledgements

I am grateful to the Wellcome Trust for the studentship which allowed me to do this PhD.

I am deeply indebted to David Attwell, for his invaluable supervision, inexhaustible encouragement and exceptional enthusiasm. His guidance has made my last three years in the lab most enjoyable.

I also thank Peter Mobbs for his inspiration and help. I was very fortunate to be surrounded by friendly and stimulating environment in the lab, and give my thanks to all the people in the past and present: Yury Kovalchuk, Monique Sarantis, Brian Billups, Martine Hamann, David Rossi, Alessandra Amato, Viola Bonness, Suzette Allcorn, and especially Marina Catsicas for her constant scientific and non-scientific help. I enjoyed discussions with people in the Pharmacology Department, in particular with Akiko Momiyama and Angus Silver.

I thank Richard Tunwell and David Becker for their help with this thesis.

My thanks go to Shaun, Louise, Martin, Leo and Michelle, for their unconditional friendship.

I would like to express my special thanks to my parents for their endless support and encouragement.

Finally, a big thank you to Richard.

Chapter 1

Introduction

In this thesis I describe experiments investigating synaptic transmission at cerebellar glutamatergic synapses. This introduction provides the background to these experiments, in particular on the role of presynaptic factors, postsynaptic receptors and glutamate uptake in shaping excitatory synaptic currents, and on synaptic transmission in the cerebellum.

1.1 Glutamate as a neurotransmitter

L-glutamate, a dicarboxylic acid, is the most important excitatory neurotransmitter in the mammalian central nervous system (CNS).

Immunohistochemical and electron microscopic studies have shown that glutamate is present in synaptic vesicles at the presynaptic membrane of excitatory synapses throughout the CNS (De Biasi and Rustioni, 1990; Hamori *et al.*, 1990; Storm-Mathisen and Ottersen, 1990; Aas *et al.*, 1992; Ottersen *et al.*, 1992). This glutamate is released in a calcium-dependent manner upon physiological stimulation, and during electric field stimulation (de Belleroche and Bradford, 1972; Hamberger *et al.*, 1978; Potashner, 1978) or depolarization with high potassium concentration (Nicholls *et al.*, 1987; Ottersen *et al.*, 1990; Storm-Mathisen and Ottersen, 1990). Furthermore, the pharmacology of excitatory transmission at proposed glutamatergic synapses is in agreement with the pharmacology of cloned glutamate receptors (Forsythe and Westbrook, 1988; Hestrin *et al.*, 1990a; Keinänen *et al.*, 1990; Nakanishi *et al.*, 1990; Keller *et al.*, 1991; Blanton and Kriegstein, 1992; Kutsuwada *et al.*, 1992; Meguro *et al.*, 1992; Silver *et al.*, 1992). However calcium-dependent release of other candidate transmitters, such as L-aspartate, L-homocysteate and L-cysteine sulphinate, which are structurally related to glutamate, has also been demonstrated (Wiklund *et al.*, 1982; Do *et al.*, 1988; Pittaluga *et al.*, 1988), and these other proposed transmitters can also activate glutamate receptors (Cuénod *et al.*, 1990; Cuénod *et al.*, 1993; Griffiths, 1993).

1.2 Synaptic transmission at glutamatergic synapses

Glutamate mediates excitatory neurotransmission at CNS synapses by activating ionotropic and metabotropic receptors. Ionotropic glutamate receptors are ligand-gated ion channels and metabotropic receptors are coupled to second messenger systems through the activation of GTP-binding proteins (reviewed by Gasic and Hollmann, 1992; Nakanishi, 1992; Seeburg, 1993; Hollmann and Heinemann, 1994). The ionotropic glutamate receptors are divided into α-amino-3-hydroxy-5-methyl-4-isoxazole propionate (AMPA), kainate and N-methyl-D-aspartate (NMDA) receptors, based on their electrophysiological and pharmacological characteristics. The subunits that constitute the glutamate receptors have recently been identified by molecular cloning techniques, and fall into several classes which are components of the AMPA (GluR1-GluR4), kainate (GluR5-GluR7, KA1-KA2), NMDA (NR1, NR2A-NR2D), and metabotropic (mGluR1-mGluR8) receptors. This classification is based on the agonist selectivity of expressed recombinant subunits, and on the degree of sequence identity between the subunits.

After glutamate has acted postsynaptically, synaptic transmission is terminated by glutamate being removed from the synaptic cleft, either by diffusion out of the cleft or by uptake into neurons and glial cells. There is no extracellular enzyme to break down glutamate, unlike for acetylcholine at the neuromuscular junction which is hydrolysed by acetylcholinestrase.

The following sections give detail of the properties of the different postsynaptic receptors that glutamate acts on.

1.2.1 AMPA receptors

The four receptor subunits (GluR1-GluR4) of AMPA receptors are of similar size (~900 amino acids) and share 68-73% amino acid sequence identity (reviewed by Hollmann and Heinemann, 1994). These subunits share a common transmembrane topology and channel architecture with other ligand-gated ion channels and contain four trans-membrane domains (TMDs), one of which is now known not to actually cross, but to dip

into the membrane (Hollmann *et al.*, 1994). When expressed in *Xenopus* oocytes and in mammalian cultured cells, the subunits form functional homomeric or heteromeric receptors, probably as a pentamer.

When expressed in oocytes, the agonist potencies of the GluR1-GluR4 subunits follow the order quisqualate > domoate ≅ AMPA > glutamate > kainate (Hollmann *et al.*, 1989; Nakanishi *et al.*, 1990; Sakimura *et al.*, 1990). The same order of agonist potency was found in [^{3}H]AMPA ligand binding experiments (Keinänen *et al.*, 1990; Kawamoto *et al.*, 1991).

Each subunit exists in two different forms created by alternative splicing of a 115-base pair region immediately preceding TMD IV (Sommer *et al.*, 1990). The two alternate exons have been termed "flop" and "flip". These two forms have different regional distributions in the brain, particularly in the hippocampus (Sommer *et al.*, 1990): CA3 pyramidal cells express only flip, while dentate gyrus granule cells contains more flop than flip. The cerebellar Purkinje cells which I have studied express five different subunits: GluR1flip and flop, GluR2 flip and flop, and GluR3 flip (Lambolez *et al.*, 1992): among these subunits, GluR2 is most abundant. In general, the flip and flop variants do not confer different pharmacological properties on the receptors, but they result in a difference in the efficacy with which glutamate activates the receptor (Sommer *et al.*, 1990). In both native AMPA receptors (Jonas and Sakmann, 1992) and recombinant AMPA receptors (Sommer *et al.*, 1990), the glutamate-evoked current has a fast desensitizing component, which is only seen if "flip" is present.

Sommer *et al.* (1991) found that, in the putative TMD II, a glutamine residue (Q) is encoded in the genes for GluR1-GluR4, however GluR2 cDNA made from adult animals contains an arginine (R) instead. This can be explained as a result of editing of the GluR2 RNA. This Q/R site plays a key role in determining the divalent permeability of AMPA receptor channels. Generally, non-NMDA receptors used to be thought to be rather impermeable to divalent cations, in particular to Ca^{2+} (Mayer and Westbrook, 1987), although in certain neurons Ca^{2+}-permeable kainate receptors were observed (Murphy *et al.*, 1987; Iino *et al.*, 1990; Gilbertson *et al.*, 1991). However, expressed

recombinant AMPA receptor subunits and their heteromeric combinations, except for GluR2 and combinations containing GluR2, were found to be quite permeable to various divalent cations including Ca^{2+} and Mg^{2+} (Hollmann *et al.*, 1991). Thus, the presence or absence of GluR2 subunit determines the Ca^{2+} permeability of the receptors, which is almost abolished in the presence of GluR2. From mutagenesis studies of AMPA receptors, the Q/R site is found to play a critical role in determining the Ca^{2+} permeability: receptors formed with unedited GluR2 subunits (Q type) have a high calcium permeability (Hume *et al.*, 1991; Burnashev *et al.*, 1992).

The role of AMPA receptors in synaptic transmission will be described below.

1.2.2 Kainate receptors

Kainate receptor subunits are divided into two subfamilies, GluR5-7 and KA1-2, based on differences in agonist affinity. GluR5-7 subunits have lower affinities for kainate (K_D is 35-95nM) than KA1-2 (K_D is 5-15nM: Bettler *et al.*, 1990; Lomeli *et al.*, 1992; Sommer *et al.*, 1992). Thus GluR5-GluR7 are called 'low-affinity' kainate receptors and KA1-2 are called 'high-affinity' kainate receptors. In addition, they share only ~43% sequence identity.

1.2.2.1 Low-affinity kainate receptors (GluR5-GluR7)

The three cloned subunits, GluR5-GluR7, share 75-80% amino acid sequence identity with each other, but only ~40% with GluR1-GluR4, thus setting them apart as a different subfamily of receptors (Bettler *et al.*, 1990; Egebjerg *et al.*, 1991, Bettler *et al.*, 1992; Morita *et al.*, 1992; Sommer *et al.*, 1992). GluR5-GluR7 also have a structure typical of ligand-gated channels with four putative TMDs.

RNA editing at a Q/R site in TMD II, homologous to that in GluR2, also occurs in GluR5 and GluR6, but not in GluR7 (Sommer *et al.*, 1991, 1992; Bettler *et al.*, 1992; Lomeli *et al.*, 1992). In contrast to GluR2, however, the editing of GluR5 and GluR6 RNA is incomplete, so both edited (R) and unedited (Q) forms coexist. In addition, two other editing sites were found in the TMD I of GluR6, editing at which results in a change from isoleucine to valine and from tyrosine to cysteine (Köhler *et al.*, 1993).

This additional RNA editing also contributes to controlling the Ca^{2+} permeability of the receptor channels. Furthermore, several splice variants, both at the C- and N-termini, have been found for GluR5 (Sommer *et al.*, 1992). Of these variants, the one with the shortest C-terminus is expressed most strongly (Sommer *et al.*, 1992).

GluR5 and GluR6 can form homomeric functional receptors, which desensitize during application of glutamate and kainate and do not produce a steady state current (Sommer *et al.*, 1992). Expression of GluR7 alone does not produce any detectable responses either in oocytes or transfected cell lines (Bettler *et al.*, 1992; Lomeli *et al.*, 1992). This could be explained if GluR7 desensitizes extremely rapidly, or does not form functional receptors on its own. Co-expressing GluR5, GluR6 or GluR7 with GluR1-4 does not produce responses different to those seen with the GluR1-4 single subunits, suggesting that GluR5-GluR7 do not form heteromeric complexes with GluR1-GluR4 (Bettler *et al.*, 1990, 1992; Sommer *et al.*, 1992).

1.2.2.2 High-affinity kainate receptors (KA1, KA2)

The two cloned receptor subunits, KA1 and KA2, share 70% amino acid sequence identity with each other but only ~37% with GluR1-GluR4 and ~43% with GluR5-GluR7, suggesting that they form a separate subfamily of glutamate receptors (Werner *et al.*, 1991; Herb *et al.*, 1992; Kamboj *et al.*, 1992; Sakimura *et al.*, 1992). KA1 and KA2 have a structure typical of ligand-gated ion channels, as have GluR1-GluR7. There are no splice variants reported for KA1 and KA2, and no indication of RNA editing at the Q/R site: both subunits express Q at the site homologous to the Q/R site in GluR2.

Binding studies show that the affinity of KA1 and KA2 for [^{3}H]KA is significantly higher than that of GluR5-GluR7, whereas [^{3}H]AMPA binding was undetectable (Werner *et al.*, 1991; Herb *et al.*, 1992; Kamboj *et al.*, 1992). The agonist potencies of the KA1 and KA2 subunits follow the order kainate > quisqualate > domoate > glutamate >> AMPA.

KA1 and KA2 do not produce any detectable response when expressed in oocytes or transfected in cell lines. Furthermore, when KA1 subunit was coexpressed with GluR1-GluR4, there was no changes in the functional properties observed, suggesting no

interaction between these receptor subunits (Werner *et al.*, 1991). However, coexpression of KA2 with GluR5 and GluR6 produced receptors with functional properties different from the respective homomeric receptors (Herb *et al.*, 1992; Sakimura *et al.*, 1992). Coexpression of KA1 with GluR5-GluR7 and coexpression of KA2 with GluR1-GluR4 and GluR7 have not been reported.

In the brain, KA1 is expressed at a high level only in CA3 pyramidal cells and in dentate granule cells of hippocampus, whereas KA2 is widely expressed.

1.2.2.3 Kainate binding proteins

Two KA binding proteins (KBPs) have been isolated from chick (KBP-chick, Gregor *et al.*, 1989) and frog (KBP-frog, Wada *et al.*, 1989). They are small proteins of ~470 amino acids, yet have a structure similar to other GluRs apart from a shortened N-terminus. There is 55% amino acid sequence identity between the two KBPs, and they share ~30% identity with other GluR subfamilies.

When expressed in oocytes or in transfected cells, KBPs did not produce any detectable ion channel activity (Wada *et al.*, 1989; Gregor *et al.*, 1992). Their affinity for agonists is in the order: domoate > kainate > quisqualate > glutamate.

The expression of KBP-chick RNA in the cerebellum is localized exclusively and abundantly in the Bergmann glial cells (Eshhar *et al.*, 1992; Gregor *et al.*, 1992). The restriction of KBP-chick RNA to Bergmann glial cells, in addition to the close association of Bergmann glia and Purkinje cells, could be interpreted as indicating a possible role for KBP-chick subunits in modulation of the strength of the Purkinje cell synapses (Gregor *et al.*, 1988; Ortega *et al.*, 1991). During development, KBP-chick RNA is expressed several days after Bergmann glial cells have developed, when granule cells start to migrate. This could also indicate a role for the KBP-chick subunit in regulating granule cell migration (Ortega *et al.*, 1991).

1.2.3 NMDA receptors

NMDAR1, a receptor subunit for NMDA receptors, shares 25-29% amino acid sequence identity with non-NMDA receptor subunits, and has a structure typical of ligand-gated ion channels, including 4 putative TMDs. Eight different functional splice variants of the subunit have been reported: some variants show different agonist and antagonist potencies (Durand *et al.*, 1992; Nakanishi *et al.*, 1992; Hollmann *et al.*, 1993), while others exhibit a higher susceptibility to modulation by PKC (Durand *et al.*, 1992). When expressed in oocytes, NMDAR1 can form homomeric functional receptors, which respond in the presence of glycine to glutamate, NMDA, quisqualate, ibotenate, L-aspartate and L-homocysteic acid, but do not respond to kainate, AMPA, *trans*-ACPD or to glycine itself. Without glycine, the response to NMDA was completely abolished (Nakanishi *et al.*, 1992) or greatly reduced (Moriyoshi *et al.*, 1991; Yamazaki *et al.*, 1992).

In the absence of Mg^{2+}, the I-V relationship of the channels formed by NMDAR1 is linear with a reversal potential of 0mV, while in the presence of Mg^{2+}, the response is reduced at membrane voltages more negative than -20mV (Moriyoshi *et al.*, 1991; Nakanishi *et al.*, 1992), due to Mg^{2+} being attracted into (and blocking) the channel at negative voltages. The receptor channel is highly permeable to Ca^{2+} (Yamazaki *et al.*, 1992), and calcium entry through NMDA receptor channels plays a key role in activating second messenger systems, such as those involved in changing synaptic strength (e.g. in long-term potentiation, reviewed by Bliss and Collingridge, 1993; Collingridge and Bliss, 1995).

NMDAR1 is expressed in almost all neuronal cells throughout the brain as well as the peripheral nervous system, with particularly high levels in the cerebellum, hippocampus, cerebral cortex and olfactory bulb (Moriyoshi *et al.*, 1991; Shigemoto *et al.*, 1992).

The four cloned NMDAR2 subunits, NMDAR2A-NMDAR2D, share 42-56% amino acid sequence identity with each other, but share only 21-27% with other GluRs, including only 26-27% with NMDAR1 (Ikeda *et al.*, 1992; Kutsuwada *et al.*, 1992; Meguro *et al.*, 1992; Monyer *et al.*, 1992). They have the same typical structure of

ligand-gated ion channels. When expressed in oocytes or in cell lines, none of the four NMDAR2 subunits forms functional homomeric ion channels (Ikeda *et al.*, 1992; Kutsuwada *et al.*, 1992; Meguro *et al.*, 1992; Monyer *et al.*, 1992). Furthermore, co-expressing NMDAR2A with other NMDAR2s did not produce functional channels (Monyer *et al.*, 1992). However, co-expression of any one of the NMDAR2 subunits with NMDAR1 produced functional heteromeric receptors with properties different from those of the homomeric NMDAR1 receptors: glycine alone is able to activate NMDAR1/NMDAR2A, NMDAR1/NMDAR2B and NMDAR1/NMDAR2D receptors in the absence of NMDA or glutamate (Kutsuwada *et al.*, 1992; Meguro *et al.*, 1992). The co-expression of NMDAR2 subunits resulted in a much larger glutamate-evoked current than with NMDAR1 alone (Ikeda *et al.*, 1992; Kutsuwada *et al.*, 1992; Meguro *et al.*, 1992). Furthermore, each NMDAR2 subunit confers different deactivation kinetics and Mg^{2+}-sensitivity to the heteromeric receptors (Monyer *et al.*, 1992).

The role of NMDA receptors in synaptic transmission will be discussed below.

1.2.4 Metabotropic glutamate receptors

1.2.4.1 Molecular biology of metabotropic receptors

The cloned metabotropic glutamate receptors, mGluRs, are much larger than previously identified G-protein-coupled receptors and do not share any sequence homology with members of that gene superfamily (Masu *et al.*, 1991). They have a large hydrophilic N-terminal, 7 putative TMDs and a large C-terminal. Based on their amino acid sequence identities, the 8 cloned mGluRs to date can be classified into 3 groups (Nakanishi, 1992; Pin and Duvoisin, 1995); mGluRs of the same group show high sequence identity, whereas between groups the sequence identity is only about 45%. Group-I consists of mGluR1 and mGluR5, group-II of mGluR2 and mGluR3, and group-III of mGluR4 and mGluR6-8. Splice variants have been found for mGluR1, mGluR4 and mGluR5, and they show slightly different agonist potency.

The agonist potency for group-I receptors is in the order quisqualate > glutamate ≥ ibotenate > (2*S*, 1'*S*, 2'*S*)-2-(carboxycyclopropyl)glycine (CCG-I) > *trans*-1-amino-

cyclopentane-1,3-dicarboxylate (*t*ACPD). Phenylglycine derivatives are antagonists for Group-I receptors, with (S)-4-carboxy-3-hydroxyphenylglycine (4C3HPG) and (S)-4-carboxy-phenylglycine (4CPG) being specific (Hayashi *et al.*, 1994; Thomsen *et al.*, 1994). The agonist potency for group-II receptors is: 2-(2,3-dicarboxycyclopropyl)glycine (DCG-IV) ≥ L-CCG-I > glutamate > *t*ACPD > ibotenate > quisqualate. (+)-α-methyl-4-carboxyphenylglycine ((+)MCPG) is an antagonist known for mGluR2, but its potency is weak, and it blocks mGluR1 at the same concentration (Hayashi *et al.*, 1994; Thomsen *et al.*, 1994). Group-III receptors have a distinctive sensitivity to L-2-amino-4-phosphonobutyrate (L-AP4) and insensitivity to *t*ACPD. There are no selective antagonists for Group-III mGluRs.

1.2.4.2 Transduction mechanisms and physiological role of metabotropic receptors

Expression in oocytes or in cell lines shows that the sequence-based classification of mGluRs also applies to their respective transduction mechanisms and pharmacology. Group-I receptors couple to G-proteins which activate phospholipase C, while group-II and group-III receptors, on the other hand, couple with G-proteins which inhibit adenylyl cyclase activity.

Some native mGluRs, with a pharmacology comparable to Group-I mGluRs, activate PLC and thus produce IP_3, resulting in Ca^{2+} release from internal stores in neurones (reviewed by Pin and Duvoisin, 1995). This [Ca^{2+}] rise can then stimulate arachidonic acid release as a consequence of phospholipase A_2 activation (Dumuis *et al.*, 1990). In brain slices, some glutamate analogues stimulate cyclic AMP (cAMP) formation by activating adenylyl cyclase (Casabona *et al.*, 1992; Schoepp and Johnson, 1993; Winder and Conn, 1992, 1993). *t*ACPD was the most potent agonist for cAMP production (Schoepp and Johnson, 1993), however its action does not result from the direct coupling of an mGluR to the G-protein stimulating adenylyl cyclase, but from a potentiation of the stimulation of adenylyl cyclase by endogenous adenosine acting on adenosine A_2 receptors (Schoepp and Johnson, 1993; Winder and Conn, 1993). In contrast, group-II and group III mGluRs inhibit adenylyl cyclase activity via inhibitory G-proteins (Prézeau *et al.*, 1992; 1994; Kemp *et al.*, 1994; Cartmell *et al.*, 1993, 1994).

Some mGluR agonists have been shown to inhibit voltage-sensitive Ca^{2+}-channels in cultured hippocampal cells, olfactory neurons and cerebellar granule cells. Both L-type (Chavis *et al.*, 1994a; Lester and Jahr, 1990; Sayer *et al.*, 1992) and N-type (Swartz and Bean, 1992; Swartz *et al.*, 1993) Ca^{2+} channels can be inhibited by mGluRs, but the mechanism involved in these effects has yet to be characterized. Similarly, several subtypes of K^+ channels are regulated by mGluR agonists (Baskys, 1992). Furthermore, group-I mGluRs also regulate three major ionotropic receptors, $GABA_A$, NMDA and AMPA receptors, presumably by raising $[Ca^{2+}]_i$ and thus activating PKC (reviewed by Pin and Duvoisin, 1995).

ACPD and other mGluR agonists induce a slowly developing depolarization and inward current, associated with an increase in cell firing, in many neurons, including hippocampal pyramidal cells (Stratton *et al.*, 1990; Liu *et al.*, 1993) and cerebellar Purkinje cells (Glaum *et al.*, 1992; Linden *et al.*, 1994). In contrast, in ON-bipolar cells (Nawy and Copenhagen, 1987; Slaughter and Miller; 1981, 1985), mGluRs produce hyperpolarizing effects. In cerebellar Purkinje cells (Batchelor and Garthwaite, 1993; Glaum *et al.*, 1992; Staub *et al.*, 1992; Vranesic *et al.*, 1993), ACPD produced a very slow hyperpolarization following a slow depolarization. mGluRs also mediate presynaptic inhibition at glutamatergic synapses, by lowering the presynaptic level of cAMP (cf. Chavez-Noriega and Stevens, 1992), inhibiting presynaptic calcium channels (Scanziani *et al.*, 1995), or by other mechanisms coupled to part of the exocytotic machinery (Barnes-Davies and Forsythe, 1995), while in the presence of arachidonic acid they potentiate glutamate release from synaptosomes (Herrero *et al.*, 1992).

In the hippocampus, the induction of long-term potentiation (LTP) requires the activation of mGluRs (Bashir *et al.*, 1993, Bortolotto *et al.*, 1994). Similarly, from antibody studies, induction of cerebellar long-term depression (LTD, see below) has been shown to require the activation of mGluR1 (Shigemoto *et al.*, 1994).

1.2.5 Glutamate toxicity

Although vital for normal brain function, the excitatory transmitter glutamate can also act as a toxin. Raising the extracellular glutamate concentration to 100μM for 5 minutes

was found to cause the death of more than 50% of cultured cortical neurons (Choi *et al.*, 1987). This glutamate toxicity is largely mediated by an excess influx of Ca^{2+} through NMDA receptor channels (Choi *et al.*, 1988). Application of APV, a potent NMDA receptor antagonist, largely prevents the late neuronal degeneration induced by brief glutamate exposure (Choi *et al.*, 1988), and removal of extracellular calcium has a similar effect (Choi, 1985; Garthwaite and Garthwaite, 1986; Rothman *et al.*, 1987). In addition, neuronal swelling and death induced soon after exposure to glutamate, which results in an excessive cation influx through non-NMDA receptor channels followed by osmotic movement of water into the cell, can be blocked by the removal of extracellular sodium or chloride (Rothman, 1985; Olney *et al.*, 1986).

During ischaemia or hypoxia, the intracellular ATP level falls, and this is followed by a rundown of transmembrane ion concentration gradients, and release of glutamate (reviewed by Szatkowski and Attwell, 1994). This release of glutamate, which leads ultimately to neuronal death, is attributed to the reversed operation of glutamate uptake carriers (reviewed in section 1.5.5).

1.3 Presynaptic modulation of glutamate release

Experiments described in Chapter 3 investigate the role of presynaptic receptors at excitatory synapses in the cerebellum. This section reviews what is currently known about the properties of such receptors.

1.3.1 Mechanisms of presynaptic modulation

When an action potential reaches the presynaptic terminal, voltage-dependent Ca channels are activated and Ca^{2+} influx through them elicits the release of transmitter: an elevated intracellular Ca^{2+} concentration increases the probability of the transmitter-containing vesicles fusing with the presynaptic membrane. G-protein coupled receptors, situated in the membrane of the presynaptic terminal, can inhibit the transmitter release by blocking Ca^{2+} entry through voltage-gated Ca^{2+} channels (Wu and Saggau, 1995), by increasing K^+ conductance (Zoltay and Cooper, 1990), and by activating (Gereau and Conn, 1994; Dunwiddie *et al.*, 1992) or by inhibiting second messenger systems such as

adenylate cyclase (Dunwiddie and Fredholm, 1989; Scanziani *et al.*, 1992; Chavez-Noriega and Stevens, 1994). The presynaptic receptors found to date are as follows: adenosine A_1 (Dunwiddie, 1985; Lupica *et al.*, 1992; Prince and Stevens, 1992; Barrie and Nicholls, 1993), $GABA_B$ (Thompson and Gahwiler, 1989; Scanziani *et al.*, 1992; Isaacson *et al.*, 1993; Pfrieger *et al.*, 1994), kainate (glutamate: Chittajallu *et al.*, 1996), mGluRs (glutamate: Forsythe and Clements, 1990; Lovinger and McCool, 1995; Baskys and Malenka, 1991; Herrero *et al.*, 1992; Barnes-Davies and Forsythe, 1995, Vignes *et al.*, 1995; Glaum and Miller, 1995), P_2 purinergic (Motin and Bennett, 1995), α_2 adrenergic (Limberger *et al.*, 1988; Wichmann and Starke, 1988), M2 muscarinic (Kawashima *et al.*, 1990; Allen and Brown, 1993), μ- (Capogna *et al.*, 1993), δ- (Rogers and Henderson, 1990; Jiang and North, 1992; Glaum *et al.*, 1994), κ- (Ueda *et al.*, 1987) opioid, neuropeptide Y (Colmers *et al.*, 1987; Johansen, 1993; Ellis and Davies, 1994), and cannabinoid (Sheng *et al.*, 1996) receptors.

Evidence that many presynaptic receptors operate via G-proteins came from experiments in which GTPγS mimicked the effect and GDPβS and pertussius toxin inhibited the effect (reviewed by Dolphin *et al.*, 1994). For example, presynaptic inhibition of IPSPs by baclofen in CA3 pyramidal cells was blocked by pertussis toxin treatment (Capogna *et al.*, 1993). However, some effects of presynaptic receptors are insensitive to pertussis toxin treatment (Thompson and Gähwiler, 1992; Dutar and Nicoll, 1988), suggesting that a different type of G-protein was involved.

1.3.2 Function of presynaptic receptors

Presynaptic receptors may have several important functions. At some synapses, the presynaptic receptors present are autoreceptors (Waldmeier *et al.*, 1988; Forsythe and Clements, 1990; Baskys and Malenka, 1991; Martin *et al.*, 1991; Barnes-Davies and Forsythe, 1995), which may provide negative feedback limiting the amount of transmitter which can be released, and thus preventing too much excitation or inhibition occurring (Baskys and Malenka, 1991). At some other synapses, GABAergic inhibitory presynaptic receptors limit the release of excitatory glutamate (as characterized in Chapter 3 of this thesis for cerebellar synapses). Presynaptic inhibition provides the

nervous system with a means of specifically reducing transmission at a particular synapse (in contrast to postsynaptic inhibition which often reduces the effectiveness of transmission at all the synapses impinging on the dendrite where the inhibitory synapse is located). Finally, some presynaptic receptors may be neuroprotective in pathological situations. During ischaemia or hypoxia, a massive release of glutamate can lead to neuronal death. At the same time, there is a large release of adenosine into the extracellular space (Hagberg *et al.*, 1987). This activates presynaptic adenosine receptors which reduce the amount of glutamate release and so may reduce neuronal death (Rudolphi *et al.*, 1992).

1.4 Determinants of EPSC waveform

In most mammalian CNS neurones, EPSCs consist of two components that differ in kinetics; a fast component, which is selectively blocked by 6-cyano-7-nitroquinoxaline-2,3-dione (CNQX), but is insensitive to D(-)-2-amino-5-phosphopentanoic acid (D-APV D-APV); and a slow component, which is blocked by D-APV but not by CNQX, and is also blocked by Mg^{2+} in a voltage-dependent manner (Nowak *et al.*, 1984). These results suggest that the two components of the EPSC are mediated by two different types of ionotropic glutamate receptors: AMPA/kainate-type (fast) and NMDA-type (slow) glutamate receptors (Silver *et al.*, 1992; Stern *et al.*, 1992; Forsythe and Barnes-Davies, 1993; Bekkers and Stevens, 1989; McBain and Dingledine, 1992).

Interestingly, the cerebellar Purkinje cells studied in this thesis lack functional NMDA receptors after postnatal day 10 (Perkel *et al.*, 1990; Llano *et al.*, 1991; Rosenmund *et al.*, 1992), and consequently the EPSCs evoked by stimulating the climbing fibre or parallel fibre inputs to Purkinje cells (see section 1.6) are mediated by non-NMDA receptors (Konnerth *et al.*, 1990; Perkel *et al.*, 1990; Llano *et al.*, 1991; Momiyama *et al.*, 1996). Thus I shall focus on factors shaping non-NMDA receptor-mediated EPSCs in the following sections.

The rise time of EPSC is determined by both the rate of rise of neurotransmitter concentration in the synaptic cleft and the activation kinetics of the receptors. The

factors that determine the rate of the decay of the synaptic current are more complicated. There are three possible models:

i) If the decay of neurotransmitter concentration in the synaptic cleft is very rapid, then the synaptic current will be terminated by receptor deactivation following the removal of neurotransmitter from the synaptic cleft, as has already been proposed for the neuromuscular junction (Katz and Miledi, 1973; Anderson and Stevens, 1973; Magleby and Stevens, 1972).

ii) If the decay of neurotransmitter concentration is very slow, the synaptic current may be terminated by receptor desensitization in the presence of a sustained level of neurotransmitter.

iii) If the neurotransmitter concentration decays with a time course between that of receptor deactivation and of receptor desensitization, the synaptic current decay time course will be determined partly by the time course of the fall of neurotransmitter concentration (as transformed through the dose-response curve for receptor activation), and so will be determined by the rate at which transmitter is removed from the synaptic cleft by diffusion and uptake.

I shall review briefly each of these mechanisms in turn.

1.4.1 Role of receptor deactivation

Deactivation is the closing of a receptor ion channel after a fall in concentration of the transmitter which activates the channel. Deactivation time constants of non-NMDA receptors have been studied in various CNS neurones, including cerebellar Purkinje cells (Barbour *et al.*, 1994), cochlear nucleus neurones (Raman and Trussell, 1992; Trussell *et al.*, 1993), cerebellar granule cells (Silver *et al.*, 1994), inhibitory neurons of neocortex (Hestrin, 1993; Jonas *et al.*, 1994), hippocampal spiny mossy cells and aspiny hilar interneurons (Livsey *et al.*, 1993), hippocampal granule cells (Colquhoun *et al.*, 1992), hippocampal pyramidal neurones (Colquhoun *et al.*, 1992), and neocortical pyramidal neurones (Hestrin, 1992; Hestrin, 1993; Jonas *et al.*, 1994). The time constants varied from 1 to 3 ms in the different cells.

In some cell types, the deactivation time constant (measured for AMPA receptors in membrane patches pulled from the cell soma) is close to the synaptic current decay time constant (Stern *et al.*, 1992; Colquhoun *et al.*, 1992; Jonas *et al.*, 1993;Jonas *et al.*, 1994). Thus, if the properties of postsynaptic receptors are similar to those in the soma, this suggests that the EPSC decay might be largely due to deactivation, following a fast fall of glutamate concentration in the synaptic cleft. However, this is not the case in cerebellar Purkinje cells (Barbour *et al.*, 1994), where the decay time constants of the climbing and parallel fibre EPSCs are 6-10msec, while the deactivation time constant is ≈1msec.

1.4.2 Role of receptor desensitization

Desensitization is the decrease of current flow through a receptor ion channel in the continued presence of the transmitter which activates the channel. Desensitization time constants of non-NMDA receptors have been well studied in many CNS neurones, and vary between 1 and 15msec (Tang *et al.*, 1989; Koh *et al.*, 1995; Hestrin, 1993; Livsey *et al.*, 1993; Jonas *et al.*, 1994; Colquhoun *et al.*, 1992; Trussell and Fischbach, 1989; Barbour *et al.*, 1994; Trussell *et al.*, 1993). In most of the cell types studied, desensitization of glutamate receptors in membrane patches is two- to four-fold slower than the decay time course of non-NMDA EPSCs (Silver *et al.*, 1992; Stern *et al.*, 1992; Trussell *et al.*, 1993; Jonas *et al.*, 1993; Hestrin, 1992, 1993; Colquhoun *et al.*, 1992; Jonas *et al.*, 1994; Raman and Trussell, 1992), suggesting a minor role for desensitization in terminating the EPSC. However, at a cochlear nucleus synapse, the synaptic current decay is apparently dominated by desensitization of the postsynaptic receptors (Trussell *et al.*, 1993), because the time constant of the EPSC decay and of desensitization are the same.

1.4.3 Diffusion

Computer modelling of transmitter diffusion through the extracellular space away from its release site suggests that the neurotransmitter concentration should fall very rapidly at CNS synapses (reviewed by Clements, 1996), falling to 10% of its peak value in 0.5msec. At synapses in cultured hippocampal neurons, the average time course of the

transmitter concentration was measured using a rapidly dissociating (low-affinity) antagonist (Clements *et al.*, 1992). The glutamate concentration decay was estimated to be a double exponential with 2.7mM and 0.4mM as the amplitude of the exponentials of time constant 100μs and 2.1ms, similar to what is predicted by the computer modelling. Rapid removal of glutamate by diffusion depends on the glutamate concentration in the extracellular space around a synapse being kept low by uptake into surrounding cells.

1.4.4 Uptake

Uptake of neurotransmitter, either directly from the synaptic cleft, or at more distant locations after the neurotransmitter has diffused out of the cleft, plays a key role in terminating the action of most CNS transmitters, including glutamate. This role can be demonstrated by inhibiting uptake, which should prolong the postsynaptic action of released neurotransmitter and thus alter the decay time course of EPSCs.

Carrying out this experiment for GABAergic synapses has demonstrated that GABA uptake carriers do contribute to terminating synaptic transmission via $GABA_A$ receptors (Thompson and Gähwiler, 1992). In addition, GABA uptake prevents GABA released from active inhibitory neurons spreading through the extracellular space and inhibiting neurotransmitter release from nearby excitatory neurons by activating $GABA_B$ receptors (Isaacson *et al.*, 1993).

At glutamatergic synapses, the effect of uptake blockers varies from synapse to synapse. At cerebellar mossy fibre to granule cell synapses and hippocampal Schaffer collateral to pyramidal cell synapses, inhibiting glutamate uptake does not affect the EPSC decay time course (Hestrin *et al.*, 1990b; Isaacson and Nicoll, 1993; Sarantis *et al.*, 1993), which may be dominated by the time course of channel deactivation following rapid diffusion of glutamate out of the synaptic cleft (Colquhoun *et al.*, 1992; Silver *et al.*, 1992; 1994). However, at cerebellar climbing fibre and parallel fibre to Purkinje cell synapses, blocking uptake prolongs the EPSCs as will be shown in this thesis (see also Barbour *et al.*, 1994).

1.5 Glutamate uptake

A substantial fraction of the experiments described in this thesis are on the properties of glutamate uptake. This section provides background information on the properties of glutamate transporters relevant to the experiments carried out.

1.5.1 Stoichiometry of glutamate uptake carrier

Radiotracing experiments and electrophysiological studies using patch-clamp techniques have suggested that glutamate uptake by uptake carriers in the membrane of rat (Kanner and Sharon, 1978), salamander (Brew and Attwell, 1987; Barbour *et al.*, 1988; Amato *et al.*, 1994), and rabbit (Sarantis and Attwell, 1990) glial cells is associated with the co-transport of two Na^+ ions into the cell and the counter-transport of one K^+ ion out of the cell per glutamate anion taken up. There are four cloned mammalian glutamate transporters reported so far, and all of them appear to transport Na^+ ions into and K^+ ions out of the cell (Pines *et al.*, 1992; Kanai and Hediger, 1992; Klockner *et al.*, 1993; Fairman *et al.*, 1995). Furthermore, glutamate uptake carriers generate pH changes, acidifying the inside and alkalinizing the outside of the cells (Erecinska *et al.*, 1983; Bouvier *et al.*, 1992). In salamander retinal glial cells, it has been suggested that uptake carriers transport an OH^- ion out of the cell (Bouvier *et al.*, 1992). The experiments leading to these conclusions are summarised in the following sections.

1.5.1.1 Glutamate

A single glutamate anion seems to be transported on each cycle of the carrier's operation. Previous studies of high affinity glutamate uptake carriers found a first order Michaelis-Menten dependence of uptake on external glutamate concentration (Hertz, 1979; Erecinska, 1987) with apparent K_m values between 2 and 70μM.

1.5.1.2 Sodium

Sodium ions are necessary outside cells to drive the uptake of radioactive glutamate (Hertz 1979; Erecinska, 1987). Glutamate uptake by all four cloned expressed carriers was almost abolished by removal of extracellular sodium. Furthermore, glutamate

stimulates uptake of radioactive sodium (Stallcup *et al.*, 1979; Baetge *et al.*, 1979), suggesting that sodium ions are co-transported on the uptake carrier with glutamate. The sigmoid dependence of glutamate uptake on external sodium concentration suggests that at least two sodium ions are transported with each glutamate anion. Direct measurements of radioactive glutamate and sodium fluxes suggest that two sodium ions are transported per glutamate (Stallcup *et al.*, 1979; Baetge *et al.*, 1979). A similar conclusion (2 Na^+ per glu^-) was deduced from the sodium-dependence of the equilibrium accumulation of D-aspartate into synaptosomes (Erecinska *et al.*, 1983). Consistent with this, the current produced by glutamate transport (which partly reflects the co-transport with glutamate of an excess of Na^+ ions) has a sigmoid dependence on external sodium concentration (Barbour *et al.*, 1991).

1.5.1.3 Potassium

Radiotracing experiments suggested that glutamate uptake needs, in addition to extracellular sodium, intracellular potassium (Kanner and Sharon, 1978; Burckhardt *et al.*, 1980). Similarly, when uptake is studied by whole-cell clamping (Barbour *et al.*, 1988), the glutamate-evoked current is activated by intracellular potassium (controlled by the whole-cell pipette). The current depends on internal potassium concentration in a first order Michaelis-Menten manner, showing that one K^+ has to bind to an intracellular activating site. Direct confirmation that K^+ is transported out of the cell, rather than just binding at a regulatory site, was obtained by measuring K^+ efflux using K^+-sensitive microelectrodes positioned outside the cell (Amato *et al.*, 1994).

1.5.1.4 pH-changing ions

In addition to transporting 2 Na^+ and a glu^- into the cell, and transporting a K^+ out of the cell, glutamate transporters also generates pH changes, acid inside and alkali outside the cell, and these are not a secondary consequence of glutamate transport raising $[Na^+]_i$ and modulating the action of pH-regulating carriers (Erecinska *et al.*, 1983; Nelson *et al.*, 1983; Bouvier *et al.*, 1992). The magnitude of the pH change implies that the glutamate transporter in salamander glial cells (Bouvier *et al.*, 1992) and the cloned carrier EAAC1 (Kanai *et al.*, 1995) transport approximately one proton equivalent into the cell with each

unitary charge, i.e. presumably each cycle. These pH changes may therefore be produced either by the transport of an H^+ into the cell or of one OH^- out of the cell with each glu^-. Bouvier *et al.* (1992), on the basis of anion substitution experiments, suggested that an OH^- was transported out of the cell rather than an H^+ into the cell, but the discovery that glutamate transporters activate an anion conductance (Wadiche *et al.*, 1995a; Fairman *et al.*, 1995; Billups *et al.*, 1996) undermines the methods used to reach this conclusion: it is currently unknown whether an H^+ or an OH^- is transported.

1.5.2 Molecular structure of glutamate uptake carrier

Four distinct glutamate transporters have been cloned. The cloning of homologous transporters in different species brings to seven the total number of transporters cloned. The amino acid sequences of these seven transporters (4 from human, EAAT1-4, 2 from rat, GLT-1 and GLAST, and 1 from rabbit, EAAC1) are shown in Fig. 1.1. Based on this alignment made by the Clustal method (Higgins *et al.*, 1992), the sequence identity of the same transporter in different species is highly (more than 90%) conserved: human EAAT1 (Arriza *et al.*, 1994) has 96% identity with the rat GLAST (Storck *et al.*, 1992); human EAAT2 (Arriza *et al.*, 1994) has 90% identity with the rat GLT1 (Pines *et al.*, 1992); human EAAT3 (Arriza *et al.*, 1994) has 91% identity with the rabbit EAAC1 (Kanai and Hediger, 1992). GLAST and EAAT1, which are glial transporters, are closest in sequence to EAAT4, a neuronal transporter, and (surprisingly) furthest in sequence from the glial transporters GLT1 and EAAT2 (Fig. 1.2). The most homologous region of the transporters is at the C terminus. The number of transmembrane domains has not been established yet, but is believed to be between 6 and 12.

1.5.3 Coupling with an anion channel

The four cloned human glutamate transporters (Fairman *et al.*, 1995; Wadiche *et al.*, 1995a) and the transporters in salamander photoreceptors and glial cells (Sarantis *et al.*, 1988; Eliasof and Werblin, 1993; Billups *et al.*, 1996) have been shown to activate an anion conductance when they bind external glutamate and Na^+ ions. The fact that expressing the cloned transporters also leads to the anion conductance being expressed

Fig. 1.1 Alignment of glutamate transporter sequences. The alignment was made by the Clustal method, based on maximizing sequence identity. The conserved amino acids are boxed. Gaps are introduced to optimize sequence identity. Sequences are taken from the following references: EAAT1-3 (Arriza *et al.*, 1994), EAAT4 (Fairman *et al.*, 1994), EAAC1 (Kanai & Hediger, 1992), GLAST (Storck *et al.*, 1992) and GLT1 (Pines *et al.*, 1992).

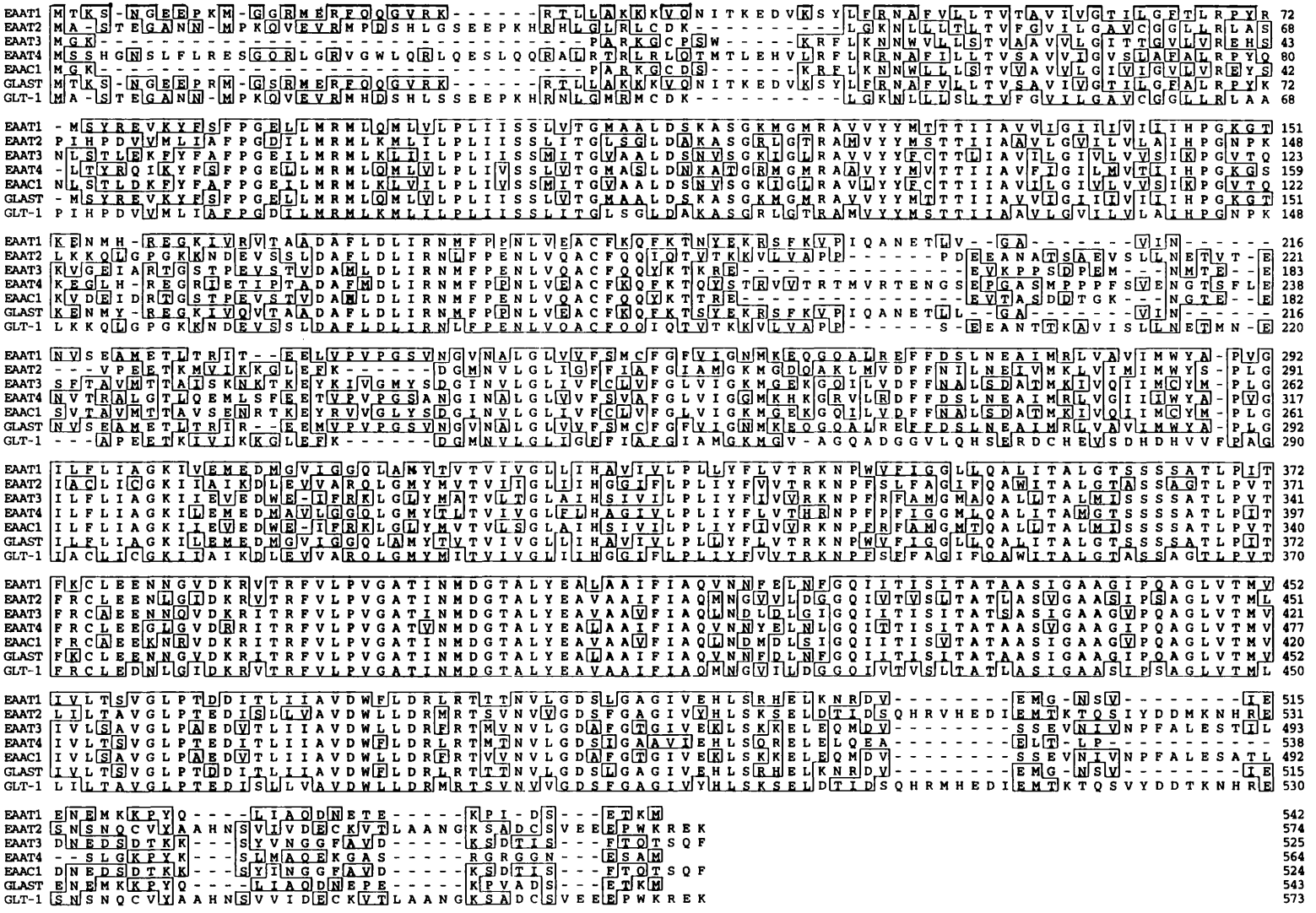
EAAT1
EAAT2
EAAT3
EAAT4
EAAC1
GLAST
GLT-1

Fig. 1.2 A phylogenetic tree of glutamate transporters. This was generated from the optimal alignment shown in fig. 1.1 to determine the ancestral relationship. Branch distances from ancestral nodes correspond to sequence divergence.

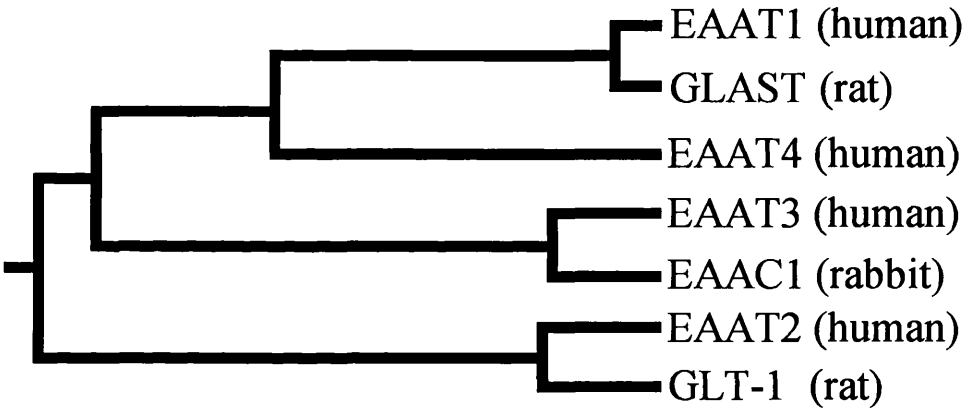
EAAT1 (human)
GLAST (rat)
EAAT4 (human)
EAAT3 (human)
EAAC1 (rabbit)
EAAT2 (human)
GLT-1 (rat)

suggests that the anion conductance is in the structure of the transporter. Patch-clamp studies show that the anion conductance in salamander retinal glial cells can be activated by glutamate binding to either side of the membrane (i.e. both during forward and reversed uptake), and can occur independently of the transport of glutamate (Billups *et al.*, 1996).

1.5.4 Distribution of glutamate uptake carriers in the central nervous system

In situ hybridization indicates that mRNA for the four distinct cloned transporters is produced only in certain cells of the brain. Two of the first transporters to be cloned, GLAST or EAAT1 (Storck *et al.*, 1992; Arriza *et al.*, 1994) and GLT-1 or EAAT2 (Pines *et al.*, 1992; Arriza *et al.*, 1994), are located predominantly in glial cells. GLT-1 is expressed widely among astrocytes throughout the brain, while GLAST is much more localized, being concentrated in Bergmann glial cells of the cerebellum. One cloned carrier, EAAC1 or EAAT3, is expressed in neurons throughout the brain (Kanai and Hediger, 1992; Arriza *et al.*, 1994), while the more recently cloned EAAT4 (Fairman *et al.*, 1995) is expressed mainly in the cerebellum, primarily in Purkinje cells, and occasionally in astrocytes.

Antibody staining has revealed in detail the subcellular localization of cloned transporters in the cerebellum. Interestingly, GLT-1 transporters are not expressed uniformly in the membrane of astrocytes: there are more carriers in the parts of the glial cell membrane that face nerve terminals, axons and dendritic spines than in the membrane that faces other glial cells, capillaries, pia or stem dendrites (Chaudhry *et al.*, 1995), consistent with a major role for glial uptake being to maintain the glutamate concentration around neurons below neurotoxic levels. The subcellular location of the neuronal transporters EAAC1 and EAAT4 is also of interest. Conventionally neuronal glutamate uptake has been thought of as being in presynaptic terminals, where it would serve the dual function of being in a good location to terminate the synaptic action of glutamate and of recycling glutamate to synaptic vesicles for re-use as a transmitter. However, EAAC1 (Rothstein *et al.*, 1994) and EAAT4 (Rothstein, personal communication) are found to be expressed throughout the soma and dendritic tree of Purkinje cells, and experiments described in

Chapter 5 show that this uptake is present in the surface membrane. Purkinje cells are not even glutamatergic neurons (although they may need to take up glutamate as a precursor for synthesis of their transmitter GABA), and this subcellular location suggests a role in terminating the synaptic action of glutamate released from climbing and parallel fibres onto the Purkinje cells: a possibility investigated in Chapter 5.

A different function for the glial transporters GLAST and GLT-1, and for the neuronal transporter EAAC1, has been suggested by experiments in which antisense techniques were used to prevent transporter expression (Rothstein *et al.*, 1996). The loss of glial transporters produced a rise of extracellular glutamate concentration which caused cell death. By contrast, preventing EAAC1 function did not raise the extracellular glutamate concentration, but produced a mild neurotoxicity and resulted in epilepsy. These results suggest that glial transporters may mainly function to keep the glutamate concentration low in the extracellular space, while neuronal transporters play a more specific role in synaptic transmission.

1.5.5 Reversed uptake

The direction of glutamate transport by the uptake carrier is determined partly by the concentration gradient of the ions other than glutamate that this carrier transports. During brain hypoxia or ischaemia, these ion gradients will be altered (reviewed by Attwell *et al.*, 1993; Szatkowski and Attwell, 1994). The first ionic concentration to change is that of $[H^+]$: because of the switch to anaerobic respiration the pH starts to go acid, eventually reaching about 6.1 both inside and outside cells. Next, the fall of ATP levels produced by lack of oxygen leads to inhibition of the sodium/potassium pump and a rundown of the transmembrane gradients for $[K^+]$, $[Na^+]$ and voltage. Initially the extracellular potassium concentration, $[K^+]_o$ rises slowly, but after 2 minutes $[K^+]_o$ suddenly rises to about 60mM, while $[Na^+]_o$ falls, and the cells are depolarized to -20mV. These changes leads to the reversed operation of glutamate transporters with the stoichiometry described above, resulting in release of glutamate into the extracellular space which can then lead to neuronal death.

This release of glutamate by reversed uptake has been shown in two ways. First, raising the potassium concentration around glial cells whole-cell clamped to a depolarized potential with pipettes containing sodium and glutamate (to mimic the conditions during ischaemia) evoked an outward membrane current produced by reversed operation of the transporters (Szatkowski *et al.*, 1990). Second, glutamate release from a glial cell produced by depolarizing in high [K^+] solution was detected as an opening of glutamate receptor channels in a neuron placed next to the glial cell (Billups and Attwell, 1996).

In Chapter 5 of this thesis I investigate whether the glutamate transporters in Purkinje cells can operate at a significant rate in the reversed direction.

1.5.6 Glutamate-cystine exchange

Apart from Na^+-dependent glutamate transporters as described above, a Na^+-independent transport mechanism for glutamate in the cell membrane has been reported (Bannai and Kitamura, 1980, 1981; Bannai, 1986). This is called cystine-glutamate exchange, and is found in human fibroblasts (Bannai and Kitamura, 1980, 1981), in mouse macrophages (Watanabe and Bannai, 1987; Bannai *et al.*, 1991), in hepatocytes (Bannai *et al.*, 1986), in opossum kidney cells (States and Segal, 1990), and in fetal rat brain primary culture (Sagara *et al.*, 1993). This transport activity is designated as system x_c^- and is a non-electrogenic process (Bannai, 1986). This exchanger normally transports cystine into the cell and glutamate out of the cell, since the concentration of cystine is lower inside the cell while that for glutamate is lower in the extracellular space. The uptake of cystine mediated by this transporter is important in maintaining intracellular levels of glutathione (an anti-oxidant), since cystine is converted to cysteine inside the cell, which is the rate limiting precursor for glutathione synthesis (Bannai and Tateishi, 1986).

The stoichiometry of this transporter has not been defined, however, it is thought to be Na-independent, Cl-dependent (Waniewski and Martin, 1984), and to be pH-dependent (Ishii *et al.*, 1991): the uptake of cystine is slower at an acid pH (6.0) than at pH 7.5. This protein transports glutamate, cystine, homocysteic acid, α-aminoadipate, and α-aminopinelate, but not aspartate. The cDNA for this transporter has not been cloned, however, from an expression study, mRNA encoding this transport is thought to be of

length 1.5-2.9 kb (Ishii *et al.*, 1991). In the brain, autoradiography suggests that this Cl-dependent transporter is most common in the cerebral cortex, the molecular layer of the dentate gyrus and the superior colliculus (Anderson *et al.*, 1990), but it is also expressed in the cerebellum. In Chapter 6 of this thesis I investigate the possible contribution of cystine-glutamate exchange to glutamate removal at cerebellar synapses.

1.6 Cerebellum

The experiments discovered in this thesis were all carried out on slices of cerebellum, so I shall review briefly the structure and function of the cerebellum.

The cerebellar cortex functions largely to modulate motor commands, and to integrate various forms of sensory information to smooth and fine-tune voluntary movements and reflexes (Ito, 1984). Both lesion studies and *in vivo* electrical recordings have suggested that the intrinsic cerebellar circuitry is involved in various forms of motor learning, including adaptation of the vestibulo-ocular reflex (Ito, 1984; Watanabe, 1984), associative eyeblink conditioning (Berther and Moore, 1986; McCormick and Thompson, 1984; Yeo and Hardiman, 1992), and limb load adjustment (Gilbert and Thatch, 1977).

1.6.1 Structure of the cerebellum

In the cerebellar cortex, neurons are arranged uniformly and simply as shown in Fig.1.3, which represents a portion of the structure which repeats throughout the cerebellum (reviewed by Marr, 1969; Albus, 1971; Gilbert, 1974). The cerebellar cortex consists of three layers, the granule cell layer, the Purkinje cell layer and the molecular layer containing the Purkinje cell dendrites and parallel fibres (the axons of granule cells).

Climbing fibres and mossy fibres are the only afferent pathways to the cerebellum. The climbing fibres originate in the inferior olive; the mossy fibres are all the other afferents to the cerebellar cortex which arrive from the cerebral cortex, spinal cord, vestibular cortex and reticular formation. Each climbing fibre sends excitatory synaptic input to a single Purkinje cell. By contrast, each mossy fibre arborizes throughout the granule cell layer, and contacts more than 500 granule cells as well as Golgi cells.

Fig. 1.3 Diagram of the cerebellar cortex of adult rat. The afferents are the climbing fibres and the mossy fibres. Each climbing fibre makes synapses onto one Purkinje cell, and sends weak collaterals to other cells of the cortex. The mossy fibres synapse with granule cells, whose axons form the parallel fibres. The parallel fibres, running longitudinally down the folium, make synapses onto Purkinje cells and inhibitory interneurons, the stellate, basket and Golgi cells. The stellate and basket cell axons make synapses with the Purkinje cells and Golgi cell axons make synapses with granule cells and mossy fibres. The Purkinje cell axons are the only output from the cortex. (Drawing created and kindly provided by Dr Barbara Lom.)

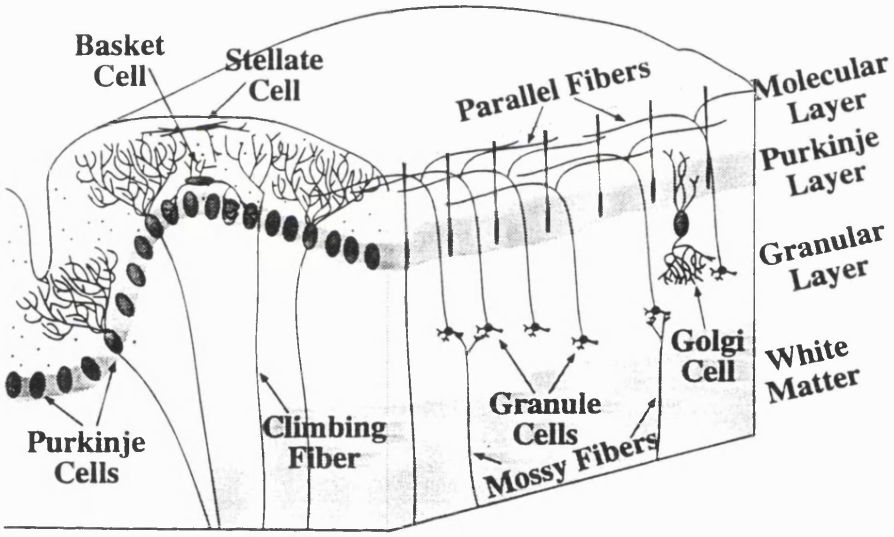
Basket Cell
Stellate Cell
Parallel Fibers
Molecular Layer
Purkinje Layer
Granular Layer
Golgi Cell
White Matter
Granule Cells
Mossy Fibers
Climbing Fiber
Purkinje Cells

Granule cells receive inputs from mossy fibres, and send their output axons to Purkinje cells. Each granule cell axon rises to the molecular layer, where it makes a T-shaped branch and runs longitudinally, parallel to all the other granule axons (hence it is called a parallel fibre) and perpendicular to the Purkinje cells' dendritic trees. The parallel fibres make excitatory synapses with Purkinje cells, basket cells, stellate cells and Golgi cells. Golgi cells are inhibitory interneurons situated in the granule cell layer, which have elaborate axons making GABAergic synapses onto granule cells.

Purkinje cells (Fig. 1.3) have a large and very dense dendritic tree flattened in the parasagittal plane in the molecular layer. More than 150,000 parallel fibres make synapses onto each Purkinje cell, and each parallel fibre makes synapses onto about 300 Purkinje cells. Despite the large number of parallel fibre inputs, only 50 of these inputs have to be active to make the Purkinje cell fire an action potential (Barbour, 1993). The climbing fibre to Purkinje cell synapse is extremely reliable - activating the climbing fibre always makes the Purkinje cell fire. The only output from the cerebellar cortex is through the axons of the Purkinje cells which make inhibitory synapses on the cells of the deep cerebellar nuclei. Purkinje cell axons also send inhibitory recurrent collaterals to other Purkinje cells, basket cells, stellate cells and Golgi cells.

Basket cells, with somata situated just above the Purkinje cell bodies, also have dense dendritic trees which receive inputs from parallel fibres. Basket cells axons make strong inhibitory synapses onto Purkinje cells. Each basket cell inhibits about 50 Purkinje cells. Stellate cells, located higher up in the molecular layer, are smaller inhibitory interneurons, which also receive inputs from parallel fibres, and inhibit Purkinje cells.

The Purkinje cells are partly surrounded by a glial sheath formed from the membrane of Bergmann glia (not shown in Fig. 1.3) which express glutamate transporters (Chaudhry *et al.*, 1995) whose role is to terminate transmission at the excitatory synapses onto the Purkinje cell.

1.6.2 The Purkinje cell and its glutamatergic synapses

At parallel fibre synapses, glutamate activates two types of postsynaptic receptor: those activated by AMPA, and metabotropic receptors (mGluRs). Glutamate is also believed to be the transmitter released at the climbing fibre to Purkinje cell synapse, where it activates postsynaptic AMPA receptors. In adult cerebellum (after about 10 days old: Konnerth *et al.*, 1990; Perkel *et al.*, 1990; Rosenmund *et al.*, 1992; Momiyama *et al.*, 1996), neither type of synapse possesses functional NMDA receptors.

1.6.3 Synaptic plasticity

It is widely believed that long-term changes in synaptic strength underlie the storage of information in the brain, eventually yielding learning and memory. In recent years, considerable amounts of work have been done to identify persistent, use-dependent mechanisms that increase synaptic strength, termed collectively long-term potentiation (LTP), or those which decrease synaptic strength, termed long-term depression (LTD). In the cerebellum, LTD occurs at the synapses from parallel fibres to Purkinje cells, and indirect evidence suggests that this form of synaptic plasticity may be one of the mechanisms underlying some simple forms of learning (reviewed by Thompson and Krupa, 1994).

1.6.3.1 Synaptic requirements for cerebellar LTD

In intact animals or *in vitro* cerebellar slices, co-activation of parallel fibre and climbing fibre inputs to Purkinje cells at low frequencies (1-4Hz) results in depression of transmission at the parallel fibre synapses (reviewed by Linden and Connor, 1995). The duration of this depression is not well defined, but is thought to persist for many days or weeks and is therefore termed long-term synaptic depression, or LTD.

LTD has many interesting features as a model of synaptic plasticity and a memory substrate. First, it shows input specificity, i.e., LTD is confined to those parallel fibre-Purkinje cell synapses that are active at the time of climbing fibre stimulation (Ito *et al.*, 1982; Ekerot and Kano, 1985). Second, it can be observed at many levels of experimental analysis, ranging from intact animals to slices and even cultured Purkinje

cells. Third, unlike some other forms of long-lasting synaptic plasticity, the locus of expression of LTD is defined: cerebellar LTD appears to be a purely postsynaptic phenomenon.

1.6.3.2 Postsynaptic glutamate receptors involved in LTD

The activation of both AMPA receptors and mGluRs by parallel fibres appears to be important in LTD. In cerebellar slices, activation of the metabotropic glutamate receptor in conjunction with depolarization, which replaces activation of AMPA receptors (to produce a postsynaptic calcium action potential like climbing fibre activation does: see below), is sufficient to induce LTD (Daniel *et al.*, 1992; Linden *et al.*, 1993). Furthermore, mice in which mGluR1 receptors have been genetically knocked-out do not have LTD (Aiba *et al.*, 1994). It is likely that activation of these receptors provides one or more intracellular messengers essential for the induction of LTD (see below).

The postsynaptic electrical responses at parallel fibre to Purkinje cell synapses are primarily mediated by AMPA receptors (Konnerth *et al.*, 1990) and these receptors also play a central role in LTD. First, their activation is required for LTD induction, because inhibiting them with CNQX also inhibits LTD induction (Linden *et al.*, 1991). More importantly, a decrease in the amount of current flowing through postsynaptic AMPA receptors at parallel fibre to Purkinje cell synapses is thought to be the mechanism underlying LTD (Hémart *et al.*, 1994; Linden and Connor, 1995). For example, LTD results in a progressive decrease in electrical responses to AMPA application (Linden *et al.*, 1991; Linden and Connor, 1991). Quantal analysis indicates that quantal size changes during LTD, which is also consistent with this interpretation (Hirano, 1991). Thus, cerebellar LTD might be mediated entirely postsynaptically, by an alteration in the properties of AMPA receptors at the parallel fibre synapse. However, the nature of these changes is not yet clear.

1.6.3.3 Intracellular signalling mechanisms involved in LTD

Climbing fibre activation normally triggers an action potential associated with Ca^{2+} influx in the Purkinje cell (Konnerth *et al.*, 1992). For induction of LTD, climbing fibre input

can be replaced with depolarization of the Purkinje cell: postsynaptic depolarization coincident with presynaptic parallel fibre stimulation is sufficient for LTD induction (Crépel and Krupa, 1988; Konnerth *et al.*, 1992). This depolarization (or climbing fibre stimulation) appears to act by elevating the intracellular calcium concentration. Evidence for this includes observations that intracellular application of calcium buffers prevents the induction of LTD (Sakurai, 1990; Konnerth *et al.*, 1992) and that elevation of intracellular calcium permits LTD induction (Lev-Ram *et al.*, 1995). Thus, a rise in intracellular calcium within the Purkinje cell is one signal for LTD.

Other signalling pathways have also been implicated in LTD. Nitric oxide (NO) has been suggested to play an important role in several models of neuronal plasticity (reviewed by Schuman and Madison, 1994). Recently, it was found that photolytic generation of NO could completely replace parallel fibre activation in the induction of LTD (Lev-Ram *et al.*, 1995). NO is a potent activator of soluble guanylate cyclase, the enzyme catalyzing cyclic GMP formation (Shibuki and Okada, 1991; Daniel *et al.*, 1993). Since the main biological action of cyclic GMP is to activate protein kinase G, the activation of this kinase by NO may play a role in the induction of LTD.

Recent work has shown that AMPA receptors can be phosphorylated by protein kinases (Moss *et al.*, 1993; McGlade-McCulloh *et al.*, 1993; Raymond *et al.*, 1993; Tingley *et al.*, 1993; Tan *et al.*, 1994; Nakazawa *et al.*, 1995). Some of the phosphorylation sites on cloned AMPA receptor subunits have been identified, and phosphorylation of these sites was found to decrease their response to glutamate. It has been postulated that protein kinases participate in LTP, LTD and receptor desensitization by phosphorylating glutamate receptors (reviewed by Roche *et al.*, 1994). For the case of cerebellar LTD, Nakazawa *et al.* (1995) have suggested a requirement for phosphorylation of receptors by protein kinase C (PKC). In agreement with this hypothesis, it has been shown that activation of PKC is necessary to induce LTD in cultured Purkinje cells (Crépel and Krupa, 1988, 1990; Linden and Connor, 1991): PKC inhibitors block LTD whilst activators of PKC mimic LTD. Protein kinase G is also proposed to be involved in the induction of LTD (Ito and Karachot, 1990; Daniel *et al.*, 1993). Furthermore, inhibition of protein phosphatase-1 (PP-1) by calyculin A mimics LTD (Ajima and Ito, 1995).

While these data imply a role for protein phosphorylation in LTD, the possible mechanism of the link between receptor phosphorylation and LTD has not been established.

1.6.4 Purkinje cell death in ischaemia

Cerebellar Purkinje cells are known to be selectively vulnerable to ischaemia among neurons in CNS, yet the reason for this vulnerability is not well understood. As discussed in section 1.2.5, for most neurons an elevation of intracellular free Ca^{2+} concentration mediated by NMDA receptor activation is thought to be important in causing neuronal death following ischaemia (Choi, 1990), but Purkinje cells have no functional NMDA receptors (Rosenmund *et al.*, 1992). One possible explanation of selective vulnerability among neurons is a lower than normal ability to buffer cytoplasmic Ca^2, since a high level of the cytoplasmic Ca^{2+}-binding protein calbindin-D28k may give a resistance to excitotoxic death in hippocampal neurons (Scharfman and Schwartzkroin, 1989); however, Purkinje cells do express calbindin-D28k at a high level. (Sequier *et al.*, 1990), so this does not explain the vulnerability of Purkinje cells. Recently, it has been shown that cultured Purkinje cells express Ca^{2+} permeable AMPA receptors (Brorson *et al.*, 1992), some of which do not show complete desensitization when AMPA is applied (Brorson *et al.*, 1995). Purkinje cells express largely the flip form of GluR3, as well as both splice variants of GluR1 and GluR2 (Lambolez *et al.*, 1992). Since homomeric GluR3 flip receptor channels were shown to have the slowest desensitization time constant (Mosbacher *et al.*, 1994), this expression pattern of AMPA receptors might be responsible for the selective vulnerability of Purkinje cells during ischaemia, by producing a long lasting calcium influx.

Another possibility is that Purkinje cells may be exposed to high level of NO during ischaemia (since NO is believed to play an important role in producing LTD in these cells) - NO is known to be able to damage cells by forming peroxynitrite anions. In Chapter 5, based on my work on glutamate transporters in Purkinje cells, I will suggest other possible explanations for their vulnerability to ischaemic insults.

Chapter 2

Methods

2.1 Preparation of rat cerebellar slices

2.1.1 Preparation of tissue for slicing

Cerebellar slices were prepared from 10-18 day old (usually 12 day old) Sprague-Dawley rats. The rat was killed by cervical dislocation followed by decapitation, and the whole brain was removed. After removal, the brain was immediately submerged in ice-cold oxygenated saline solution A or B (solution recipes are given at the end of this chapter: table 2.1). Then the two side lobes and the vermis of the cerebellum were cut off using a razor blade, leaving the central part of the cerebellum intact.

2.1.2 Slicing

The slicing chamber was filled with saline solution A or B, and pre-cooled in a freezer until the solution was frozen. A sagittal surface (for EPSC and iontophoresis experiments) or coronal surface (for recording the parallel fibre presynaptic volley) of the cerebellar block was glued with a cyanoacrylate glue to the stage of the slicing chamber, then the slicing chamber was immediately filled with ice-cold saline solution. A vibrating tissue slicer (Campden Instruments) was used to cut slices, and the chamber was continuously oxygenated. Four to ten 200μm thick slices were usually obtained from one cerebellum.

After slicing, each slice was immediately transferred to a holding chamber containing oxygenated saline solution A or B, which was kept either in a water bath at a temperature of 37°C or at room temperature for one hour to ensure the recovery of cells from slicing, then stored at room temperature until required. All the experiments were done at room temperature, 22 to 25°C.

2.1.3 Mechanical fixation of brain slices for recording

One slice was placed in a glass-bottomed recording chamber (0.8ml volume), and during recording, the chamber was perfused with oxygenated saline solution at a flow rate of 2ml/min. The slice was held in place with a grid of parallel nylon threads. The U-shaped frame (8×10mm) of the grid was made from 0.5mm platinum wire flattened with a vice (Konnerth *et al.*, 1987), and the threads were taken from nylon stockings and glued to this frame.

2.1.4 Isolation of Purkinje cells

To isolate cells, first a 200μm thick cerebellar slice was incubated in 2ml of medium containing (mM): Na-pyruvate 1; NaCl 86; $NaHCO_3$ 25; NaH_2PO_4 10; KCl 3.7; glucose 15; DL-cysteine 10; bubbled with 100% O_2 and about 10 units of papain for 12-15 minutes at 32°C. Then the slice was rinsed by dropping it through 4ml of solution B four times. Next the slice was triturated in 1ml of solution B by passing it in and out of the tip of a Pasteur pipette, which was fire polished to produce an internal diameter of about 0.5mm.

The resulting cell suspension was then immediately plated into the recording chamber. Prior to superfusing the external solution, cells were allowed to settle on the bottom of the chamber for 2-3 minutes. Purkinje cells were easily recognised morphologically by their large cell body and the presence of an axon and some dendritic processes (Fig. 2.1), as well as electrically by their sodium current after going to the whole-cell configuration.

2.2 Whole-cell clamping

2.2.1 Visualization of cells

The recording chamber was mounted on the fixed stage of an upright microscope (Axioskop, Zeiss, Germany) and slices were viewed with a 40× water immersion objective (Achroplan, Zeiss) with 0.9-NA condenser (Zeiss). Purkinje cell somata were easily identified by their position, shape and size in the slice (Fig. 2.2).

Fig. 2.1 An isolated Purkinje cell. The cell has a large pear-shaped cell body, an axon (at the bottom) and some dendritic processes (at the top). Cell body is about 18μm diameter.

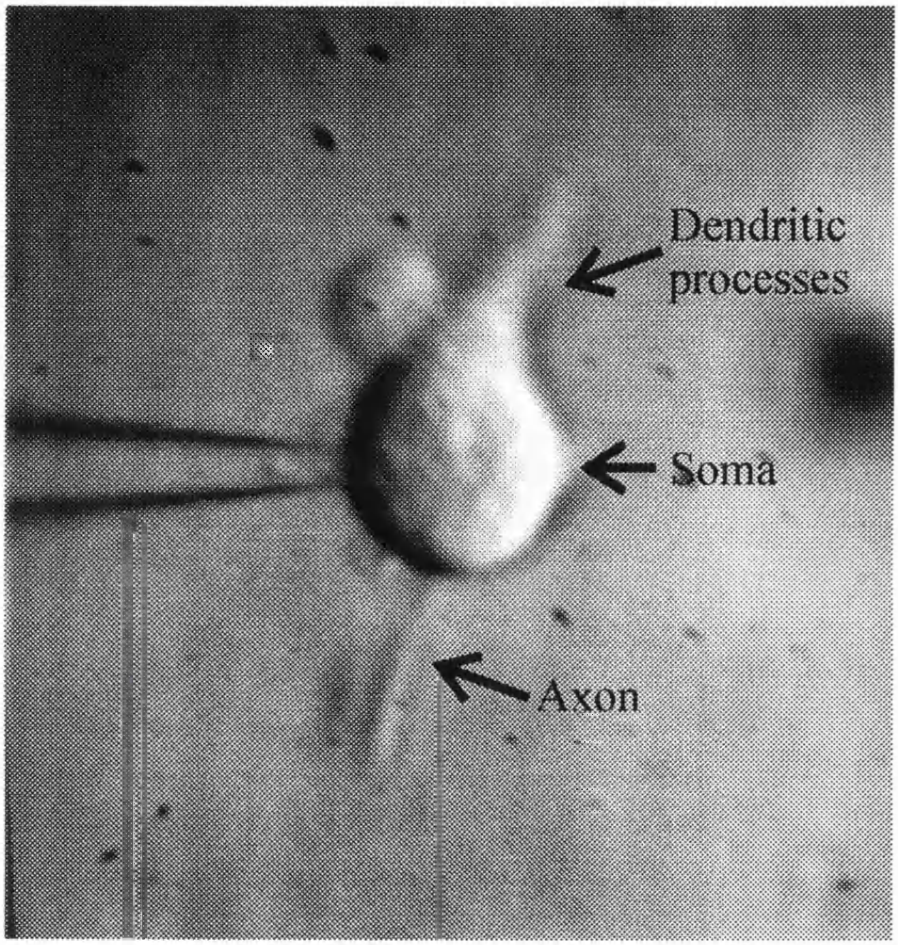
Dendritic processes
Soma
Axon

Fig. 2.2 A confocal image of a Lucifer yellow-filled Purkinje cell from a 12 day old rat.

2.2.2 Patch-clamp recording

The microscope was placed on a vibration isolation air table (Ealing Electro-Optics, U.S.A.) within a Faraday cage. Patch electrodes were pulled from thin-walled borosilicate glass capillaries (GC150TF-10, Clark Electromedical, England) using a two-stage pull on a BB-CH horizontal puller (Mecanex, Geneva). Immediately prior to use, the pipette tip was heat polished with a platinum wire: the pipette tip was observed under a microscope (Laborlux 11, Leitz) at a magnification of 400. The resistance of the pipettes before sealing was 2-2.5 MΩ when filled with solution D (table 2.2) and bathed in solution A or B (table 2.1).

The headstage of the patch clamp amplifier (RK300, Biologic, France or Axopatch-200A, Axon Instruments, U.S.A.) was mounted on a mechanical micromanipulator (MX-1, Narishige, Japan). The earth electrode was usually an Ag/AgCl pellet immersed in the bath solution. For experiments in which the external chloride concentration was altered, a 4M NaCl agar bridge was used (see section 2.2.4). The patch pipette was inserted in a perspex electrode holder with an Ag/AgCl pellet (Clark Electromedical) or a Teflon electrode holder with a chlorided silver wire (Axon Instruments).

During seal formation, 10mV voltage steps were applied to the electrode to monitor its resistance. When the patch electrode was put into the bath, offset potentials were cancelled to zero. A slight positive pressure was continuously applied until the electrode tip touched the membrane of the cell. Following contact of the electrode with the membrane, the positive pressure was immediately released and a small negative pressure was applied until a high-resistance seal (> 1GΩ) was established, and the electrode was hyperpolarized by 60-80mV to help make a better seal. Then application of brief pulses of suction to the patch electrode ruptured the membrane at the end of the electrode to obtain the whole-cell configuration.

2.2.3 Double-patch experiments

To exchange intracellular solutions in the same cell, double-patch experiments were performed (section 5.8.3). First, a Purkinje cell was whole-cell clamped with the first

patch electrode (electrode 1), and necessary recordings were made. Next, immediately prior to attaching the second patch electrode (electrode 2), electrode 1 was switched to the current-clamp configuration from the voltage-clamp configuration, and a seal was obtained with electrode 2. Rupture of the patch of membrane under electrode 2 was then achieved to obtain the whole-cell configuration. Then electrode 2 was set to current-clamp mode, while electrode 1 was switched back to voltage-clamp mode so that subsequent EPSC recordings were made with the same electrode as before electrode 2 was attached. The series resistance of electrode 1 was continuously monitored by giving 2mV steps prior to the stimuli used to evoke a synaptic current.

2.2.4 Correction of liquid junction potentials

Potential differences between two solutions, called liquid junction potentials, occur at all boundaries between solutions of differing compositions. They result from the charge separation that occurs when anions and cations of different mobilities diffuse across boundaries. Apparent offset potentials were cancelled before seal formation, at a time when the pipette solution was diffusing into the bath solution. However, after entering the whole-cell recording configuration, the liquid junction and the concentration gradients at the electrode tip no longer exist. Thus, the apparent zero voltage read by the amplifier was actually shifted by the size of the liquid junction potential, existing at the end of the pipette when immersed in the bath solution.

The measurement of liquid junction potentials was carried out as described by Neher (1992). To ensure the accurate measurement of the liquid junction potentials, a 4M NaCl agar bridge was used as a bath electrode to avoid changes of potential at that electrode. The bath was first filled with the test pipette solution, which was also in the pipette. The amplifier was switched to current clamp mode, and the voltage reading was set to zero by adjusting the offset. The bath solution was then quickly exchanged for normal external solution and the new pipette voltage was read: this new voltage is the liquid junction potential between the test pipette solution and the bath solution. For all the data of this thesis, the liquid junction potential was corrected using this method.

2.2.5 Voltage-clamp quality

2.2.5.1 Space-clamp quality

To improve voltage control, when recording EPSCs, cell somata were usually clamped to between -30mV and -40mV to inactivate the voltage-gated sodium current. For the pipette solution, caesium was used as a major cation instead of potassium to reduce voltage-dependent potassium currents and to obtain better voltage-clamp uniformity. Earlier work suggests that with these conditions, combined with the use of young animals (usually 12 days old), the climbing and parallel fibre EPSCs are reasonably well voltage-clamped and their decay time constants are reasonably accurately measured (Llano *et al.*, 1991; Häusser, 1994).

2.2.5.2 Modelling the Purkinje cell dendritic tree

Purkinje cells have an extensive dendritic arborization in adult cerebellum, which would cause serious problems of voltage-clamp quality. However, using rats younger than 20 days old is thought to give considerably better voltage-control and at this age the Purkinje cell can be represented by a 2 compartment model, as shown in Fig. 2.3A (Llano *et al.*, 1991). This model represents the cell in terms of a proximal compartment comprising the soma and proximal (main) dendrites (where the climbing fibre synapses impinge in rats of the age that I have studied) and a distal compartment representing the distant dendrites (where the parallel fibre synapses impinge). To assess the parameters in this model, voltage steps (10 or 2mV) were applied to the pipette in whole-cell mode, and the resulting capacity transient (for an example see Fig. 2.3B) was analysed as follows. The symbols used in this derivation are as follows:

I: current

V_0: pipette (command) potential

V_1: potential in the soma and in the main dendrites

V_2: potential in the distal dendrites

Fig. 2.3 Two compartment model of a Purkinje cell. **A.** Circuit equivalent to a whole-cell clamped Purkinje cell. V_0 is the holding potential, V_1 the somatic membrane potential, V_2 the membrane potential of distal dendrites, I the current flowing in response to a change of voltage, R_1 the series resistance between the pipette and the cell, R_2 the series resistance between the soma compartment and the distal dendrites, R_3 the membrane resistance of the distal dendrites, R_4 the membrane resistance of the soma and proximal dendrites, C_1 the somatic and main dendritic membrane capacitance and C_2 the (distal) dendritic membrane capacitance. **B.** Specimen capacity transient, showing the current flow in response to a 10mV depolarization from a holding potential of -90mV. I_∞ is the steady state current.

A

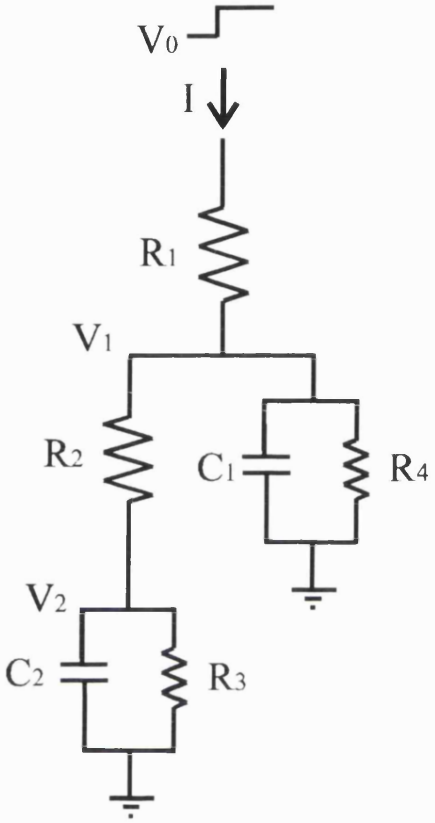

B

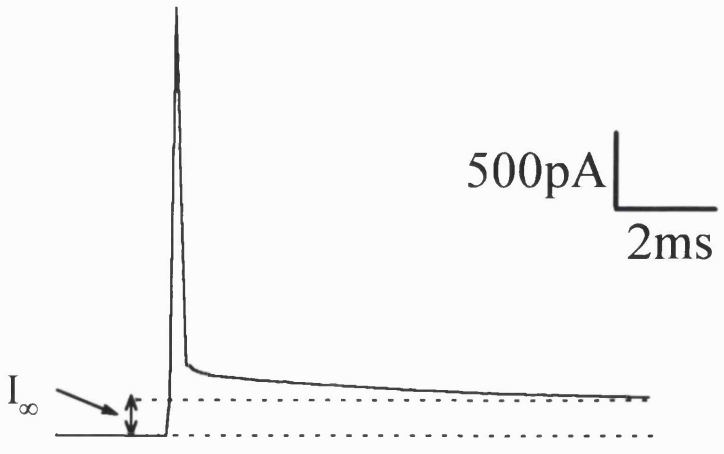

C_1: somatic and main membrane capacitance

C_2: distal dendritic membrane capacitance

R_1: pipette access resistance

R_2: resistance between main dendrites and distal dendrites

R_3: distal dendritic membrane resistance

R_4: somatic and main dendritic membrane capacitance

The following derivation leads to results different from those in the maths of Llano *et al.* (1991) whose treatment involved making erroneous assumptions.

When a sudden voltage jump is given at the electrode, the current which flows is given by,

$$I = \frac{V_0 - V_1}{R_1} = C_1 \frac{dV_1}{dt} + \frac{V_1}{R_4} + \frac{V_1 - V_2}{R_2} \qquad (1)$$

and

$$\frac{V_1 - V_2}{R_2} = \frac{V_2}{R_3} + C_2 \frac{dV_2}{dt} \quad . \qquad (2)$$

From (1),

$$V_2 = V_1 R_2 \left(\frac{1}{R_2} + \frac{1}{R_4} \right) + R_2 C_1 \frac{dV_1}{dt} - IR_2 \, . \qquad (3)$$

Therefore from (3),

$$\frac{dV_2}{dt} = \frac{dV_1}{dt} R_2 \left(\frac{1}{R_2} + \frac{1}{R_4} \right) + R_2 C_1 \frac{d^2 V_1}{dt^2} - R_2 \frac{dI}{dt} \qquad (4)$$

From (2),

$$C_2\frac{dV_2}{dt}=\frac{V_1}{R_2}-V_2\left(\frac{1}{R_2}+\frac{1}{R_3}\right) \tag{5}$$

Inserting (3) and (4) into (5),

$$\begin{aligned}&C_2R_2\left(\frac{1}{R_2}+\frac{1}{R_4}\right)\frac{dV_1}{dt}+C_2R_2C_1\frac{d^2V_1}{dt^2}-C_2R_2\frac{dI}{dt}\\&=\frac{V_1}{R_2}-\left(\frac{1}{R_2}+\frac{1}{R_3}\right)\left\{V_1R_2\left(\frac{1}{R_2}+\frac{1}{R_4}\right)+R_2C_1\frac{dV_1}{dt}-IR_2\right\}\end{aligned} \tag{6}$$

Now, from (1) $V_1=V_0-R_1I$, so

$$\frac{dV_1}{dt}=-R_1\frac{dI}{dt},$$

$$\frac{d^2V_1}{dt^2}=-R_1\frac{d^2I}{dt^2}.$$

So,

$$\begin{aligned}&-R_1R_2C_1C_2\frac{d^2I}{dt^2}-R_2C_2\frac{dI}{dt}-R_1\left\{C_2R_2\left(\frac{1}{R_2}+\frac{1}{R_4}\right)+R_2C_1\left(\frac{1}{R_2}+\frac{1}{R_3}\right)\right\}\frac{dI}{dt}\\&=(V_0-R_1I)\left\{\frac{1}{R_2}-\left(\frac{1}{R_2}+\frac{1}{R_3}\right)\left(1+\frac{R_2}{R_4}\right)\right\}+I\left(1+\frac{R_2}{R_3}\right)\end{aligned},$$

and collecting terms gives

$$\begin{aligned}&\frac{d^2I}{dt^2}+\frac{dI}{dt}\left\{\frac{1}{R_1C_1}+\frac{1}{C_1}\left(\frac{1}{R_2}+\frac{1}{R_4}\right)+\frac{1}{C_2}\left(\frac{1}{R_2}+\frac{1}{R_3}\right)\right\}+\frac{I}{R_1R_2C_1C_2}\left(1+\frac{R_2}{R_3}+\frac{R_1}{R_3}+\frac{R_1}{R_4}+\frac{R_1R_2}{R_3R_4}\right)\\&=\frac{V_0}{R_1R_2C_1C_2}\left(\frac{1}{R_3}+\frac{1}{R_4}+\frac{R_2}{R_3R_4}\right)\end{aligned} \tag{7}$$

Hence the steady state current is

$$I_\infty = \frac{V_0\left(\frac{1}{R_3}+\frac{1}{R_4}+\frac{R_2}{R_3R_4}\right)}{1+\frac{R_2}{R_3}+\frac{R_1}{R_3}+\frac{R_1}{R_4}+\frac{R_1R_2}{R_3R_4}} \qquad (8)$$

Now, in general the solution of (7) is

$$I(t) = I_\infty + A_1 e^{-t/\tau_1} + A_2 e^{-t/\tau_2} \qquad (9)$$

and the boundary conditions are $V_1=V_2=0$ at t=0.

Therefore, from (1)

$$I(t=0) = \frac{V_0}{R_1} = I_\infty + A_1 + A_2$$

Hence generally (independent of the values of R_3 and R_4) the pipette series resistance can be obtained from the values of A_1 and A_2 derived from fitting the sum of 2 exponentials to the capacity transient, as:

$$R_1 = \frac{V_0}{I_\infty + A_1 + A_2}. \qquad (10)$$

When $\tau \equiv \tau_1, \tau_2$, inserting (9) into (7) gives

$$\frac{1}{\tau_1}, \frac{1}{\tau_2} \equiv \frac{1}{\tau} = \frac{x \pm \sqrt{x^2 - 4y}}{2} \qquad (11)$$

where

$$x = \frac{1}{R_1C_1} + \frac{1}{C_1}\left(\frac{1}{R_2}+\frac{1}{R_4}\right) + \frac{1}{C_2}\left(\frac{1}{R_2}+\frac{1}{R_3}\right) \qquad (12)$$

and

$$y = \frac{1}{R_1R_2C_1C_2}\left(1+\frac{R_2}{R_3}+\frac{R_1}{R_3}+\frac{R_1}{R_4}+\frac{R_1R_2}{R_3R_4}\right). \qquad (13)$$

Now at t=0, since $V_1=V_2=0$, equation (1) becomes

$$C_1\frac{dV_1}{dt} = I = \frac{V_0}{R_1} \tag{14}$$

However, $V_1=V_0-IR_1$. Hence at t=0,

$$\begin{aligned} C_1\frac{dV_1}{dt} &= -R_1\frac{dI}{dt}C_1 \\ &= R_1C_1\left(\frac{A_1}{\tau_1}+\frac{A_2}{\tau_2}\right) \end{aligned} \tag{15}$$

Thus from (14) and (15), generally (independent of the values of R_3 and R_4) the capacitance of the soma and main dendrite component can be obtained as:

$$C_1 = \frac{V_0}{R_1^2\left(\frac{A_1}{\tau_1}+\frac{A_2}{\tau_2}\right)} \tag{16}$$

$$\therefore C_1 = \frac{\left(I_\infty + A_1 + A_2\right)^2}{V_0\left(\frac{A_1}{\tau_1}+\frac{A_2}{\tau_2}\right)}. \tag{17}$$

Now, if $\tau_2>\tau_1$, (11), (12) and (13) give

$$\frac{1}{\tau_1}+\frac{1}{\tau_2} = \frac{1}{R_1C_1}+\frac{1}{C_1}\left(\frac{1}{R_2}+\frac{1}{R_4}\right)+\frac{1}{C_2}\left(\frac{1}{R_2}+\frac{1}{R_3}\right) \tag{18}$$

and

$$\begin{aligned} \frac{1}{\tau_1}-\frac{1}{\tau_2} &= \sqrt{x^2-4y} \\ &= \sqrt{\left(\frac{1}{\tau_1}+\frac{1}{\tau_2}\right)^2 - 4\frac{1}{R_1R_2C_1C_2}\left(1+\frac{R_2}{R_3}+\frac{R_1}{R_3}+\frac{R_1}{R_4}+\frac{R_1R_2}{R_3R_4}\right)} \end{aligned}$$

therefore, squaring both sides,

$$\frac{4}{R_1R_2C_1C_2}\left(1+\frac{R_2}{R_3}+\frac{R_1}{R_3}+\frac{R_1}{R_4}+\frac{R_1R_2}{R_3R4}\right)=\left(\frac{1}{\tau_1}+\frac{1}{\tau_2}\right)^2-\left(\frac{1}{\tau_1}-\frac{1}{\tau_2}\right)^2$$
$$=\frac{4}{\tau_1\tau_2}. \qquad (19)$$

Since equations (8), (18) and (19) are 3 equations with 4 unknown values (i.e. R_2, C_2, R_3, R_4), either $R_3=\infty$ or $R_4=\infty$ must be assumed to proceed.

Suppose $R_3=\infty$ (i.e. no distant dendritic conductance), then (8) becomes

$$I_\infty=\frac{V_0}{R_1+R_4},$$

therefore

$$R_4=\frac{V_0}{I_\infty}-R_1$$
$$=\frac{V_0}{I_\infty}-\frac{V_0}{I_\infty+A_1+A_2} \qquad (20)$$

and (18) becomes

$$\frac{1}{\tau_1}+\frac{1}{\tau_2}=\frac{1}{R_1C_1}+\frac{1}{R_2C_1}+\frac{1}{C_1R_4}+\frac{1}{R_2C_2}$$

$$\therefore \frac{1}{\tau_1}+\frac{1}{\tau_2}-\frac{1}{C_1}\left(\frac{1}{R_1}+\frac{1}{R_4}\right)=\frac{1}{R_2}\left(\frac{1}{C_1}+\frac{1}{C_2}\right), \qquad (21)$$

and (19) becomes

$$R_2C_2=\frac{\tau_1\tau_2}{R_1C_1}\left(1+\frac{R_1}{R_4}\right). \qquad (22)$$

The values of R_2 and C_2 can be obtained in terms of other known parameters, as follows. From (21) and (22):

$$\frac{R_1(C_1+C_2)}{\tau_1\tau_2\left(1+\frac{R_1}{R_4}\right)} = \frac{1}{\tau_1}+\frac{1}{\tau_2}-\frac{1}{C_1}\left(\frac{1}{R_1}+\frac{1}{R_4}\right)$$

$$\therefore C_2 = \left\{\tau_1+\tau_2-\frac{\tau_1\tau_2}{C_1}\left(\frac{1}{R_1}+\frac{1}{R_4}\right)\right\}\left(\frac{1}{R_1}+\frac{1}{R_4}\right)-C_1 \qquad (23)$$

and

$$R_2 = \frac{\tau_1\tau_2\left(\frac{1}{R_1}+\frac{1}{R_4}\right)}{C_1\left[\left\{\tau_1+\tau_2-\frac{\tau_1\tau_2}{C_1}\left(\frac{1}{R_1}+\frac{1}{R_4}\right)\right\}\left(\frac{1}{R_1}+\frac{1}{R_4}\right)-C_1\right]} \qquad (24)$$

or more simply

$$R_2 = \frac{\tau_1\tau_2\left(\frac{1}{R_1}+\frac{1}{R_4}\right)}{C_1C_2}.$$

Alternatively, the equations (8), (18) and (19) can be solved by postulating that $R_4=\infty$, i.e. no soma conductance. In this case (8) becomes

$$I_\infty = \frac{V_0}{R_1+R_2+R_3}, \qquad (25)$$

(18) becomes

$$\frac{1}{\tau_1}+\frac{1}{\tau_2}-\frac{1}{R_1C_1} = \frac{1}{C_1R_2}+\frac{1}{C_2}\left(\frac{1}{R_2}+\frac{1}{R_3}\right), \qquad (26)$$

and (19) becomes

$$\frac{R_1R_2C_1C_2}{\tau_1\tau_2} = \frac{R_1+R_2+R_3}{R_3} = \frac{V_0}{R_3I_\infty}. \qquad (27)$$

From (27),

$$R_2R_3C_2 = \frac{V_0\tau_1\tau_2}{R_1C_1I_\infty}. \tag{28}$$

Now, (26) becomes

$$\frac{1}{\tau_1}+\frac{1}{\tau_2}-\frac{1}{R_1C_1} = \frac{1}{C_1R_2}+\frac{R_2+R_3}{R_2R_3C_2}. \tag{29}$$

Inserting (25) and (28) into (29) gives

$$\frac{1}{\tau_1}+\frac{1}{\tau_2}-\frac{1}{R_1C_1} = \frac{1}{C_1R_2}+\frac{\left(\frac{V_0}{I_\infty}-R_1\right)R_1C_1I_\infty}{V_0\tau_1\tau_2}.$$

$$\therefore R_2 = \frac{\frac{1}{C_1}}{\frac{1}{\tau_1}+\frac{1}{\tau_2}-\frac{1}{R_1C_1}-\frac{R_1C_1(V_0-R_1I_\infty)}{V_0\tau_1\tau_2}}. \tag{30}$$

From (25),

$$R_3 = \frac{V_0}{I_\infty}-R_1-R_2. \tag{31}$$

From (28),

$$C_2 = \frac{V_0\tau_1\tau_2}{R_1R_2R_3C_1I_\infty}. \tag{32}$$

Equations (30) and (32) reduce to equations (23) and (24) when $R_3=R_4=\infty$.

These equations were used to derive the parameters of the model circuit in Fig. 2.3 from experimentally derived capacity transients. Capacity transients could be fit well by the sum of 2 exponentials, as required for this modelling.

A typical response to a 10mV pulse (average of 25 traces) is shown in fig. 2.3B. A curve fitting program, Clampfit, was used to fit two exponentials to this response. The fitting region was from 95% of the peak response to the steady state. To use the equations derived above I obtained the following parameters from the curve fitting:

A_1: amplitude of the first exponential

A_2: amplitude of the second exponential

I_∞: amplitude of the steady state current

τ_1: decay time constant of the first exponential

τ_2: decay time constant of the second exponential

These values were then inserted into the equations above. For example, the fit for the cell in Fig.2.3B generated the following values: A_1=1681pA, A_2=220pA, I_∞=256pA, τ_1=0.13ms, τ_2=5.25ms. Therefore, R_1=4.64MΩ and C_1=35.86pF. When $R_3=\infty$ (no distal dendritic conductance), R_4=34.4MΩ, C_2=141pF and R_2=33.0MΩ; and when $R_4=\infty$ (no somatic conductance), R_3=17.6MΩ, C_2=541pF and R_2=33.0MΩ. Note that the value obtained for C_2 (distal dendrite capacitance) depends critically on whether it is assumed that $R_3=\infty$ or that $R_4=\infty$.

Average values of the parameters in 14 cells were: R_1 (pipette series resistance before compensation)=9.7MΩ, C_1=112pF, and when $R_3=\infty$ (no dendritic conductance), R_4=69.1MΩ, C_2=137pF and R_2=76.0MΩ; and when $R_4=\infty$ (no somatic conductance), R_3=47.2MΩ, C_2=383pF and R_2=21.8MΩ.

2.2.5.3 Series resistance

No correlation of EPSC decay time constant with series resistance value (R_1 in Fig. 2.3) was found when the series resistance was less than 15MΩ, suggesting no significant shaping of the EPSC by series resistance by filtering. Furthermore, series resistance compensation was usually employed to reduce the effective pipette series resistance.

Nevertheless, control experiments (described in section 3.7) and theoretical calculations (see below) were performed to check that changes of EPSC waveform produced experimentally, by reducing transmitter release with adenosine or baclofen, were not due to defective voltage control produced by series resistance errors.

The voltage drop generated by the synaptic current flowing across the series resistance, or access resistance, R_1, of the whole cell pipette can lead to a distortion of the decay time course of EPSC and altering the synaptic current amplitude (as in Chapter 3) will alter this distortion. To analyse this, the cell capacitance (C_1 and C_2) and conductance ($1/R_3$ and $1/R_4$) were ignored: numerical simulations using MathCad showed that including them reduced the speeding of the EPSC decay predicted to be produced by the series resistance when the synaptic current is reduced with adenosine or baclofen, so the following is a worst case analysis. In addition the cell was treated as isopotential. Series resistance alteration of the EPSC time course is most likely to occur for the climbing fibre synapses because of their large current. Most of the climbing fibre synapses in 12 day old rats are likely to be located in the proximal compartment (soma and proximal dendrites: Llano *et al.*, 1991).

The following symbols are used in the analysis.

I_{syn}: inward synaptic current produced at proximal dendrites or soma

g_{max}: peak ion channel conductance

I_{max}: peak synaptic current in the absence of blockers to reduce g_{max}

V_{rev}: the reversal potential of the synaptic current

V_{cell}: the voltage inside the cell

V_{pip}: the clamped pipette potential

τ: "real" time constant of decay of the synaptic conductance

τ_{obs}: the decay time constant of the observed current

The inward synaptic current can be expressed as

$$I_{syn} = g_{max} e^{-t/\tau} \left(V_{rev} - V_{cell} \right). \qquad (33)$$

This current will generate a voltage drop across the pipette series resistance R_1, therefore

$$V_{cell} = V_{pip} + I_{syn} R_1. \qquad (34)$$

Inserting (34) into (33) gives the observed (non-exponential) time course of the synaptic current as

$$I_{syn} = \frac{g_{max} \left(V_{rev} - V_{pip} \right) e^{-t/\tau}}{1 + g_{max} R_1 e^{-t/\tau}}. \qquad (35)$$

The instantaneous time decay constant of the observed current is defined as

$$\frac{1}{\tau_{obs}} = -\frac{1}{I_{syn}} \frac{dI_{syn}}{dt}. \qquad (36)$$

At the time when the underlying conductance has decreased to half its initial value, equations (35) and (36) give the observed instantaneous decay time constant (an estimate of what will be obtained from fitting from 90% to 10% of the EPSC decay) as

$$\begin{aligned} \tau_{obs} &= \tau \left(1 + \frac{g_{max} R_1}{2} \right) \\ &= \tau \frac{1 + \left(\frac{I_{max} R_1}{2} \right)}{V_{rev} - V_{pip} - I_{max} R_1} \end{aligned} \qquad (37)$$

Thus, when adenosine, GABA or baclofen are used to decrease g_{max} (see Chapter 3), the observed decay time constant will decrease. If the resulting peak current is decreased by a fraction *f*, (37) predicts a fractional change of observed time constant of

$$\frac{\Delta\tau_{obs}}{\tau_{obs}} = \frac{f I_{max} R_1 \left(V_{rev} - V_{pip}\right)}{\left\{2\left(V_{rev} - V_{pip}\right) I_{max} R_1\right\}\left\{V_{rev} - V_{pip} - (1-f) I_{max} R_1\right\}}. \qquad (38)$$

For each cell studied in which the synaptic current amplitude was altered experimentally, equation (38) was used to calculate the change of EPSC decay time constant expected from series resistance errors. Fig. 3.18 shows that for cells with low (uncompensated) series resistance (R_s in Fig. 3.18 is equal to R_1 above), these errors generate only a small fraction (open squares) of the observed change of time constant (filled squares). For the data in Fig. 3.18 with $R_s I_{max}$<10mV, the predicted fractional change of time constant due to series resistance errors is on average 24% of that actually observed.

The presence of series resistance error can also be shown to produce a small distortion of the dose-response curves describing the action of adenosine or baclofen on the peak synaptic current (Figs. 3.3, 3.4, 3.8 and 3.9) from that which would be observed for the underlying conductance. For typical values of series resistance (10MΩ) and synaptic current amplitude, mathematical analysis showed that this will lead to the adenosine dose needed to produce a half-maximal effect on the synaptic current being 12% higher for the climbing fibre and 6% higher for the parallel fibre input than that which has a half-maximal effect on the synaptic conductance, i.e. negligible errors.

2.3 Stimulation of inputs

Stimulation electrodes were pulled from thin-walled borosilicate theta glass capillaries (TGC150-10, Clark Electromedical, England). For EPSC experiments, the climbing fibre or parallel fibre input to Purkinje cells was stimulated at 0.1Hz with a bipolar theta glass electrode filled with 1M NaCl (Konnerth et al, 1990; Perkel et al, 1990). Identification of synaptic inputs is described in section 3.3.

To record the parallel fibre presynaptic volley, stimuli were given by electrodes containing extracellular solution in the molecular layer, and the resulting extracellular compound action potentials were recorded with an electrode containing extracellular solution placed about 300μm from the stimulation electrode. The intensity of the stimuli

was set to produce a half-maximal response, to enhance the chance of detecting any effect of the drugs on the number of fibres stimulated.

2.4 Iontophoresis

Iontophoresis electrodes were pulled from thin-walled borosilicate glass capillaries (GC150TF-10, Clark Electromedical, England) using a single-stage pull on a PG-1 horizontal puller (Narishige, Japan). Electrodes were filled with 100mM sodium D-aspartate, 100mM sodium glutamate or 100mM PDC (resistance around 100MΩ) and backfilled with 1M NaCl, and were placed near Purkinje cell bodies (usually 5-10μm from the cell bodies) with the superfusion solution flowing in the direction from the electrode to the Purkinje cell. D-aspartate, glutamate or PDC was ejected by switching from a holding current of +20nA to an ejection current of -40nA. The position of electrodes was always monitored by a TV camera on the microscope and thus maintained constant relative to the cell.

2.5 Superfusion

The extracellular solutions were bath applied in all experiments. Solutions were fed into the recording chamber through plastic tubing by gravity flow. Excess solution was constantly removed with a hypodermic needle connected to a small tube with suction provided by a vacuum pump.

2.5.1 Superfusion for slice experiments

For slice experiments, syringe barrels containing different solutions were connected to a common tube at the bottom of them to ensure good oxygenation even while switching the flowing solutions (i.e. there was no dead space containing unoxygenated solution): with this system, it took less than 2 minutes to change the solution in the recording chamber when solutions flowed at a rate of 2 ml/min.

2.5.2 Superfusion for isolated cell experiments

For isolated cell experiments, syringe barrels containing different solutions were connected together at the common inlet into the bath to allow a faster change (around 10 seconds) of the recording chamber solution. To investigate the effect of high external potassium concentration as described in Chapter 5, rapid changes of the extracellular solutions around isolated Purkinje cells were achieved by high speed perfusion through a cannula (inner diameter 0.6mm) placed near the cell, and by lifting the whole-cell clamped cell from the bottom of the bath.

2.6 Solutions

The extracellular solutions used frequently are listed in Table 2.1. Modifications of these are stated in the appropriate figure legends. HCO_3^- buffered solutions (solution A) were made freshly on the day of experiments, and their pH was 7.4 when bubbled with 95% O_2/5% CO_2. This solution was used for the experiments described in Chapters 3 and 4. HEPES-buffered solutions (solution B) were made either on the day of experiments, or made up before and kept in a freezer. These solutions were used for the experiments described in Chapter 5, to allow zero-sodium external experiments.

Picrotoxin (Sigma) were made up as a 2.5mM stock in extracellular solution, and kept frozen until needed. CNQX (Tocris) and DNQX (Tocris or Sigma) were made up as either a 10mM or 20mM stock in DMSO. DMSO was then also added to the control solution. D-APV (Tocris) was made up as a 10 or 20mM stock in water. PDC (Tocris) was made up as a 100mM stock in water. Diazoxide (Sigma), glibenclamide (RBI), and sodium kynurenate (Sigma) were dissolved directly in the external solution. ACPD (Tocris), MCPG (Tocris) were made up as a 100mM stock in water with equimolar NaOH. After adding drugs, pH of the solution was always checked, and adjusted to 7.4 as necessary.

The intracellular solutions used frequently are listed on Table 2.2; any others used are stated in the appropriate figure legend. All intracellular solutions were made as a stock

and kept frozen. On the day of experiments, the solutions were thawed. When filling the pipette, the solutions were passed through a filter with the pore diameter of 0.2μm.

2.7 Data analysis

In most of the experiments, data were acquired with pClamp5.5.1 (Axon Instrument), and recorded on a hard disk of a personal computer (486, 33kHz, Samsung, South Korea) after being filtered between 1 (iontophoresis experiments and reversed uptake experiments) and 50kHz (capacity transients) with a low pass filter (Barr & Stroud). Data was then analysed using pClamp5.5.1.

For reversed uptake experiments (section 5.9), data were stored on magnetic tape (Racal Store 4DS) and recorded with a chart recorder (Gould, BS-272), and the currents were measured directly from the chart recordings.

2.7.1 Fitting the decay of the EPSCs

The decay time constant was calculated using Clampfit or a home-made spread sheet. The fitting region was 10-90% of the amplitude. The rise time was similarly acquired with Clampfit, and the fitting region was roughly 10-90% of the amplitude.

Table 2.1

Standard extracellular solutions A-C

	A	B	C
NaCl	124	140	131
KCl	2.5	2.5	2.5
$BaCl_2$			6
NaH_2PO_4	1	1	1
$CaCl_2$	2.5	10	10
$MgCl_2$	2	2	2
$NaHCO_3$	26		
HEPES		10	10
Glucose	10	10	10
Bubbled with	95% O_2/5% CO_2	100%O_2	100%O_2
pH	7.4	7.4	7.4
pH adjusted with	5% CO_2	NaOH	NaOH

All concentrations are in mM.

A: Standard extracellular solution used in experiments described in Chapters 3, 4 and 6.

B: Standard extracellular solution used in experiments described in Chapters 5 and 6.

C: Barium extracellular solution used in experiments described in Chapter 5.

Table 2.2

Standard intracellular solutions D-F

	D	E	F
CsF	110		
CsCl	30		
KCl		140	
$KClO_4$			140
NaCl	4	4	4
$CaCl_2$	0.5	0.5	0.5
$NMDG_2$ -EGTA	5	5	5
HEPES	10	10	10
pH	7.3	7.3	7.3
pH adjusted with	NMDG	NMDG	NMDG
Junction potential	-6mV	-2mV	-3mV

All concentrations are in mM.

D: Standard intracellular solution.

E: KCl intracellular solution used in Chapter 5.

F: $KClO_4$ intracellular solution used in Chapter 5.

Table 2.3

Intracellular solutions G and H

	G	H
CsF	110	110
CsCl	14	14
NaCl	20	
Na-D-aspartate		20
CaCl2	0.5	0.5
$NMDG_2$-EGTA	5	5
HEPES	10	10
pH	7.3	7.3
pH adjusted with	NMDG	NMDG
Junction potential	-3mV	-3mV

All concentrations are in mM.

G: Control intracellular solution for H

H: Intracellular solution to block glutamate uptake from inside the cell

Chapter 3

Differential effects of adenosine and GABA on parallel fibre and climbing fibre synapses

3.1 Introduction

Adenosine acts on presynaptic A_1 receptors to inhibit transmitter release (Dunwiddie, 1985; Lupica *et al.*, 1992; Prince and Stevens, 1992), either by inhibiting voltage-dependent Ca^{2+} influx (Scholz and Miller, 1991; Yawo and Chuhma, 1993) or by another mechanism such as inhibition of adenylate cyclase (Dunwiddie and Fredholm, 1989; Scanziani *et al.*, 1992; Chavez-Noriega and Stevens, 1994). GABA, acting on $GABA_B$ receptors, inhibits glutamate release in a similar manner (Scanziani *et al.*, 1992; Isaacson *et al.*, 1993; Pfrieger *et al.*, 1994). The role of adenosine and $GABA_B$ receptors in the cerebellum is poorly understood. The cerebellum contains a high level of adenosine, as well as A_1 (but not A_2) receptors on parallel fibre terminals (Jarvis and Williams, 1989), and a high level of 5'-nucleotidase which converts AMP into adenosine (reviewed by Do *et al.*, 1991). $GABA_B$ receptors are localized in the molecular layer (Turgeon and Albin, 1993) where parallel fibres make synapses with Purkinje cells. Adenosine is released by climbing fibres (Cuenod *et al.*, 1989), and by granule cells (Schousboe *et al.*, 1989) which provide the parallel fibre input to Purkinje cells, while GABA is released by basket, Golgi and stellate cells. Adenosine and GABA reduce parallel fibre to Purkinje cell transmission (Hackett, 1974; Kocsis *et al.*, 1984; Batchelor and Garthwaite, 1992).

This chapter describes experiments which show that adenosine and GABA affect differentially the strengths of the parallel and climbing fibre synapses to Purkinje cells.

3.2 Methods

These are described in detail in Chapter 2. Purkinje cells were whole-cell clamped in slices of rat cerebellum. To evoke synaptic currents, the climbing or parallel fibre input to Purkinje cells was stimulated with a bipolar theta glass electrode filled with 1M NaCl. For iontophoresis experiments, electrodes filled with 100mM sodium glutamate were

placed near Purkinje cell bodies and glutamate was ejected by switching from a holding current of +20nA to an ejection current of -40nA. Iontophoresis experiments were done in calcium-free external solution (Fig. 3.12 legend) to avoid trans-synaptic effects. All the drugs were added to external solutions and 100μM picrotoxin was present to block $GABA_A$ receptors.

3.3 Identification of inputs

EPSCs evoked by stimulating the climbing fibre or parallel fibre inputs to Purkinje cells in cerebellar slices are shown in Fig. 3.1. These EPSCs are mediated by non-NMDA receptors (Konnerth *et al.*, 1990; Perkel *et al.*, 1990). Stimulation in the granule cell layer elicited a climbing fibre response. An inward synaptic current elicited by the climbing fibre was easily recognised by its large amplitude (typically 1-4nA at -36mV) and its all-or-none characteristic when increasing the stimulus strength (Fig. 3.1A and B; Perkel *et al.*, 1990; Konnerth *et al.*, 1990). Stimulation of the molecular layer resulted in a parallel fibre response, the magnitude of which was smoothly graded with stimulus intensity (Fig. 3.1C and D; Perkel *et al.*, 1990; Konnerth *et al.*, 1990). These results are consistent with the idea that a single climbing fibre innervates each Purkinje cell, whereas more than 100,000 parallel fibres make synapses onto each Purkinje cell. Occasionally the stimulus-response curve for the climbing fibre input showed two increments rather than one, suggesting multiple innervation by 2 climbing fibres, as reported previously in 8 to 14 day old rats (Crépel *et al.*, 1976).

The climbing and parallel fibre EPSCs were also distinguished by their response to two stimuli applied at a short interval (Perkel *et al.*, 1990; Konnerth *et al.*, 1990). The climbing fibre EPSC evoked by the second of the two closely spaced stimuli is smaller than the EPSC evoked by the first stimulus (Fig. 3.2A). By contrast, the EPSC evoked by a second stimulus to the parallel fibre input was larger in amplitude than the first EPSC (Fig. 3.2B).

Fig. 3.1 Two types of excitatory postsynaptic currents in Purkinje cells. **A.** The synaptic currents elicited by stimulating climbing fibre with an intensity of 10, 30, 50, 70 and 90V. There was no response to the stimuli of 10 and 30V. **B.** Amplitude of climbing fibre EPSC as a function of stimulus intensity. Each point is the mean of the response to three stimuli. The reduction of amplitude with higher stimulation intensity is probably due to a rise of series resistance during the experiment. **C.** The synaptic currents of graded response elicited by stimulating the parallel fibres, with an intensity of 5, 20, 35, 50, 70 and 90V. **D.** Amplitude of parallel fibre EPSC as a function of stimulus intensity. Each point represents the mean from three stimuli. The holding potential was -36mV.

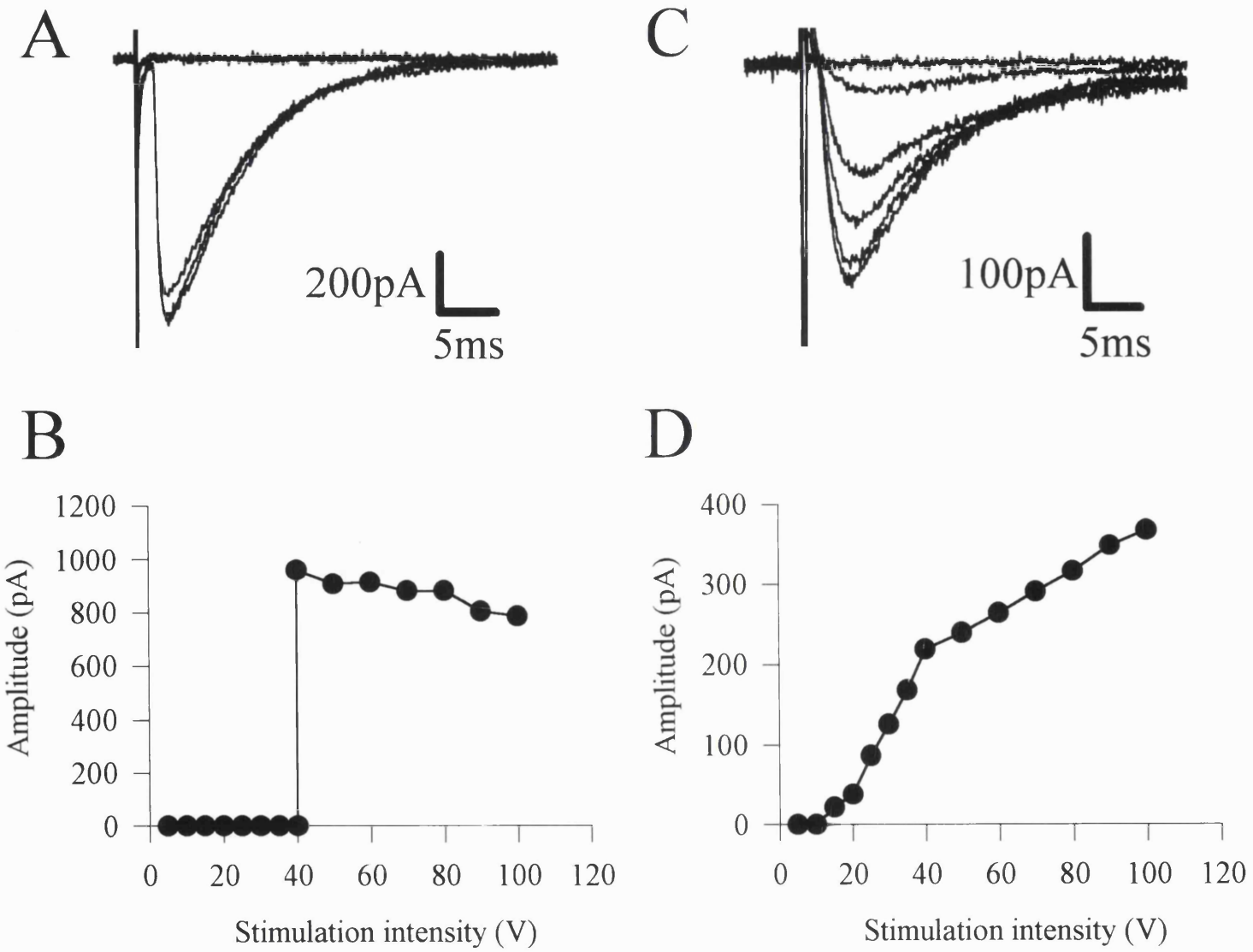
A
200pA
5ms
C
100pA
5ms
B
Amplitude (pA)
1200
1000
800
600
400
200
0
0
20
40
60
80
100
120
Stimulation intensity (V)
D
Amplitude (pA)
400
300
200
100
0
0
20
40
60
80
100
120
Stimulation intensity (V)

Fig. 3.2 The response of the two inputs to paired stimuli. **A.** Paired-pulse depression of a climbing fibre EPSC. **B.** Ratio of the climbing fibre EPSC amplitude produced by the 2nd stimulus to that produced by the 1st stimulus as a function of the interval between the stimuli. Curve best-fit through the points has the form

$$I_0 + (100 - I_0)(1 - e^{-t/\tau}),$$

where I_0 is the initial amplitude (55%) and τ is the time constant for the interval needed for the recovery of the 2nd EPSC amplitude (650ms).

C. The parallel fibre EPSC showed facilitation when two stimuli were given at a close interval. **D.** Ratio of the parallel fibre EPSC amplitude produced by the 2nd stimulus to that produced by the 1st stimulus as a function of the interval between the stimuli. Curve best-fit through the points has the form

$$100 + (I_0 - 100)e^{-t/\tau},$$

where I_0 is the initial amplitude (253%) and τ is the time constant for the interval needed for the recovery of the 2nd EPSC amplitude (103ms). The holding potential was -36mV.

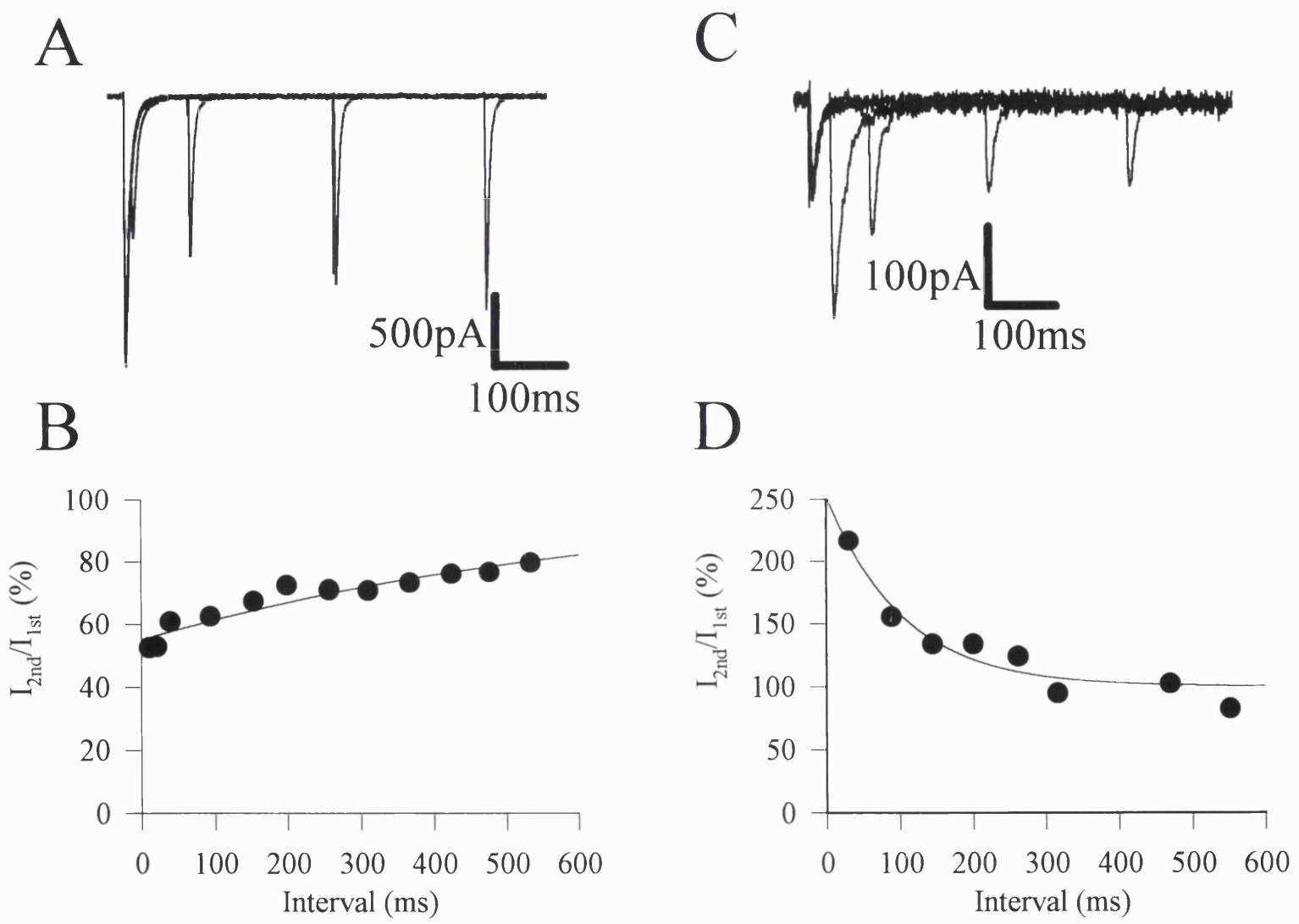
A
500pA
100ms
C
100pA
100ms
B
I_{2nd}/I_{1st} (%)
100
80
60
40
20
0
0 100 200 300 400 500 600
Interval (ms)
D
I_{2nd}/I_{1st} (%)
250
200
150
100
50
0
0 100 200 300 400 500 600
Interval (ms)

3.4 Effects of adenosine, GABA and baclofen on the amplitude of EPSCs

Superfused adenosine reduced the EPSC amplitude at both synapses (Figs. 3.3, 3.4). Fig. 3.3 shows that adenosine suppressed the climbing fibre EPSC amplitude in a dose-dependent manner. Mean dose-response data for the suppressive effect of adenosine on the climbing fibre EPSC are shown in Fig. 3.3C. Similarly, adenosine suppressed the parallel fibre EPSC in a dose-dependent manner (Figs. 3.4A and B), and mean dose-response data for this effect are shown in Fig. 3.4C. The fractional suppression produced by high doses of adenosine was much larger for the parallel fibre synapses (78%) than for the climbing fibre synapses (31%), as shown in Figs. 3.3 and 3.4.

The reduction of EPSC amplitude by adenosine is presumably due to a reduction of presynaptic glutamate release, as in the hippocampus (Lupica *et al.*, 1992; Prince and Stevens, 1992). Postsynaptic effects of adenosine on potassium currents should be minimized by the use of caesium instead of potassium in the whole-cell pipette solution.

Dose-response curves for the suppressive effect of adenosine on the EPSCs (Figs. 3.3C, 3.4C) could be fit empirically by Michaelis-Menten functions, and showed that the larger effect of adenosine on the parallel fibre synapses was not due to a large difference in apparent affinity for adenosine at the two synapses. The dose producing a half-maximal suppression was 3.4μM at the climbing, and 1.1μM at the parallel fibre synapse.

Evidence confirming that adenosine was reducing the EPSCs by acting on A_1 receptors came from experiments showing that the A_1 receptor antagonist 8-cyclopentyl-theophylline (CPT, 20μM) blocked the action of adenosine (Fig. 3.5). Applying CPT on its own potentiated the parallel fibre response by 24±5 (S.E.M.) % in 6 cells, but had little effect on the climbing fibre response (Fig. 3.5, data typical of 3 cells). This suggests that there is some tonic adenosine release in cerebellar slices which tonically suppresses the parallel fibre EPSC. The lack of effect on the climbing fibre EPSC is consistent with the lower sensitivity of this EPSC to adenosine. However, the potentiation of the parallel fibre EPSC in Fig. 3.5 is much less than the 200% potentiation seen for the hippocampal Schaffer collateral EPSC (Garaschuk *et al.*, 1992).

Fig. 3.3 Suppressive effect of adenosine (Ado) on the EPSC produced in Purkinje cells by stimulation of the climbing fibre input. **A.** Specimen EPSCs recorded in control solution (largest amplitude current) and with increasing doses of superfused adenosine (smaller currents), 3, 30, and 300μM. The holding potential was -40mV. **B.** EPSC amplitude for the cell shown in **A** as a function of time during application of different adenosine doses. **C.** Mean dose-response data (±S.E.M.) obtained as in **B** at potentials between -30 and -65mV. Number of cells shown by each point. Curve best-fit through the points has the form

$$I \propto 1 - \frac{F_{max}[\mathrm{Ado}]}{[\mathrm{Ado}] + K_m},$$

where F_{max} is the maximum fractional suppression (0.31), and K_m (3.4μM) is the dose producing a half-maximal suppression.

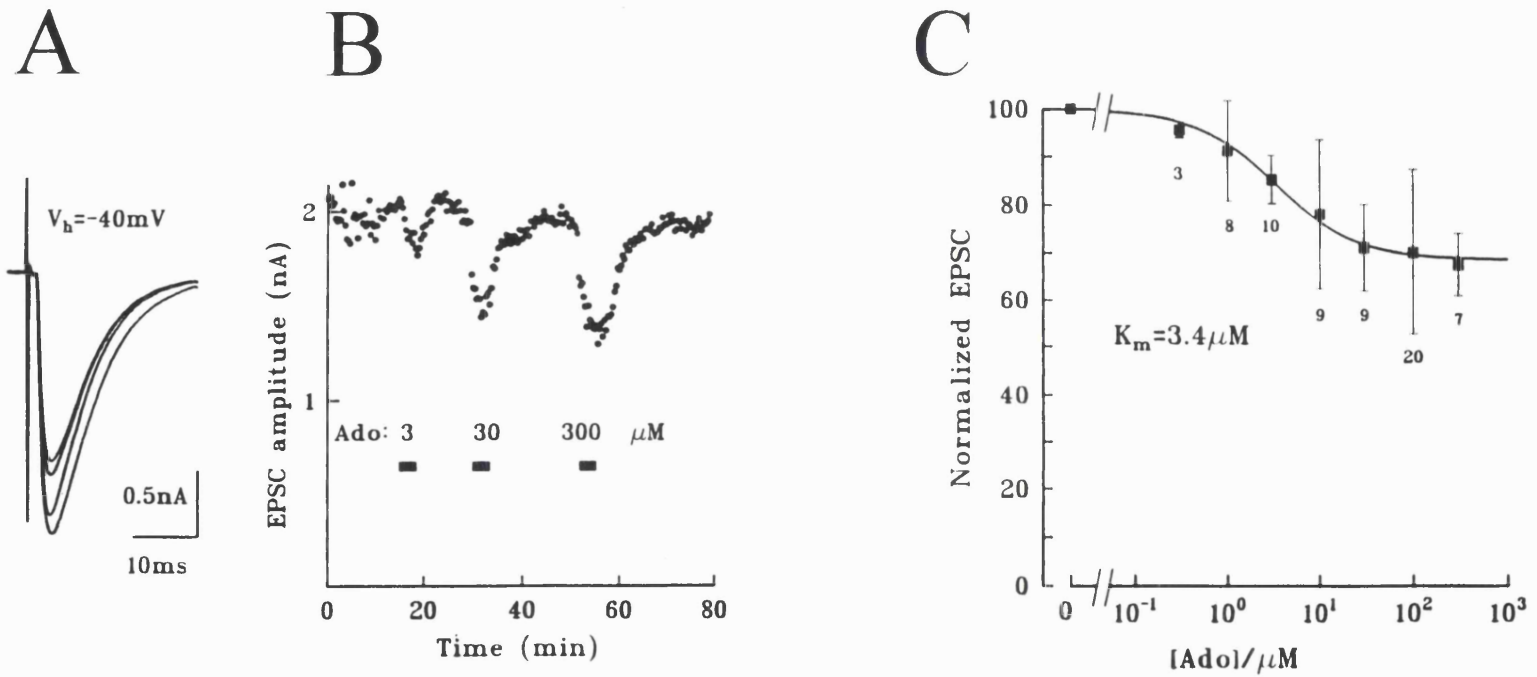
A
B
C
V_h=-40mV
0.5nA
10ms
EPSC amplitude (nA)
2
1
Ado: 3 30 300 μM
0 20 40 60 80
Time (min)
Normalized EPSC
100
80
60
40
20
0
3
8
10
9
9
20
7
K_m=3.4μM
0 10^{-1} 10^0 10^1 10^2 10^3
[Ado]/μM

Fig. 3.4 Suppressive effect of adenosine (Ado) on the EPSC produced in Purkinje cells by stimulation of the parallel fibre input. **A.** Specimen EPSCs recorded in control solution (largest amplitude current) and with increasing doses of superfused adenosine (smaller currents), 1, 10, and 100μM. The holding potential was -55mV. **B.** EPSC amplitude for the cell shown in **A** as a function of time during application of different adenosine doses. **C.** Mean dose-response data (±S.E.M.) obtained as in **B** at potentials between -30 and -65mV. Number of cells shown by each point. Curve best-fit through the points has the form

$$100 - \frac{F_{max}[\text{Ado}]}{[\text{Ado}] + K_m},$$

where F_{max} is the maximum fractional suppression (0.78) and K_m (1.1μM) is the dose producing a half-maximal suppression.

A
V_h=-55mV
200pA
10ms
B
EPSC amplitude (pA)
0
200
400
600
Ado: 1 10 100 μM
0
20
40
60
Time (min)
C
Normalized EPSC
0
20
40
60
80
100
K_m=1.1μM
0
10^{-1}
10^0
10^1
10^2
10^3
[Ado]/μM

Fig. 3.5 Effect of the A_1 receptor blocker 8-cyclopentyl-theophylline (CPT) on the parallel and climbing fibre EPSCs. **A.** Peak amplitude of the parallel fibre EPSC as a function of time during application of CPT. The holding potential was -66mV. Adenosine suppresses the EPSC less in the presence of CPT than in its absence. Line through the points was drawn by eye. **B.** Peak amplitude of the climbing fibre EPSC as a function of time during application of CPT. The holding potential was -51mV.

A

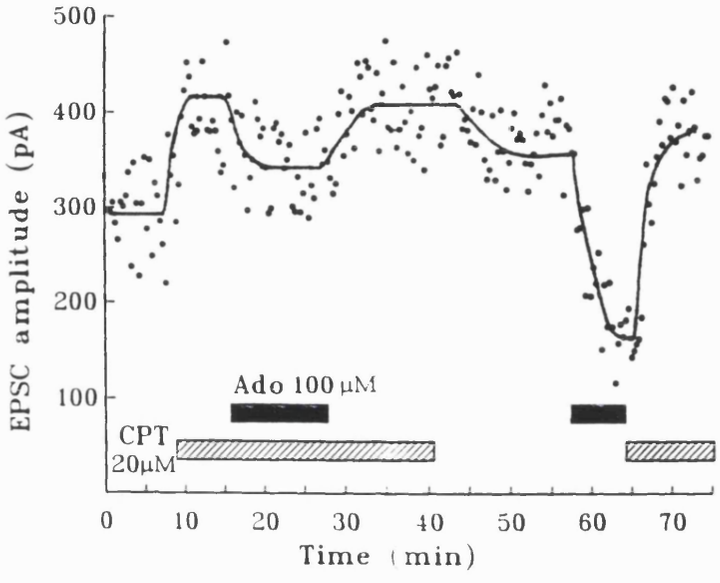
500
400
300
200
100
EPSC amplitude (pA)
Ado 100 μM
CPT
20μM
0
10
20
30
40
50
60
70
Time (min)

B

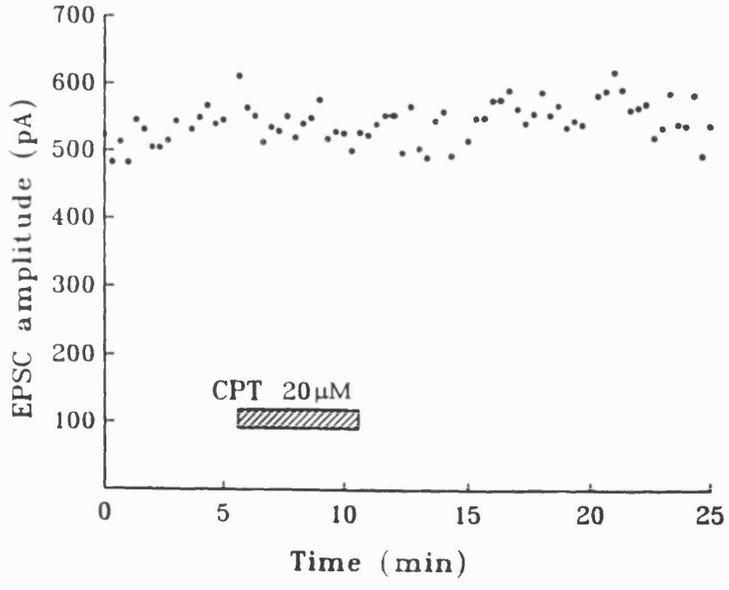
700
600
500
400
300
200
100
EPSC amplitude (pA)
CPT 20μM
0
5
10
15
20
25
Time (min)

In the presence of picrotoxin (to block $GABA_A$ receptors), GABA (100μM) also reduced the climbing and parallel fibre EPSC amplitude (Figs. 3.6 and 3.7). To confirm that GABA is acting on $GABA_B$ receptors, baclofen, a $GABA_B$ receptor agonist, was applied. Baclofen also reduced the climbing and parallel fibre EPSCs (Figs. 3.8 and 3.9). Fig. 3.8 shows that the suppressive effect of baclofen on the climbing fibre EPSC is dose-dependent. Likewise baclofen suppressed the parallel fibre EPSC in a dose-dependent manner (Fig. 3.9). As for adenosine, the parallel fibre response was suppressed more (93%) than the climbing fibre response (44%) at high baclofen doses. Dose-response curves for the suppressive effect of baclofen on the EPSCs (Figs. 3.8C, 3.9C) could be fit empirically by Michaelis-Menten functions. The dose producing a half-maximal suppression was 4.1μM at the climbing, and 0.47μM at the parallel fibre synapse. Thus there was some difference in the affinity of the receptors at the two synapses (Figs. 3.8C and 3.9C).

The GABA or baclofen-evoked reduction of the EPSC is presumably due, as at other synapses (Scanziani *et al.*, 1992; Isaacson *et al.*, 1993; Pfrieger *et al.*, 1994), to a reduction of glutamate release from the presynaptic terminal. Effects due to gating of postsynaptic potassium channels by $GABA_B$ receptors should be minimised in these experiments by the use of caesium in the whole-cell pipette solution.

The $GABA_B$ antagonist 2-hydroxy-saclofen blocked the action of baclofen (Fig. 3.10), but did not produce a tonic potentiation of the EPSC at the 4 parallel fibre and 8 climbing fibre synapses tested, indicating little tonic release of GABA into the cerebellar slice.

The effects of adenosine and baclofen do not result from changes in the number of presynaptic afferents stimulated. In the case of the climbing fibre synapses, stimulus-response curves (Fig. 3.1A) showed that there was only one climbing fibre sending input to each cell recorded from (or sometimes two climbing fibres, as found previously in young rats: Konnerth *et al.*, 1990; Llano *et al.*, 1991), and a failure of excitation would have been immediately apparent. For the parallel fibres, extracellular recording of the presynaptic compound action potential in 12 coronal cerebellar slices showed that

Fig. 3.6 Suppressive effect of GABA on the EPSC produced in a Purkinje cell by stimulation of the climbing fibre input. **A.** Specimen EPSCs recorded in control solution and in the presence of 100μM GABA. The holding potential was -35mV. **B.** EPSC amplitude for the cell shown in **A** as a function of time during application of GABA. In this cell, the suppression by GABA was larger than the average value of suppression by baclofen.

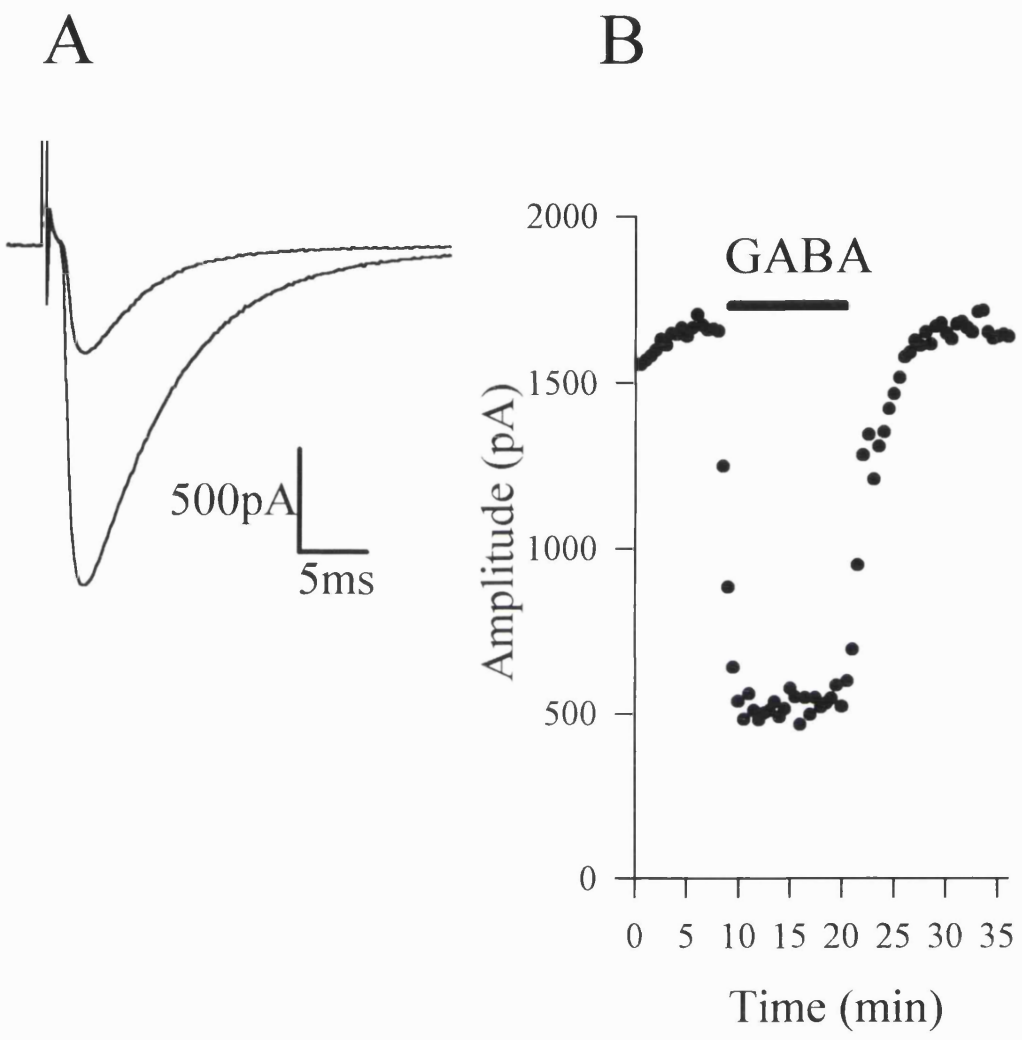
A
B
500pA
5ms
GABA
2000
1500
1000
500
0
Amplitude (pA)
0 5 10 15 20 25 30 35
Time (min)

Fig. 3.7 Suppressive effect of GABA on the EPSC produced in a Purkinje cell by stimulation of the parallel fibre input. **A.** Specimen EPSCs recorded in control solution and in the presence of 100μM GABA. The holding potential was -35mV. **B.** EPSC amplitude for the cell shown in **A** as a function of time during application of GABA.

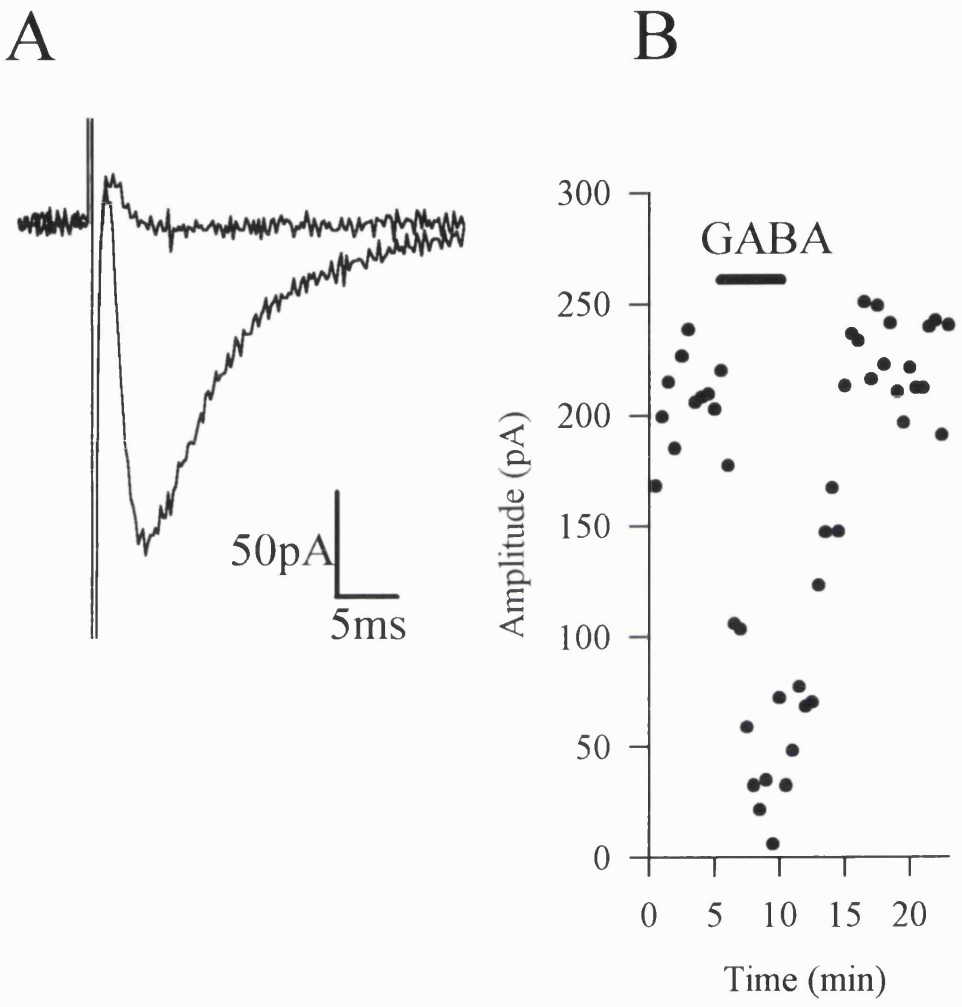
A
B
50pA
5ms
GABA
300
250
200
150
100
50
0
Amplitude (pA)
0
5
10
15
20
Time (min)

Fig. 3.8 Suppressive effect of the $GABA_B$ agonist baclofen (Bac) on the EPSC evoked in Purkinje cells by stimulation of the climbing fibre input. **A.** Specimen EPSCs recorded in control solution (largest amplitude current) and with increasing doses of superfused baclofen (smaller currents), 1, 3, and 30μM. The holding potential was -36mV. **B.** EPSC amplitude for the cell shown in **A** as a function of time during application of different baclofen doses. **C.** Mean dose-response data (±S.E.M.) obtained as in **B** at potentials between -25 and -45mV. Number of cells shown by each point. Curve best-fit through the points has the form

$$100\chi - \frac{F_{max}[\text{Bac}]}{[\text{Bac}] + K_m},$$

where F_{max} is the maximum fractional suppression (0.44), and K_m (4.1μM) is the dose producing a half-maximal suppression.

A
0.5nA
5ms
B
Amplitude (nA)
2.5
2.0
1.5
1.0
0.5
0.0
1
3
30 (μM)
0
20
40
60
80
Time (min)
C
Normalized EPSC
100
80
60
40
20
0
6
9
10
13
3
K_m=4.1μM
0
10^{-1}
10^{0}
10^{1}
10^{2}
10^{3}
[Bac] (μM)

Fig. 3.9 Suppressive effect of the $GABA_B$ agonist baclofen (Bac) on the EPSC evoked in Purkinje cells by stimulation of the parallel fibre input. **A.** Specimen EPSCs recorded in control solution (largest amplitude current) and with increasing doses of superfused baclofen (smaller currents), 0.3, 1, and 3μM. The holding potential was -32mV. **B.** EPSC amplitude for the cell shown in **A** as a function of time during application of different baclofen doses. **C.** Mean dose-response data (±S.E.M.) obtained as in **B** at potentials between -25 and -45mV. Number of cells shown by each point. Curve best-fit through the points has the form

$$\propto \frac{F_{max}[Bac]}{[Bac]+K_m},$$

where F_{max} is the maximum fractional suppression (0.93), and K_m(0.47μM) is the dose producing a half-maximal suppression. .

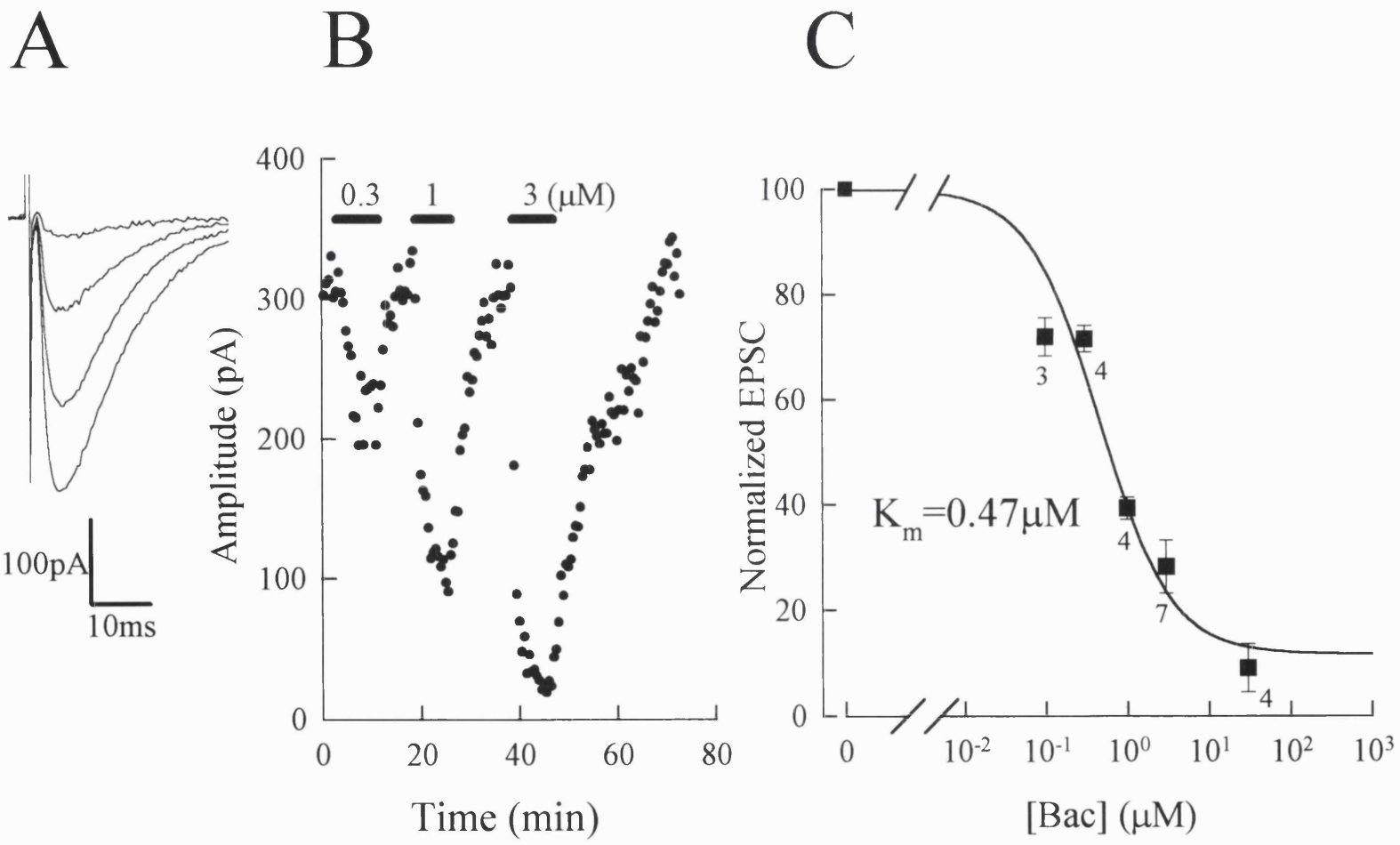
A
B
C
100pA
10ms
Amplitude (pA)
0.3
1
3 (μM)
Time (min)
Normalized EPSC
K_m=0.47μM
[Bac] (μM)

Fig. 3.10 Effect of the $GABA_B$ receptor blocker 2-hydroxy-saclofen (Sac) on the EPSC suppression produced by baclofen. **A.** Peak amplitude of the parallel fibre EPSC as a function of time during application of baclofen in the presence and absence of saclofen. **B.** Peak amplitude of the climbing fibre EPSC as a function of time during application of baclofen in the presence and absence of saclofen. Baclofen suppresses the EPSC less in the presence of saclofen than in its absence. The holding potential was -36mV.

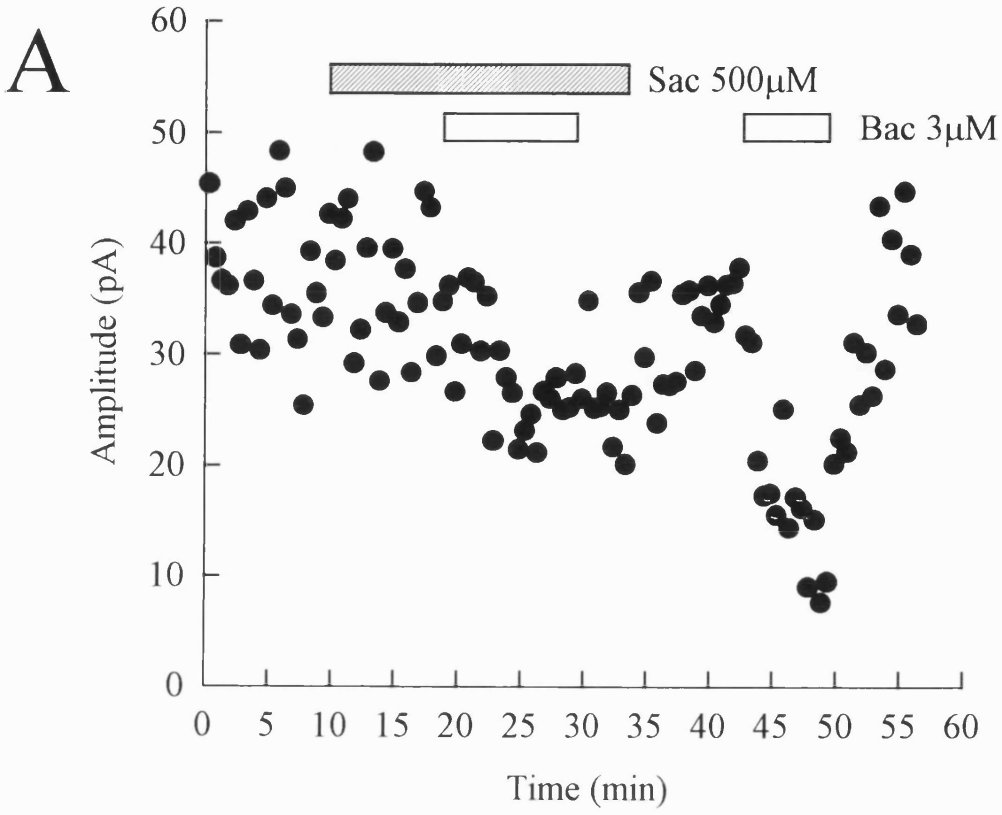
A
Sac 500μM
Bac 3μM
Amplitude (pA)
60
50
40
30
20
10
0
0 5 10 15 20 25 30 35 40 45 50 55 60
Time (min)

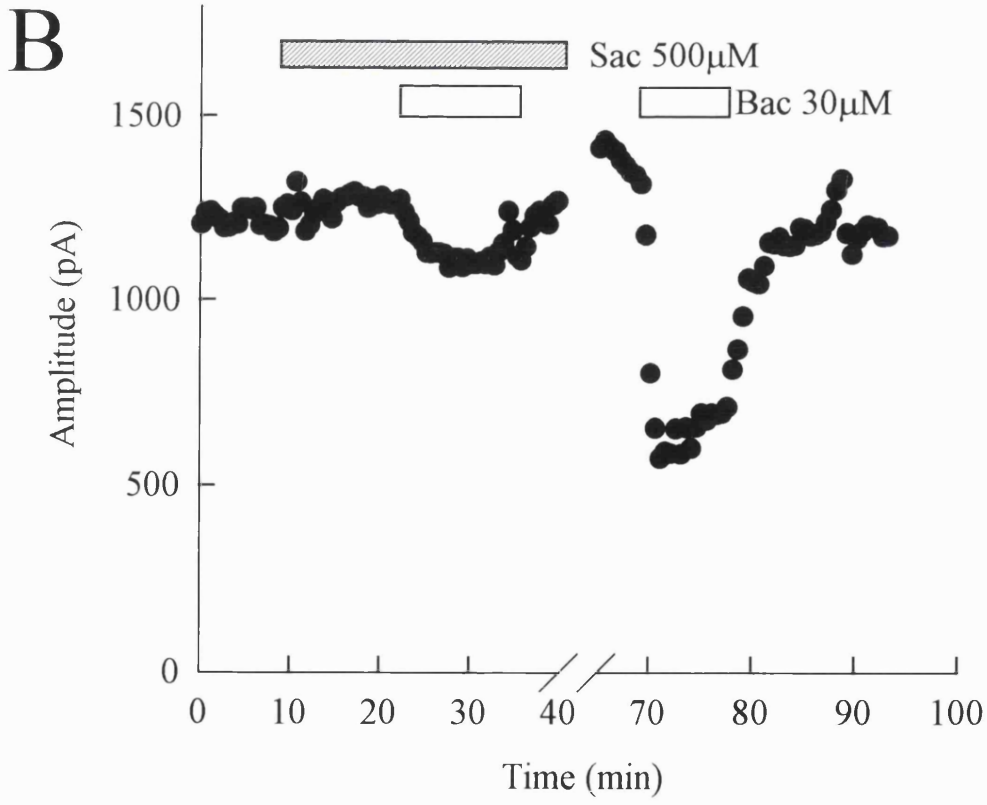
B
Sac 500μM
Bac 30μM
Amplitude (pA)
1500
1000
500
0
0 10 20 30 40 70 80 90 100
Time (min)

100μM adenosine and 100μM baclofen reduced the presynaptic volley by only 6% and 9%, respectively (Fig. 3.11), much less than the 80-90% reduction they produced in the EPSC amplitude.

3.5 Adenosine and baclofen do not affect non-NMDA receptors in Purkinje cells

To eliminate the possibility that the decrease in EPSC amplitude produced by adenosine or baclofen application is due to an effect on postsynaptic non-NMDA receptors, the effects of adenosine and baclofen were tested on the current produced in Purkinje cells by applying glutamate iontophoretically. Adenosine (100μM) had little effect on the current generated in Purkinje cells in response to iontophoresed glutamate. The current was reduced by <3% in 3 cells (Fig. 3.12A), studied in zero-calcium solution to eliminate trans-synaptic effects of glutamate. Similarly, 100μM baclofen had little effect on the current generated in Purkinje cells by iontophoresed glutamate (Fig. 3.12: reduced by <6% in 3 cells). These results confirm that the effects of adenosine and baclofen were presynaptic. In contrast to the lack of effect of adenosine and baclofen, CNQX greatly reduced the glutamate-evoked current, as expected (Fig. 3.12C).

3.6 Effects of adenosine and baclofen on the decay time course of the EPSCs

As well as reducing the EPSC amplitude, at both the climbing and the parallel fibre synapses adenosine, GABA and baclofen speeded the decay of the EPSC (Figs. 3.13, 3.14 and 3.15). Fig. 3.13 shows the effects of 300μM adenosine on the climbing fibre EPSC, and of 100μM adenosine on the parallel fibre EPSC decay time course. The effects of 30μM baclofen on the climbing fibre EPSC, and of 3μM baclofen on the parallel fibre EPSC decay are shown in Fig. 3.14. GABA also speeded the decay time of the climbing fibre EPSC as shown in Fig. 3.15. However, 100μM GABA almost completely suppressed parallel fibre EPSCs so that the decay time course could not be measured, and smaller doses were not tested.

For cells where the voltage error due to the pipette series resistance at the peak of the synaptic current was less than 10mV (see section 3.7.2, and Fig. 3.18), fitting the EPSC decay at the climbing fibre synapse by a single exponential showed that the normal decay

Fig. 3.11 Effect of adenosine and baclofen on the parallel fibre action potential. The parallel fibre action potential was recorded extracellularly, with the stimulus to the parallel fibres adjusted to give a half-maximal response. Graph shows the amplitude of the extracellular action potential during application (indicated by bars) of adenosine and baclofen. Data taken from 13 slices. Error bars are S.E.M.

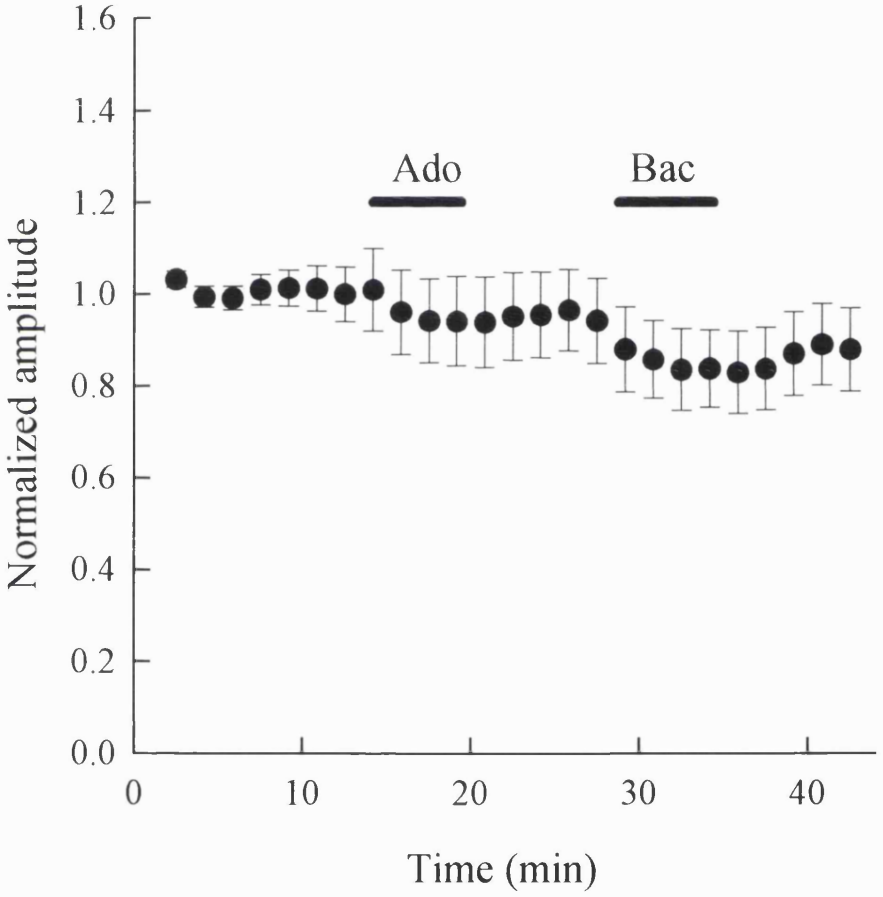
1.6
1.4
1.2
1.0
0.8
0.6
0.4
0.2
0.0
Normalized amplitude
Ado
Bac
0
10
20
30
40
Time (min)

Fig. 3.12 Effect of adenosine, baclofen and CNQX on non-NMDA receptor currents evoked by iontophoresing glutamate onto a Purkinje cell. **A.** Superfusion of 100μM adenosine (bar) did not change the amplitude of the non-NMDA current (ordinate). Data typical of 3 cells. **B.** Superfusion of 100μM baclofen (bar) had little effect on the amplitude of the non-NMDA current (ordinate). Data typical of 3 cells. **C.** Superfusion of 5μM CNQX (bar) suppressed the non-NMDA current (ordinate). Data typical of 3 cells. The holding potential was -82mV. Experiments were done in calcium-free external solution (2.5mM $CaCl_2$ replaced by 2.5mM Na_2EGTA) to eliminate effects of glutamate, on cells other than the Purkinje cell, being transmitted synaptically to the Purkinje cell.

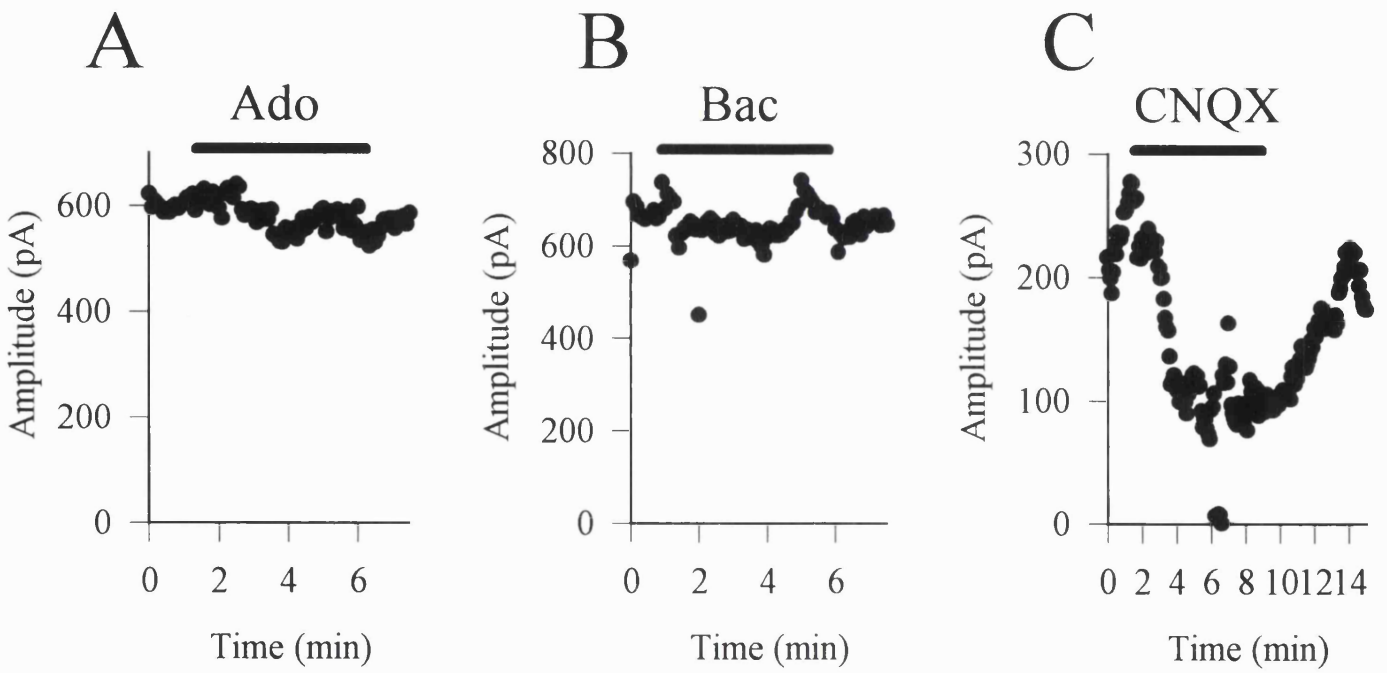
A
Ado
Amplitude (pA)
600
400
200
0
0 2 4 6
Time (min)
B
Bac
Amplitude (pA)
800
600
400
200
0
0 2 4 6
Time (min)
C
CNQX
Amplitude (pA)
300
200
100
0
0 2 4 6 8 10 12 14
Time (min)

Fig. 3.13 Effect of adenosine on the decay of EPSCs. **A.** Climbing fibre EPSCs recorded in control solution, in 300μM adenosine, and again in control solution (wash). **B.** The climbing fibre EPSCs in **A** normalised to the same peak current. The holding potential was -46mV. **C.** Parallel fibre EPSCs recorded in control solution, in 100μM adenosine and again in control solution (wash). **D.** The parallel fibre EPSCs in **C** normalised to the same peak current. The holding potential was -61mV.

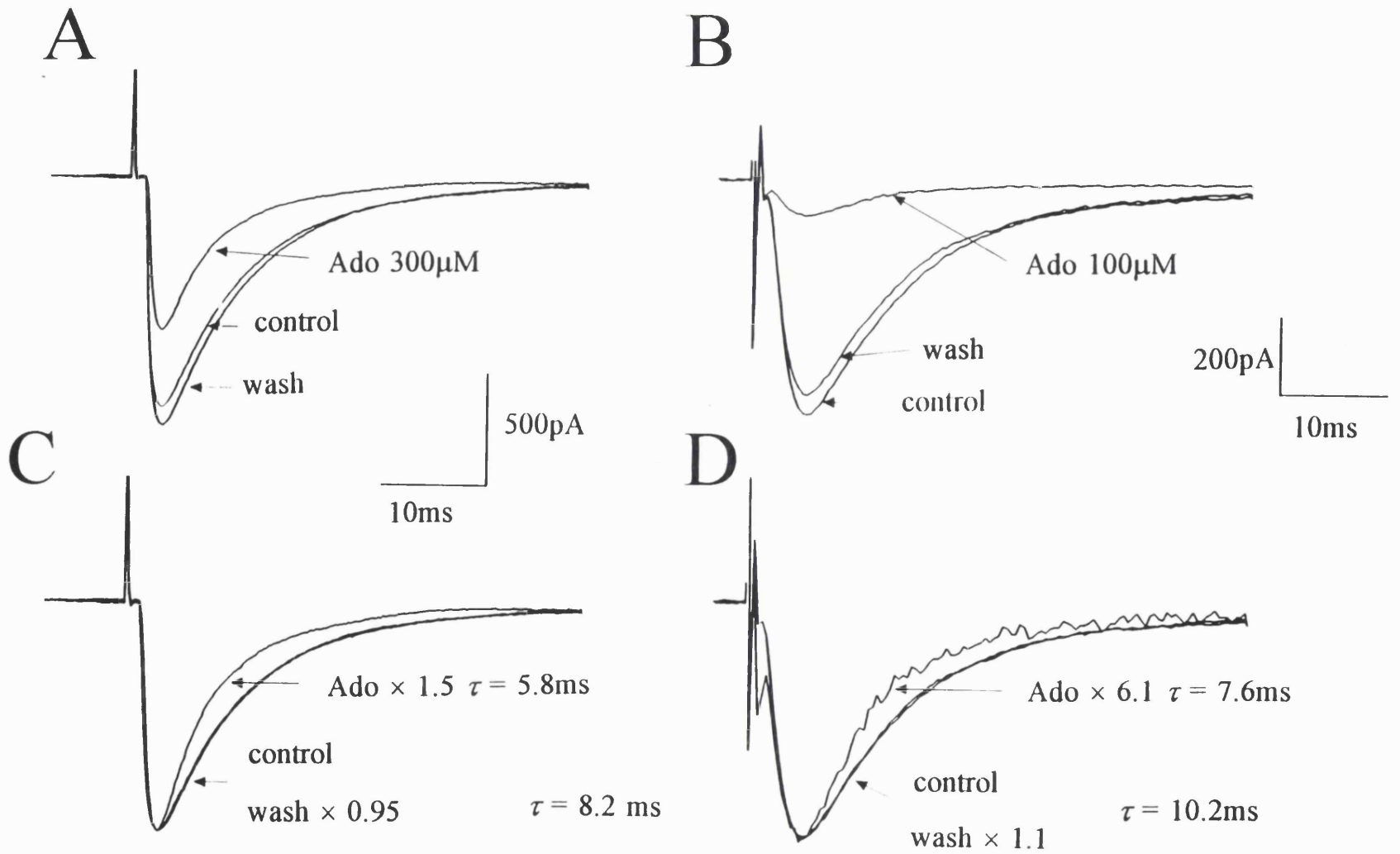
A
Ado 300μM
control
wash
500pA
10ms
B
Ado 100μM
wash
control
200pA
10ms
C
Ado × 1.5 τ = 5.8ms
control
wash × 0.95
τ = 8.2 ms
D
Ado × 6.1 τ = 7.6ms
control
wash × 1.1
τ = 10.2ms

Fig. 3.14 Effect of baclofen on the decay of EPSCs. **A.** Climbing fibre EPSCs recorded in control solution, in 30μM baclofen, and again in control solution (wash). **B.** The climbing fibre EPSCs in **A** normalised to the same peak current. The holding potential was -27mV. **C.** Parallel fibre EPSCs recorded in control solution, in 3μM adenosine and again in control solution (wash). **D.** The parallel fibre EPSCs in **C** normalised to the same peak current. The holding potential was -36mV.

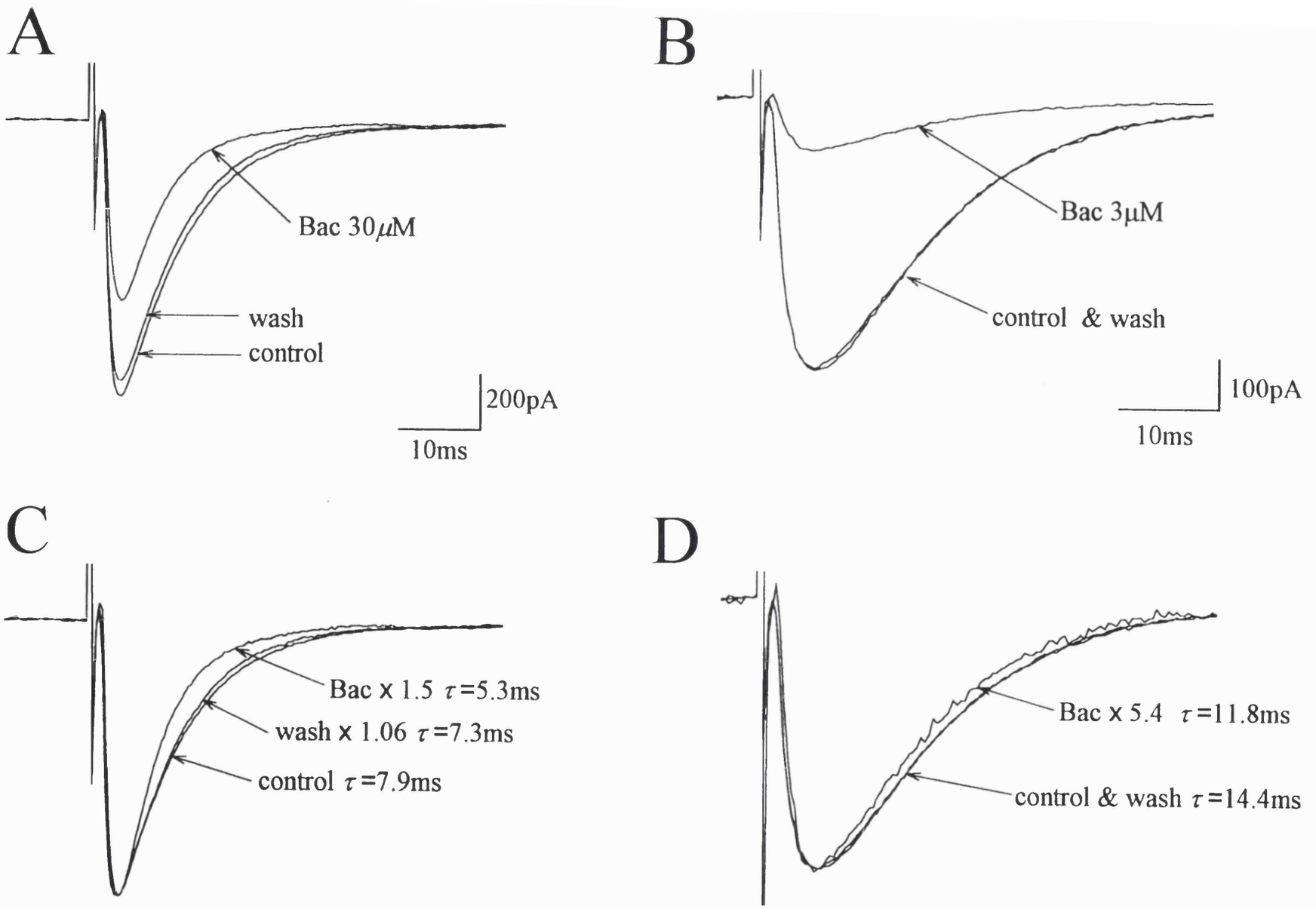
A
Bac 30μM
wash
control
200pA
10ms
B
Bac 3μM
control & wash
100pA
10ms
C
Bac x 1.5 τ=5.3ms
wash x 1.06 τ=7.3ms
control τ=7.9ms
D
Bac x 5.4 τ=11.8ms
control & wash τ=14.4ms

Fig. 3.15 Effect of GABA on the decay of the climbing fibre EPSC. **A.** Climbing fibre EPSCs recorded in control solution, in 100μM GABA, and again in control solution (wash). **B.** The climbing fibre EPSCs in **A** normalised to the same peak current. The holding potential was -35mV.

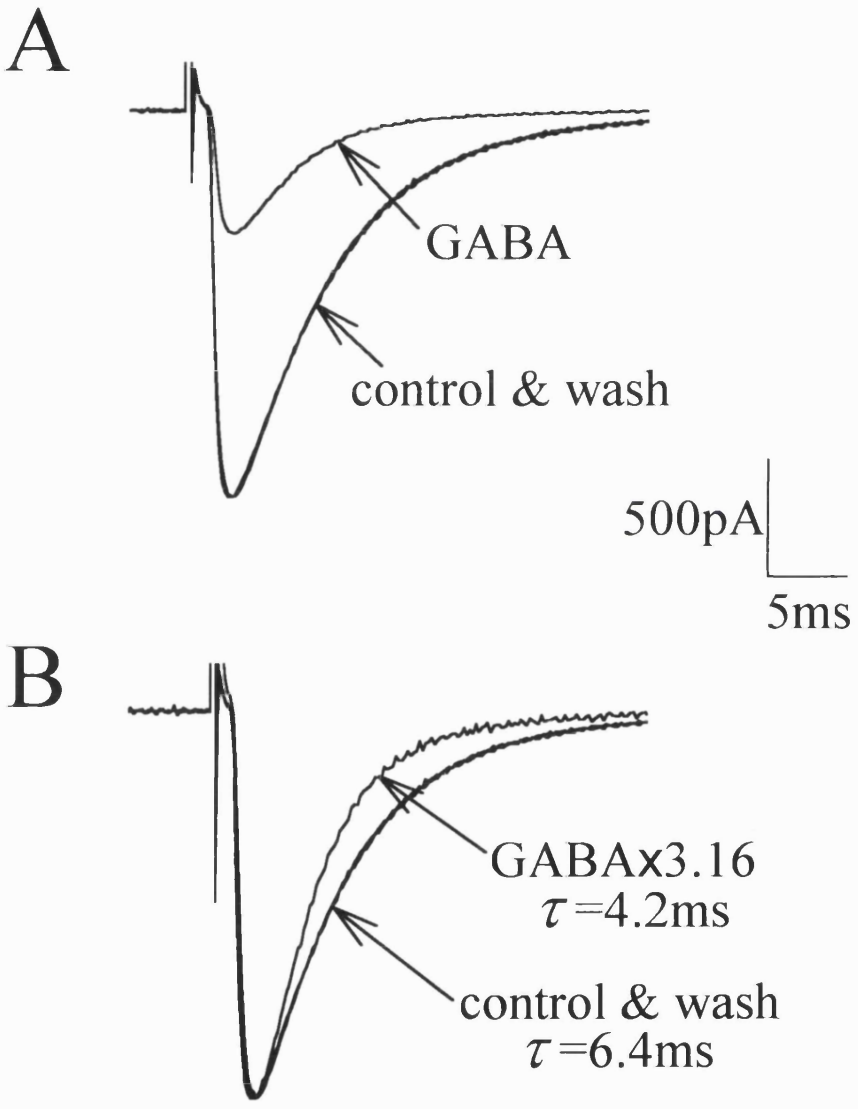
A
GABA
control & wash
500pA
5ms
B
GABAx3.16
τ=4.2ms
control & wash
τ=6.4ms

time constant (mean±S.E.M., 7.0±0.4msec in 29 cells) was reduced by 17±2% (15 cells) by 10-300μM adenosine and by 18±4% (4 cells) by 3-30μM baclofen. At the parallel fibre synapse the normal decay time constant (mean value 10.7±0.8msec in 27 cells) was reduced by 14±2% (13 cells) by 10-100μM adenosine and by 14±2% (6 cells) by 0.3-3μM baclofen.

3.7 Speeding of the EPSC decay does not result from a voltage-clamp artefact

A change of EPSC kinetics on reducing the amount of glutamate released could result from two kinds of artefact. First, if the EPSC significantly depolarised a poorly voltage-clamped cell (more of a problem for the climbing fibre EPSCs which have larger amplitude), then voltage-gated currents might be activated and contribute to the EPSC waveform, and their contribution might be smaller when the EPSC amplitude was reduced, leading to an apparent change of EPSC waveform. Secondly, mathematical analysis (see Chapter 2, and also Llano *et al.*, 1991) indicates that the voltage drop across the series resistance of the whole-cell pipette is expected to result in a speeding of the EPSC decay kinetics when the EPSC is reduced in amplitude. To rule out these possibilities the three sets of experiments described below were carried out.

3.7.1 The speeding of the decay also occurs at positive potentials

First, the speeding of the EPSC decay by adenosine and baclofen was seen both at negative potentials and at positive potentials where activation of voltage-gated currents would be different to that occurring at negative potentials (Fig. 3.16, data typical of 3 cells). These experiments were done on the climbing fibre EPSC because it is larger and therefore more likely to be affected by this kind of artefact.

3.7.2 Postsynaptically-reduced EPSCs do not show speeding of the decay

Second, reducing the climbing fibre response by around 70% postsynaptically (instead of by reducing glutamate release presynaptically), by blocking non-NMDA receptors with 1μM CNQX (Honore *et al.*, 1988), did not affect the decay of the EPSC at the climbing fibre synapse (Fig. 3.17). The time constant in 6 cells was reduced by 0.5±5.2 (S.E.M.)

Fig. 3.16 Baclofen speeded the climbing fibre EPSC decay at positive potentials as well as at negative potentials. **A.** Climbing fibre EPSCs recorded in control solution, in 30μM baclofen, and again in control solution (wash). **B.** The EPSCs in **A** normalised to the same peak current. The holding potential was +24mV.

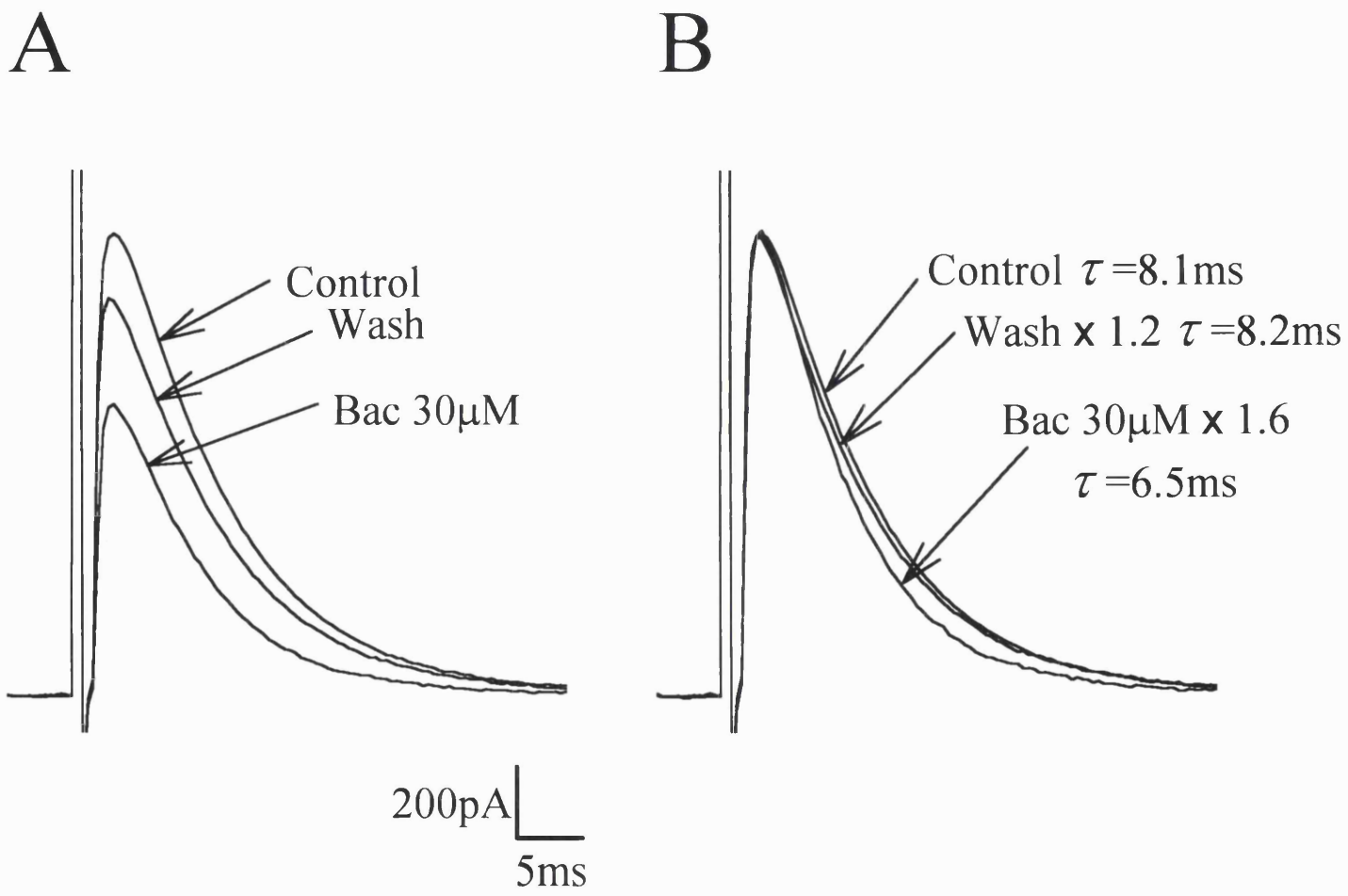
A
B
Control
Wash
Bac 30µM
200pA
5ms
Control τ =8.1ms
Wash x 1.2 τ =8.2ms
Bac 30µM x 1.6
τ =6.5ms

Fig. 3.17 Postsynaptic reduction of the EPSC does not speed the EPSC decay. **A.** Climbing fibre EPSCs recorded in control solution, in a dose of CNQX (1μM) chosen to produce a reduction of EPSC amplitude similar to that produced by baclofen or adenosine, and again in control solution (wash). **B.** The EPSC in CNQX scaled up to the amplitude of the control EPSC, to show the lack of any change of decay time constant. The holding potential was -37mV.

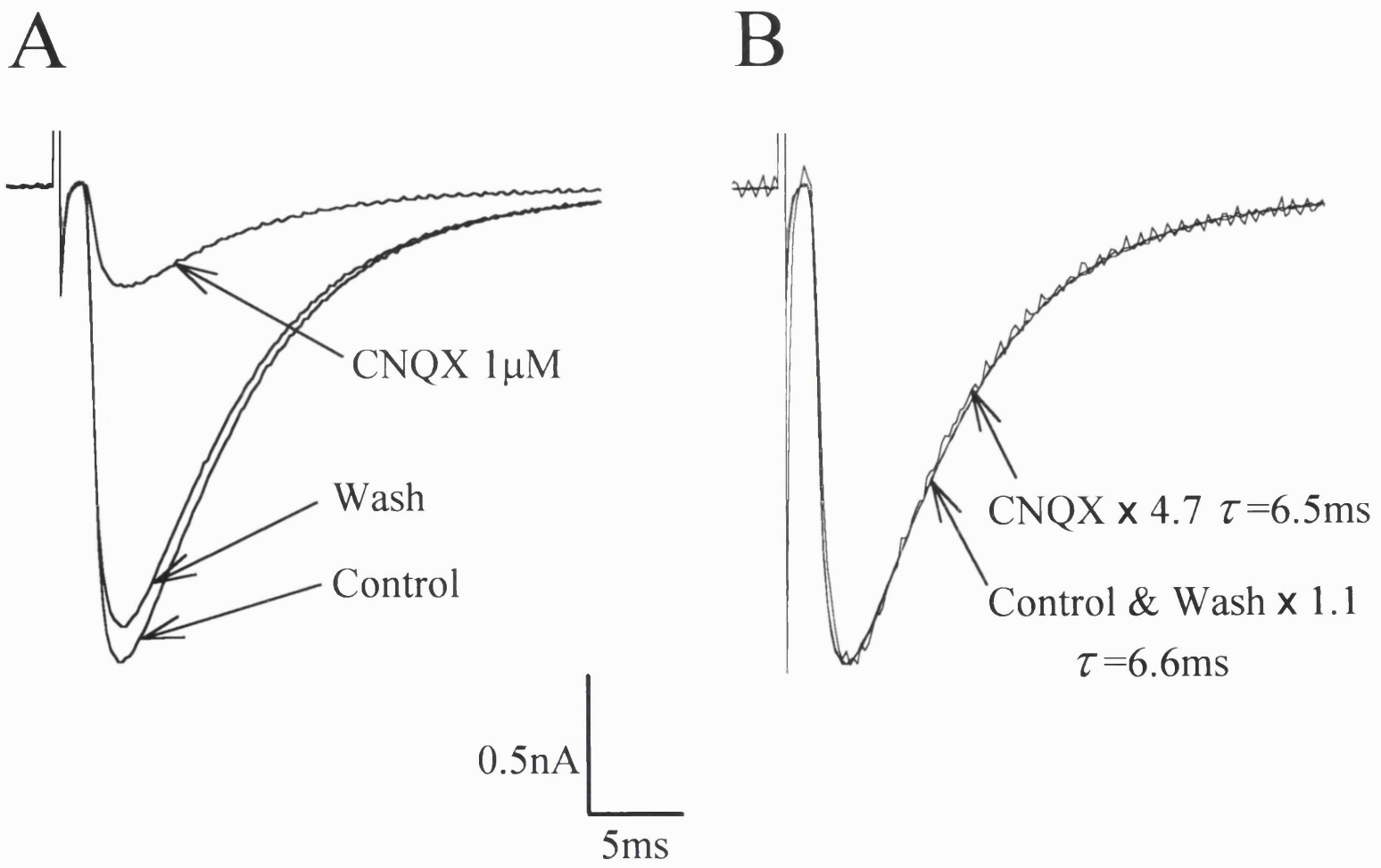
A
B
CNQX 1μM
Wash
Control
0.5nA
5ms
CNQX x 4.7 τ=6.5ms
Control & Wash x 1.1
τ=6.6ms

%, and the series resistance remaining uncompensated in these cells (10.3±2.5MΩ) was slightly larger than that for the cells to which adenosine and baclofen were applied (5.9±1.2 and 9.2±8MΩ respectively). A similar experiment showing CNQX having no effect on the kinetics of the EPSC at the parallel fibre synapse has been carried out by Barbour *et al.* (1994).

3.7.3 Speeding of the decay is not due to a series resistance error

Third, for cells in which the series resistance voltage error was not excessive (peak EPSC × uncompensated series resistance <10mV), the speeding of the EPSC decay produced by 10-300μM adenosine at the climbing fibre synapse was found to be uncorrelated with the series resistance voltage error (Fig. 3.18), and to be on average four-fold greater than the speeding predicted to occur as a result of the series resistance (from eqn.38, Chapter 2). A similar result was found for the effects of baclofen on the climbing fibre EPSC (on average the decay speeding was 2.4-fold greather than that predicted as a result of series resistance aretefact), and for the effects of adenosine on the parallel fibre EPSCs (Fig. 3.19), although for these the more distant synaptic location makes the applicability of eqn. 38 in Chapter 2 uncertain, since much of the series resistance may be along the dendrites rather than at the electrode tip.

3.8 Discussion

These experiments give insight into two aspects of the operation of the excitatory synapses from parallel and climbing fibres to Purkinje cells: the differential control of synaptic strength at different synapses by presynaptic receptors, and the effect of the amount of glutamate released on the speed of the EPSC decay.

3.8.1 Differential control of synaptic strength by presynaptic receptors

Both adenosine and GABA (baclofen) had a much stronger suppressive effect on the EPSC at the parallel fibre synapse than at the climbing fibre synapse (see also Hackett (1974) and Kocsis *et al.* (1984) who failed to detect a suppression of the climbing fibre response by applying adenosine or GABA, when they recorded the response

Fig. 3.18 Speeding of the EPSC decay at the climbing fibre synapse was not correlated with the series resistance voltage error. Fractional change of climbing fibre EPSC decay time constant, $\Delta\tau/\tau$, produced experimentally by 10-300μM adenosine (solid squares), and predicted theoretically from Equation 38 (Chapter 2) for the same cells to occur as a result of pipette series resistance R_s, plotted as a function of the product of R_s and the peak synaptic current I_{Max}, in control solution (abscissa). Straight line is a best fit to the solid squares. Curve (dotted line) through open squares is a second order spline curve showing the trend of Equation 38. On average the decay speeding predicted to occur artefactually (open squares) is only 23.5±7.1% of the decay speeding actually observed.

Climbing fibre

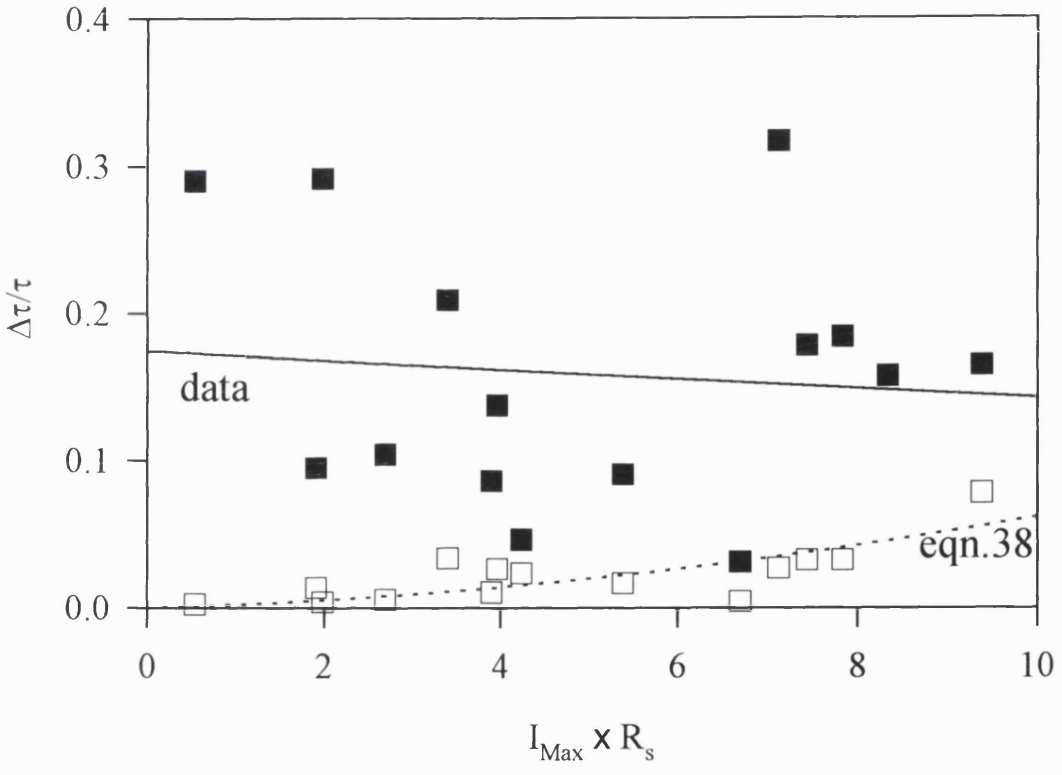

Fig. 3.19 Speeding of the EPSC decay at the parallel fibre synapse was not correlated with the series resistance voltage error. Fractional change of parallel fibre EPSC decay time constant, $\Delta\tau/\tau$, produced experimentally by 0.3-30μM adenosine (solid squares), and predicted theoretically from Equation 38 (Chapter 2) for the same cells to occur as a result of pipette series resistance $R_{s,}$, plotted as a function of the product of R_s and the peak synaptic current I_{Max}, in control solution (abscissa). Straight line (continuous) is a best fit to the solid squares. Dotted line through open squares is a best fit to show the trend of Equation 38. On average the decay speeding predicted to occur artefactually (open squares) is only 30.2±6.7% of the decay speeding actually observed.

Parallel fibre

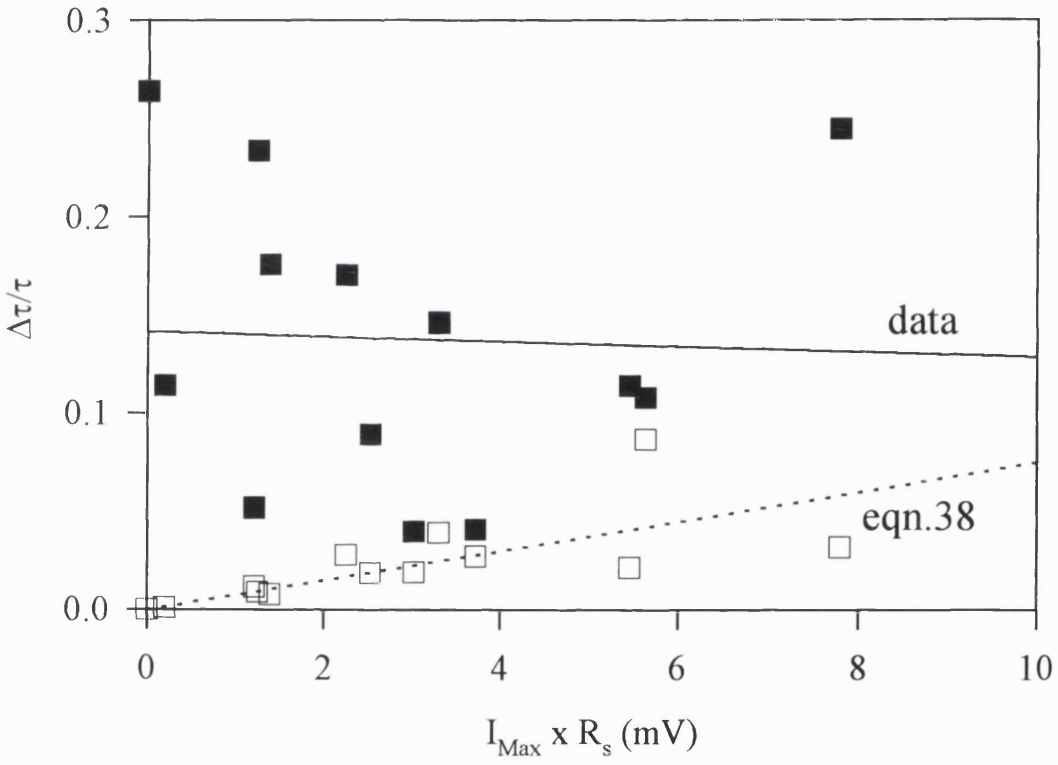

extracellularly). Functionally this may correlate with the notion (Marr, 1969) that the powerful climbing fibre input is an all-or-none signal triggering adjustment of the parallel fibre synaptic gains, so that subtle modulation of its strength by presynaptic receptors is not required. However, during ischaemia, suppression of glutamate release by release of adenosine (Hagberg *et al.*, 1987) is neuroprotective (Gribkoff and Bauman, 1992; Fowler, 1990; Rudolphi *et al.*, 1992; Goldberg *et al.*, 1988), and it is not obvious why such a protective mechanism is not employed at the climbing fibre synapse. Interestingly, of cerebellar neurones, Purkinje cells are particularly vulnerable to ischaemic damage (Brierley and Graham, 1984), triggered by activation of non-NMDA receptors (Balchen and Diemer, 1992).

3.8.2 Dependence of the EPSC duration on the amount of glutamate released

Reducing the amount of glutamate released, using adenosine or a $GABA_B$ receptor agonist, baclofen, speeded the decay of the EPSC at both the climbing fibre and the parallel fibre to Purkinje cell synapses, and the experiments described in section 3.7 show that is not an artefact resulting from poor voltage control. In principle the EPSC speeding could be a purely presynaptic effect, if the duration of the EPSC partly reflects temporal dispersion in the release of different vesicles of transmitter, and if reducing transmitter release with adenosine and GABA increases synchrony in the release of different vesicles. However, reducing the amount of glutamate released could also result in a faster EPSC decay by three non-presynaptic mechanisms, occurring after the glutamate has been released. First, when less glutamate is released, there may be a larger extracellular concentration gradient for diffusion of glutamate out of the synaptic cleft, so the glutamate concentration falls with a faster time constant, as suggested by Trussell *et al.* (1993, Fig. 7). Second, the glutamate concentration may fall with a faster time constant because glutamate uptake is less saturated. Finally, even if the glutamate concentration ([glu]) falls with the same time constant (τ_{glu}), saturation of the dose-response curve for glutamate activating AMPA receptors can result in a faster EPSC decay when the peak glutamate concentration is lower, as described by Sarantis *et al.* (1993, Methods). Sarantis *et al.* (1993) analysed a simple model which assumes that receptor deactivation is much quicker than the decay of [glu], and which ignores

receptor desensitisation. For this situation, the EPSC decay time constant, τ_I, is related to the time constant with which [glu] falls, τ_{glu}, by the equation:

$$\tau_I = \tau_{glu} \frac{1+(\frac{[glu]}{K})^n}{n}$$

where K is the EC_{50} for glutamate activating AMPA receptors, and n is the Hill coefficient for that activation. This equation predicts that τ_I is smaller when [glu] is smaller.

These explanations for how reduced release could speed the EPSC decay assume that a reduction of release decreases the [glu] seen by all the postsynaptic receptors. This is appropriate if each release site normally releases several vesicles per action potential, and adenosine or baclofen decreases the number released. However, it is possible that each site normally releases only one vesicle, and that adenosine or baclofen stops release completely at some sites (where the release probability is then 0) while leaving the release and the [glu] transient unaltered at other, spatially separate, release sites. There is no information available on the number of vesicles released at single release sites at parallel and climbing fibre synapses. However, for the climbing fibre, the relatively open extracellular space between different release sites (onto different Purkinje cell dendritic "thorns": Palay and Chan-Palay, 1974) may well result in a reduced [glu] at all postsynaptic receptors even if only a fraction of release sites stop releasing in the presence of adenosine or baclofen (i.e. there may well be crosstalk between different release sites).

One of the possible explanations suggested above, for the EPSC speeding which occurs when glutamate release is reduced, is that when more glutamate is released from the presynaptic cell it is cleared from the synaptic cleft more slowly because glutamate uptake is saturated at high glutamate doses. To test the role of glutamate uptake in clearing glutamate from the synaptic cleft, and to investigate the role of receptor

desensitisation in shaping the EPSC, the experiments in the next chapter were carried out.

Chapter 4

Factors determining the EPSC decay time course

4.1 Introduction

This chapter describes experiments to investigate further the factors determining the synaptic current waveform at the two excitatory synapses onto cerebellar Purkinje cells from climbing fibres and parallel fibres. These experiments test the role of glutamate uptake and receptor desensitization in terminating the EPSC, by using blockers of these processes, and by using adenosine and baclofen as tools to vary the amount of glutamate released presynaptically.

4.2 Methods

These are described in detail in Chapter 2. Excitatory synaptic input was activated by stimulating the climbing fibre or parallel fibres projecting to the Purkinje cell. Inputs were identified as described in Chapter 3 (section 3.3). All experiments in this chapter were done in the presence of 100μM picrotoxin to block inhibitory $GABA_A$ receptors on the Purkinje cell.

4.3 Blocking glutamate uptake slows the decay of the EPSCs

To test for a rate limiting role of glutamate removal in setting the EPSC decay rate, the competitive glutamate uptake blocker L-*trans*-pyrrolidine-2,4-dicarboxylate (PDC, 300μM: Bridges *et al.*, 1994) was used. This should roughly halve the rate of uptake of 1mM glutamate (Sarantis *et al.*, 1993), which may be the peak concentration of glutamate in the synaptic cleft during the EPSC (Clements *et al.*, 1992). PDC does not affect AMPA receptor currents in hippocampal neurones (Sarantis *et al.*, 1993) and in Purkinje cells (Billups and Attwell, 1996).

Consistent with the results of Barbour *et al.* (1994), whose paper was published while I was doing this work, PDC prolonged the EPSC at both the climbing fibre and the parallel fibre synapses. At the climbing fibre synapses, the decay time constant increased

by 10±2 (S.E.M.)% in 6 cells as shown in Fig. 4.1. At the parallel fibre synapses, the decay time constant increased more strikingly by 101±27% in 12 cells, as shown in Fig. 4.2. In PDC the parallel fibre EPSC decay was better fit by the sum of two exponentials, rather than just one exponential: however, for simplicity here, the slowing of the EPSC decay was characterised by using the time constant of a single exponential fitted to the part of the decay between approximately 90% and 10% of the peak current amplitude.

In addition to slowing the EPSC decay, PDC reduced its amplitude at both synapses by 30-40% (Figs. 4.1 & 4.2), presumably because blocking uptake raises the extracellular glutamate level, $[glu]_o$, in the slice and desensitizes the postsynaptic glutamate receptors. Consistent with a rise of $[glu]_o$, PDC evoked a tonic inward current in the Purkinje cell (typically about 200pA at -36mV), as reported by Sarantis *et al.* (1993) and Barbour *et al.* (1994). The slowing of the EPSC decay time constant cannot reflect an effect of desensitization on the receptor deactivation rate, because pre-desensitization apparently speeds deactivation (Colquhoun *et al.*, 1992, Fig. 14).

These data show that the rate of glutamate removal affects the EPSC decay rate, implying that there is a prolonged glutamate transient in the synaptic cleft at these two synapses when uptake is blocked (and possibly in the absence of uptake blockers as well).

4.4 Differential effect of adenosine on the 1st and 2nd EPSC produced by double pulse stimulation of the climbing fibres

If there is a prolonged glutamate transient in the synaptic cleft, as suggested by the experiments above, then one might expect AMPA receptor desensitization to contribute to setting the decay time of the EPSC. Desensitization typically occurs on a time scale of 1-15msec (Raman and Trussell, 1992; Colquhoun *et al.*, 1992; Barbour *et al.*, 1994), similar to the EPSC decay time constant at the parallel and climbing fibre synapses. Such desensitization could explain the fact that, as in calyceal synapses (Trussell *et al.*, 1993), the EPSC evoked by the 2nd of two closely spaced climbing fibre stimuli is smaller than the EPSC evoked by the 1st stimulus, as shown in Fig. 3.2A (Konnerth *et al.*, 1990; Perkel *et al.*, 1990). Unlike at some synapses (Davies *et al.*, 1990), paired pulse

Fig. 4.1 The effect of PDC, a glutamate uptake blocker, on the decay time course of the climbing fibre EPSC. **A.** Climbing fibre EPSCs recorded in control solution, in 300μM PDC, and again in control solution (wash). **B.** The same climbing fibre EPSCs as in **A** normalised to the same peak current. The holding potential was -36mV.

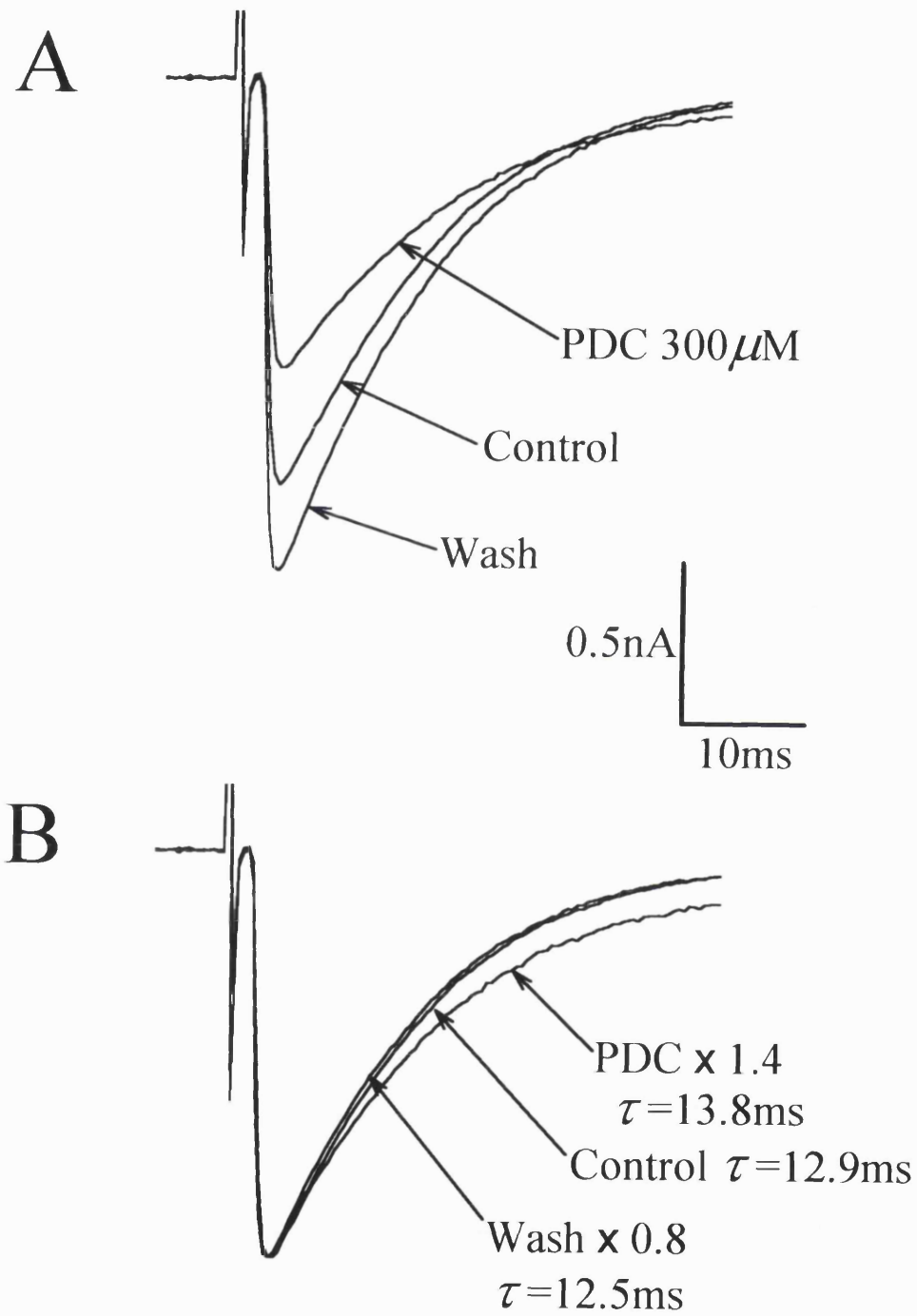
A
PDC 300μM
Control
Wash
0.5nA
10ms
B
PDC x 1.4
τ=13.8ms
Control τ=12.9ms
Wash x 0.8
τ=12.5ms

Fig. 4.2 The effect of PDC, a glutamate uptake blocker, on the decay time course of parallel fibre EPSC. **A.** Parallel fibre EPSCs recorded in control solution, in 300μM PDC, and again in control solution (wash). **B.** The same parallel fibre EPSCs as in **A** normalised to the same peak current. The holding potential was -36mV.

A

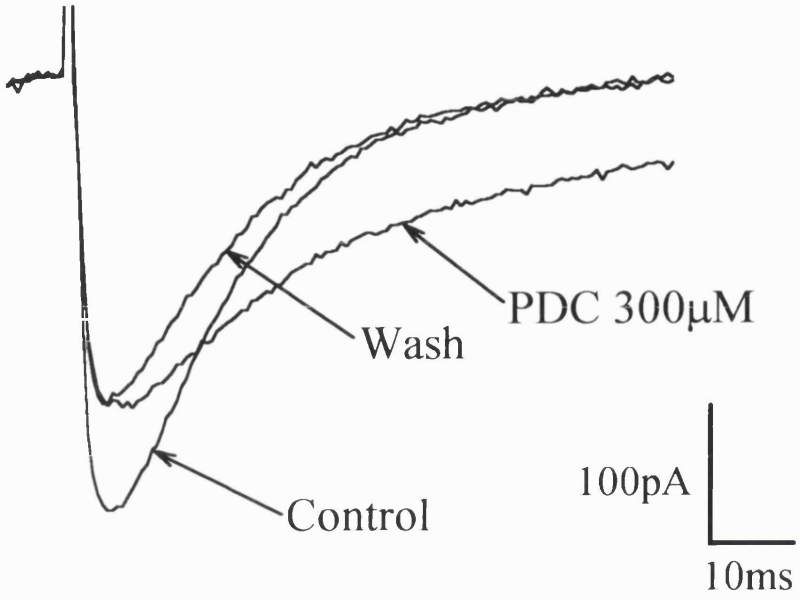
PDC 300μM
Wash
Control
100pA
10ms

B

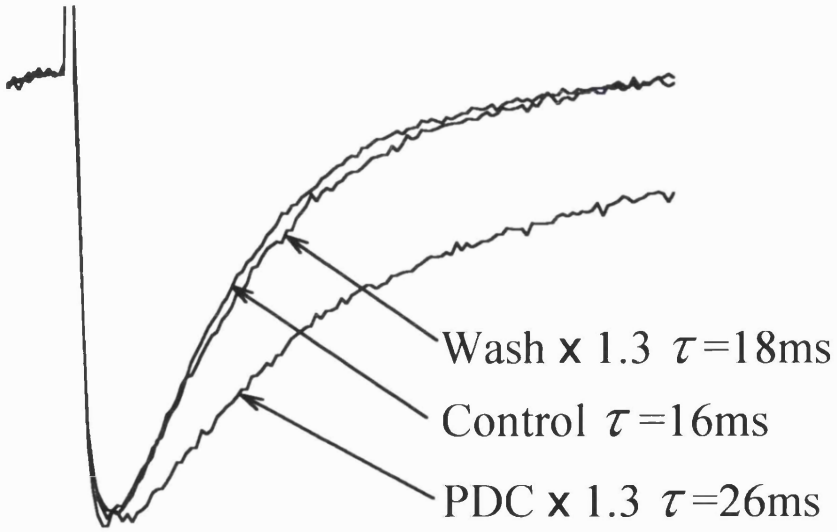
Wash x 1.3 τ=18ms
Control τ=16ms
PDC x 1.3 τ=26ms

depression at the climbing fibre synapse is not due to GABA release from interneurons produced by the 1st stimulus acting on $GABA_B$ receptors to suppress glutamate release produced by the 2nd stimulus: in 9 cells the $GABA_B$ receptor blocker 2-hydroxy-saclofen (500μM) had no effect on the ratio of the 2nd EPSC amplitude to that of the 1st EPSC (increased by only 0.9±1.5%).

As a first step in investigating how desensitization might shape the climbing fibre EPSC, I tested how reducing glutamate release with adenosine or baclofen affected the EPSCs evoked by twin stimuli to the climbing fibres. The rationale behind this experiment was that reducing glutamate release should result in less desensitization at the time of the 2nd EPSC (cf. Trussell *et al.*, 1993). As a result adenosine or baclofen is expected to produce less reduction of the 2nd EPSC than of the 1st. This prediction was found to be correct, indeed adenosine sometimes increased the amplitude of the second EPSC while decreasing the amplitude of the first (Figs. 4.3 & 4.6A). This effect presumably results from less desensitization of non-NMDA receptors at the time of the 2nd stimulus, outweighing the reduction in amplitude produced by adenosine decreasing glutamate release. For stimuli separated by 30-55msec, in 22 cells 100μM adenosine decreased the 1st EPSC by 32±3% but did not significantly affect the 2nd EPSC (decreased by 2±5%). Corresponding figures for 100μM baclofen (3 cells) were 43±4% and 20±6%.

It appears, therefore, that postsynaptic receptor desensitization may contribute to shaping the climbing fibre EPSC. To test this interpretation, the experiments in the following section were carried out, using a blocker of desensitization.

4.5 Effects of diazoxide on EPSCs

Diazoxide (500μM) which, among other effects, reduces desensitization of AMPA receptors (Yamada and Rothman, 1992), was applied to test the hypothesis given above, and to test directly whether desensitization helps to terminate the EPSC. At both the climbing fibre synapse (Fig. 4.4) and the parallel fibre synapse (Fig. 4.5), diazoxide greatly prolonged the EPSC decay. In 9 cells the climbing fibre time constant increased from 7.5±0.7msec in control solution to 48±6msec in diazoxide. In 2 cells the parallel

Fig. 4.3 Differential effect of adenosine on the first and second of two EPSCs evoked by twin pulse stimulation to the climbing fibre input of a Purkinje cell. Adenosine decreased the amplitude of the 1st EPSC but increased the amplitude of the 2nd EPSC. (More commonly adenosine had approximately no effect on the 2nd EPSC amplitude as in Fig. 4.6A). **A.** Specimen EPSCs in control solution, in 100μM adenosine, and again in control solution (wash). Stimulus timing is shown by sharp stimulus artefacts on current traces. **B.** Amplitude of the first (solid square) and second (open square) EPSCs as a function of time during the experiment. The holding potential was -51mV.

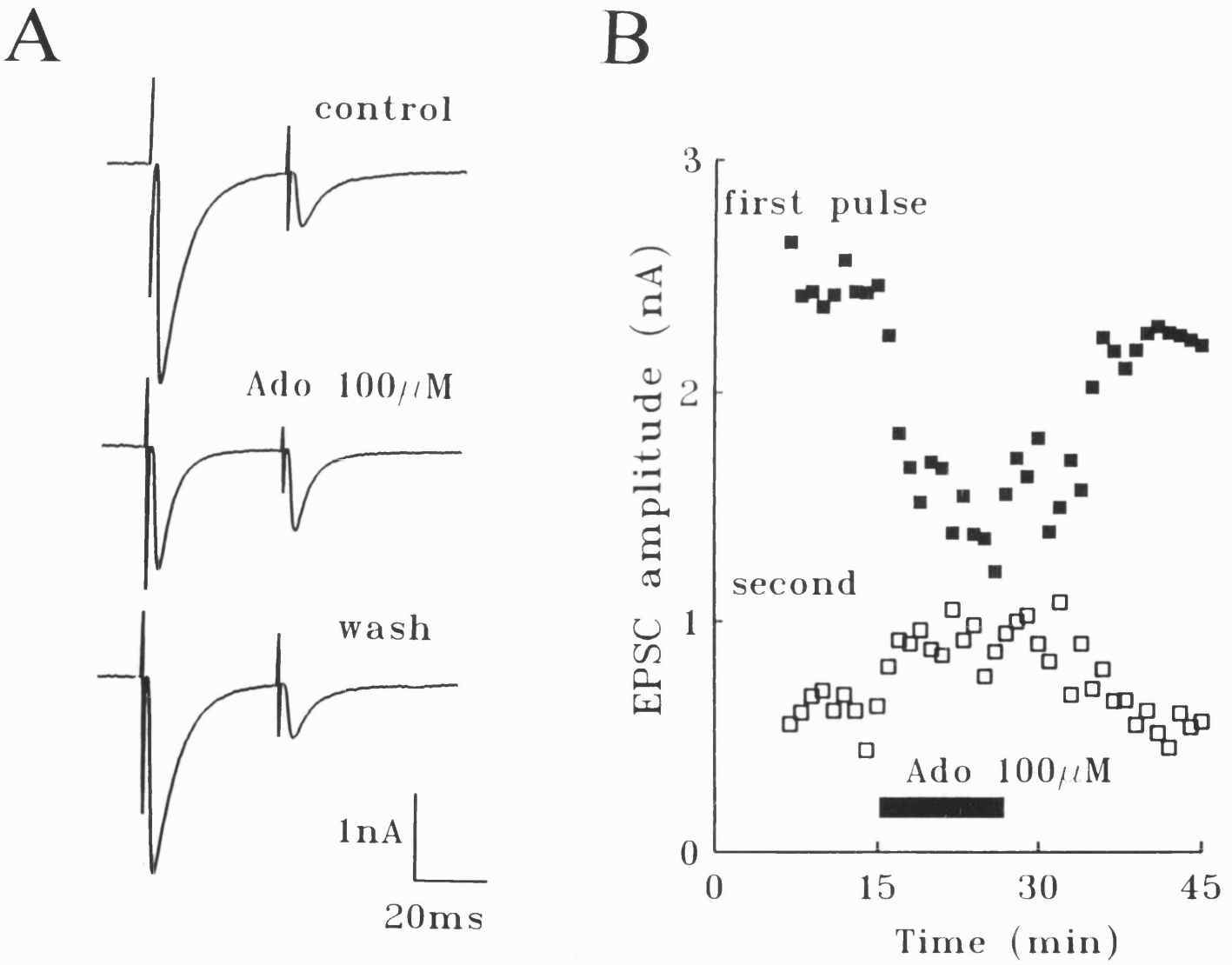
A
control
Ado 100μM
wash
1nA
20ms
B
3
2
1
0
first pulse
second
Ado 100μM
EPSC amplitude (nA)
0
15
30
45
Time (min)

Fig. 4.4 Effect of diazoxide on the climbing fibre EPSC. **A.** Climbing fibre EPSCs recorded in control solution and in 0.5mM diazoxide (DZ). **B.** The same climbing fibre EPSCs as in **A** normalised to the same peak current. The holding potential was -36mV.

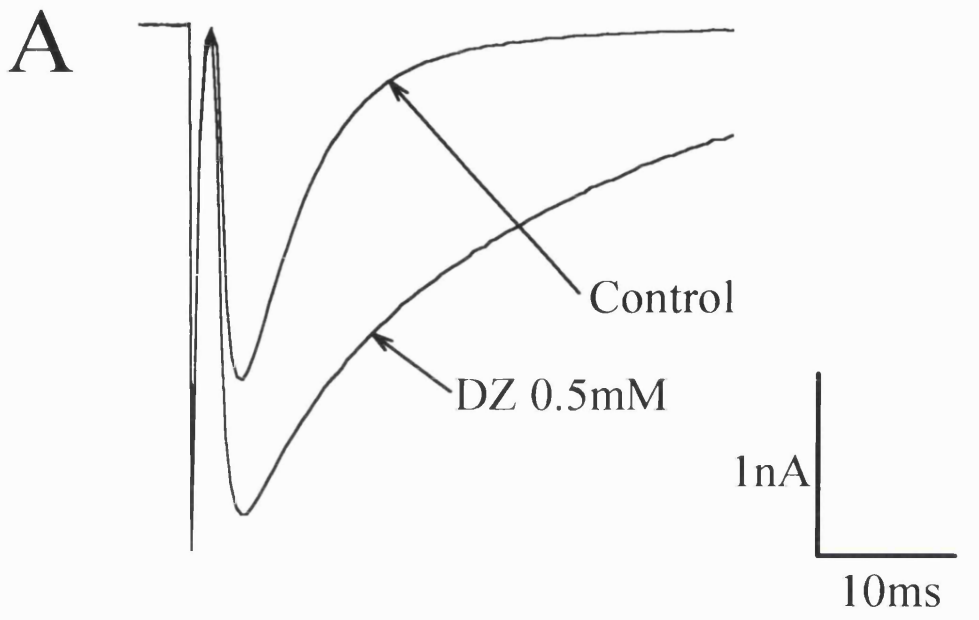
A
Control
DZ 0.5mM
1nA
10ms

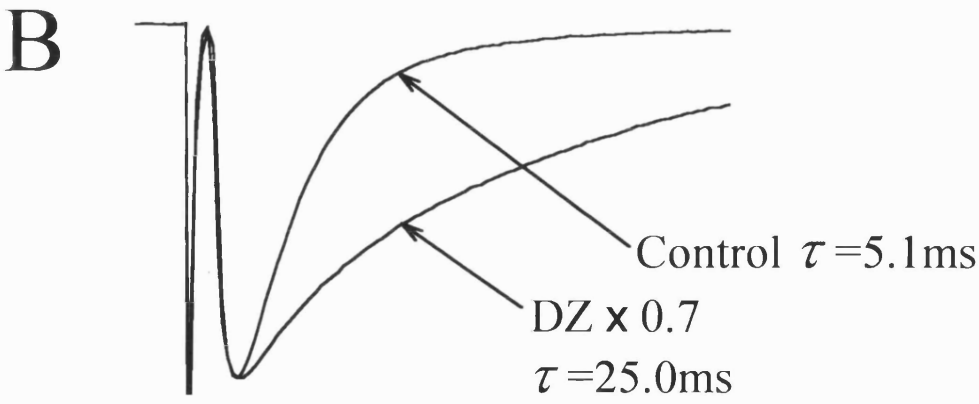
B
Control τ =5.1ms
DZ x 0.7
τ =25.0ms

Fig. 4.5 Effect of diazoxide on the decay time course of the parallel fibre EPSC. **A.** Parallel fibre EPSCs recorded in control solution and in 0.5mM diazoxide (DZ). **B.** The same climbing fibre EPSCs as in **A** normalised to the same peak current. The holding potential was -36mV.

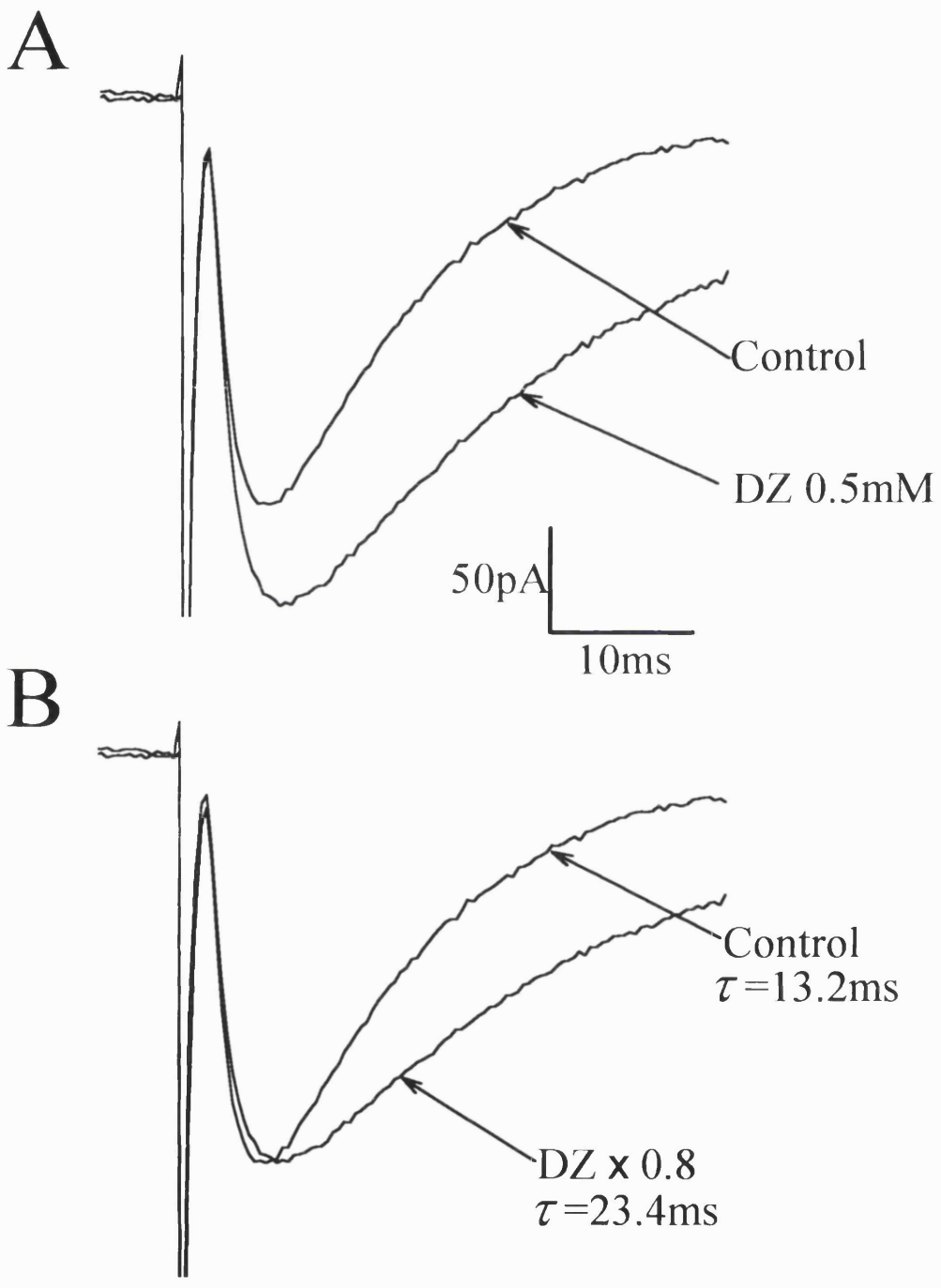
A
Control
DZ 0.5mM
50pA
10ms
B
Control
τ=13.2ms
DZ x 0.8
τ=23.4ms

fibre time constant increased from 11.2±2msec to 27.6±4.2msec. A similar result was found by Barbour *et al.* (1994) who blocked desensitization with aniracetam (and also showed that this only increased the deactivation time constant from about 1msec to about 2msec, so the prolongation of the EPSC decay is unlikely to reflect slowed receptor deactivation). The slowing of the EPSC decay is unlikely to be due to diazoxide inhibiting glutamate uptake. Control experiments on salamander glial cells (Billups and Attwell, 1996) showed that 500μM diazoxide slightly speeded uptake (the uptake current produced by 200μM glutamate was increased by 17±8% in 3 cells).

In addition diazoxide potentiated the 2nd of two climbing fibre EPSCs more than it potentiated the 1st EPSC as shown in Fig. 4.6B (see also Trussell *et al.*, 1993): in 9 cells the ratio of the 2nd EPSC amplitude to the 1st EPSC amplitude was 0.60±0.02 (S.E.M.) in control solution and 0.84±0.02 in diazoxide. For these experiments, in diazoxide the current produced by the second stimulus starts from the decaying current tail produced by the first stimulus. Assuming that glutamate is released at the same sites by both stimuli (consistent with diazoxide increasing the size of the second response more than the first), I defined the amplitude of the second EPSC as the peak current measured relative to the baseline before the first stimulus (i.e., without subtracting the first EPSC tail), a definition different to that of Trussell *et al.* (1993). This is because I am interested in the current produced by the amount of glutamate present in the synaptic cleft at the peak of the second EPSC: I assume this glutamate concentration is the same with or without diazoxide present, so the long current tail of the first EPSC in diazoxide reflects a prolonged presence of glutamate in the synaptic cleft which occurs even when diazoxide is absent (without diazoxide the glutamate generates no current because desensitization occurs and the receptor affinity may be lower).

In 4 of the 9 cells studied 30μM glibenclamide was applied with the diazoxide, to prevent diazoxide activating ATP-gated potassium channels (Quast and Cook, 1989; Yamada and Rothman, 1992) and the results obtained were similar to those in the 5 cells studied without glibenclamide: increase in the decay time constant was 522±70% with glibenclamide and 725±138% without glibenclamide. Thus, these effects of diazoxide do

Fig. 4.6 Effect of adenosine on the climbing fibre EPSC evoked by twin pulse stimulation with and without AMPA receptor desensitization blocked. **A.** In control solution, the second of two EPSCs is smaller than the first, and 100μM adenosine reduced the first EPSC much more than the second. **B.** 500μM Diazoxide prolongs both EPSCs, and increases the second EPSC more than the first. **C.** In diazoxide, adenosine has a more similar effect on the first and second EPSCs. The holding potential was -25mV.

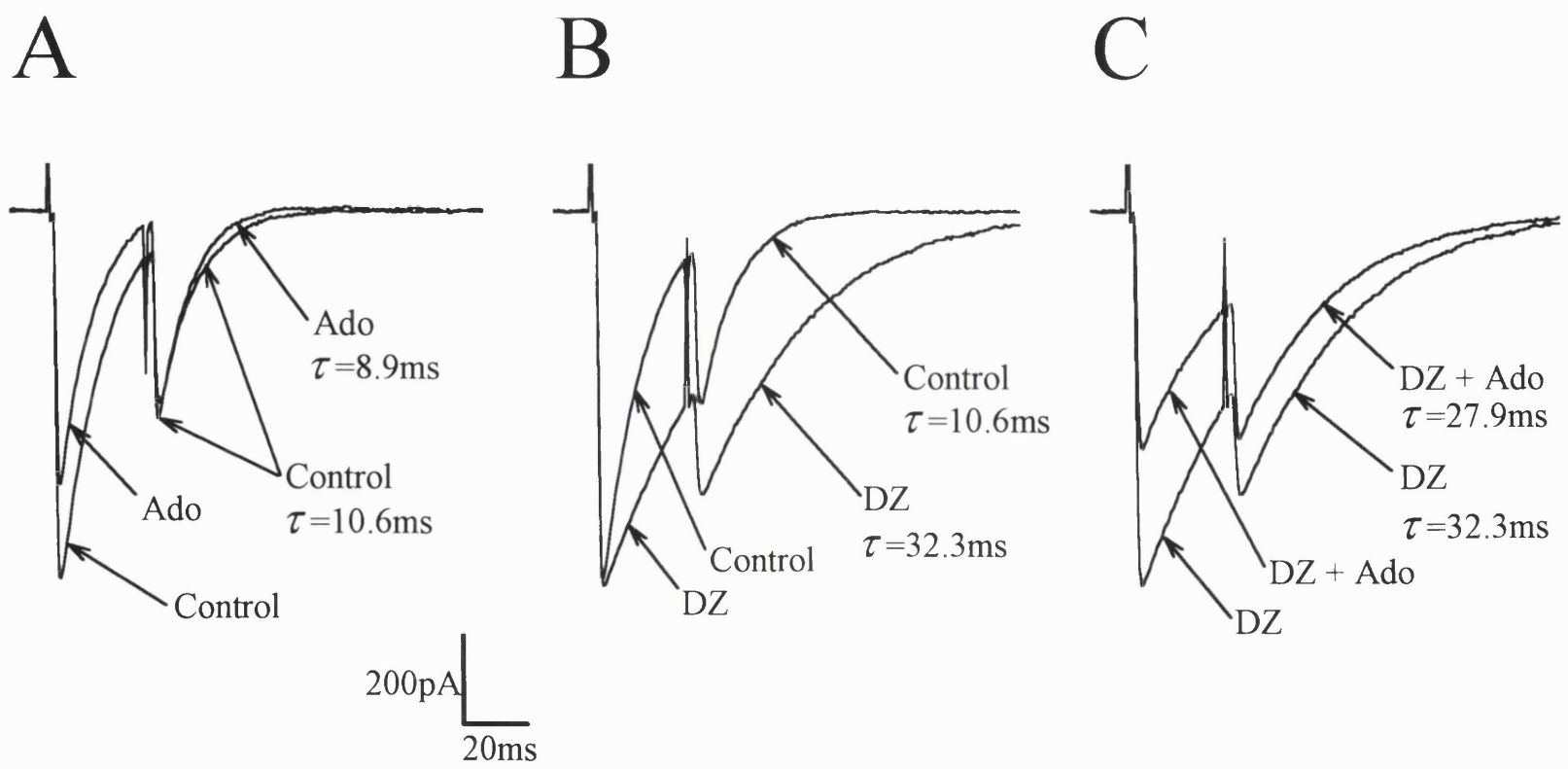
A
Ado
τ=8.9ms
Control
τ=10.6ms
Ado
Control
200pA
20ms
B
Control
τ=10.6ms
DZ
τ=32.3ms
Control
DZ
C
DZ + Ado
τ=27.9ms
DZ
τ=32.3ms
DZ + Ado
DZ

not reflect a change of glutamate release produced by activation of presynaptic ATP-gated potassium channels.

Both the prolonging effect of diazoxide on the EPSC duration, and its greater potentiation of the 2nd EPSC than the 1st EPSC, are consistent with desensitization contributing to the 2nd EPSC being smaller, and to setting the EPSC decay time course. Presumably the longer EPSC seen in diazoxide is a more faithful reflection of the underlying glutamate transient in the synaptic cleft (but see section 4.7.2 for more discussion).

4.6 Interaction of receptor desensitization and amount of glutamate release in setting the EPSC decay time

A decreased sensitivity of the 2nd EPSC to a blockade (with adenosine or baclofen) of presynaptic calcium entry, as described in section 4.4 and attributed to a change in postsynaptic desensitization, might instead be attributed to a presynaptic effect. For example, decreasing (with adenosine) the number of vesicles released on the 1st pulse might leave more to be released by the 2nd pulse. The explanation in terms of desensitization, for the differential effects of adenosine and baclofen on the 1st and 2nd EPSCs, could be tested by blocking desensitization: with desensitization blocked, adenosine (or baclofen) should reduce both EPSC amplitudes equally.

Applying adenosine (100μM) in the presence of diazoxide (Fig. 4.6C) led to the 2nd EPSC amplitude (measured from the prestimulus baseline as explained in section 4.5) being suppressed by an amount (13±2 % in 9 cells) more similar to the suppression of the 1st EPSC (18±3%), as expected with desensitization greatly reduced. This is in contrast to what was seen in the absence of diazoxide, as shown in Figs. 4.3 & 4.6A. It appears, therefore, that the explanation given in terms of desensitization for the results in section 4.4 is plausible. Consequently, for brief intervals between presynaptic action potentials, the climbing fibre EPSC size and kinetics will be set by an interaction between the amount of glutamate released presynaptically and the amount of desensitization occurring postsynaptically.

4.7 Discussion

The experiments described in this chapter give insight into the role of glutamate uptake and of receptor desensitization in terminating the synaptic current at excitatory synapses onto Purkinje cells.

4.7.1 Role of glutamate uptake in terminating the EPSC

Blocking glutamate uptake prolonged the EPSC at both the climbing and the parallel fibre to Purkinje cell synapses (see also Barbour *et al.*, 1994), consistent with the rate of removal of glutamate from the synaptic cleft partly determining the EPSC duration. This is in contrast to the behaviour of cerebellar mossy fibre to granule cell synapses and hippocampal Schaffer collateral to pyramidal cell synapses where blocking uptake has no effect on the EPSC decay (Hestrin *et al.*, 1990b; Sarantis *et al.*, 1993; Isaacson and Nicoll, 1993). Interestingly these differential effects of blocking uptake on the EPSCs at the three cerebellar synapses correlate with the fact that mossy fibre terminals do not express much glutamate uptake, unlike climbing fibre terminals and the granule cells which provide the parallel fibre terminals (Garthwaite and Garthwaite, 1988; Wilklund *et al.*, 1982). The dramatic effect of uptake block on the parallel fibre EPSC (Fig. 4.2) may be due partly to a number of parallel fibres being stimulated (perhaps 20 for Fig. 4.2, estimated by dividing the EPSC amplitude by the current generated per parallel fibre as measured by Barbour, 1993). Removal of glutamate by diffusion out of the synaptic cleft, rather than uptake, may be more important if only one parallel fibre is active, so that the glutamate concentration is not elevated in the extracellular space around that synapse and there is a larger concentration gradient driving diffusion.

An effect of uptake rate on EPSC duration has also been found for synapses in cultured hippocampal neurones when desensitization is blocked (Mennerick and Zorumski, 1994a, b). By contrast Tong and Jahr (1994) found that blocking uptake did not affect the EPSC decay (although it did affect the EPSC amplitude): this may be because the [glu] falls more rapidly at their cultured synapses than at the cerebellar synapses I have studied, due to the good diffusive contact with the bath solution, so the EPSC decay rate is dominated by the time course of receptor deactivation.

4.7.2 Does receptor desensitization contribute to the EPSC decay?

The changes of the EPSC decay produced by decreasing glutamate release (Chapter 3) or blocking glutamate uptake suggest that the glutamate transient in the synaptic cleft decays on a time scale comparable to that of the EPSC. A prolonged glutamate transient could result in some of the decay of the EPSC being due to AMPA receptor desensitization, which in other preparations proceeds with a time constant of 1-15msec (Colquhoun *et al.*, 1992; Raman and Trussell, 1992). Consistent with this, diazoxide, which reduces desensitization (Yamada and Rothman, 1992), prolonged the EPSC at both the climbing fibre and parallel fibre synapses, and reduced the paired pulse depression seen when applying two stimuli separated by a brief interval to the climbing fibre. Similar effects of agents which remove desensitization at cochlear nucleus and Purkinje cell synapses have been interpreted as proving that desensitization contributes to terminating the EPSC (Trussell *et al.*, 1993; Barbour *et al.*, 1994). However, agents like diazoxide have effects other than removal of desensitization. First, they prolong deactivation time, although apparently not enough to explain the lengthening of the EPSC produced (Trussell *et al.*, 1993; Barbour *et al.*, 1994). Second, they may increase the AMPA receptor affinity for glutamate (Patneau *et al.*, 1993; Yamada and Tang, 1993) and could thus generate a large long lasting current decay from a small tail of elevated glutamate concentration in the synaptic cleft. This alternative explanation for the effect of diazoxide on the EPSC decay would require, though, that the glutamate transient in the synaptic cleft decays on a time scale longer than the EPSC seen in the absence of diazoxide, and so would in any case be likely to produce desensitization during the EPSC.

The effects of adenosine in the absence and presence of diazoxide also suggest a role for desensitization in setting the amplitude of the second of two closely spaced EPSCs (Figs. 4.3 & 4.6). In the absence of diazoxide adenosine had little effect on the amplitude of the second EPSC while reducing the first EPSC. This is presumably because, by reducing glutamate release on the first stimulus, it reduced desensitization at the time of the second stimulus, and the removal of desensitization counteracted the reduction of glutamate release produced by adenosine. By contrast, in the presence of diazoxide

adenosine reduced both the first and second EPSCs, as expected with desensitization removed.

Thus, desensitization is one determinant of the climbing fibre EPSC amplitude and duration, and the glutamate transient in the synaptic cleft outlasts the EPSC seen in normal solution. It is interesting to consider how both desensitization and uptake can contribute to shaping the EPSC (decay time constant ~7msec at the climbing fibre synapse), when complete desensitization to a high maintained [glu] occurs with a time constant of around 4msec (Barbour *et al.*, 1994). The answer may lie in the [glu]-dependence of desensitization: the fall of [glu] occurring after the EPSC peak may slow desensitization or make it less complete, so that the current seen late in the EPSC can be increased either by removing desensitization or by prolonging the [glu] transient (with an uptake blocker) and thus increasing the number of channels activated at late times. Alternatively, desensitization may set the EPSC duration at the (possibly saturated) receptors opposite a presynaptic release site, with uptake determining how far glutamate diffuses laterally in the synaptic cleft: inhibiting uptake could then allow more lateral diffusion and later activation of receptors at a distance from the release site (cf. Isaacson *et al.*, 1993).

4.7.3 Determinants of the EPSC duration at different cerebellar synapses

From the experiments reported here it appears that a number of factors contribute to determining the EPSC duration at the parallel and climbing fibre synapses: the amount of glutamate released presynaptically, the rate of glutamate uptake, and the rate of AMPA receptor desensitization. By contrast the fast decay of the cerebellar mossy fibre to granule cell synapse is dominated by the speed of receptor deactivation following fast removal of glutamate from the synaptic cleft (Silver *et al.*, 1992,1994; Sarantis *et al.*, 1993). It remains to be determined whether these differences are of functional importance for the operation of cerebellum.

Chapter 5

Electrogenic glutamate uptake in Purkinje cells

5.1 Introduction

Experiments in Chapter 4 showed that glutamate uptake plays a role in terminating synaptic transmission at the climbing and parallel fibre synapses. In this chapter experiments were carried out to determine whether *post*synaptic glutamate uptake may be important in this regard. Conventionally, uptake is thought of as being in *pre*synaptic terminals or glial cells. These experiments were carried out because of recent work on the location of cloned mammalian uptake carriers, in particular the discovery that they can be expressed in postsynaptic cells.

Of the four cloned glutamate uptake carriers, one (EAAC1) is known to be expressed in neurones (Kanai and Hediger, 1992). When expressed in oocytes, this carrier generates a Na^+-dependent inward membrane current when transporting glutamate into the cell (Kanai and Hediger, 1992), like the uptake carrier in salamander retinal glial cells (Brew and Attwell, 1987). Within the cerebellum, the cloned glutamate uptake carrier subtypes are differentially localised. An antibody staining study (Rothstein *et al.*, 1994) showed that EAAC1 is expressed in the soma and dendrites of cerebellar Purkinje cells, i.e. approximately postsynaptic to the climbing fibre and parallel fibre synapses. The glial transporters GLT-1 and GLAST were found to be expressed in astrocytes and Bergmann glial cells. The fourth cloned transporter, EAAT4, is also expressed in cerebellum (Fairman *et al.*, 1995) but its cellular localization has not yet been published.

The antibody labelling experiments of Rothstein *et al.* (1994), while showing that EAAC1 is present in Purkinje cells, did not establish whether it was present and functioning in the cell's surface membrane. This chapter describes experiments which attempted to detect glutamate uptake electrophysiologically in cerebellar Purkinje cells. The aims were to investigate the properties of an identified cloned mammalian glutamate transporter *in situ* in the cell where it is normally expressed (allowing a comparison to be

made with its properties when expressed in *Xenopus* oocytes: Kanai and Hediger, 1992; Kanai *et al.*, 1995), and to test its role in terminating synaptic transmission to Purkinje cells.

5.2 Methods

These are described in detail in Chapter 2. In brief, glutamate uptake was activated by applying glutamate analogues like D-aspartate iontophoretically to Purkinje cells in cerebellar slices from 12 day old rats (Fig. 5.1A). Excitatory synaptic input was activated by stimulating the climbing fibre or parallel fibres projecting to the Purkinje cell. All experiments in this chapter were done in the presence of 100μM picrotoxin to block inhibitory input to the Purkinje cell via $GABA_A$ receptors.

5.3 The D-aspartate uptake current and its pharmacology

D-aspartate is transported on glutamate uptake carriers, as shown by radiotracing in mammalian preparations (Erecinska *et al.*, 1983), and by electrical recording in salamander Müller cells (Barbour *et al.*, 1991) and in *Xenopus* oocytes expressing, for example, EAAC1 transporters (Kanai and Hediger, 1992). However D-aspartate has a low affinity for non-NMDA receptors (Monaghan *et al.*, 1984). In Purkinje cells from 12 day old rats, the only ionotropic glutamate receptors are non-NMDA receptors (NMDA receptors are not expressed after postnatal day 10: Konnerth *et al.*, 1990; Perkel *et al.*, 1990; Momiyama *et al.*, 1996), so D-aspartate has a suitable pharmacological profile for selectively activating uptake instead of channels. By contrast (as shown below) L-glutamate mainly produces a current in the Purkinje cell by activating non-NMDA receptors. Fig. 5.1B shows the membrane current of a whole-cell clamped Purkinje cell during iontophoresis of D-aspartate onto its soma. D-aspartate evokes an inward membrane current.

How does D-aspartate evoke this current? There are three possibilities (Fig. 5.2). First, D-aspartate might open glutamate-gated channels directly, although D-aspartate is a poor agonist for non-NMDA receptors (Monaghan *et al.*, 1984). Secondly, D-aspartate may

Fig. 5.1 Application of D-aspartate iontophoretically, to cerebellar Purkinje cells. **A.** Schematic diagram of iontophoresis experiment. Purkinje cells were whole-cell clamped, and D-aspartate was applied onto the soma by changing the iontophoresis holding current of +20nA to an ejecting current of -40nA. **B.** Iontophoresing D-aspartate evoked an inward current. Pipette solution was solution D, Table 2.2. The holding potential was -96mV.

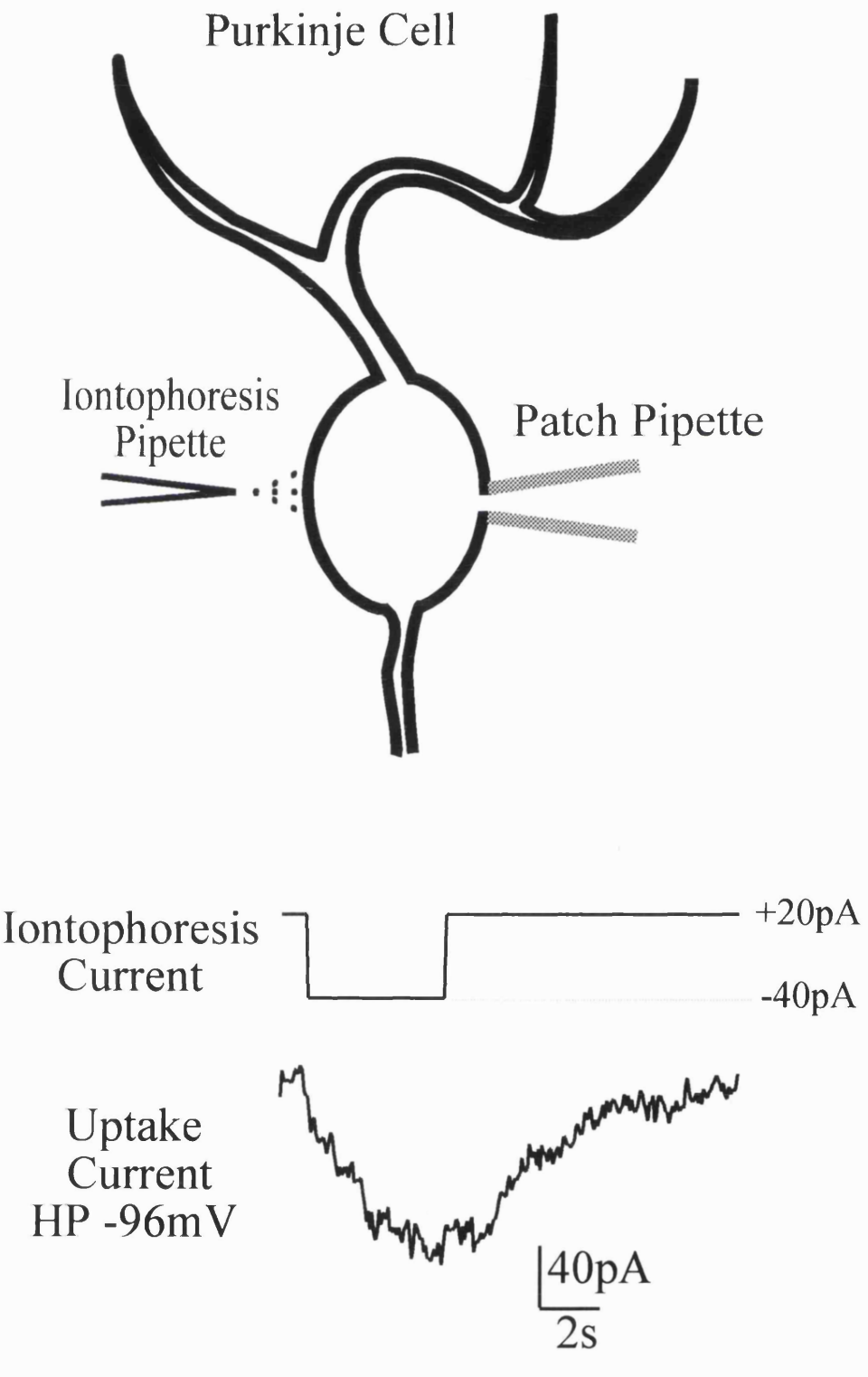
Purkinje Cell
Iontophoresis Pipette
Patch Pipette
Iontophoresis Current
+20pA
-40pA
Uptake Current HP -96mV
40pA
2s

Fig. 5.2 Diagram of three possible causes of D-aspartate-evoked current in Purkinje cells. **Top arrow:** D-aspartate might directly open the non-NMDA receptor channels in Purkinje cells. **Bottom arrow:** D-aspartate might inhibit the uptake of glutamate in surrounding cells, and raise the extracellular glutamate concentration which leads to opening of non-NMDA channels in Purkinje cells. **Middle arrow:** D-aspartate may be taken up directly by glutamate uptake carriers in Purkinje cells.

How does D-asp evoke a current?

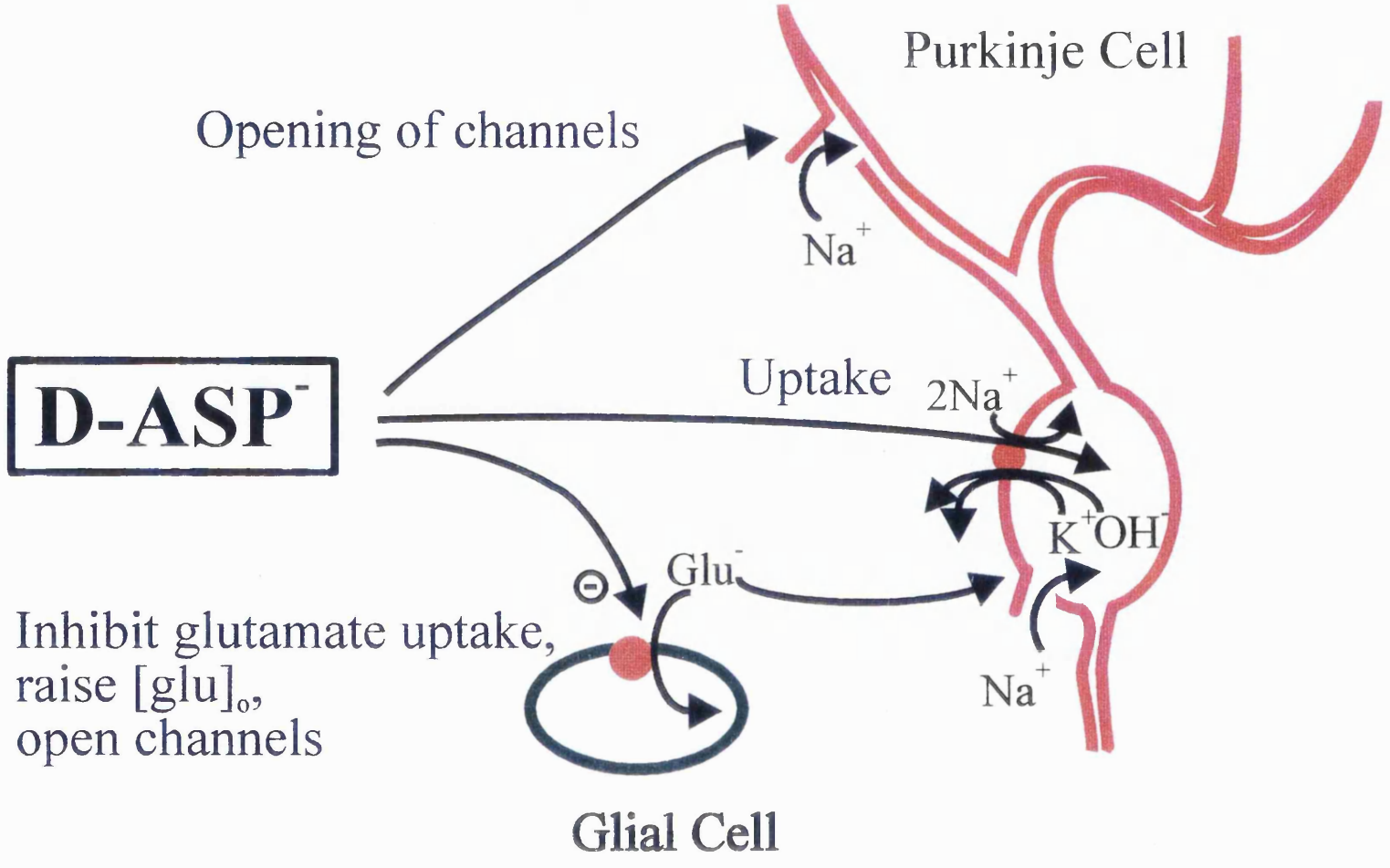

inhibit uptake in surrounding cells (i.e. glial cells or presynaptic terminals), and thus raise the extracellular glutamate concentration, leading to opening of non-NMDA channels in the Purkinje cells. Thirdly, D-aspartate may be directly taken up into the Purkinje cells by glutamate uptake carriers. To distinguish these possibilities the following experiments were performed.

Fig. 5.3A and B shows the effect on the current evoked by D-aspartate of superfusing kynurenate (1mM) which blocks non-NMDA and NMDA receptors (Perkins and Stone, 1985, Stone and Burton, 1988), D-APV (50μM) which blocks NMDA receptors (Davies and Watkins, 1982, Evans *et al.*, 1982), and TTX (1μM) which blocks voltage-gated sodium channels (reviewed by Mosher, 1986). This cocktail of blockers had little effect on the D-aspartate-evoked current: in 19 cells it reduced the current by 19±6 (S.E.M.) %. Even superimposing 50μM CNQX on top of the cocktail of kynurenate, D-APV and TTX had little effect on the D-aspartate-evoked current (Fig. 5.3C). In 19 cells the current was reduced by a further 11±5%. The relatively weak effect of antagonists to non-NMDA and NMDA receptors suggests that most of the current evoked by D-aspartate does not result from the opening of glutamate-gated ion channels. Fig. 5.3D and E show, however, that the glutamate analogue PDC (300μM), which is known to block glutamate uptake (Bridges *et al.*, 1994), reversibly reduced the current when applied on top of the channel blockers mentioned above. In 20 cells the current was reduced by 71±4%, suggesting that D-aspartate generates a current by binding to the glutamate uptake carrier. Purkinje cells can also show aspartate-evoked currents caused by glutamate, released by aspartate-glutamate exchange on uptake carriers, activating non-NMDA receptors (Renard and Crepel, 1996), or caused by aspartate activating a Ca^{2+}-permeable channel (Yuzaki *et al.*, 1996). Both of those currents were abolished by CNQX and so do not contribute significangly to the D-aspatate-evoked current I observed (Fig. 5.3C).

By contrast, when L-glutamate was iontophoresed instead of D-aspartate, the blockers kynurenate, APV and TTX reduced the current by 76±6 (S.E.M.) % (6 cells), and 50μM CNQX reduced the current remaining in these blockers by 93±3% (2 cells). These

Fig. 5.3 Pharmacology of the current evoked by iontophoresis of D-aspartate (bar) onto whole-cell clamped Purkinje cells in cerebellar slices. **A-C.** Effect of glutamate receptor blockers. **A.** Control response with 100μM picrotoxin present to block $GABA_A$ receptors. **B.** Superfusing 1mM kynurenate, 50μM D-APV and 1μM TTX on top of the picrotoxin in **A**. **C.** Superfusing 50μM CNQX on top of the blockers in **B**. **D, E.** Effect of the glutamate uptake carrier blocker PDC. **D.** Superfusing 300μM PDC on top of the blockers in **C**. **E.** recovery from **D**. All traces were taken from the same cell. Pipette solution was solution D, Table 2.2. The holding potential was -96mV.

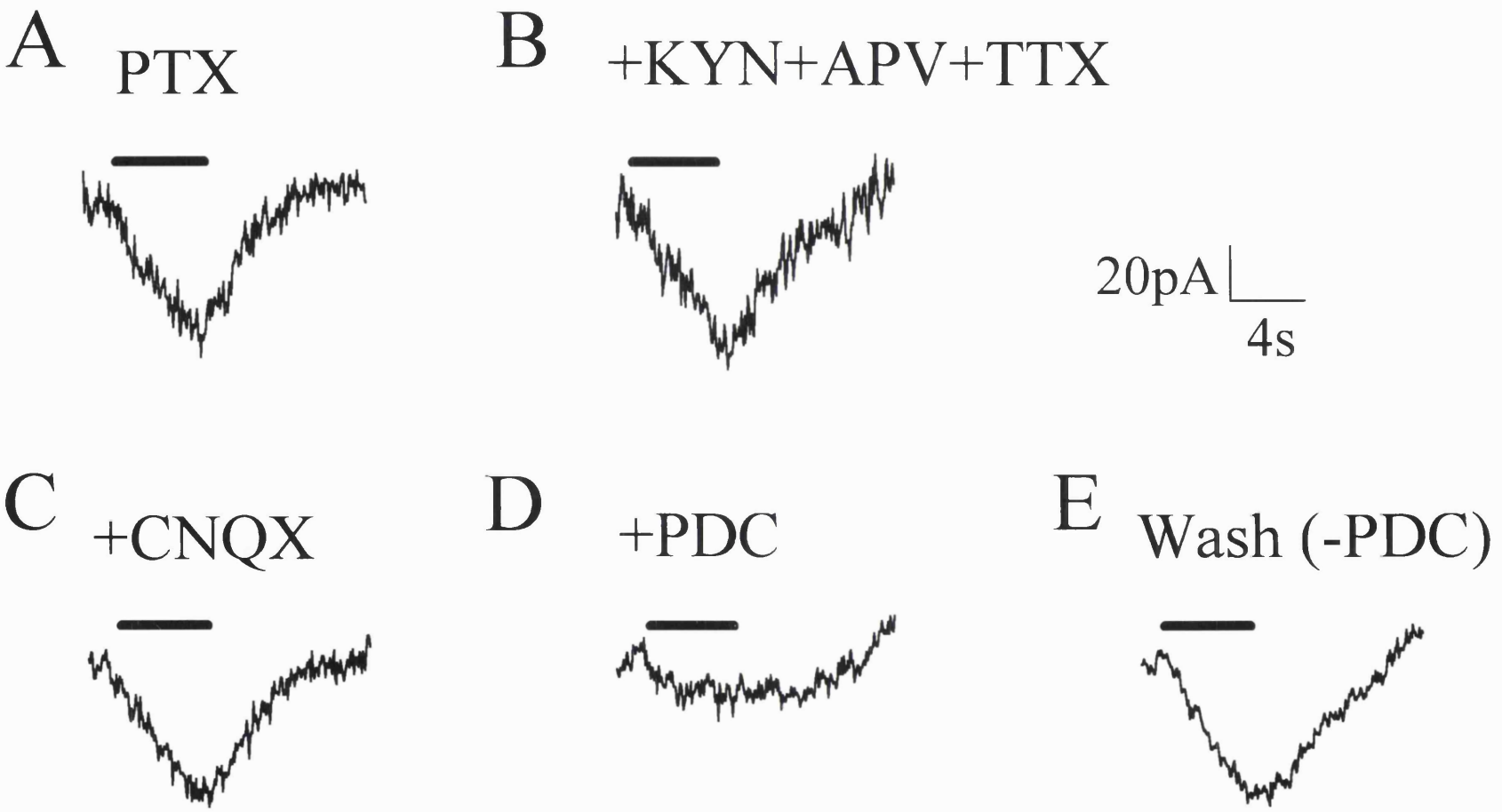
A
PTX
B
+KYN+APV+TTX
20pA
4s
C
+CNQX
D
+PDC
E
Wash (-PDC)

results suggest that the glutamate-evoked current is generated largely by the activation of non-NMDA channels, and confirm that the doses of blockers used would have greatly reduced the response to D-aspartate if it had been produced by glutamate-gated channels.

The need for a further set of control experiments was suggested by the work of Linden *et al.* (1994), who observed inward currents in cerebellar Purkinje cells when glutamate analogues activating metabotropic glutamate receptors were applied. They suggested that the metabotropic agonists raised $[Ca]_i$ which activated the Na^+/Ca^{2+} exchanger and thus generated an inward current (since 3 Na^+ enter the cell on this exchanger for each Ca^{2+} that leaves the cell). To investigate the possibility that D-aspartate activates metabotropic receptors and thus generates a Na^+/Ca^{2+} exchange current, the following experiments were carried out (in the presence of 100μM picrotoxin, 1mM kynurenate, 50μM D-APV and 50μM CNQX). Application of 500μM (+)-α-methyl-4-carboxyphenylglycine (MCPG), an antagonist to the $mGluR_1$ type of metabotropic receptor (Ito *et al.*, 1992, Jane *et al.*, 1993, Collingridge and Watkins, 1994) found in Purkinje cells (Batchelor *et al.*, 1994), had no effect on the D-aspartate evoked current (reduced by 7±11% in 3 cells: Fig. 5.4A). Similarly application of 100μM (1S,3R)-1-aminocyclopentane-1,3-dicarboxylic acid (*trans*-ACPD), a metabotropic receptor agonist, did not alter the current (increased by 4±3% in 4 cells: Fig. 5.4B), although one might have expected this dose of *trans*-ACPD to nearly saturate the metabotropic receptors (East and Garthwaite, 1992; Palmer *et al.*, 1989) and thus reduce any current produced by D-aspartate acting on those receptors. To test further the possible involvement of the Na^+/Ca^{2+} exchanger, 100μM dichlorobenzamil and 200μM La^{3+}, putative exchanger blockers (Andreeva *et al.*, 1991; Plasman *et al.*, 1991; Niggli and Lederer, 1993), were applied. Neither of them had any effect on the current (reduced by 5±12% in 4 cells in the presence of dichlorobenzamil, and increased by 5±8% in 5 cells in the presence of La^{3+}: Fig. 5.5).

The D-aspartate evoked current was also unaffected by Ba^{2+} (Fig. 5.6), ruling out the possibility that K^+, which could be released from glial cells depolarised by D-aspartate uptake, generates the current by passing through inward rectifier channels (which have a

Fig. 5.4 Effect of a metabotropic receptor blocker and agonist on the current evoked by D-aspartate (bar). **A.** (*Left*) Response to iontophoretically applied D-aspartate. (*Right*) Response to D-aspartate in the presence of the metabotropic glutamate receptor blocker MCPG (500μM). Pipette solution contained ClO_4^- (solution F, Table 2.2) to increase the carrier-generated current as described in section 5.6. **B.** (*Left*) Response to iontophoretically applied D-aspartate. (Right) Response to D-aspartate in the presence of the metabotropic glutamate receptor agonist *trans*-ACPD (100μM). Pipette solution was solution D, Table 2.2. The holding potential was -96mV.

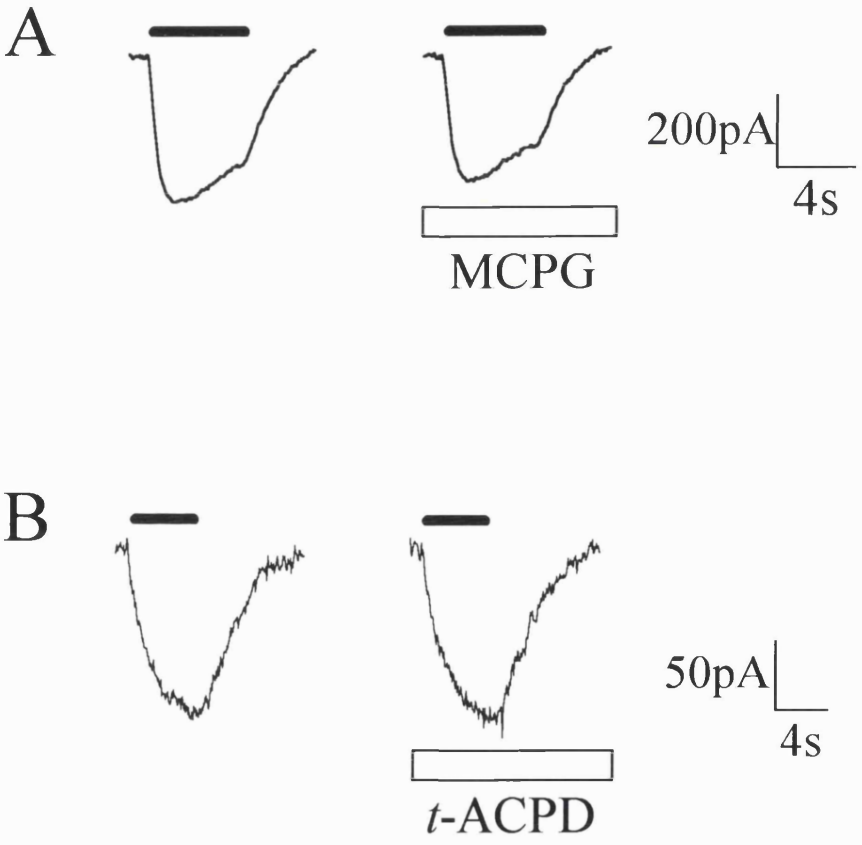
A
200pA
4s
MCPG
B
50pA
4s
t-ACPD

Fig. 5.5 Effect of Na/Ca exchange blockers on the current evoked by D-aspartate (bar). **A.** (*Left*) Response to iontophoretically applied D-aspartate. (*Right*) Response to D-aspartate in the presence of 100 μM dichlorobenzamil (DCB). Pipette solution contained ClO_4^- (solution F, Table 2.2) to increase the carrier-generated current (see section 5.6). **B.** (*Left*) Response to iontophoretically applied D-aspartate. (*Right*) Response to D-aspartate in the presence of 200μM lanthanum (La^{3+}). Pipette solution was solution D, Table 2.2. The holding potential was -96mV.

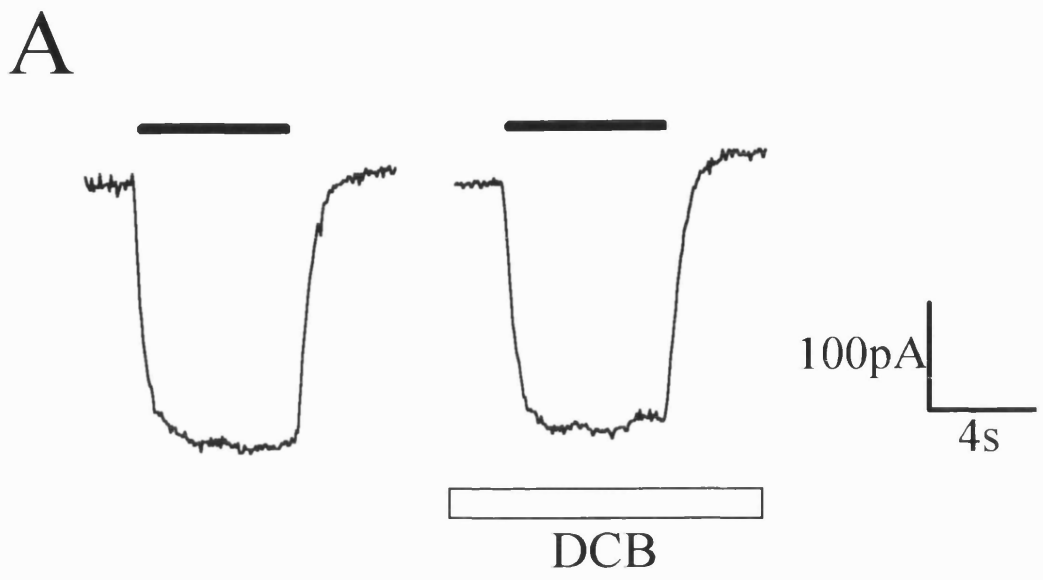
A
100pA
4s
DCB

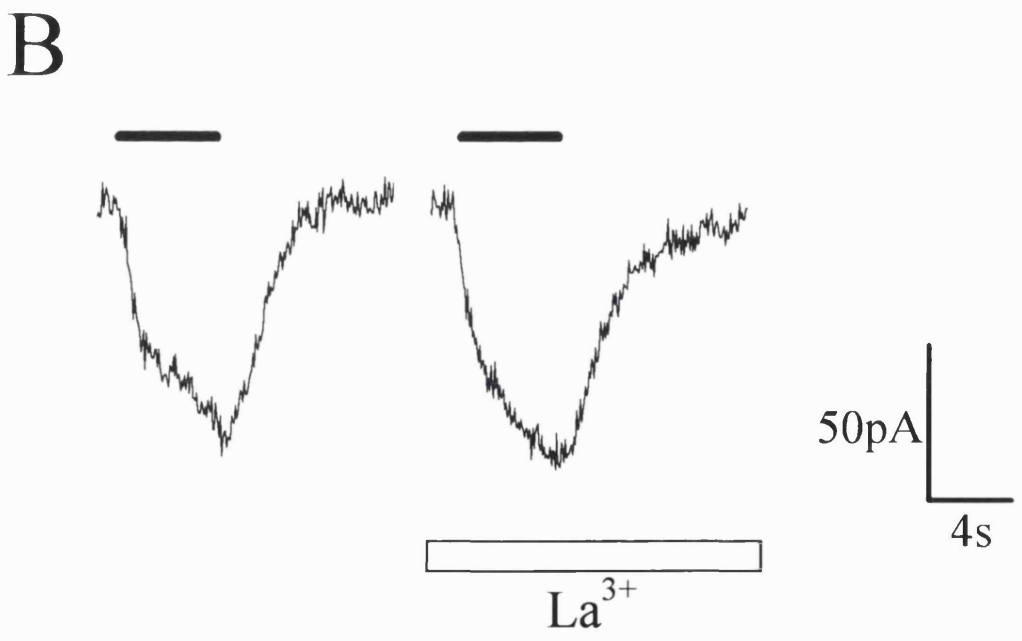
B
50pA
4s
La3+

Fig. 5.6 Effect of the inward-rectifying potassium channel blocker (Ba^{2+}) on the current evoked by D-aspartate (bar). (*Left*) Response to iontophoretically applied D-aspartate. (*Right*) Response to D-aspartate in the presence of 6mM barium (Ba^{2+}) (solution C, Table 2.1). Pipette solution was solution D, Table 2.2. The holding potential was -96mV.

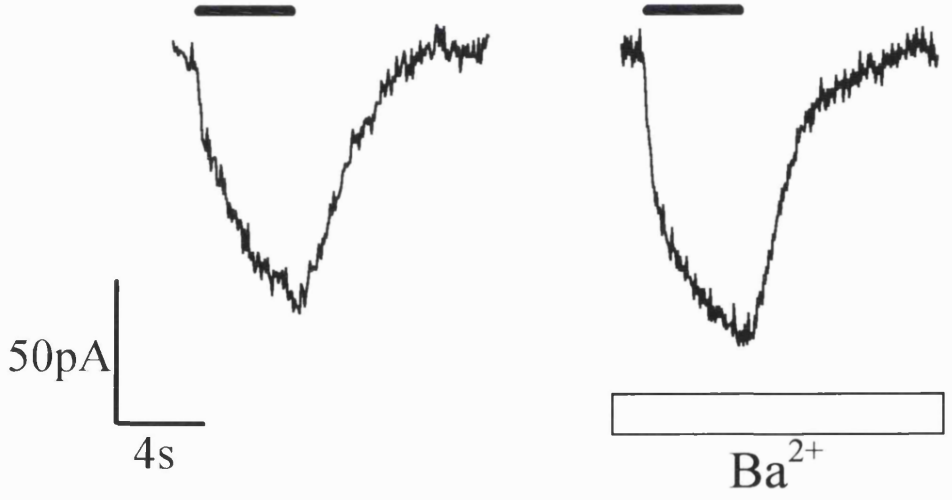
50pA
4s
Ba2+

voltage-dependence similar to that of the current evoked by D-aspartate, see below; Newman, 1985).

These pharmacological data suggest that the current is generated by D-aspartate being taken up into Purkinje cells by glutamate transporters (with the inward current being generated partly by co-transported Na^+ ions and partly by Cl^- movement through an anion channel in the carrier's structure, as described below).

5.4 Voltage-dependence of the current

Glutamate uptake carriers are thought to cotransport 2 Na^+ ions into the cell with each glutamate anion, and to counter-transport a K^+ and a OH^- out of the cell, so that a net positive charge is carried in with every cycle (Bouvier *et al.*, 1992). The resulting inward current is smaller at more positive potentials because at a positive potential it is harder to move positive charge into the cell. Consequently the current generated by salamander glial glutamate uptake (Brew and Attwell, 1987), and by EAAC1 glutamate uptake (Kanai *et al.*, 1995), has a strong voltage-dependence, being reduced at positive potentials. Fig. 5.7 shows the current-voltage relationship of the D-aspartate-evoked current in Purkinje cells in the presence of 1mM kynurenate and 50μM D-APV. The current was inward at large negative potentials. As the potential was made less negative the current got smaller. At positive potentials it was small but could be either inward or outward. Overall the current-voltage relationship showed quite strong inward rectification. This I-V relation is similar to that of the salamander glial and mammalian EAAC1 glutamate transporters, which tends towards zero at positive potentials (Barbour *et al.*, 1991; Kanai *et al.*, 1995), but may show a small outward current generated by a Cl^- channel in the transporter structure (Wadiche *et al.*, 1995a).

By contrast, iontophoresing L-glutamate evoked a membrane current with a different current-voltage relationship, as shown in Fig. 5.8. The current-voltage relationship is roughly ohmic or outwardly rectifying, with a clear outward current at positive potentials and a reversal potential around zero. Like the pharmacological data presented above, these results suggest that glutamate generates mostly non-NMDA receptor-mediated

Fig. 5.7 Voltage-dependence of D-aspartate-evoked currents in whole-cell clamped Purkinje cells in cerebellar slices in the presence of 100μM picrotoxin, 1mM kynurenate and 50μM D-APV. **A.** Specimen currents evoked by D-aspartate (applied onto the soma during bar) in one cell at different voltages. **B.** I-V relationship for the current evoked by D-aspartate. Pipette solution was solution D, Table 2.2. Data are mean ± S.E.M., and normalised at -96mV for each cell. Data are taken from 17 cells.

A
D-Asp
+24mV
-6mV
-36mV
-66mV
-96mV
40pA
4s
B
Normalized Current
0.8
0.4
0.0
-0.4
-0.8
-1.2
-1.6
-150
-100
-50
0
50
mV
17 cells

Fig. 5.8 Voltage-dependence of L-glutamate-evoked currents in whole-cell clamped Purkinje cells in cerebellar slices in the presence of 100μM picrotoxin. **A.** Specimen currents evoked by L-glutamate (applied during bar) in one cell at different voltages. **B.** I-V relationship for the current evoked by L-glutamate. Pipette solution was solution D, Table 2.2. Data are mean ± S.E.M., and normalised at -96mV for each cell. Data are taken from 6 cells.

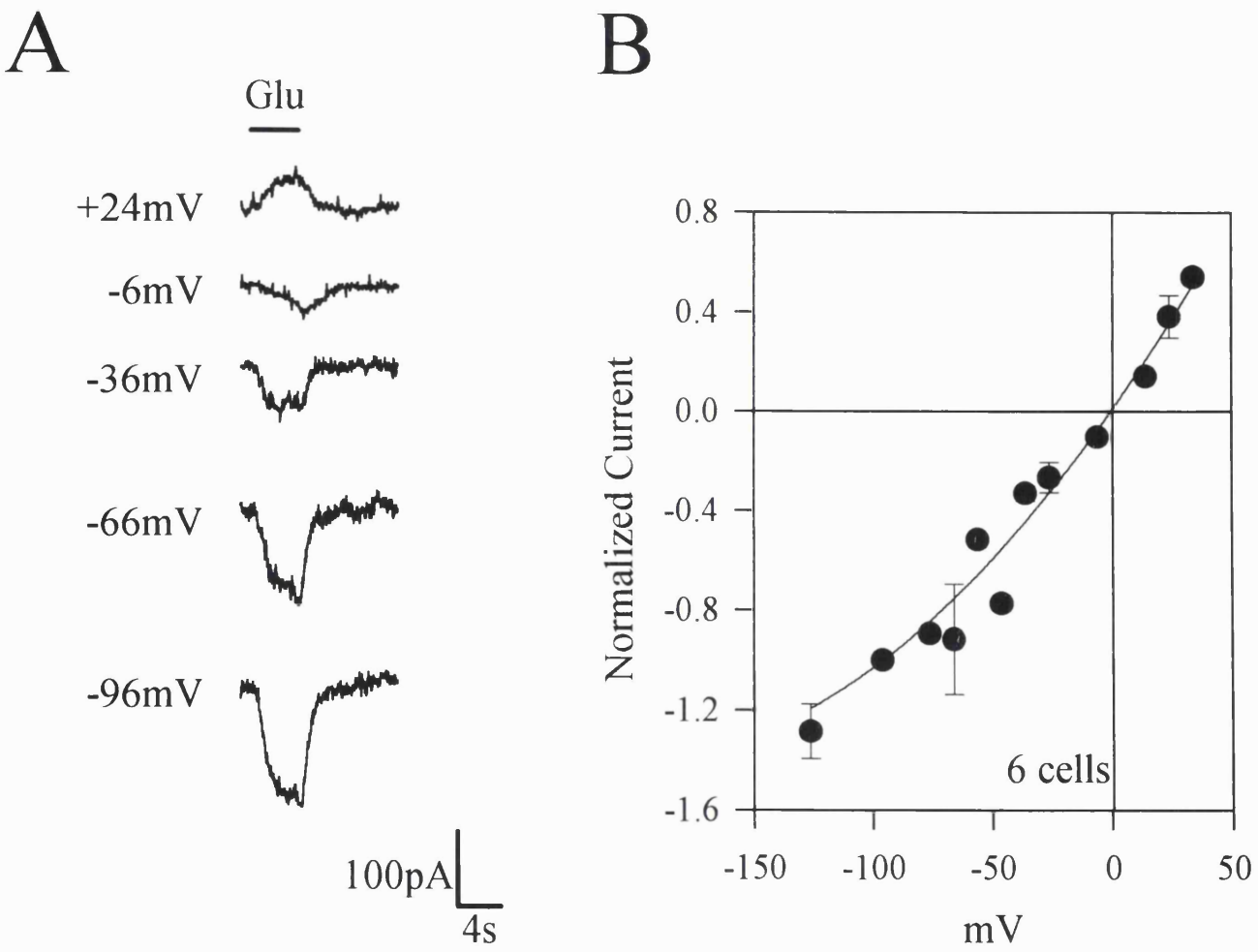
A
Glu
+24mV
-6mV
-36mV
-66mV
-96mV
100pA
4s
B
Normalized Current
0.8
0.4
0.0
-0.4
-0.8
-1.2
-1.6
6 cells
-150
-100
-50
0
50
mV

current, while D-aspartate activates a current generated mainly by glutamate uptake carriers.

Interestingly, iontophoresing the glutamate uptake blocker PDC onto a Purkinje cell also generated a membrane current in the presence of kynurenate, APV and CNQX (Fig. 5.9; current seen in all 3 cells to which PDC was applied). This current is probably generated by PDC being transported into Purkinje cells by glutamate uptake carriers, since PDC is a substrate for the uptake carriers in salamander glial cells (Sarantis *et al.*, 1993).

5.5 Dependence on external sodium

The glutamate-evoked uptake current in salamander glial cells has a strong dependence on external sodium (Brew and Attwell, 1987), as has the current generated by EAAC1 uptake carriers expressed in *Xenopus* oocytes (Kanai and Hediger, 1992). Fig. 5.10 shows that replacement of external sodium with choline reversibly abolished the D-aspartate-evoked current in Purkinje cells (in the presence of 100μM picrotoxin, 1mM kynurenate and 50μM D-APV), consistent with the current being produced by uptake.

5.6 Dependence on internal perchlorate

Bouvier *et al.* (1992) have shown that intracellular perchlorate ions increase the inward current generated by the salamander glial uptake carrier when glutamate is applied extracellularly . This is now known to be because perchlorate ions are more permeant than chloride ions (Billups *et al.*, 1996; Eliasof and Jahr, 1996) through the carrier's anion channel (Wadiche *et al.*, 1995a). Replacement of internal chloride ions with perchlorate ions increased the size of the inward current evoked at -93mV by D-aspartate in Purkinje cells by 261%, from 115.3±42.4pA (10 cells) to 301.5±85.5pA (4 cells), as shown in Fig. 5.11A. These values are significantly different with $p=0.048$ (2 tailed t-test). The current-voltage relationship for the D-aspartate-evoked current with perchlorate ions inside is shown in Fig. 5.11B. Including perchlorate ion in the pipette solution made the current clearly inward at potentials as positive as +30mV (done in 4 cells).

Fig. 5.9 Voltage-dependence of PDC-evoked current in whole-cell clamped Purkinje cells in a cerebellar slice in the presence of 100μM picrotoxin, 1mM kynurenate and 50μM D-APV. **A.** Specimen currents evoked by PDC (applied during bar) in one cell at different voltages. **B.** I-V relationship for the current evoked by PDC. Pipette solution was solution D, Table 2.2. Data are normalised at -96mV.

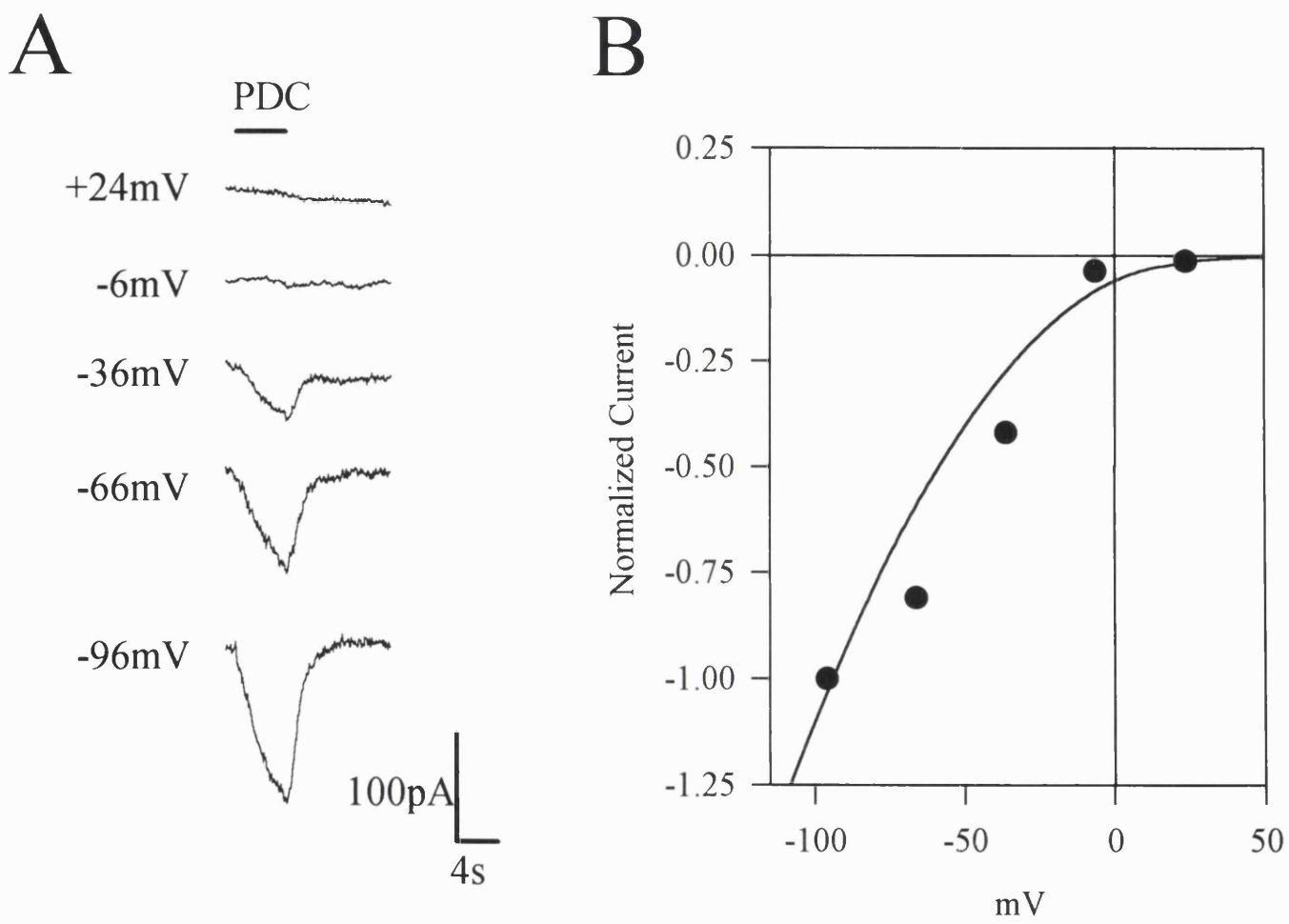
A
PDC
+24mV
-6mV
-36mV
-66mV
-96mV
100pA
4s
B
Normalized Current
0.25
0.00
-0.25
-0.50
-0.75
-1.00
-1.25
-100
-50
0
50
mV

Fig 5.10 Na^+-dependence of D-aspartate-evoked current in whole-cell clamped Purkinje cells in a cerebellar slice in the presence of 100μM picrotoxin, 1mM kynurenate and 50μM D-APV. **A.** D-aspartate (bar) evoked an inward current. Bath solution was solution B, Table 2.1. **B.** The D-aspartate-evoked current was abolished when external sodium ions were completely replaced by choline. Bath solution was (in mM): CholineCl 141; KCl 1.5; $CaCl_2$ 2.5; $MgCl_2$ 2; HEPES 10; glucose 10; KH_2PO_4 1, pH 7.4 adjusted with NMDG. **C.** On replacing the choline with sodium ions the current was recovered. Pipette solution was solution D, Table 2.2. Data are typical of 3 cells. The membrane was held at -96mV.

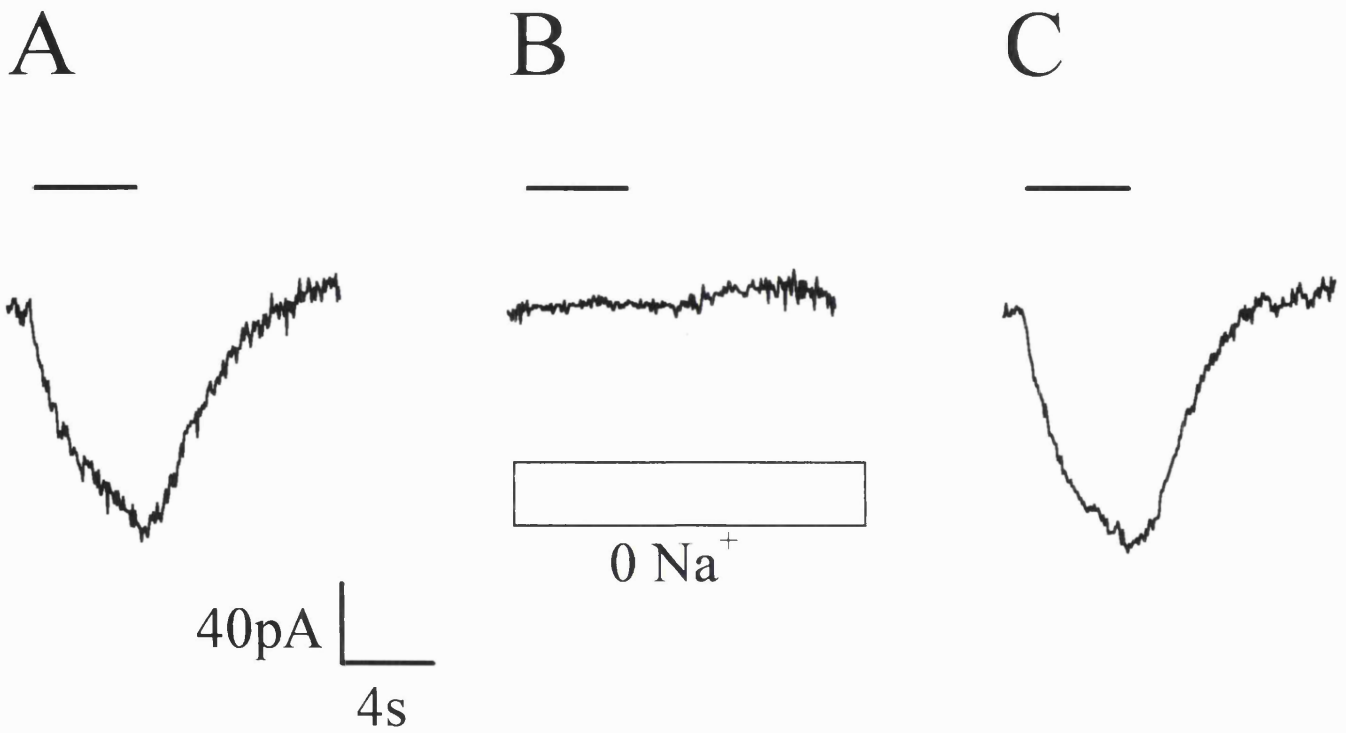
A
B
C
0 Na+
40pA
4s

Fig 5.11 Anion-dependence of D-aspartate-evoked current in whole-cell clamped Purkinje cells (in the presence of 1mM kynurenate, 50μM D-APV and 50μM CNQX). **A.** Specimen records from different cells showing the current evoked at +27mV and -93mV by D-aspartate with chloride or perchlorate as the main internal anion (solution E and F, Table 2.2). Extracellular solution contained Ba^{2+} to block K^+ conductance (solution C, Table 2.1). **B.** Current-voltage relationship of the D-aspartate-evoked current with perchlorate inside (•, 4 cells) or Cl^- inside (◦, 5 cells). Data for the different anions were first normalised at -93mV for each cell, and then averaged over the different cells. The average D-aspartate-evoked currents with Cl^- inside were then scaled down using the ratio of the mean current sizes at -93mV with perchlorate or Cl^- inside. Error bars show S.E.M.

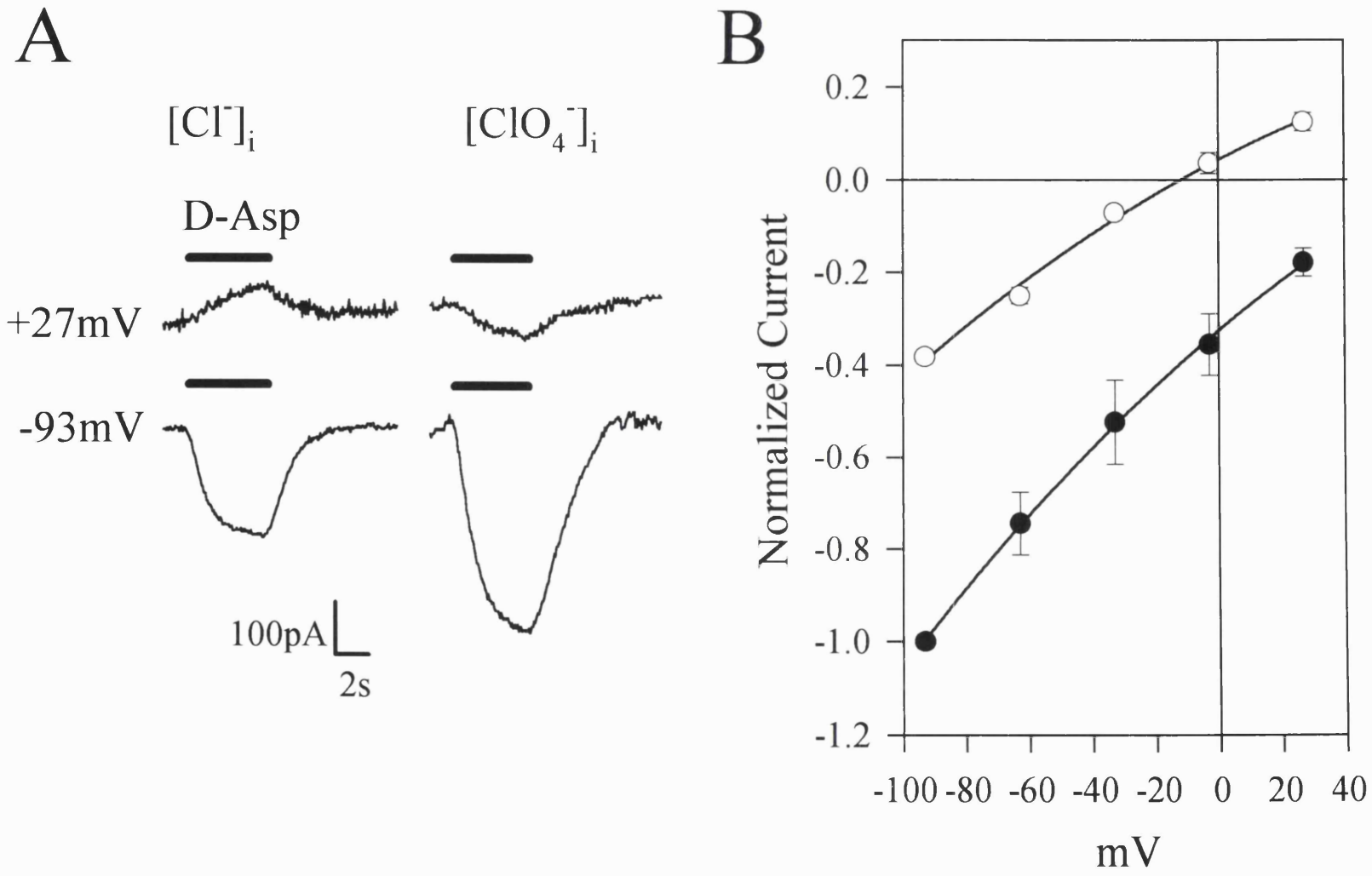
A
$[Cl^-]_i$
$[ClO_4^-]_i$
D-Asp
+27mV
-93mV
100pA
2s
B
Normalized Current
0.2
0.0
-0.2
-0.4
-0.6
-0.8
-1.0
-1.2
-100 -80 -60 -40 -20 0 20 40
mV

5.7 Dependence on external chloride

All of the four cloned mammalian glutamate transporters have been shown to activate an anion conductance when they bind external glutamate and Na^+ ions (Fairman *et al.*, 1995; Wadiche *et al.*, 1995a). Consistent with this, lowering the extracellular chloride concentration from 155mM to 45mM resulted in a shift of the reversal potential positive by 24±5mV in 5 cells (Fig. 5.12), as has been observed previously for the EAAT1 transporter (Wadiche *et al.*, 1995a). The Nernst potential for a Cl^--specific channel would be shifted 32mV by this $[Cl^-]_o$ change.

5.8 Change of EPSC kinetics by inhibiting postsynaptic glutamate uptake

The data described above established the presence of electrogenic glutamate uptake in Purkinje cells which are postsynaptic to the climbing and parallel fibre synaptic terminals. Although it is not known how closely uptake carriers may be located in the postsynaptic membrane to the sites where glutamate is released presynaptically, it would be interesting to know whether postsynaptic uptake is significant for terminating the synaptic action of glutamate. As described in Chapter 4, superfusing the glutamate uptake blocker PDC prolonged the EPSC at the climbing fibre and parallel fibre synapses onto the Purkinje cells. However, such experiments do not determine whether the EPSC prolongation is due to a slowing of postsynaptic uptake in Purkinje cells, of uptake into presynaptic terminals, or of glial uptake in surrounding Bergmann glial cells. Therefore an attempt was made to block glutamate uptake specifically in the Purkinje cells without changing glial or presynaptic uptake.

The strategy used to block Purkinje cell uptake alone was to include D-aspartate in the whole-cell pipette used to clamp the cell. It is known that internal glutamate slows the uptake of external glutamate (Barbour *et al.*, 1991), presumably by binding to the carriers' glutamate-binding site at the inner surface of the membrane, making it harder for the carrier to lose glutamate at that surface and re-orient to the outer surface to pick up more glutamate. Since D-aspartate can also bind to the glutamate transport site, then internal D-aspartate ought be expected to slow glutamate uptake. The next section

Fig. 5.12 Effect of external chloride concentration on the D-aspartate-evoked current (in the presence of 1mM kynurenate, 50μM D-APV and 50μM CNQX). Mean normalised I-V data for the response with normal $[Cl^-]_o$ (155mM; •) or with $[Cl^-]_o$ reduced to 45mM by replacement with gluconate (◦). Bath solution was (in mM): NaCl (131 or 21); Na-gluconate (0 or 110); $BaCl_2$ 6; KCl 2.5; $CaCl_2$ 2.5; HEPES 10; $MgCl_2$ 2; glucose 10. Major cation in the pipette solution was K^+ (solution E, Table 2.2). A 4M NaCl agar bridge was used to earth the bath, to avoid changes in junction potential when the external $[Cl^-]$ was altered.

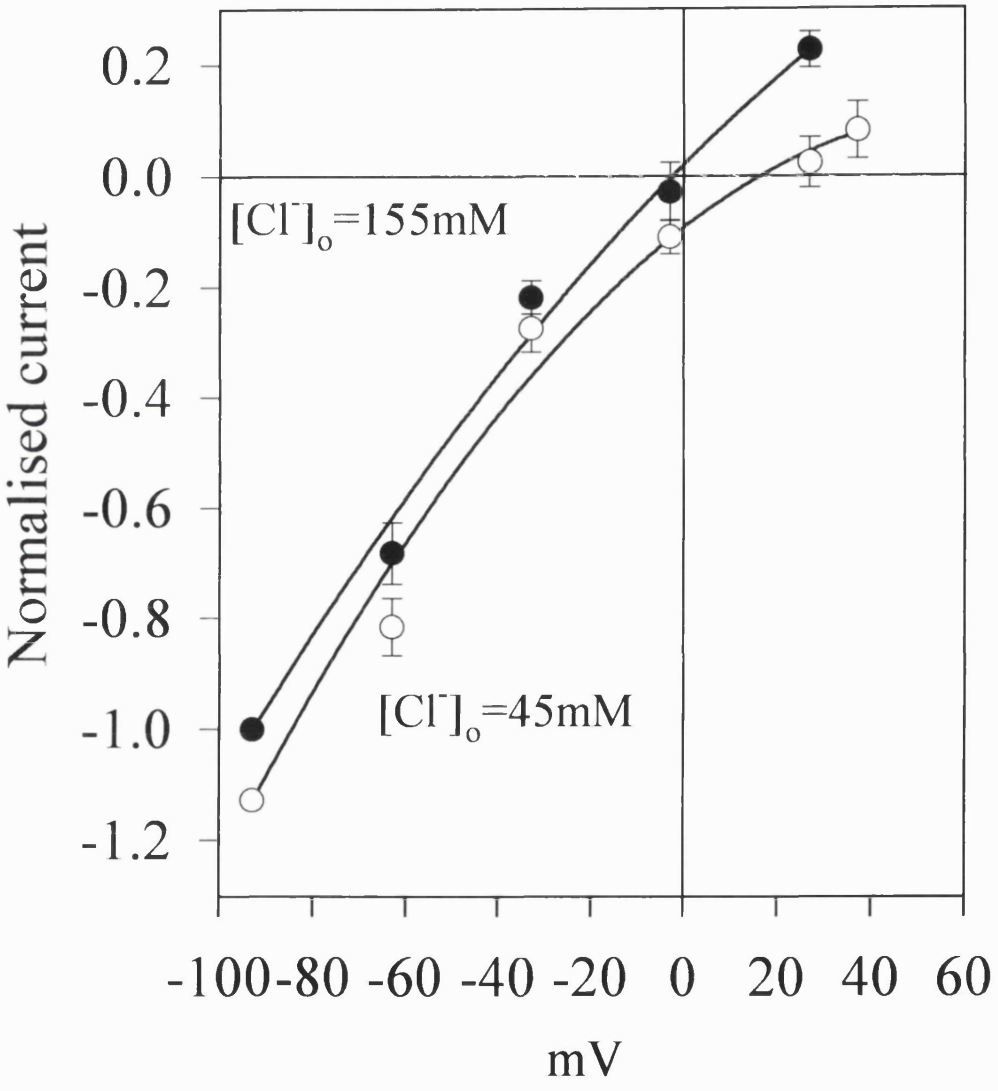
0.2
0.0
-0.2
-0.4
-0.6
-0.8
-1.0
-1.2
Normalised current
[Cl-]o=155mM
[Cl-]o=45mM
-100 -80 -60 -40 -20 0 20 40 60
mV

(5.8.1) describes experiments which verify this hypothesis. Having shown that internal D-aspartate slows uptake, I then went on to test the effect of this manoeuvre on the EPSC evoked in the Purkinje cell by stimulation of the climbing fibre input (sections 5.8.2 and 5.8.3). The climbing fibre synapses were chosen for this analysis because, in the 12 day old rats used, they impinge much closer to the soma where D-aspartate is introduced than do the parallel fibre synapses (Altman, 1972).

5.8.1 Effect of internal D-aspartate on iontophoretically-evoked uptake current

Adding 20mM Na-D-aspartate to the pipette solution (replacing NaCl) to try to slow uptake, reduced the current produced by iontophoresed D-aspartate (Fig. 5.13). The reduction was by 53%, from 111±24pA in 14 cells studied with D-aspartate inside to 52±14pA in 11 cells without D-aspartate ($p<0.06$, 2-tailed t-test).

5.8.2 Comparison of climbing fibre EPSC decay with and without uptake inhibited in different cells

The effect on the climbing fibre EPSC of blocking uptake with internal D-aspartate was investigated in two different ways. In the first set of experiments, climbing fibre EPSCs evoked in different cells clamped with a solution either containing or lacking D-aspartate were compared (Fig. 5.14). With D-aspartate inside the EPSC decay time constant (8.89±0.96msec, measured from 90% to 10% of the current amplitude, 16 cells) was significantly longer ($p<0.02$, 2-tailed t-test) than that with no D-aspartate inside (6.33±0.58msec, 24 cells). In addition, the EPSC amplitude was reduced (Fig. 5.14) as was also seen with an extracellularly applied uptake blocker (Fig. 4.1). Although this reduction of amplitude was not significant ($p=0.195$), it may occur because a local rise in $[glu]_o$ produced by blocking uptake desensitized postsynaptic receptors (Chapter 4).

Replacing 20mM Cl^- by D-asp^- is expected to increase the resistivity of the pipette solution by 5% because of the lower mobility of D-asp^-, but the series resistance remaining uncompensated in the two groups of the cells was similar (1.04±0.46MΩ in control cells, 0.95±0.32MΩ with D-aspartate inside), suggesting that the longer EPSC

Fig. 5.13 Effect of intracellular D-aspartate on the D-aspartate-evoked current (in the presence of 1mM kynurenate, 50μM D-APV and 50μM CNQX). **A.** Response to iontophoresed D-aspartate (bar) in a cell clamped with a pipette lacking D-aspartate (solution G, Table 2.3). Data typical of 14 cells. **B.** Response of a different Purkinje cells clamped with a pipette containing 20mM D-aspartate (Solution H, Table 2.3). Data typical of 11 cells. The holding potential was -96mV.

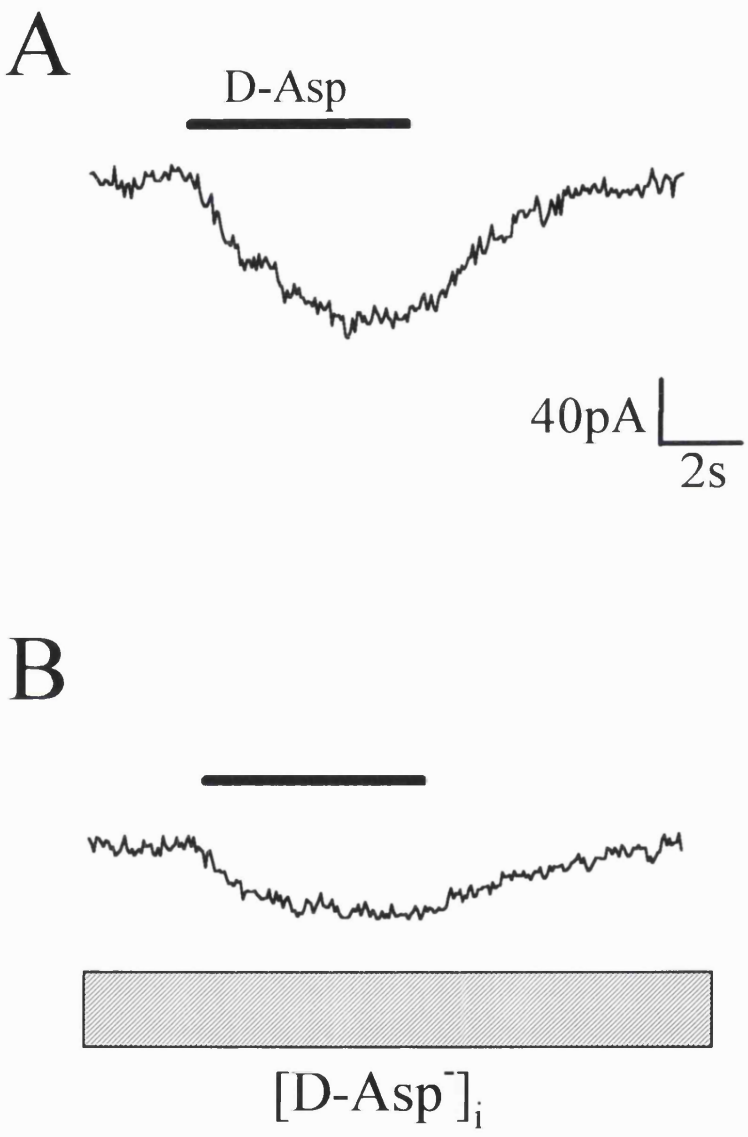
A
D-Asp
40pA
2s
B
[D-Asp⁻]i

Fig. 5.14 Effect of inhibiting postsynaptic uptake on the climbing fibre EPSC decay. **A.** The climbing fibre EPSC decay time constant ± S.E.M. in 24 control cells clamped with electrodes lacking D-aspartate (open bar; solution G, Table 2.3) and in 16 cells clamped with electrodes containing 20mM Na-D-aspartate (filled bar; solution H, Table 2.3). **B.** Peak amplitude ± S.E.M. in the same groups of cells as in **A**. The holding potential was -36mV to inactivate voltage gated Na^+ and Ca^{2+} currents (see Methods).

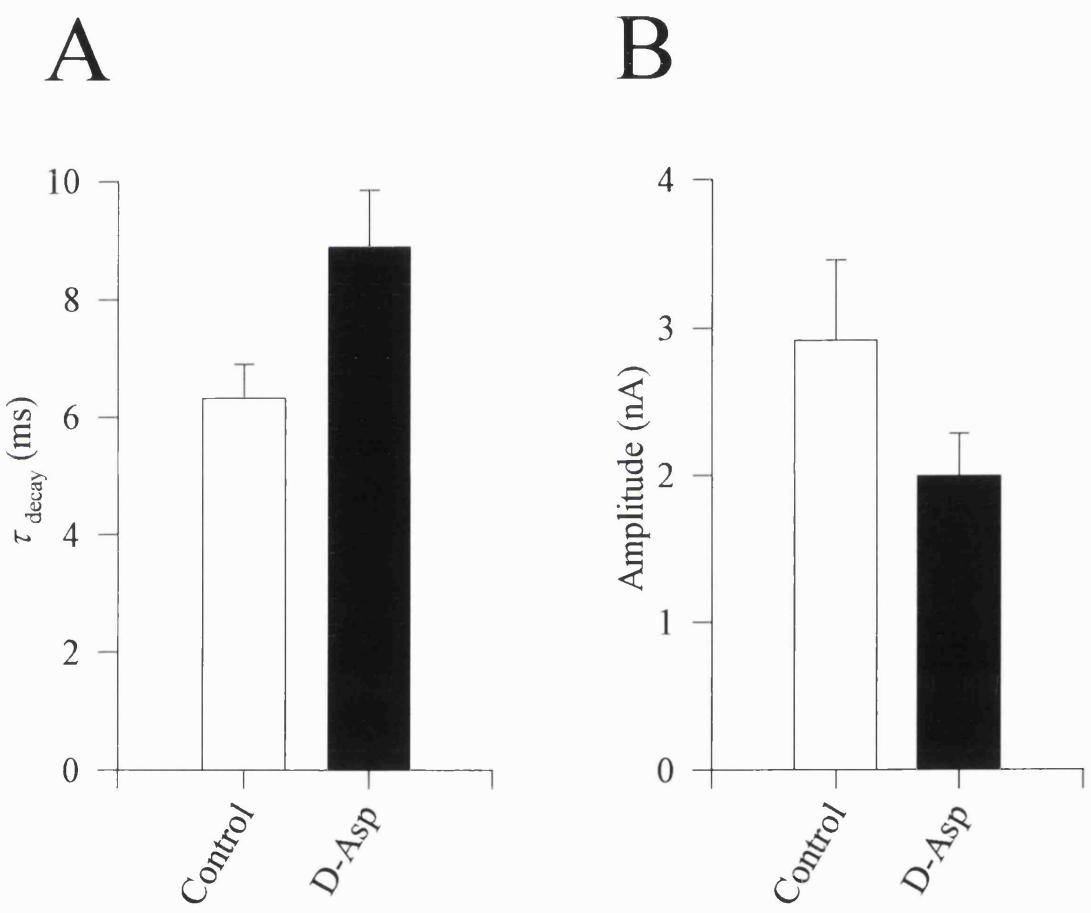
A
B
10
8
6
4
2
0
τ_{decay} (ms)
Control
D-Asp
4
3
2
1
0
Amplitude (nA)
Control
D-Asp

decay with D-aspartate inside was not due to more filtering by the combination of the series resistance and cell capacitance.

5.8.3 Comparison of climbing fibre EPSC decay with and without uptake inhibited in the same cells

Next, an attempt was made to measure the time constant without and with uptake blocked in the same cell (Fig. 5.15). First, the EPSC decay in a cell clamped with a pipette lacking D-aspartate was measured. Then, a second whole-cell electrode containing D-aspartate was attached and the EPSC decay was measured again (Fig. 5.15). The time constant just after the second (D-aspartate) electrode was attached was increased by about 20% from its value before the electrode was attached ($p=0.097$, 2-tailed paired t-test, $n=4$) in cells studied in this way, while in cells to which a second electrode filled with control internal solution was attached there was no change in time constant ($p=0.93$, $n=3$; Fig. 5.15A). These results are similar to those in Fig. 5.14 obtained by comparing separate cells clamped with and without internal D-aspartate. However, the amplitude reduction produced by D-aspartate in Fig. 5.14 was not routinely seen in these experiments. Indeed, on average, both for the cells for which the second electrode contained control solution, and for those for which it contained D-aspartate solution, the amplitude increased slightly when the second electrode was attached. The reason for this is unclear, but conceivably it is a result of leaving the cell not voltage-clamped briefly while attaching the second electrode (see Methods).

The parallel fibre EPSC decay was also studied by attaching a second electrode containing D-aspartate. The time constant was not affected by this operation (done in 3 cells, $p>0.87$, 2-tailed paired t-test: Fig. 5.16). This might well be explained by the fact that the parallel fibre synapses are much further from the soma, where D-aspartate was introduced, than are the climbing fibre synapses, so that enough D-aspartate did not reach the parallel fibre synapses to significantly reduce postsynaptic uptake. Alternatively, for the parallel fibre synapses, postsynaptic uptake may be less important than uptake into surrounding glial cells or into the presynaptic terminal.

Fig. 5.15 Effect of inhibiting postsynaptic uptake on the climbing fibre EPSC. **A.** Normalized climbing fibre decay time constant (mean ± S.E.M.) for cells clamped with a pipette containing the control solution (solution G, Table 2.3), and then with an extra pipette (in current-clamp mode) containing control solution (∘, 3 cells) or 20mM D-aspartate solution (•, 4 cells; solution H, Table 2.3). The second pipette was attached at the time indicated. **B.** Specimen data from one cell for the experiment of **A**, showing the EPSC before (control) and after (D-asp) the D-aspartate electrode was attached (*Left* and *Middle*), and these traces normalised and superimposed (*Right*).

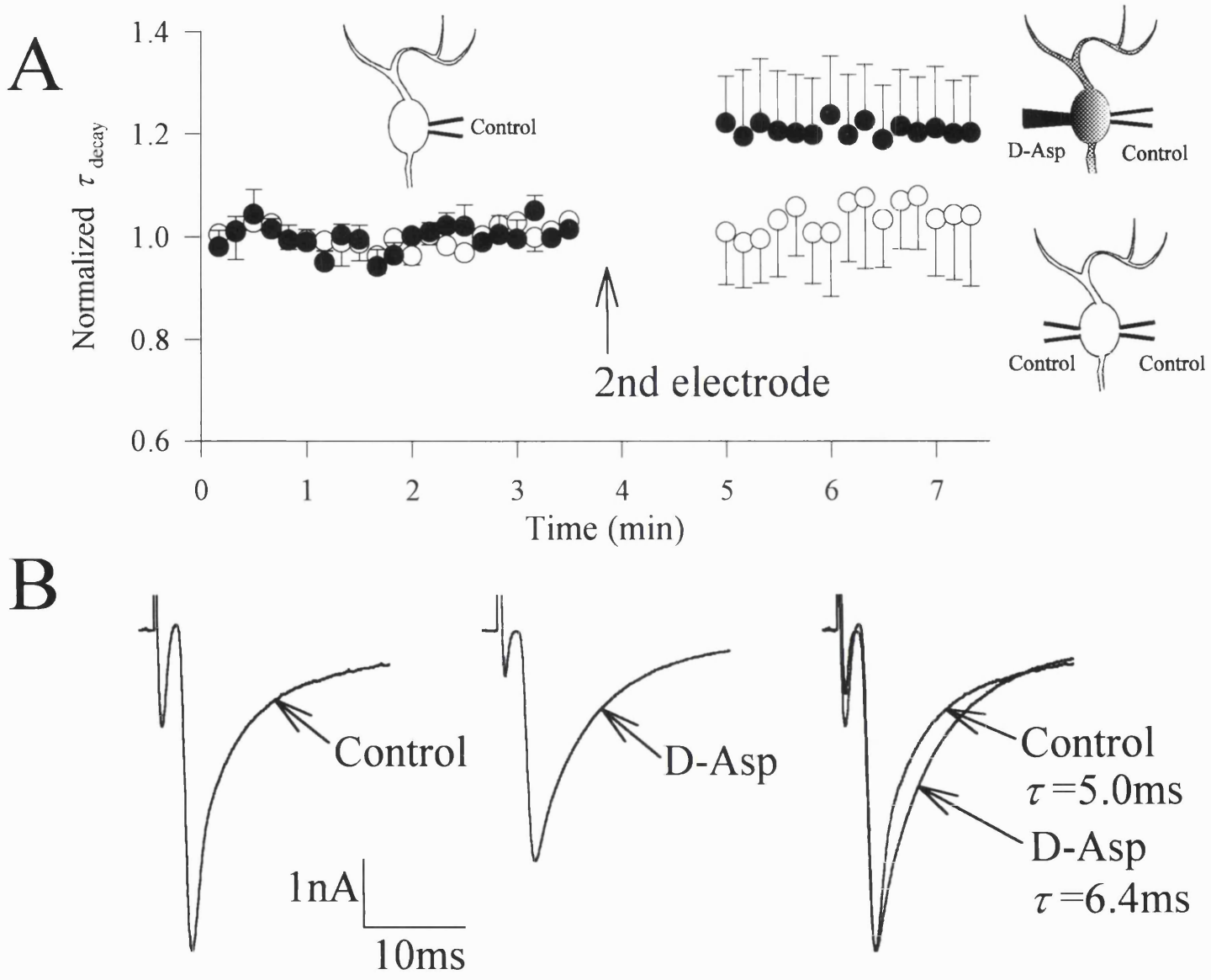
A
Normalized τ_{decay}
1.4
1.2
1.0
0.8
0.6
0
1
2
3
4
5
6
7
Time (min)
Control
2nd electrode
D-Asp
Control
Control
Control
B
Control
D-Asp
1nA
10ms
Control
τ =5.0ms
D-Asp
τ =6.4ms

Fig. 5.16 Effect of inhibiting postsynaptic uptake on the parallel fibre EPSC. Normalized parallel fibre decay time constant for 3 cells clamped to -36mV with a pipette containing the control solution (solution G, Table 2.3), and then with an extra pipette (in current-clamp mode) containing 20mM D-aspartate solution (solution H, Table 2.3) at the time shown. Error bars show S.E.M.

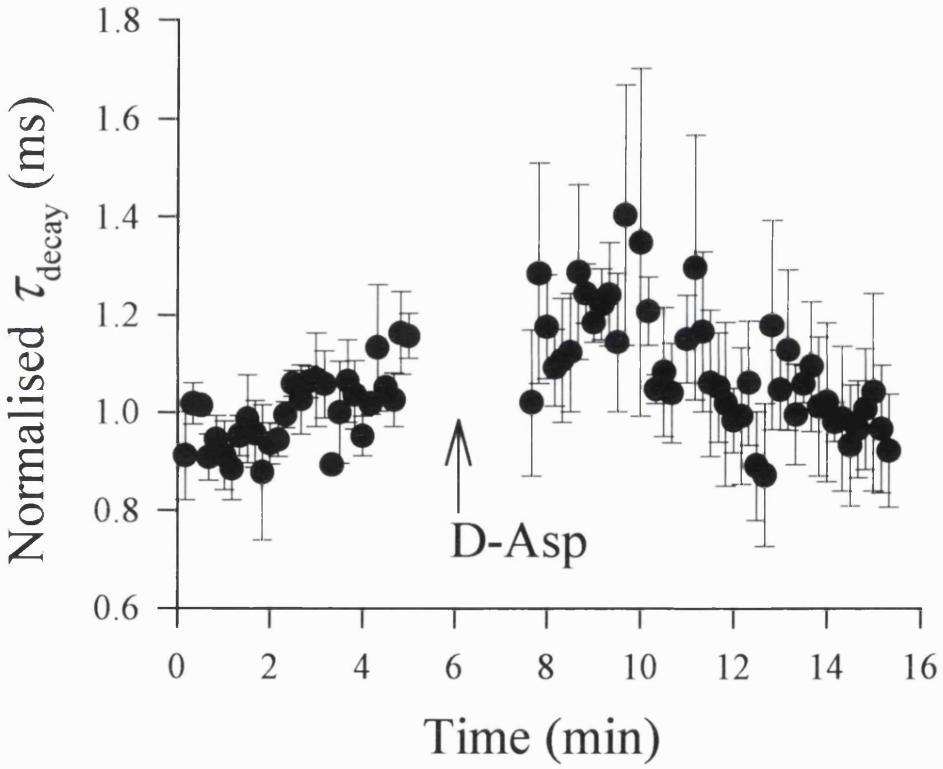
Normalised τ_{decay} (ms)
1.8
1.6
1.4
1.2
1.0
0.8
0.6
D-Asp
0
2
4
6
8
10
12
14
16
Time (min)

5.9 Reversed uptake in Purkinje cells

Glutamate uptake carriers have been shown to be able to operate backwards under certain conditions (Szatkowski *et al.*, 1990), releasing glutamate into the extracellular space. As explained in Chapter1, the stoichiometry of this process is thought to involve one glu^- anion and 2 Na^+ being transported out of the cell, while one K^+ and one OH^- enter (Szatkowski *et al.*, 1990; Bouvier *et al.*, 1992; Billups and Attwell, 1996). Consequently reversed uptake generates an outward membrane current.

To test whether the Purkinje cell glutamate transporters can generate significant current by this reversed operation, the external $[K^+]$ was raised around Purkinje cells clamped to a depolarised potential with electrodes containing 20mM Na-glutamate: conditions which mimic the ion gradient changes occurring in ischaemia (Szatkowski and Attwell, 1994). Fig. 5.17 shows that this operation generated an outward current (46±8pA in 9 cells) at positive potentials, which was suppressed by external D-aspartate. A similar current in salamander glial cells (Szatkowski *et al.*, 1990) has been shown to be correlated with glutamate release by reversed uptake (Billups and Attwell, 1996). At more negative potentials raising the potassium concentration evoked an inward current shift. This suggests that the outward reversed uptake current which presumably occurs in the Purkinje cells was obscured by a K^+-evoked inward current that may be due to K^+ entry through unblocked K^+ channels.

For cells clamped with a pipette solution containing NaCl instead of Na-glutamate, raising K^+ evoked no outward current at +40mV in 4 out of 6 cells tried (Fig. 5.18), but in the remaining cells it gave current changes like those seen in cells with glutamate inside, possibly indicating a lack of complete dialysis of endogenous glutamate out of the cell. The mean K^+-evoked current in all 6 cells was 19±12pA.

Fig. 5.17 K^+-evoked outward current produced by reversed uptake in Purkinje cells. **A.** Raising $[K^+]$ from 0 to 30mM (bar) evoked an outward current. **B.** Superfusing 100μM D-aspartate suppressed the current. **C.** The current was recovered after washing out the D-aspartate. Data typical of 9 cells. Pipette solution contained (in mM): TEACl (to block K^+ channels; reviewed by Stanfield, 1983) 119; Na-glutamate 20; $CaCl_2$ 0.5; $NMDG_2$-EGTA 5; HEPES 10; malonic acid 0.2 (to block succinate dehydrogenase, Horn, 1989); aminooxyacetic acid 5 (to block glutamate transaminases, Horn, 1989). Bath solution contained (in mM): NaCl 103.5; CholineCl (30 or 0); KCl (0 or 30); $BaCl_2$ 6; $CaCl_2$ 2.5; HEPES 10; $MgCl_2$ 2; glucose 10; picrotoxin 0.1; DNQX 0.1; ouabain 0.1 (to block Na^+ pump; reviewed by Yingst, 1988). The holding potential was +37mV.

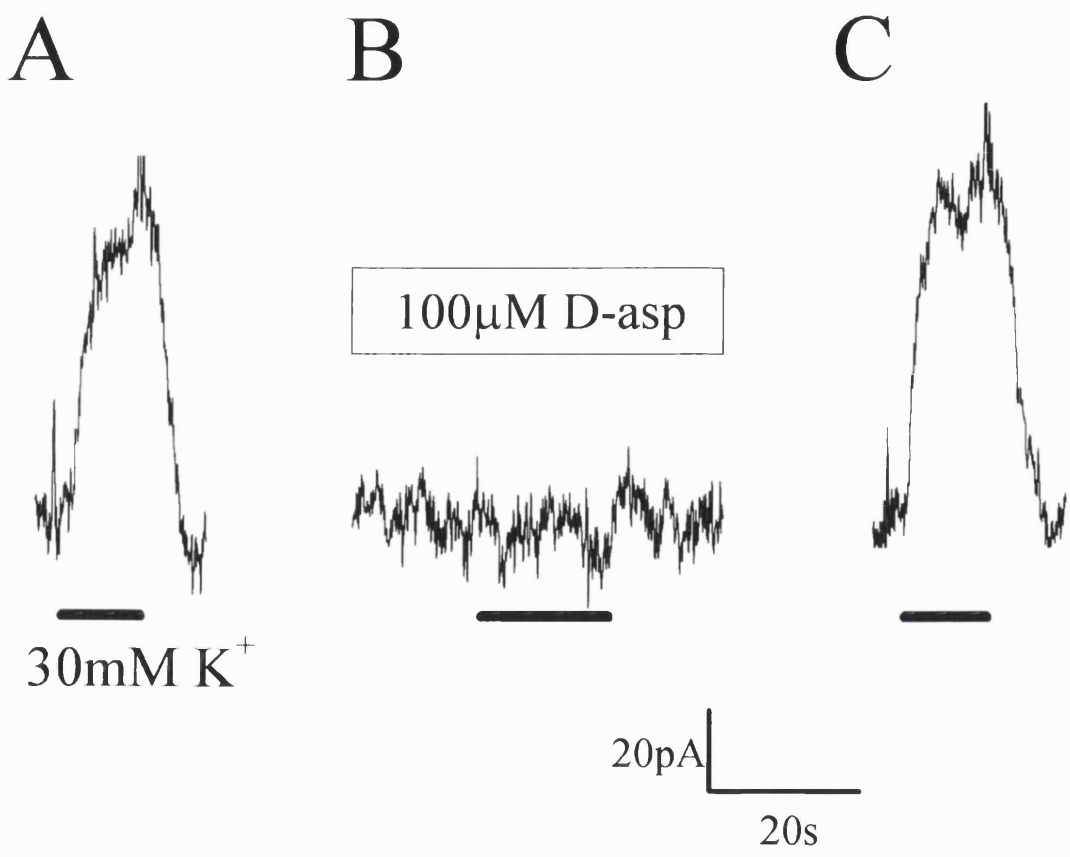
A
B
C
100μM D-asp
30mM K+
20pA
20s

Fig. 5.18 Raising [K^+] does not evoke outward current in a Purkinje cell lacking [glu]. **A-C.** Raising [K^+] from 0 to 30mM (bar) did not change the membrane current in the presence and absence of 100μM D-aspartate. This result was seen in 4 cells, but in 2 other cells an outward K^+-evoked current was seen (see text). Pipette solution contained (in mM): TEACl 119; NaCl 20; $CaCl_2$ 0.5; $NMDG_2$-EGTA 5; HEPES 10; malonic acid 0.2; aminooxyacetic acid 5. Bath solution contained (in mM): NaCl 103.5; CholineCl (30 or 0); KCl (0 or 30); $BaCl_2$ 6; $CaCl_2$ 2.5; HEPES 10; $MgCl_2$ 2; glucose 10; picrotoxin 0.1; DNQX 0.1; ouabain 0.1. The holding potential was +37mV.

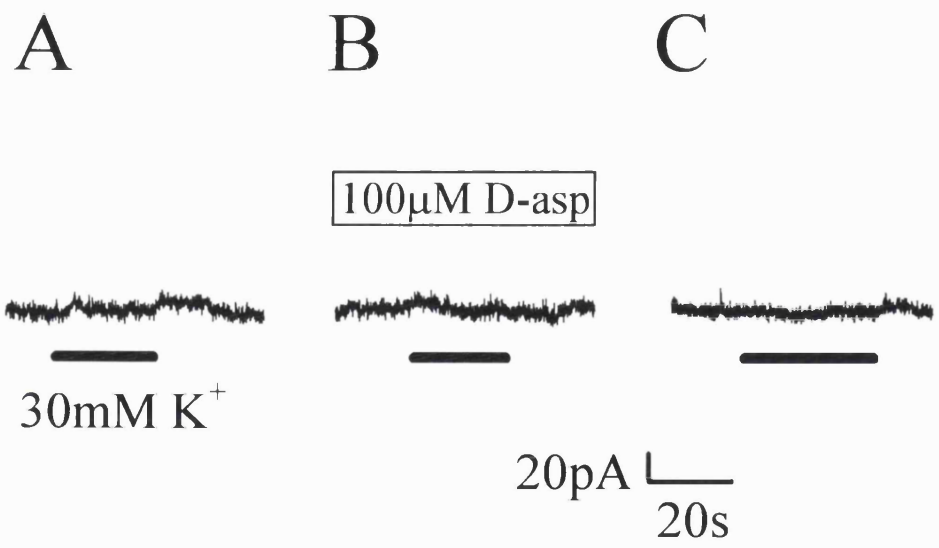
A
B
C
100μM D-asp
30mM K+
20pA
20s

5.10 Discussion

5.10.1 Identification of the carriers

The experiments described above show that glutamate uptake carrier expression in Purkinje cells can be detected electrophysiologically. Antibody staining (Rothstein *et al.*, 1994) suggested the presence of EAAC1 transporters in Purkinje cells. Kanai and Hediger (1992) reported that EAAC1 transporters, when expressed in *Xenopus* oocytes, are electrogenic and their activity is completely Na^+-dependent as for the glutamate transporters in salamander Müller cells. The data reported here show that the same is true for the transporters in Purkinje cells. Furthermore the voltage-dependence of the D-aspartate-evoked current recorded with caesium in the Purkinje cells (Fig. 5.7A) is similar to that for uptake currents in salamander Müller cells and for EAAC1 expressed in oocytes (Brew and Attwell, 1987; Kanai *et al.*, 1995).

In Purkinje cells, non-NMDA receptors mediate synaptic transmission in response to glutamate released presynaptically (Perkel *et al.*, 1990; Konnerth *et al.*, 1990). To explain the small outward current evoked sometimes by D-aspartate at positive potentials (Fig. 5.7A), there are three possibilities: (1) D-aspartate opened AMPA receptors directly; (2) D-aspartate inhibits uptake in surrounding cells and raises the extracellular glutamate concentration which leads to opening of non-NMDA channels in Purkinje cells; or (3) uptake generates an outward current by opening an anion channel in the carrier structure (Wadiche *et al.*, 1995a). Arguing against the first two possibilities, Fig. 5.3 showed that there was little effect of glutamate receptor blockers on the D-aspartate-evoked current. In addition, experiments done by Barbour (1994) showed that membrane patches ripped off Purkinje cells did not respond to D-aspartate. Therefore, the third possibility would be the more probable explanation. Consistent with this, lowering the external Cl^- concentration altered the potential at which the D-aspartate-evoked current became outward (Fig. 5.12). Thus, the current generated when D-aspartate activates the glutamate transporters is the sum of 2 components: an inward current produced by the co-transport of sodium into the cell, and a current generated by

an anion channel activated during uptake, the sign of which depends on the [Cl^-] gradient and the cell membrane potential.

In contrast to the D-aspartate or PDC-evoked current, the I-V relationship of the glutamate-evoked current did not show strong inward rectification, and was largely blocked by kynurenate and CNQX, so the current was presumably generated largely by non-NMDA receptor-gated channels.

Although the data reviewed above are all consistent with the uptake current I observe being produced by the EAAC1 transporters which Purkinje cells have been shown to express (Rothstein *et al.*, 1994), unpublished work of Rothstein (personal communication) has also found expression of EAAT4 transporters on the soma and the dendrites of Purkinje cells. EAAT4 has a larger anion conductance than EAAC1 in its structure, which is activated when glutamate binds, and its I-V relation shows a clear outward current at positive potentials (Fairman *et al.*, 1995). The I-V relation I find with Cs^+ as the intracellular cation shows little outward current (Fig. 5.7A) suggesting little contribution of EAAT4 transporters. However with K^+ as the intracellular cation, a significant outward current was produced by D-aspartate (even in the presence of kynurenate, D-APV and CNQX: see section 5.6), and the I-V relation of the D-aspartate-evoked current (Figs. 5.11 & 5.12) is more ohmic like that for EAAT4. These results may indicate a contribution of EAAT4 to the D-aspartate-evoked current when K^+ is inside. The lack of a large outward current with Cs^+ inside might then be due to EAAT4 transporters having an intracellular K^+-binding site which is more selective (less able to accept Cs^+) than the corresponding site on EAAC1 transporters (or on the salamander carrier which does accept Cs^+: Barbour *et al.*, 1991).

5.10.2 The strength of postsynaptic uptake

The mean uptake current evoked by D-aspartate at -70mV with Cs^+ as the internal cation was I_m=64±11 (S.E.M.) pA in 12 Purkinje cell somata. An estimate of the strength of uptake can be made by assuming that the iontophoresed D-aspartate only acts on the soma at the surface of the slice (and does not diffuse into the slice and act on

transporters in the dendrites: the rapid flow of solution over the surface of the slice may make this a reasonable assumption). For a measured soma diameter of 18.6±0.5μm (measured for 10 cells from a TV monitor linked to the microscope), an uptake current of 64pA implies an uptake current density (0.06pA/μm^2) similar to that in salamander glial cells (Barbour *et al.*, 1991) (≈0.03pA/μm^2 for high [D-asp] at -70mV) and cerebellar astrocytes (Wyllie *et al.*, 1991) (≈0.1pA/μm^2 for 30μM [glu], assuming 1μF/cm^2 capacitance). Thus, the strength of Purkinje cell uptake suggests it has a significant role in lowering the extracellular glutamate concentration.

In vivo the uptake current will be increased by the presence of internal K^+ instead of Cs^+, but will be reduced by the presence of internal glutamate (Barbour *et al.*, 1991). The ability of uptake to lower $[glu]_o$ near the Purkinje cell can be estimated as follows, provided uptake is not powerful enough to reach equilibrium (i.e. to lower $[glu]_o$ to its equilibrium value of 0.2μM: Attwell *et al.*, 1993). If the maximum current evoked by a high [glu] *in vivo* is similar to the mean D-aspartate-evoked current of I_m=64pA (see above), at low $[glu]_o$ glutamate will be taken up at a rate

$$U = \frac{I_m[glu]_o}{zFK_m}$$

(from the low dose limit of the Michaelis-Menten equation), where F is the Faraday constant, K_m is the Michaelis-Menten constant for uptake being activated by glutamate, and z≈2 positive charges are moved (at -70mV) per glutamate (Wadiche *et al.*, 1995b: the human EAAT3 for which z=2 is homologous to rat EAAC1): one charge is moved because of the glutamate transport stoichiometry and one charge passes through the carrier's anion channel. At a distance r from the soma centre, the rate (Sarantis *et al.*, 1993) at which glutamate diffuses (with a coefficient $D \approx 7.6\times10^{-10} m^2 s^{-1}$) towards the soma through the extracellular space of tortuosity factor f=1.55 and volume fraction v=0.21 (Sarantis *et al.*, 1993, Nicholson and Phillips, 1981) is

$$\frac{Dv}{f^2} 4\pi r^2 \frac{d[glu]}{dr}$$

and in a steady state this must equal U. Thus

$$\frac{Dv}{f^2} 4\pi r^2 \frac{d[glu]}{dr} = \frac{I_m[glu]_o}{zFK_m}$$

Integrating this equation from the soma radius a to r= ∞ gives

$$\frac{[glu]_r}{[glu]_o} = 1 + \frac{I_m f^2}{4\pi zDFvK_m a}.$$

For a=9.3μm and Km=12μM (Kanai and Hediger, 1992) this gives $[glu]_o/[glu]_\infty$=0.2. Thus, the local [glu] will be reduced to 1/5 of its bulk value, i.e. from ≈3μM (Benveniste *et al.*, 1984; Hagberg *et al.*, 1985; Wahl *et al.*, 1994) to 0.6μM, which may reduce AMPA receptor desensitization (IC_{50}≈5μM, Colquhoun *et al.*, 1992, and see Chapter 4) and metabotropic receptor activation (Yuzaki and Mikoshiba, 1992), thus altering information processing by the Purkinje cell.

It is important to note, however, that if a substantial fraction of the D-aspartate-evoked current is produced by EAAT4 transporters (with z≈20, instead of 2 as assumed above, because of their large anion conductance: Fairman *et al.*, 1995), then the local reduction of [glu] produced by Purkinje cell uptake (calculated as above) would be only from 3μM to 2.2μM (instead of to 0.6μM).

5.10.3 A role for postsynaptic glutamate uptake in synaptic transmission

Postsynaptic uptake might provide glutamate to the Purkinje cell for formation of its transmitter GABA, but the transporter distribution in the cell's dendritic tree (Rothstein *et al.*, 1994) suggests a role in terminating synaptic transmission. A calculation suggests that Purkinje cell uptake could in principle contribute to terminating glutamate's synaptic action. If the carrier cycling rate (Wadiche *et al.*, 1995b) is 14/sec, and each cycle moves ≈2 unitary charges (at -70mV) into the cell (Wadiche *et al.*, 1995b), an uptake current of I_m=64pA at -70mV evoked by D-aspartate in a D=18.6μm diameter cell soma implies a mean density of 13,150 carriers/$(\mu m)^2$. If this density of carriers exists near

glutamate release sites (antibody labelling shows carriers throughout the dendritic tree; Rothstein *et al.*, 1994), the number of carriers within a 1.2μm radius circle (the distance glutamate diffuses in 1msec) is 6×10^4. Even if all the uptake current were generated by EAAT4 carriers, which have $z\approx20$ instead of $z\approx2$ as assumed above (Fairman *et al.*, 1995), the number of carriers close to a release site would still be 6×10^3. This is far greater than the number (80) of postsynaptic channels opened per vesicle at the climbing fibre synapse (Momiyama *et al.*, 1996) and greater than the number (4700) of transmitter molecules in a vesicle (Bruns and Jahn, 1995). If glutamate binding to carriers is rapid (Tong and Jahr, 1994), these carriers could, in principle, bind a significant fraction of the glutamate released in a single quantum, thus contributing to terminating synaptic transmission.

5.10.4 A role for postsynaptic glutamate uptake in ischaemia

The Purkinje cell glutamate transporters could also be run backwards at a significant rate by raising K^+ at a depolarised potential (Fig. 5.17) with glutamate and sodium present inside the cell. A similar current in salamander glia (Szatkowski *et al.*, 1990) has been shown to reflect glutamate release from the cell by reversed operation of glutamate transporters (Billups and Attwell, 1996), transporting $2Na^+$ and glu^- out of the cell and K^+ and OH^- into the cell. Purkinje cells are particularly prone to be killed by glutamate release in ischaemia (Cervos-Navarro and Diemer, 1991; Balchen and Diemer, 1992), despite having no NMDA receptors. Reversed operation (Szatkowski *et al.*, 1990; Szatkowski and Attwell, 1994) of the uptake carriers in their membrane (Fig. 5.17), releasing glutamate which will activate the cells' non-NMDA and metabotropic receptors, might account for this selective vulnerability.

Another possible cause of cell death in ischaemia is the glutamate transporter's anion conductance. Some cell death in ischaemia results from cell swelling following the entry of Na^+ and Cl^- into the cell, followed by water (Choi *et al.*, 1987). If the transporter's anion conductance is a significant fraction of the cell's anion conductance, Cl^- entry via the transporters' anion channel could facilitate cell swelling and death.

Chapter 6

Other factors which might contribute to shaping the EPSC waveform

6.1 Introduction

In this chapter I consider two other factors which might contribute to shaping the EPSC waveform: glutamate transport by cystine-glutamate exchangers, and glutamate buffering by NMDA receptor subunits.

Cystine, a disulfide amino acid, is abundant in the extracellular space (≈50μM: Bannai, 1986) and plays an important role in the body, being a precursor for the synthesis of glutathione, an anti-oxidant within cells. Once inside the cell, cystine is soon reduced to two cysteine molecules, whereby its intracellular level is kept negligibly low. The intracellular level of glutamate, on the other hand, is quite high (≈10mM) but its extracellular concentration is maintained very low (≈1μM) by diffusion and uptake into cells (Nicholls and Attwell, 1990). In cell membranes there is a cystine-glutamate exchanger which may normally use the outwardly directed glutamate concentration gradient to drive the movement of cystine into the cells. It seems possible therefore that, in addition to the Na^+-dependent glutamate transporters considered so far in this thesis, the glutamate-cystine exchanger might contribute to buffering glutamate or controlling the concentration of glutamate in the synaptic cleft.

Cerebellar Purkinje cells do not express functional NMDA receptors after postnatal day 10 in the rat (Konnerth *et al.*, 1990; Perkel *et al.*, 1990; Momiyama *et al.*, 1996). However, immunohistochemical data showed that Purkinje cells do express NR1 subunits abundantly after postnatal day 10 (Petralia *et al.*, 1994), and the antibody staining showed dense expression at the postsynaptic density. Thus NR1 subunits might, in principle, help to buffer extracellular glutamate.

This chapter describes experiments which investigate whether these two additional factors contribute to determining the synaptic current waveform at the climbing fibre to Purkinje cell synapse.

6.2 Methods

These are described in detail in Chapter 2. Excitatory synaptic input was activated by stimulating the climbing fibre projecting to the Purkinje cell. Inputs were identified as described in Chapter 3 (section 3.3). All experiments in this chapter were carried out in the presence of 100μM picrotoxin to block inhibitory $GABA_A$ receptors on the Purkinje cell.

6.3 Effect of internal and external cystine

To try to detect an effect of glutamate-cystine exchange on buffering or removal of extracellular glutamate during the EPSC, cystine (1mM) was introduced into the Purkinje cell via the whole-cell pipette. If the glutamate-cystine exchanger can help to remove glutamate from the synaptic cleft, and thus shape the climbing fibre EPSC, this manipulation should increase the rate of glutamate removal, and the decay of the climbing fibre EPSC would be faster. Concentrations of internal cystine higher than 1mM were not tested since they were insoluble at physiological pH. Of four cells studied, the decay time constant of the climbing fibre EPSC (6.0±1.8ms) was similar to that of the control cells ($p=0.84$; control cells were the cells in fig. 5.14), and so was its amplitude (2.04±0.57nA; $p=0.52$), as shown in figs. 6.1 and 6.2A, B. Conceivably a small difference of time constant would have been detected if a large number of control and cystine-filled cells were compared, but I did not have time to do such an extensive study. Instead, for the cells recorded with solutions containing 1mM cystine, I tested the role of the cystine-glutamate exchanger by superfusing 100μM cystine to block the release of internal cystine and uptake of external glutamate. This dose of external cystine blocks the release of cystine and uptake of glutamate in other cell types (Van Winkle *et al.*, 1992). This protocol allowed me to investigate the role of the exchanger in individual cells, rather than by comparing groups of different cells studied with different intracellular solutions. In the 4 cells studied, external cystine had no effect on the EPSC decay time (1.5±1.5% increase) or on the amplitude (1.9±2.1% increase), as shown in Fig. 6.1 and 6.2C, D.

Fig. 6.1 Effect of internal and external cystine on the decay of the climbing fibre EPSCs. **A.** Climbing fibre EPSCs recorded with 1mM cystine in the whole-cell pipette: EPSCs from one cell are shown in control solution, with 100μM external (ext.) cystine and again in control solution (wash). The holding potential was -36mV. **B.** The climbing fibre EPSCs in **A** normalised to the same peak current. Pipette solution contained (in mM): CsCl 139; L-cystine 1; NaCl 4; $CaCl_2$ 0.5; $NMDG_2$-EGTA 5; HEPES 10; pH 7.3 adjusted with NaOH. Bath solution was solution B (Table 2.1).

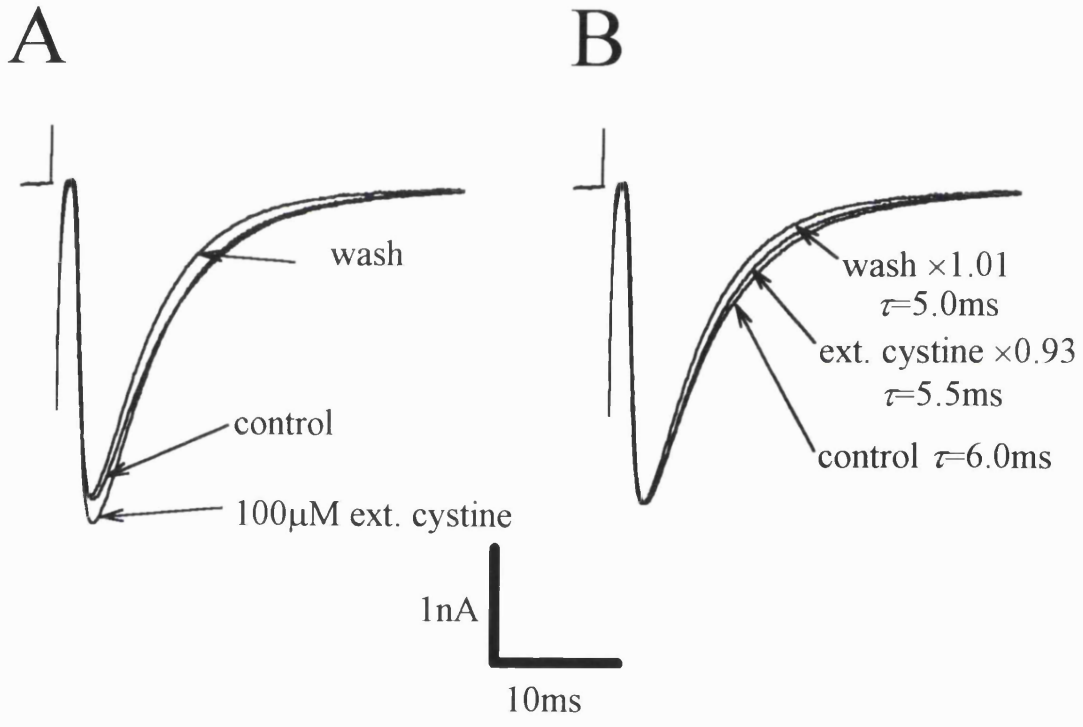
A
B
wash
control
100μM ext. cystine
1nA
10ms
wash ×1.01
τ=5.0ms
ext. cystine ×0.93
τ=5.5ms
control τ=6.0ms

Fig. 6.2 Effect of internal (int.) and external (ext.) cystine on the decay time constant and the amplitude of the climbing fibre EPSC. **A.** The mean climbing fibre EPSC decay time constant ± S.E.M. in 24 control cells clamped with electrodes lacking cystine (open bar; solution G, Table 2.3) and in 4 cells clamped with an electrode containing 1mM cystine (filled bar). **B.** Peak amplitude ± S.E.M. in the same groups of cells as in **A**. **C.** The mean climbing fibre EPSC decay time constant ± S.E.M. of cells clamped with electrodes containing 1mM cystine (solution as in Fig. 6.1) in control solution (filled bar) and in the presence of 100μM external cystine (hatched bar); data normalized to the value in control solution. The holding potential was -36mV. **D.** The mean peak amplitude ± S.E.M. in the same groups of cells as in **C**; normalized to the value in control solution.

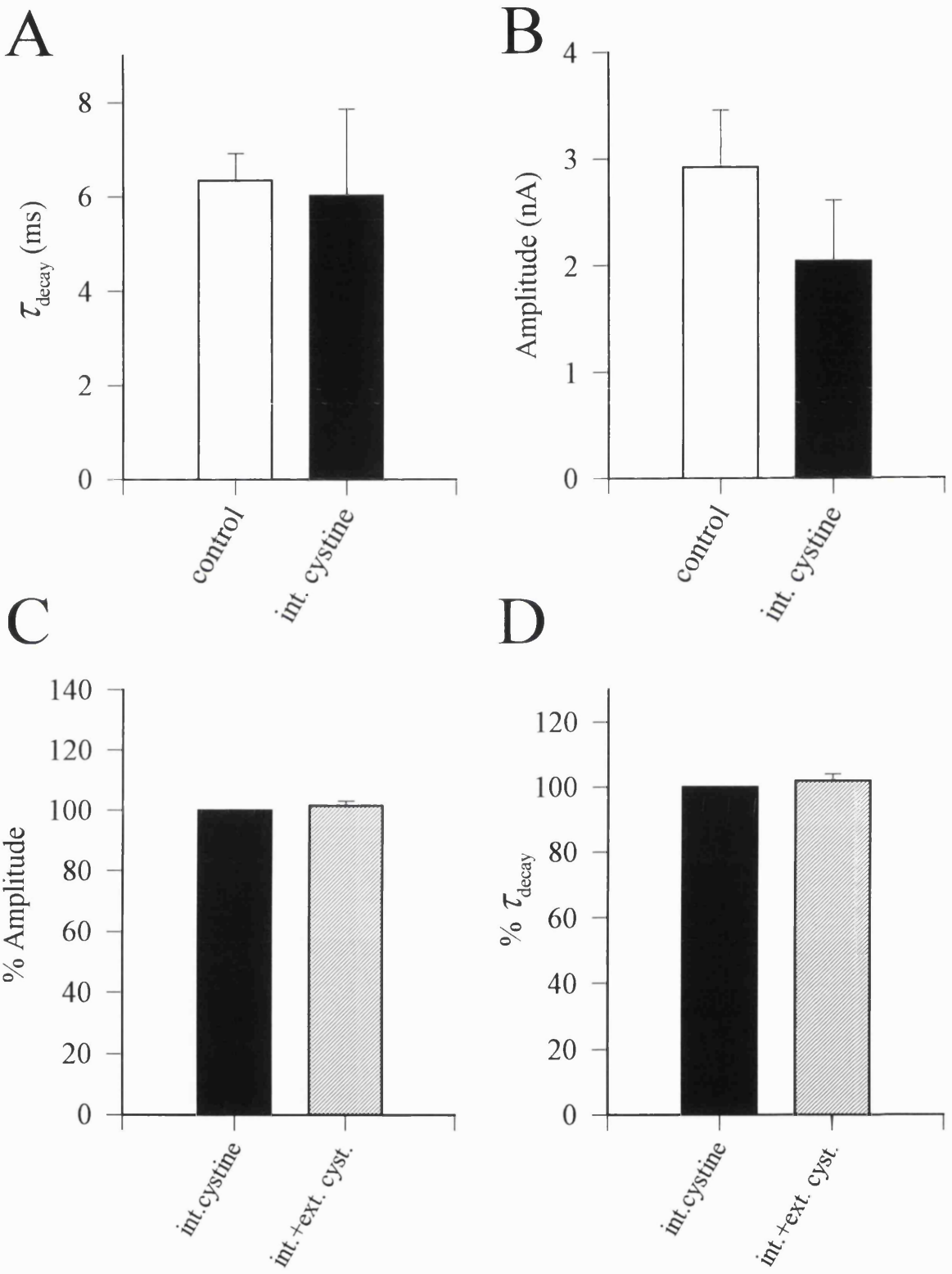
A
8
6
4
2
0
τ_{decay} (ms)
control
int. cystine
B
4
3
2
1
0
Amplitude (nA)
control
int. cystine
C
140
120
100
80
60
40
20
0
% Amplitude
int.cystine
int.+ext. cyst.
D
120
100
80
60
40
20
0
% τ_{decay}
int.cystine
int.+ext. cyst.

6.4 Effect of internal glutamate and external cystine

To test further for a possible effect of the cystine-glutamate exchanger, I carried out experiments with glutamate (20mM) added to the whole-cell pipette. Climbing fibre EPSCs were then evoked, first in control solution and then in solution to which 100μM cystine was added (Fig. 6.3A, B). The rationale was that cystine-glutamate exchange would operate, when the external cystine was added, releasing glutamate into the synaptic cleft, and thus decreasing the EPSC amplitude by desensitizing non-NMDA receptors and possibly slowing the decay of the EPSC. In fact, superfusing 100μM cystine changed neither the amplitude of the climbing fibre EPSC nor its decay rate, as shown in Fig. 6.3. Of three cells studied, the change of amplitude was -4.2±9.1 (mean ± S.E.M.) % and that of the decay time constant was -7.8±6.7% (Fig. 6.3C, D).

In 3 cells, the effect of external cystine (in the presence of internal glutamate) on the parallel fibre EPSC was also tested. The results were similar to those for the climbing fibre EPSCs: the change of amplitude when adding external cystine was -8.0±9.7% and that of the decay time constant was -6.4±6.7%.

6.5 Effect of NMDA

To test whether NMDA receptor subunits buffer glutamate in the synaptic cleft of the climbing fibre synapse, the following experiments were carried out. Superfused NMDA should compete with glutamate for binding to NMDA receptor subunits, and so should prevent buffering by these subunits and prolong the climbing fibre EPSC decay. Experimentally, superfusing 100μM NMDA did not alter the EPSC decay time constant (slowed by 2.2±2.8% in 4 cells), as shown in figs. 6.4A, B. The amplitude of the climbing fibre EPSC was reduced slightly, by 12.3 ±1.6% ($p < 0.05$ in 4 cells; fig. 6.4C).

Fig. 6.3 Effect of internal glutamate and external cystine on the decay of the climbing fibre EPSCs. **A.** Climbing fibre EPSCs recorded with 20mM glutamate in the whole-cell solution. EPSCs are shown in control solution, in 100μM cystine and again in control solution (wash). The holding potential was -36mV. **B.** The climbing fibre EPSCs in **A** normalised to the same peak current. **C.** Mean climbing fibre EPSC decay time constant ± S.E.M. in control solution (open bar) and in the presence of 100μM external cystine (hatched bar; normalized to the value in control solution), in 4 cells. **D.** EPSC peak amplitude ± S.E.M. in the same group of cells as in **C**. Pipette solution contained (in mM): CsCl 120; Na-glutamate 20; NaCl 4; $CaCl_2$ 0.5; $NMDG_2$-EGTA 5; HEPES 10; pH 7.3 adjusted with NaOH. Bath solution was solution B (Table 2.1).

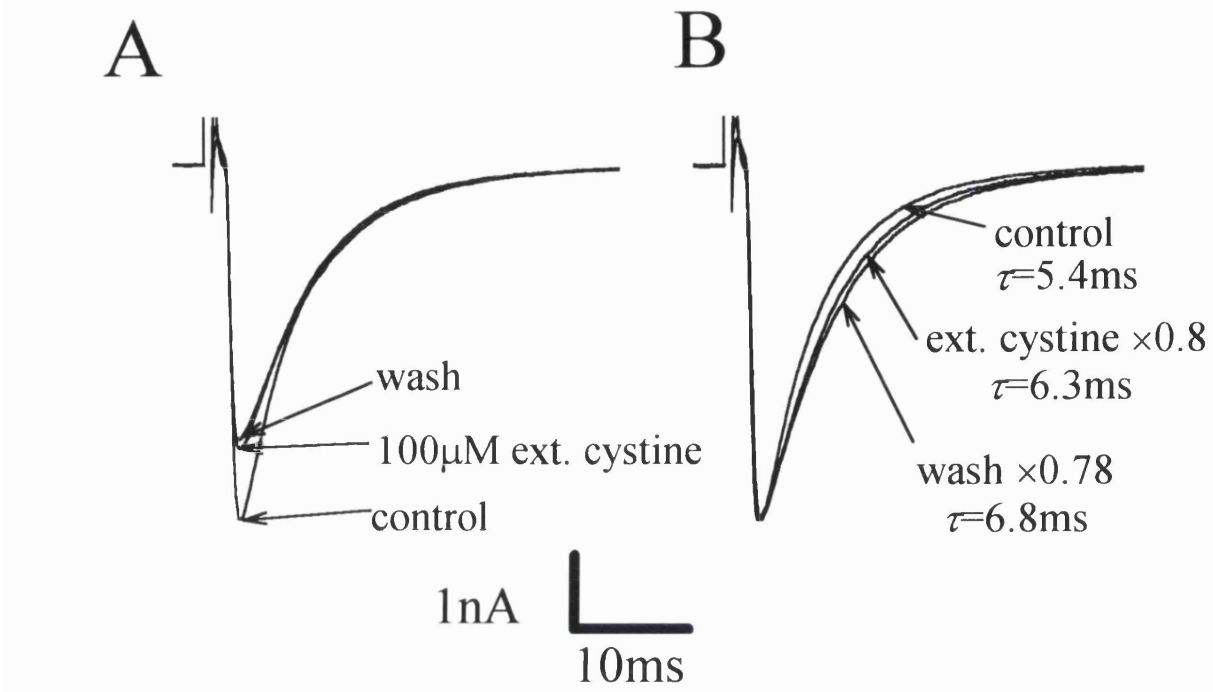
A
B
wash
100μM ext. cystine
control
control
τ=5.4ms
ext. cystine ×0.8
τ=6.3ms
wash ×0.78
τ=6.8ms
1nA
10ms

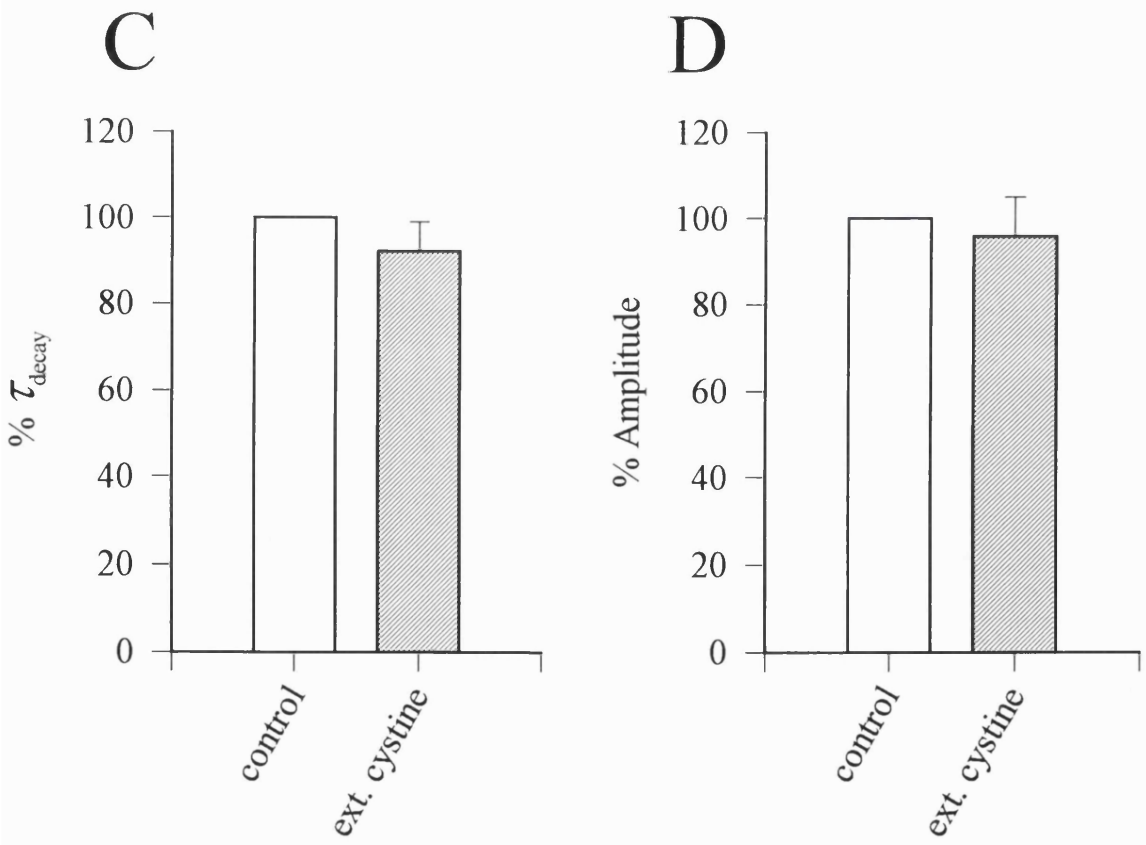
C
D
% τdecay
% Amplitude
120
100
80
60
40
20
0
control
ext. cystine

Fig. 6.4 Effect of NMDA on the decay of the climbing fibre EPSC. **A.** Climbing fibre EPSCs recorded in control solution, in 100μM NMDA and again in control solution (wash). **B.** The climbing fibre EPSCs in **A** normalised to the same peak current. The holding potential was -63mV. **C.** EPSC amplitude for the cell shown in **A** as a function of time during application of NMDA. The pipette solution was solution D (Table 2.2) and the bath solution was solution A (Table 2.1).

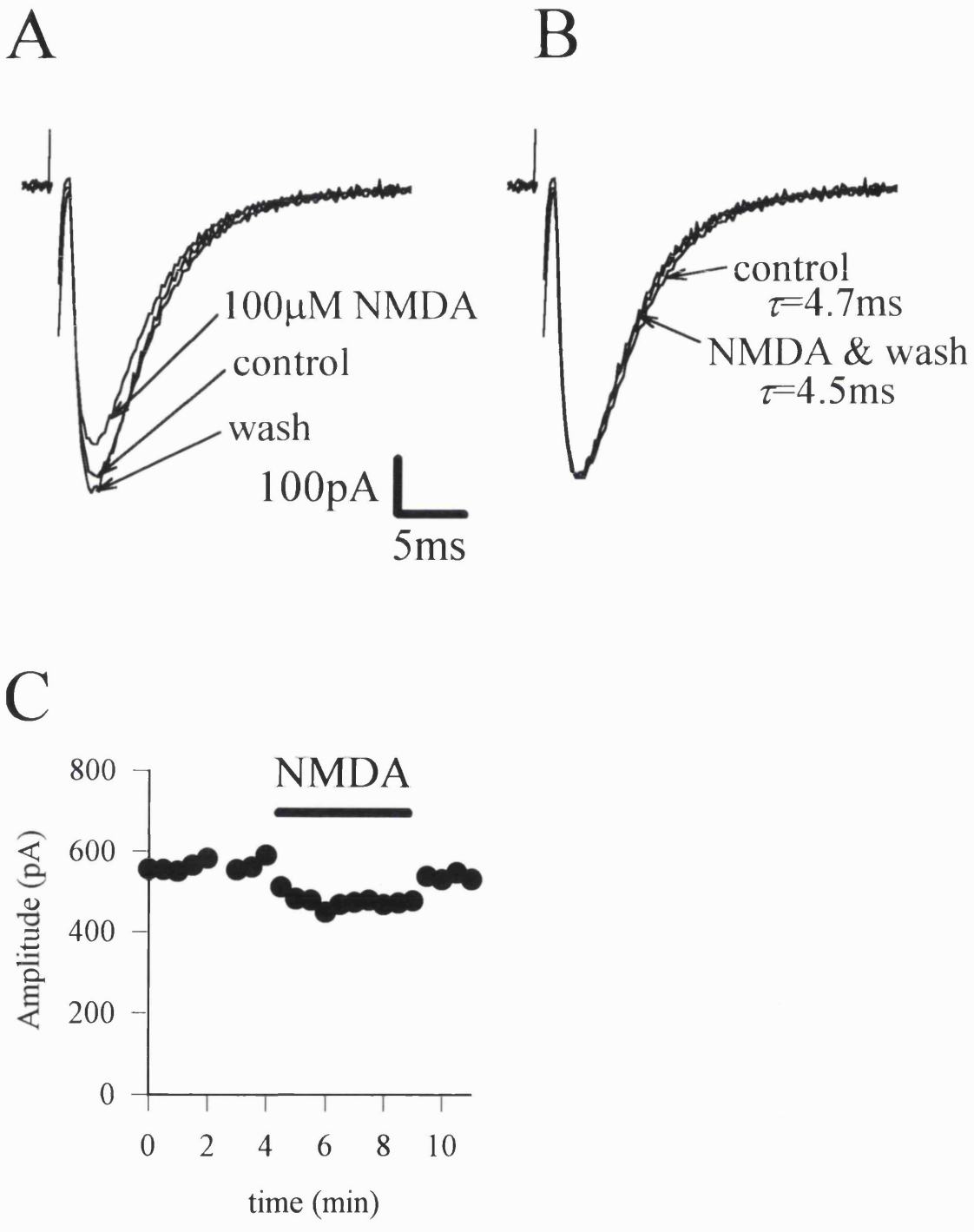
A
100μM NMDA
control
wash
100pA
5ms
B
control
τ=4.7ms
NMDA & wash
τ=4.5ms
C
NMDA
800
600
400
200
0
Amplitude (pA)
0
2
4
6
8
10
time (min)

6.6 Discussion

The experiments described above showed that the waveform of climbing fibre EPSC was not affected by activating or inhibiting cystine-glutamate exchange, nor by occupying putative glutamate binding sites on NMDA receptor subunits with NMDA.

Although autoradiographical studies have shown expression of the glutamate-cystine exchanger in the cerebellum (Anderson *et al.*, 1990), shaping of the EPSC decay time course by this exchanger was not detected. This could be interpreted in two ways. First, cystine-glutamate exchange may not be expressed, or may be insignificant compared to Na^+-dependent glutamate uptake, at the climbing fibre to Purkinje cell synapses. Alternatively the cystine concentrations used in my experiments may not have been sufficient to change the rate of the exchanger's operation. For example 1mM cystine added to the cell might be immediately reduced to cysteine. Furthermore, even with a high level of internal cystine, synaptically released glutamate might not be able to enter the cell in exchange for internal cystine if the dialysis of endogenous glutamate out of the cell was not complete, because this internal glutamate could greatly slow the carrier-mediated influx of glutamate by preventing the carrier from losing glutamate at the inner membrane surface.

NMDA receptor subunits do not seem to contribute to buffering glutamate at the climbing fibre to Purkinje cell synapses at postnatal day 12 (P12). In younger animals (P5 and P6), superfusion of D-APV (100μM) or 7-chlorokynurenate (30μM) reduces the climbing fibre EPSC peak amplitude by 10 to 15%, because these animals have functional NMDA receptors which contribute to generating the EPSC (Momiyama, A., personal communication). The results obtained here were quite surprising, since expression of the NR1 subunit on the Purkinje cell body and dendrites is particularly high (the highest of all areas in the cerebellum: Petralia *et al.*, 1994).

Chapter 7

Discussion

This thesis described experiments carried out to determine what factors contribute to shaping the EPSC decay time course at cerebellar climbing fibre and parallel fibre to Purkinje cell synapses. For the convenience of the reader, a detailed discussion was given at the end of each chapter. This final Discussion summarizes the main results obtained, and suggests work for the future based on the experiments I have carried out.

7.1 Summary

In Chapter 3, I showed that presynaptic adenosine A_1 and $GABA_B$ receptors have a far stronger suppressive effect on the EPSC at the parallel fibre synapse than at the climbing fibre synapse. Reducing glutamate release with adenosine or baclofen also speeded the decay of the EPSCs. This effect was not an artefact due to a poor voltage control, because: (1) this speeding also occurred at positive potentials; (2) reducing the EPSC amplitude postsynaptically by blocking postsynaptic non-NMDA receptors with CNQX did not change the decay time constant; and (3) the speeding of the decay was not correlated with the voltage error produced by the series resistance. The speeding of the EPSC decay time could be a pure presynaptic effect, but it could also be a result of non-presynaptic mechanisms such as a greater concentration gradient between the synaptic cleft and the extrasynaptic space (which would cause faster diffusion of glutamate away from the synaptic cleft), less saturation of glutamate uptake carriers or a lower peak glutamate concentration produced in the synaptic cleft (which, when transformed through the non-NMDA receptor dose-response curve, results in a faster decay of the EPSC: Sarantis *et al.*, 1993). The first two of these possibilities suggest that the role of glutamate uptake in clearing glutamate from the synaptic cleft could be important in determining the decay of the EPSC at these synapses, so, in Chapter 4 I investigated the role of glutamate uptake and the rate of postsynaptic receptor desensitization in shaping the EPSC time course.

Blocking glutamate uptake prolonged the decay of the EPSC at both the climbing and parallel fibre synapses and reduced its amplitude, presumably because of postsynaptic receptor desensitization produced by a rise in the background glutamate level. This result suggested the presence of a prolonged glutamate transient in the synaptic cleft, which might lead to receptor desensitization, which might also contribute to shaping the EPSC decay time course. To test the role of desensitization, first, paired-pulse experiments were carried out on the climbing fibre EPSC. The EPSC evoked by the 2nd of two closely spaced stimuli has a smaller amplitude, possibly due to desensitization caused by glutamate release in response to the first stimulus. Adenosine reduced the EPSC produced by the first stimulus, but had little effect on the 2nd EPSC. This could be because reducing the amount of glutamate released from the 1st stimulus leads to less desensitization at the time of the 2nd EPSC. Next, blocking postsynaptic non-NMDA receptor desensitization with diazoxide increased the amplitude of the EPSC and prolonged its decay. Furthermore, application of adenosine in the presence of diazoxide reduced the amplitude of the 1st and 2nd EPSC similarly at the climbing fibre synapse. These results support the idea that the rate of receptor desensitization is one of the factors which set the decay time course of the EPSC. To summarise, the experiments in Chapter 3 and Chapter 4 showed that the EPSC decay time course at the climbing fibre and the parallel fibre synapse is determined by the amount of glutamate released, by the rate of glutamate removal by uptake, and by the rate of postsynaptic receptor desensitization.

In Chapter 5, further studies of glutamate uptake were carried out based on immunohistochemical data of Rothstein and his colleagues (1994), whose showed that Purkinje cells, which are postsynaptic to the climbing and parallel fibre inputs, express the glutamate transporter EAAC1. Glutamate uptake has generally been believed to be located in glial cells and in the presynaptic terminals of neurons, therefore it was of great interest to know whether Purkinje cells express functional glutamate transporters in their cell surface membrane. By iontophoresing a glutamate analogue, D-aspartate, onto the Purkinje cell somata, I detected a current with the pharmacology, voltage- and ion-dependence of a glutamate uptake current. Part of this current was generated by an

anion channel associated with the transporter. Furthermore, by raising the external potassium concentration to mimic an ischaemic insult, an outward current attributable to reversed operation of glutamate uptake carriers was observed when sodium and glutamate were included inside the cell, as observed previously in salamander glial cells. Next, the role of this postsynaptic glutamate uptake in shaping the EPSC decay time course was examined, since the experiments in Chapter 3 only showed the effect of blocking glutamate uptake everywhere in the slice (i.e. of blocking presynaptic, postsynaptic and glial uptake). Blocking glutamate uptake specifically in the Purkinje cell, by introducing D-aspartate into the cell via the patch pipette, prolonged the climbing fibre EPSC. Thus, modulation of this postsynaptic glutamate uptake in Purkinje cells, like modulation of presynaptic receptors, could alter the strength of synaptic transmission.

In Chapter 6, two other additional factors which might shape the climbing fibre EPSC decay time course were studied. First, I tested the possible role in shaping the EPSC of the cystine-glutamate exchanger, another type of glutamate transporter which transports cystine into and glutamate out of the cell in normal conditions. Altering the rate of this exchange did not affect the EPSC decay. Second, the possible role of NMDA receptor subunits, which are expressed abundantly in Purkinje cells, was also examined. There are no functional NMDA receptors reported after postnatal 10 day electrophysiologically, yet the presence of these subunits might help to buffer glutamate in the synaptic cleft. However, application of NMDA did not alter the EPSC decay.

7.2 Suggestions for further work

In this section, I will suggest experiments which could build on the data I obtained.

7.2.1 Quantal analysis of the climbing fibre and parallel fibre to Purkinje cell synapses

In Chapter 3, the effect of adenosine and baclofen on the climbing fibre and the parallel fibre to the Purkinje cell synapses was described. Adenosine and baclofen were assumed to act presynaptically, based on data in the literature (see section 3.1) and on the fact that

neither of them modulate an iontophoretically-generated non-NMDA receptor current. However, by quantal analysis, a reduction of glutamate release from the presynaptic terminal might be demonstrated directly.

7.2.2 Detection of a synaptically-evoked uptake current

In Chapter 5, I have demonstrated an iontophoretically-generated current in the Purkinje cell attributed to uptake. The size of the current was 64±11 (S.E.M.) pA (see section 5.10.2) at -70mV when iontophoresing D-aspartate. Iontophoresing glutamate in the same way generated about 4nA of current, which is comparable to the amplitude of the climbing fibre EPSC. Therefore, it might be reasonable to suppose that an uptake component of the EPSC could be detected. By inhibiting non-NMDA receptors and by including ClO_4^- in the patch pipette to increase the current (see section 5.6), it might be possible to detect an uptake component of the EPSC at the Purkinje cell synapses.

7.2.3 Detection of glutamate release from the Purkinje cell by reversed uptake using a granule cell as a biosensor

In section 5.9, a current attributed to the reversed operation of the glutamate transporter in the Purkinje cell was shown. As in salamander glial cells, this current was evoked by raising $[K^+]_o$ while including glutamate in the patch pipette. To detect directly the release of glutamate by reversed uptake in the salamander glial cell, non-NMDA receptor channels in a Purkinje cell have been used (Billups and Attwell, 1996). Similar experiments for Purkinje cell reversed uptake could reinforce the notion of glutamate release occurring in this way, and perhaps, thereby, give an explanation for the vulnerability of Purkinje cells during ischaemia.

7.2.4 Identification of the transporter

When I was carrying out the experiments described in Chapter 5, the available immunohistochemical data (Rothstein *et al.*, 1994) indicated only the presence of the EAAC1 transporter in the Purkinje cells. However, more recent work suggests that the Purkinje cell also expresses EAAT4 transporters in the soma and in the dendrites

(Rothstein, personal communication). The I-V relation for the current generated by D-aspartate is similar to that of cloned EAAC1 transporters, however the small outward current at positive potentials suggests a contribution from an anion conductance. The EAAT4 transporter has a larger anion conductance (Fairman *et al.*, 1995) than that of EAAC1 (Wadiche *et al.*, 1995a). To distinguish the current generated by the different carriers, it might be possible to use antibodies raised against the transporters to block specifically each transporter in turn.

7.2.5 Effect of D-aspartate on the non-NMDA receptor

In section 5.8, I showed that inhibiting glutamate uptake in the Purkinje cell by adding D-aspartate inside the cell prolonged the decay of the EPSC at the climbing fibre synapse. Since the same manipulation reduced the current evoked by D-aspartate iontophoresis, I assumed that the effect of D-aspartate on the EPSC was via the glutamate transporter. However, it is possible that, in addition to blocking glutamate uptake, internal D-aspartate might affect the deactivation or desensitization kinetics of non-NMDA receptors (D-aspartate does not activate non-NMDA receptors when applied extracellularly: Monaghan *et al.*, 1984; Barbour, 1993). This could be tested by applying fast glutamate concentration jumps to an outside-out patch clamped with a pipette containing or lacking D-aspartate.

7.2.6 Contribution of the cystine-glutamate exchanger to shaping the synaptic current in other cells

Changing the rate of cystine-glutamate exchange did not alter the climbing and parallel fibre EPSC decay, as described in Chapter 6. Although cerebellar cells are known to express this exchanger (Anderson *et al.*, 1990), their expression of it is not the highest in the brain. Thus, it would be interesting to examine the effect of this exchanger on the EPSC decay in a region where it is expressed more, such as cerebral frontal cortex (Anderson *et al.*, 1990).

7.2.7 Effect of NMDA on the parallel fibre to Purkinje cell synapses

In Chapter 6, I showed that application of NMDA did not alter the EPSC decay time course at the climbing fibre to Purkinje cell synapse: a surprising result considering the high expression of NR1 in Purkinje cells (Petralia *et al.* 1994). However, it is possible that NMDA receptor subunits contribute to shaping the EPSC at the parallel fibre synapses. Therefore, experiments similar to those in section 6.5 should be carried out on the parallel fibre EPSC.

References

Aas, J.E., Laake, J.H., Brodal, P. and Ottersen, O.P. (1992). Immunocytochemical evidence for in vitro release of glutamate and GABA from separate nerve terminal populations in the rat pontine nuclei. *Exp. Brain Res.* **89,** 540-548.

Aiba, A., Kano, M., Chen, C., Stanton, M.E., Fox, G.D., Herrup, K., Zwingman, T.A. and Tonegawa, S. (1994). Deficient cerebellar long-term depression and impaired motor learning in mGluR1 mutant mice. *Cell.* **79,** 377-388.

Ajima, A. and Ito, M. (1995). A unique role of protein phosphatases in cerebellar long-term depression. *Neuroreport.* **6,** 297-300.

Albus, J.S. (1971). A theory of cerebellar function. *Math. Biosci.* **10,** 25-61.

Allen, T.G. and Brown, D.A. (1993). M2 muscarinic receptor-mediated inhibition of the Ca^{2+} current in rat magnocellular cholinergic basal forebrain neurones. *J. Physiol. (Lond.)* **466,** 173-189.

Altman, J. (1972). Postnatal development of the cerebellar cortex in the rat. II. Phases in the maturation of Purkinje cells and of the molecular layer. *J. Comp. Neurol.* **145,** 399-463.

Amato, A., Barbour, B., Szatkowski, M. and Attwell, D. (1994). Counter-transport of potassium by the glutamate uptake carrier in glial cells isolated from the tiger salamander retina. *J. Physiol. (Lond).* **479,** 371-380.

Anderson, C.R. and Stevens, C.F. (1973). Voltage clamp analysis of acetylcholine produced end-plate current fluctuations at frog neuromuscular junction. *J. Physiol. (Lond).* **235,** 655-691.

Anderson, K.J., Monaghan, D.T., Bridges, R.J., Tavoularis, A.L. and Cotman, C.W. (1990). Autoradiographic characterization of putative excitatory amino acid transport sites. *Neuroscience.* **38,** 311-322.

Andreeva, N., Khodorov, B., Stelmashook, E., Cragoe, E., Jr. and Victorov, I. (1991). Inhibition of Na^+/Ca^{2+} exchange enhances delayed neuronal death elicited by glutamate in cerebellar granule cell cultures. *Brain Res.* **548,** 322-325.

Arriza, J.L., Fairman, W.A., Wadiche, J.I., Murdoch, G.H., Kavanaugh, M.P. and Amara, S.G. (1994). Functional comparisons of three glutamate transporter subtypes cloned from human motor cortex. *J. Neurosci.* **14,** 5559-5569.

Attwell, D., Barbour, B. and Szatkowski, M. (1993). Nonvesicular release of neurotransmitter. *Neuron.* **11,** 401-407.

Baetge, E.E., Bulloch, K. and Stallcup, W.B. (1979). A comparison of glutamate transport in cloned cell lines from the central nervous system. *Brain Res.* **167,** 210-214.

Balchen, T. and Diemer, N.H. (1992). The AMPA antagonist, NBQX, protects against ischemia-induced loss of cerebellar Purkinje cells. *Neuroreport.* **3,** 785-788.

Bannai, S. (1986). Exchange of cystine and glutamate across plasma membrane of human fibroblasts. *J. Biol. Chem.* **261,** 2256-2263.

Bannai, S. and Kitamura, E. (1980). Transport interaction of L-cystine and L-glutamate in human diploid fibroblasts in culture. *J. Biol. Chem.* **255,** 2372-2376.

Bannai, S. and Kitamura, E. (1981). Role of proton dissociation in the transport of cystine and glutamate in human diploid fibroblasts in culture. *J. Biol. Chem.* **256,** 5770-5772.

Bannai, S., Sato, H., Ishii, T. and Taketani, S. (1991). Enhancement of glutathione levels in mouse peritoneal macrophages by sodium arsenite, cadmium chloride and glucose/glucose oxidase. *Biochim. Biophys. Acta.* **1092,** 175-179.

Bannai, S., Takada, A., Kasuga, H. and Tateishi, N. (1986). Induction of cystine transport activity in isolated rat hepatocytes by sulfobromophthalein and other electrophilic agents. *Hepatology.* **6,** 1361-1368.

Bannai, S. and Tateishi, N. (1986). Role of membrane transport in metabolism and function of glutathione in mammals. *J. Membr. Biol.* **89,** 1-8.

Barbour, B. (1993). Synaptic currents evoked in Purkinje cells by stimulating individual granule cells. *Neuron.* **11,** 759-769.

Barbour, B., Brew, H. and Attwell, D. (1988). Electrogenic glutamate uptake in glial cells is activated by intracellular potassium. *Nature.* **335,** 433-435.

Barbour, B., Brew, H. and Attwell, D. (1991). Electrogenic uptake of glutamate and aspartate into glial cells isolated from the salamander (Ambystoma) retina. *J. Physiol. (Lond).* **436,** 169-193.

Barbour, B., Keller, B.U., Llano, I. and Marty, A. (1994). Prolonged presence of glutamate during excitatory synaptic transmission to cerebellar Purkinje cells. *Neuron.* **12,** 1331-1343.

Barnes-Davies, M. and Forsythe, I.D. (1995). Pre- and postsynaptic glutamate receptors at a giant excitatory synapse in rat auditory brainstem slices. *J. Physiol. (Lond).* **488,** 387-406.

Barrie, A.P. and Nicholls, D.G. (1993). Adenosine A_1 receptor inhibition of glutamate exocytosis and protein kinase C-mediated decoupling. *J. Neurochem.* **60,** 1081-1086.

Bashir, Z.I., Bortolotto, Z.A., Davies, C.H., Berretta, N., Irving, A.J., Seal, A.J., Henley, J.M., Jane, D.E., Watkins, J.C. and Collingridge, G.L. (1993). Induction of LTP in the hippocampus needs synaptic activation of glutamate metabotropic receptors. *Nature.* **363,** 347-350.

Baskys, A. (1992). Metabotropic receptors and 'slow' excitatory actions of glutamate agonists in the hippocampus. *Trends. Neurosci.* **15,** 92-96.

Baskys, A. and Malenka, R.C. (1991). Agonists at metabotropic glutamate receptors presynaptically inhibit EPSCs in neonatal rat hippocampus. *J. Physiol. (Lond).* **444,** 687-701.

Batchelor, A.M. and Garthwaite, J. (1992). $GABA_B$ receptors in the parallel fibre pathway of rat cerebellum. *Eur. J. Neurosci.* **4,** 1059-1064.

Batchelor, A.M. and Garthwaite, J. (1993). Novel synaptic potentials in cerebellar Purkinje cells: probable mediation by metabotropic glutamate receptors. *Neuropharmacology*. **32,** 11-20.

Batchelor, A.M., Madge, D.J. and Garthwaite, J. (1994). Synaptic activation of metabotropic glutamate receptors in the parallel fibre-Purkinje cell pathway in rat cerebellar slices. *Neuroscience*. **63,** 911-915.

Bekkers, J.M. and Stevens, C.F. (1989). NMDA and non-NMDA receptors are co-localized at individual excitatory synapses in cultured rat hippocampus. *Nature*. **341,** 230-233.

Benveniste, H., Drejer, J., Schousboe, A. and Diemer, N.H. (1984). Elevation of the extracellular concentrations of glutamate and aspartate in rat hippocampus during transient cerebral ischemia monitored by intracerebral microdialysis. *J. Neurochem*. **43,** 1369-1374.

Berthier, N.E. and Moore, J.W. (1986). Cerebellar Purkinje cell activity related to the classically conditioned nictitating membrane response. *Exp. Brain Res.* **63,** 341-350.

Bettler, B., Boulter, J., Hermans-Borgmeyer, I., O'Shea-Greenfield, A., Deneris, E.S., Moll, C., Borgmeyer, U., Hollmann, M. and Heinemann, S. (1990). Cloning of a novel glutamate receptor subunit, GluR5: expression in the nervous system during development. *Neuron*. **5,** 583-595.

Bettler, B., Egebjerg, J., Sharma, G., Pecht, G., Hermans-Borgmeyer, I., Moll, C., Stevens, C.F. and Heinemann, S. (1992). Cloning of a putative glutamate receptor: a low affinity kainate-binding subunit. *Neuron*. **8,** 257-265.

Billups, B. and Attwell, D. (1996). Modulation of non-vesicular glutamate release by pH. *Nature*. **379,** 171-174.

Billups, B., Rossi, D. and Attwell, D. (1996). Anion conductance behavior of the glutamate uptake caurrier in salamander retinal glial cells. *J. Neurosci.* **16,** (In press).

Blanton, M.G. and Kriegstein, A.R. (1992). Properties of amino acid neurotransmitter receptors of embryonic cortical neurons when activated by exogenous and endogenous agonists. *J. Neurophysiol.* **67,** 1185-1200.

Bliss, T.V. and Collingridge, G.L. (1993). A synaptic model of memory: long-term potentiation in the hippocampus. *Nature*. **361,** 31-39.

Bortolotto, Z.A., Bashir, Z.I., Davies, C.H. and Collingridge, G.L. (1994). A molecular switch activated by metabotropic glutamate receptors regulates induction of long-term potentiation. *Nature*. **368,** 740-743.

Bouvier, M., Szatkowski, M., Amato, A. and Attwell, D. (1992). The glial cell glutamate uptake carrier countertransports pH-changing anions. *Nature*. **360,** 471-474.

Brew, H. and Attwell, D. (1987). Electrogenic glutamate uptake is a major current carrier in the membrane of axolotl retinal glial cells. *Nature*. **327,** 707-709.

Bridges, R.J., Lovering, F.E., Koch, H., Cotman, C.W. and Chamberlin, A.R. (1994). A conformationally constrained competitive inhibitor of the sodium-dependent glutamate transporter in forebrain synaptosomes: L-anti-endo-3,4-methanopyrrolidine dicarboxylate. *Neurosci. Lett.* **174,** 193-197.

Brierley, J.B. and Graham, D.I. (1984). Hypoxia and vascular disorders of the central nervous system. *Greenfields's neuropathology.* Adams, J.H., Corsellis, J.A.N. and Duchen, L.W. Eds., Arnold (London), 127-207.

Brorson, J.R., Bleakman, D., Chard, P.S. and Miller, R.J. (1992). Calcium directly permeates kainate/alpha-amino-3-hydroxy-5-methyl-4- isoxazolepropionic acid receptors in cultured cerebellar Purkinje neurons. *Mol. Pharmacol.* **41,** 603-608.

Brorson, J.R., Manzolillo, P.A., Gibbons, S.J. and Miller, R.J. (1995). AMPA receptor desensitization predicts the selective vulnerability of cerebellar Purkinje cells to excitotoxicity. *J. Neurosci.* **15,** 4515-4524.

Bruns, D. and Jahn, R. (1995). Real-time measurement of transmitter release from single synaptic vesicles. *Nature.* **376,** 62-65.

Burckhardt, G., Kinne, R., Stange, G. and Murer, H. (1980). The effects of potassium and membrane potential on sodium-dependent glutamic acid uptake. *Biochim. Biophys. Acta.* **599,** 191-201.

Burnashev, N., Monyer, H., Seeburg, P.H. and Sakmann, B. (1992). Divalent ion permeability of AMPA receptor channels is dominated by the edited form of a single subunit. *Neuron.* **8,** 189-198.

Capogna, M., Gahwiler, B.H. and Thompson, S.M. (1993). Mechanism of mu-opioid receptor-mediated presynaptic inhibition in the rat hippocampus in vitro. *J. Physiol. (Lond).* **470,** 539-558.

Cartmell, J., Curtis, A.R., Kemp, J.A., Kendall, D.A. and Alexander, S.P. (1993). Subtypes of metabotropic excitatory amino acid receptor distinguished by stereoisomers of the rigid glutamate analogue, 1-aminocyclopentane-1,3-dicarboxylate. *Neurosci. Lett.* **153,** 107-110.

Cartmell, J., Kemp, J.A., Alexander, S.P., Shinozaki, H. and Kendall, D.A. (1994). Modulation of cyclic AMP formation by putative metabotropic receptor agonists. *Br. J. Pharmacol.* **111,** 364-369.

Casabona, G., Genazzani, A.A., Di Stefano, M., Sortino, M.A. and Nicoletti, F. (1992). Developmental changes in the modulation of cyclic AMP formation by the metabotropic glutamate receptor agonist 1S,3R-aminocyclopentane-1,3-dicarboxylic acid in brain slices. *J. Neurochem.* **59,** 1161-1163.

Cervos-Navarro, J. and Diemer, N.H. (1991). Selective vulnerability in brain hypoxia. *Crit. Rev. Neurobiol.* **6,** 149-182.

Chaudhry, F.A., Lehre, K.P., van Lookeren Campagne, M., Ottersen, O.P., Danbolt, N.C. and Storm Mathisen, J. (1995). Glutamate transporters in glial plasma membranes: highly differentiated localizations revealed by quantitative ultrastructural immunocytochemistry. *Neuron.* **15,** 711-720.

Chavez-Noriega, L.E. and Stevens, C.F. (1992). Modulation of synaptic efficacy in field CA1 of the rat hippocampus by forskolin. *Brain Res.* **574,** 85-92.

Chavez-Noriega, L.E. and Stevens, C.F. (1994). Increased transmitter release at excitatory synapses produced by direct activation of adenylate cyclase in rat hippocampal slices. *J. Neurosci.* **14,** 310-317.

Chavis, P., Shinozaki, H., Bockaert, J. and Fagni, L. (1994). The metabotropic glutamate receptor types 2/3 inhibit L-type calcium channels via a pertussis toxin-sensitive G-protein in cultured cerebellar granule cells. *J. Neurosci.* **14,** 7067-7076.

Chittajallu, R., Vignes, M., Dev, K.K., Barnes, J.M., Collingridge, G.L. and Henley, J.M. (1996). Regulation of glutamate release by presynaptic kainate receptors in the hippocampus. *Nature.* **379,** 78-81.

Choi, D.W. (1985). Glutamate neurotoxicity in cortical cell culture is calcium dependent. *Neurosci. Lett.* **58,** 293-297.

Choi, D.W. (1990). Cerebral hypoxia: some new approaches and unanswered questions. *J. Neurosci.* **10,** 2493-2501.

Choi, D.W., Koh, J.Y. and Peters, S. (1988). Pharmacology of glutamate neurotoxicity in cortical cell culture: attenuation by NMDA antagonists. *J. Neurosci.* **8,** 185-196.

Choi, D.W., Maulucci Gedde, M. and Kriegstein, A.R. (1987). Glutamate neurotoxicity in cortical cell culture. *J. Neurosci.* **7,** 357-368.

Clements, J.D. (1996). Transmitter timecourse in the synaptic cleft: its role in central synaptic function. *Trends Neurosci.* **19,** 163-171.

Clements, J.D., Lester, R.A., Tong, G., Jahr, C.E. and Westbrook, G.L. (1992). The time course of glutamate in the synaptic cleft. *Science.* **258,** 1498-1501.

Collingridge, G.L. and Bliss, T.V. (1995). Memories of NMDA receptors and LTP. *Trends. Neurosci.* **18,** 54-56.

Colmers, W.F., Lukowiak, K. and Pittman, Q.J. (1987). Presynaptic action of neuropeptide Y in area CA1 of the rat hippocampal slice. *J. Physiol. (Lond).* **383,** 285-299.

Colquhoun, D., Jonas, P. and Sakmann, B. (1992). Action of brief pulses of glutamate on AMPA/kainate receptors in patches from different neurones of rat hippocampal slices. *J. Physiol. (Lond).* **458,** 261-287.

Crépel, F. and Krupa, M. (1988). Activation of protein kinase C induces a long-term depression of glutamate sensitivity of cerebellar Purkinje cells. An in vitro study. *Brain Res.* **458,** 397-401.

Crépel, F. and Krupa, M. (1990). Modulation of the responsiveness of cerebellar Purkinje cells to excitatory amino acids. *Adv. Exp. Med. Biol.* **268,** 323-329.

Crépel, F., Mariani, J. and Delhaye Bouchaud, N. (1976). Evidence for a multiple innervation of Purkinje cells by climbing fibers in the immature rat cerebellum. *J. Neurobiol.* **7,** 567-578.

Cuénod, M., Do, K.-Q., Grandes, P., Morino, P. and Streit, P. (1990). Localization and release of homocysteic acid, an excitatory sulfur-containing amino acid. *J. Histochem. Cytochem.* **38,** 1713-1715.

Cuénod, M., Do, K.-Q., Vollenweider, F., Zollinger, M., Klein, A. and Streit, P. (1989). The puzzle of the transmitters in the climbing fibres. *Exp. Brain Res.* **17,** 161-176.

Cuénod, M., Grandes, P., Zangerle, L., Streit, P. and Do, K.-Q. (1993). Sulphur-containing excitatory amino acids in intercellular communication. *Biochem. Soc. Trans.* **21,** 72-77.

Daniel, H., Hémart, N., Jaillard, D. and Crépel, F. (1992). Coactivation of metabotropic glutamate receptors and of voltage-gated calcium channels induces long-term depression in cerebellar Purkinje cells in vitro. *Exp. Brain Res.* **90,** 327-331.

Daniel, H., Hémart, N., Jaillard, D. and Crépel, F. (1993). Long-term depression requires nitric oxide and guanosine 3':5' cyclic monophosphate production in rat cerebellar Purkinje cells. *Eur. J. Neurosci.* **5,** 1079-1082.

Davies, C.H., Davies, S.N. and Collingridge, G.L. (1990). Paired-pulse depression of monosynaptic GABA-mediated inhibitory postsynaptic responses in rat hippocampus. *J. Physiol. (Lond).* **424,** 513-531.

Davies, J. and Watkins, J.C. (1982). Actions of D and L forms of 2-amino-5-phosphonovalerate and 2-amino-4-phosphonobutyrate in the cat spinal cord. *Brain Res.* **235,** 378-386.

De Biasi, S. and Rustioni, A. (1990). Ultrastructural immunocytochemical localization of excitatory amino acids in the somatosensory system. *J. Histochem. Cytochem.* **38,** 1745-1754.

Do, K.-Q., Herrling, P.L., Streit, P. and Cuénod, M. (1988). Release of neuroactive substances: homocysteic acid as an endogenous agonist of the NMDA receptor. *J. Neural. Transm.* **72,** 185-190.

Do, K.-Q., Vollenweider, F.X., Zollinger, M. and Cuénod, M. (1991). Effect of climbing fibre deprivation on the K^+-evoked release of endogenous adenosine from rat cerebellar slices. *Eur. J. Neurosci.* **3,** 201-208.

Dolphin, A.C., Menon-Johansson, A., Campbell, V., Berrow, N. and Sweeney, M.I. (1994). Modulation of voltage dependent calcium channels by $GABA_B$ receptors and G

proteins in cultured rat dorsal root ganglion neurons: relevance to transmitter release and its modulation. *Cellular mechanisms of sensory processing.* Urban, L. Ed., Springer-Verlag (Berlin). **H 79,**47-61.

Dumuis, A., Pin, J.P., Oomagari, K., Sebben, M. and Bockaert, J. (1990). Arachidonic acid released from striatal neurons by joint stimulation of ionotropic and metabotropic quisqualate receptors. *Nature*. **347,** 182-184.

Dunwiddie, T.V. (1985). The physiological role of adenosine in the central nervous system. *Int. Rev. Neurobiol.* **27,** 63-139.

Dunwiddie, T.V. and Fredholm, B.B. (1989). Adenosine A_1 receptors inhibit adenylate cyclase activity and neurotransmitter release and hyperpolarize pyramidal neurons in rat hippocampus. *J. Pharmacol. Exp. Ther.* **249,** 31-37.

Dunwiddie, T.V., Taylor, M., Heginbotham, L.R. and Proctor, W.R. (1992). Long-term increases in excitability in the CA1 region of rat hippocampus induced by beta-adrenergic stimulation: possible mediation by cAMP. *J. Neurosci.* **12,** 506-517.

Durand, G.M., Gregor, P., Zheng, X., Bennett, M.V., Uhl, G.R. and Zukin, R.S. (1992). Cloning of an apparent splice variant of the rat N-methyl-D-aspartate receptor NMDAR1 with altered sensitivity to polyamines and activators of protein kinase C. *Proc. Natl. Acad. Sci. U.S.A.* **89,** 9359-9363.

Dutar, P. and Nicoll, R.A. (1988). Pre- and postsynaptic $GABA_B$ receptors in the hippocampus have different pharmacological properties. *Neuron.* **1,** 585-591.

East, S.J. and Garthwaite, J. (1992). Actions of a metabotropic glutamate receptor agonist in immature and adult rat cerebellum. *Eur. J. Pharmacol.* **219,** 395-400.

Egebjerg, J., Bettler, B., Hermans Borgmeyer, I. and Heinemann, S. (1991). Cloning of a cDNA for a glutamate receptor subunit activated by kainate but not AMPA. *Nature.* **351,** 745-748.

Ekerot, C.F. and Kano, M. (1985). Long-term depression of parallel fibre synapses following stimulation of climbing fibres. *Brain Res.* **342,** 357-360.

Eliasof, S. and Jahr, C.E. (1996). Retinal glial cell glutamate transporter is coupled to an anionic conductance. *Proc. Natl. Acad. Sci. U.S.A.* **93,** 4153-4158.

Eliasof, S. and Werblin, F. (1993). Characterization of the glutamate transporter in retinal cones of the tiger salamander. *J. Neurosci.* **13,** 402-411.

Ellis, Y. and Davies, J.A. (1994). The effect of neuropeptides on the release of neurotransmitter amino acids from rat striatum. *Neuropeptides.* **26,** 65-69.

Erecínska, M. (1987). The neurotransmitter amino acid transport systems. A fresh outlook on an old problem. *Biochem. Pharmacol.* **36,** 3547-3555.

Erecínska, M., Wantorsky, D. and Wilson, D.F. (1983). Aspartate transport in synaptosomes from rat brain. *J. Biol. Chem.* **258,** 9069-9077.

Eshhar, N., Hunter, C., Wenthold, R.J. and Wada, K. (1992). Structural characterization and expression of a brain specific gene encoding chick kainate binding protein. *FEBS Lett.* **297,** 257-262.

Evans, R.H., Francis, A.A., Jones, A.W., Smith, D.A. and Watkins, J.C. (1982). The effects of a series of omega-phosphonic alpha-carboxylic amino acids on electrically evoked and excitant amino acid-induced responses in isolated spinal cord preparations. *Br. J. Pharmacol.* **75,** 65-75.

Fairman, W.A., Vandenberg, R.J., Arriza, J.L., Kavanaugh, M.P. and Amara, S.G. (1995). An excitatory amino-acid transporter with properties of a ligand-gated chloride channel. *Nature.* **375,** 599-603.

Forsythe, I.D. and Barnes-Davies, M. (1993). The binaural auditory pathway: excitatory amino acid receptors mediate dual timecourse excitatory postsynaptic currents in the rat medial nucleus of the trapezoid body. *Proc. R. Soc. Lond. (Biol. Sci.).* **251,** 151-157.

Forsythe, I.D. and Clements, J.D. (1990). Presynaptic glutamate receptors depress excitatory monosynaptic transmission between mouse hippocampal neurones. *J. Physiol. (Lond)*. **429,** 1-16.

Forsythe, I.D. and Westbrook, G.L. (1988). Slow excitatory postsynaptic currents mediated by N-methyl-D-aspartate receptors on cultured mouse central neurones. *J. Physiol. (Lond)*. **396,** 515-533.

Fowler, J.C. (1990). Adenosine antagonists alter the synaptic response to in vitro ischemia in the rat hippocampus. *Brain Res.* **509,** 331-334.

Garaschuk, O., Kovalchuk, Y. and Krishtal, O. (1992). Adenosine-dependent enhancement by methylxanthines of excitatory synaptic transmission in hippocampus of rats. *Neurosci. Lett.* **135,** 10-12.

Garthwaite, G. and Garthwaite, J. (1986). Neurotoxicity of excitatory amino acid receptor agonists in rat cerebellar slices: dependence on calcium concentration. *Neurosci. Lett.* **66,** 193-198.

Garthwaite, G. and Garthwaite, J. (1988). Electron microscopic autoradiography of D-[^{3}H]aspartate uptake sites in mouse cerebellar slices shows poor labelling of mossy fibre terminals. *Brain Res.* **440,** 162-166.

Gasic, G.P. and Hollmann, M. (1992). Molecular neurobiology of glutamate receptors. *Annu. Rev. Physiol.* **54,** 507-536.

Gereau, R.W.t. and Conn, P.J. (1994). Presynaptic enhancement of excitatory synaptic transmission by beta-adrenergic receptor activation. *J. Neurophysiol.* **72,** 1438-1442.

Gilbert, P.F. (1974). A theory of memory that explains the function and structure of the cerebellum. *Brain Res.* **70,** 1-18.

Gilbert, P.F. and Thach, W.T. (1977). Purkinje cell activity during motor learning. *Brain Res.* **128,** 309-328.

Gilbertson, T.A., Scobey, R. and Wilson, M. (1991). Permeation of calcium ions through non-NMDA glutamate channels in retinal bipolar cells. *Science*. **251,** 1613-1615.

Glaum, S.R. and Miller, R.J. (1995). Presynaptic metabotropic glutamate receptors modulate omega-conotoxin-GVIA-insensitive calcium channels in the rat medulla. *Neuropharmacology*. **34,** 953-964.

Glaum, S.R., Miller, R.J. and Hammond, D.L. (1994). Inhibitory actions of delta 1-, delta 2-, and mu-opioid receptor agonists on excitatory transmission in lamina II neurons of adult rat spinal cord. *J. Neurosci*. **14,** 4965-4971.

Glaum, S.R., Slater, N.T., Rossi, D.J. and Miller, R.J. (1992). Role of metabotropic glutamate (ACPD) receptors at the parallel fiber-Purkinje cell synapse. *J. Neurophysiol*. **68,** 1453-1462.

Goldberg, M.P., Monyer, H., Weiss, J.H. and Choi, D.W. (1988). Adenosine reduces cortical neuronal injury induced by oxygen or glucose deprivation in vitro. *Neurosci. Lett*. **89,** 323-327.

Gregor, P., Eshhar, N., Ortega, A. and Teichberg, V.I. (1988). Isolation, immunochemical characterization and localization of the kainate sub-class of glutamate receptor from chick cerebellum. *EMBO J*. **7,** 2673-2679.

Gregor, P., Mano, I., Maoz, I., McKeown, M. and Teichberg, V.I. (1989). Molecular structure of the chick cerebellar kainate-binding subunit of a putative glutamate receptor. *Nature*. **342,** 689-692.

Gregor, P., Yang, X., Mano, I., Takemura, M., Teichberg, V.I. and Uhl, G.R. (1992). Organization and expression of the gene encoding chick kainate binding protein, a member of the glutamate receptor family. *Brain Res. Mol. Brain Res*. **16,** 179-186.

Gribkoff, V.K. and Bauman, L.A. (1992). Endogenous adenosine contributes to hypoxic synaptic depression in hippocampus from young and aged rats. *J. Neurophysiol*. **68,** 620-628.

Griffiths, R. (1993). The biochemistry and pharmacology of excitatory sulphur-containing amino acids. *Biochem. Soc. Trans.* **21,** 66-72.

Hackett, J.T. (1974). GABA selectively blocks parallel fiber-Purkinje cell synaptic transmission in the frog cerebellum in vitro. *Brain Res.* **80,** 527-531.

Hagberg, H., Andersson, P., Lacarewicz, J., Jacobson, I., Butcher, S. and Sandberg, M. (1987). Extracellular adenosine, inosine, hypoxanthine, and xanthine in relation to tissue nucleotides and purines in rat striatum during transient ischemia. *J. Neurochem.* **49,** 227-231.

Hagberg, H., Lehmann, A., Sandberg, M., Nystrom, B., Jacobson, I. and Hamberger, A. (1985). Ischemia-induced shift of inhibitory and excitatory amino acids from intra- to extracellular compartments. *J. Cereb. Blood Flow Metab.* **5,** 413-419.

Hamori, J., Takacs, J. and Petrusz, P. (1990). Immunogold electron microscopic demonstration of glutamate and GABA in normal and deafferented cerebellar cortex: correlation between transmitter content and synaptic vesicle size. *J. Histochem. Cytochem.* **38,** 1767-1777.

Hausser, M. (1994). Kinetics of excitatory postsynaptic current in Purkinje cells studied using dendritic patch-clamp recording. *Soc. Neurosci. Abstr.* **20,** 891.

Hayashi, Y., Sekiyama, N., Nakanishi, S., Jane, D.E., Sunter, D.C., Birse, E.F., Udvarhelyi, P.M. and Watkins, J.C. (1994). Analysis of agonist and antagonist activities of phenylglycine derivatives for different cloned metabotropic glutamate receptor subtypes. *J. Neurosci.* **14,** 3370-3377.

Hémart, N., Daniel, H., Jaillard, D. and Crépel, F. (1994). Properties of glutamate receptors are modified during long-term depression in rat cerebellar Purkinje cells. *Neurosci. Res.* **19,** 213-221.

Herb, A., Burnashev, N., Werner, P., Sakmann, B., Wisden, W. and Seeburg, P.H. (1992). The KA-2 subunit of excitatory amino acid receptors shows widespread

expression in brain and forms ion channels with distantly related subunits. *Neuron.* **8,** 775-785.

Herrero, I., Miras Portugal, M.T. and Sanchez Prieto, J. (1992). Positive feedback of glutamate exocytosis by metabotropic presynaptic receptor stimulation. *Nature.* **360,** 163-166.

Hertz, L. (1979). Functional interactions between neurons and astrocytes I. Turnover and metabolism of putative amino acid transmitters. *Prog. Neurobiol.* **13,** 277-323.

Hestrin, S. (1992). Activation and desensitization of glutamate-activated channels mediating fast excitatory synaptic currents in the visual cortex. *Neuron.* **9,** 991-999.

Hestrin, S. (1993). Different glutamate receptor channels mediate fast excitatory synaptic currents in inhibitory and excitatory cortical neurons. *Neuron.* **11,** 1083-1091.

Hestrin, S., Nicoll, R.A., Perkel, D.J. and Sah, P. (1990a). Analysis of excitatory synaptic action in pyramidal cells using whole-cell recording from rat hippocampal slices. *J. Physiol. (Lond).* **422,** 203-225.

Hestrin, S., Sah, P. and Nicoll, R.A. (1990b). Mechanisms generating the time course of dual component excitatory synaptic currents recorded in hippocampal slices. *Neuron.* **5,** 247-253.

Higgins, D.G., Bleasby, A.J. and Fuchs, R. (1992). CLUSTAL V: improved software for multiple sequence alignment. *Comput. Appl. Biosci.* **8,** 189-191.

Hirano, T. (1991). Differential pre- and postsynaptic mechanisms for synaptic potentiation and depression between a granule cell and a Purkinje cell in rat cerebellar culture. *Synapse.* **7,** 321-323.

Hollmann, M., O'Shea-Greenfield, A., Rogers, S.W. and Heinemann, S. (1989). Cloning by functional expression of a member of the glutamate receptor family. *Nature.* **342,** 643-648.

Hollmann, M., Boulter, J., Maron, C., Beasley, L., Sullivan, J., Pecht, G. and Heinemann, S. (1993). Zinc potentiates agonist-induced currents at certain splice variants of the NMDA receptor. *Neuron*. **10,** 943-954.

Hollmann, M., Hartley, M. and Heinemann, S. (1991). Ca^{2+} permeability of KA-AMPA-gated glutamate receptor channels depends on subunit composition. *Science*. **252,** 851-853.

Hollmann, M. and Heinemann, S. (1994). Cloned glutamate receptors. *Annu. Rev. Neurosci*. **17,** 31-108.

Hollmann, M., Maron, C. and Heinemann, S. (1994). N-glycosylation site tagging suggests a three transmembrane domain topology for the glutamate receptor GluR1. *Neuron*. **13,** 1331-1343.

Honoré, T., Davies, S.N., Drejer, J., Fletcher, E.J., Jacobsen, P., Lodge, D. and Nielsen, F.E. (1988). Quinoxalinediones: potent competitive non-NMDA glutamate receptor antagonists. *Science*. **241,** 701-703.

Horn, L.W. (1989). L-glutamate transport in internally dialyzed barnacle muscle fibers. *Am. J. Physiol*. **257,** C442-450.

Hume, R.I., Dingledine, R. and Heinemann, S.F. (1991). Identification of a site in glutamate receptor subunits that controls calcium permeability. *Science*. **253,** 1028-1031.

Iino, M., Ozawa, S. and Tsuzuki, K. (1990). Permeation of calcium through excitatory amino acid receptor channels in cultured rat hippocampal neurones. *J. Physiol. (Lond)*. **424,** 151-165.

Ikeda, K., Nagasawa, M., Mori, H., Araki, K., Sakimura, K., Watanabe, M., Inoue, Y. and Mishina, M. (1992). Cloning and expression of the epsilon 4 subunit of the NMDA receptor channel. *FEBS Lett*. **313,** 34-38.

Isaacson, J.S. and Nicoll, R.A. (1993). The uptake inhibitor L-trans-PDC enhances responses to glutamate but fails to alter the kinetics of excitatory synaptic currents in the hippocampus. *J. Neurophysiol.* **70,** 2187-2191.

Isaacson, J.S., Solis, J.M. and Nicoll, R.A. (1993). Local and diffuse synaptic actions of GABA in the hippocampus. *Neuron.* **10,** 165-175.

Ishii, T., Nakayama, K., Sato, H., Miura, K., Yamada, M., Yamada, K., Sugita, Y. and Bannai, S. (1991). Expression of the mouse macrophage cystine transporter in Xenopus laevis oocytes. *Arch. Biochem. Biophys.* **289,** 71-75.

Ito, I., Kohda, A., Tanabe, S., Hirose, E., Hayashi, M., Mitsunaga, S. and Sugiyama, H. (1992). 3,5-Dihydroxyphenyl-glycine: a potent agonist of metabotropic glutamate receptors. *Neuroreport.* **3,** 1013-1016.

Ito, M. (1984). *The cerebellum and neural control.* Raven Press (New York).

Ito, M. and Karachot, L. (1990). Messengers mediating long-term desensitization in cerebellar Purkinje cells. *Neuroreport.* **1,** 129-132x.

Ito, M., Sakurai, M. and Tongroach, P. (1982). Climbing fibre induced depression of both mossy fibre responsiveness and glutamate sensitivity of cerebellar Purkinje cells. *J. Physiol. (Lond).* **324,** 113-134.

Jane, D.E., Jones, P.L., Pook, P.C., Salt, T.E., Sunter, D.C. and Watkins, J.C. (1993). Stereospecific antagonism by (+)-alpha-methyl-4-carboxyphenylglycine (MCPG) of (1S,3R)-ACPD-induced effects in neonatal rat motoneurones and rat thalamic neurones. *Neuropharmacology.* **32,** 725-727.

Jarvis, M.F. and Williams, M. (1989). Direct autoradiographic localization of adenosine A_2 receptors in the rat brain using the A_2-selective agonist, [^{3}H]CGS 21680. *Eur. J. Pharmacol.* **168,** 243-246.

Jiang, Z.G. and North, R.A. (1992). Pre- and postsynaptic inhibition by opioids in rat striatum. *J. Neurosci.* **12,** 356-361.

Johansen, F.F. (1993). Interneurons in rat hippocampus after cerebral ischemia. Morphometric, functional, and therapeutic investigations. *Acta Neurol. Scand. Suppl.* **150,** 1-32.

Jonas, P., Major, G. and Sakmann, B. (1993). Quantal components of unitary EPSCs at the mossy fibre synapse on CA3 pyramidal cells of rat hippocampus. *J. Physiol. (Lond).* **472,** 615-663.

Jonas, P., Racca, C., Sakmann, B., Seeburg, P.H. and Monyer, H. (1994). Differences in Ca^{2+} permeability of AMPA-type glutamate receptor channels in neocortical neurons caused by differential GluR-B subunit expression. *Neuron.* **12,** 1281-1289.

Jonas, P. and Sakmann, B. (1992). Glutamate receptor channels in isolated patches from CA1 and CA3 pyramidal cells of rat hippocampal slices. *J. Physiol. (Lond).* **455,** 143-171.

Kamboj, R.K., Schoepp, D.D., Nutt, S., Shekter, L., Korczak, B., True, R.A., Zimmerman, D.M. and Wosnick, M.A. (1992). Molecular structure and pharmacological characterization of humEAA2, a novel human kainate receptor subunit. *Mol. Pharmacol.* **42,** 10-15.

Kanai, Y. and Hediger, M.A. (1992). Primary structure and functional characterization of a high-affinity glutamate transporter. *Nature.* **360,** 467-471.

Kanai, Y., Nussberger, S., Romero, M.F., Boron, W.F., Hebert, S.C. and Hediger, M.A. (1995). Electrogenic properties of the epithelial and neuronal high affinity glutamate transporter. *J. Biol. Chem.* **270,** 16561-16568.

Kanner, B.I. and Sharon, I. (1978). Active transport of L-glutamate by membrane vesicles isolated from rat brain. *Biochemistry.* **17,** 3949-3953.

Katz, B. and Miledi, R. (1973). The binding of acetylcholine to receptors and its removal from the synaptic cleft. *J. Physiol. (Lond).* **231,** 549-574.

Kawamoto, S., Onishi, H., Hattori, S., Miyagi, Y., Amaya, Y., Mishina, M. and Okuda, K. (1991). Functional expression of the alpha 1 subunit of the AMPA-selective glutamate receptor channel, using a baculovirus system. *Biochem. Biophys. Res. Commun.* **181,** 756-763.

Kawashima, K., Fujimoto, K., Suzuki, T. and Oohata, H. (1990). Pharmacological differentiation of presynaptic M1 muscarinic receptors modulating acetylcholine release from postsynaptic muscarinic receptors in guinea-pig ileum. *Gen. Pharmacol.* **21,** 17-21.

Keinanen, K., Wisden, W., Sommer, B., Werner, P., Herb, A., Verdoorn, T.A., Sakmann, B. and Seeburg, P.H. (1990). A family of AMPA-selective glutamate receptors. *Science.* **249,** 556-560.

Keller, B.U., Konnerth, A. and Yaari, Y. (1991). Patch clamp analysis of excitatory synaptic currents in granule cells of rat hippocampus. *J. Physiol. (Lond).* **435,** 275-293.

Kemp, M., Roberts, P., Pook, P., Jane, D., Jones, A., Jones, P., Sunter, D., Udvarhelyi, P. and Watkins, J. (1994). Antagonism of presynaptically mediated depressant responses and cyclic AMP-coupled metabotropic glutamate receptors. *Eur. J. Pharmacol.* **266,** 187-192.

Klockner, U., Storck, T., Conradt, M. and Stoffel, W. (1993). Electrogenic L-glutamate uptake in Xenopus laevis oocytes expressing a cloned rat brain L-glutamate/L-aspartate transporter (GLAST-1). *J. Biol. Chem.* **268,** 14594-14596.

Kocsis, J.D., Eng, D.L. and Bhisitkul, R.B. (1984). Adenosine selectively blocks parallel-fiber-mediated synaptic potentials in rat cerebellar cortex. *Proc. Natl. Acad. Sci. U.S.A.* **81,** 6531-6534.

Koh, D.S., Geiger, J.R., Jonas, P. and Sakmann, B. (1995). Ca^{2+}-permeable AMPA and NMDA receptor channels in basket cells of rat hippocampal dentate gyrus. *J. Physiol. (Lond).* **485,** 383-402.

Kohler, M., Burnashev, N., Sakmann, B. and Seeburg, P.H. (1993). Determinants of Ca^{2+} permeability in both TM1 and TM2 of high affinity kainate receptor channels: diversity by RNA editing. *Neuron.* **10,** 491-500.

Konnerth, A., Dreessen, J. and Augustine, G.J. (1992). Brief dendritic calcium signals initiate long-lasting synaptic depression in cerebellar Purkinje cells. *Proc. Natl. Acad. Sci. U.S.A.* **89,** 7051-7055.

Konnerth, A., Llano, I. and Armstrong, C.M. (1990). Synaptic currents in cerebellar Purkinje cells. *Proc. Natl. Acad. Sci. U.S.A.* **87,** 2662-2665.

Konnerth, A., Obaid, A.L. and Salzberg, B.M. (1987). Optical recording of electrical activity from parallel fibres and other cell types in skate cerebellar slices in vitro. *J. Physiol. (Lond).* **393,** 681-702.

Kutsuwada, T., Kashiwabuchi, N., Mori, H., Sakimura, K., Kushiya, E., Araki, K., Meguro, H., Masaki, H., Kumanishi, T., Arakawa, M. and Mishina, M. (1992). Molecular diversity of the NMDA receptor channel. *Nature.* **358,** 36-41.

Lambolez, B., Audinat, E., Bochet, P., Crépel, F. and Rossier, J. (1992). AMPA receptor subunits expressed by single Purkinje cells. *Neuron.* **9,** 247-258.

Lester, R.A. and Jahr, C.E. (1990). Quisqualate receptor-mediated depression of calcium currents in hippocampal neurons. *Neuron.* **4,** 741-749.

Lev-Ram, V., Makings, L.R., Keitz, P.F., Kao, J.P. and Tsien, R.Y. (1995). Long-term depression in cerebellar Purkinje neurons results from coincidence of nitric oxide and depolarization-induced Ca^{2+} transients. *Neuron.* **15,** 407-415.

Limberger, N., Spath, L. and Starke, K. (1988). Presynaptic alpha 2-adrenoceptor, opioid kappa-receptor and adenosine A_1-receptor interactions on noradrenaline release in rabbit brain cortex. *Naunyn. Schmiedebergs. Arch. Pharmacol.* **338,** 53-61.

Linden, D.J. and Connor, J.A. (1991). Participation of postsynaptic PKC in cerebellar long-term depression in culture. *Science.* **254,** 1656-1659.

Linden, D.J. and Connor, J.A. (1995). Long-term synaptic depression. *Annu. Rev. Neurosci.* **18,** 319-357.

Linden, D.J., Dickinson, M.H., Smeyne, M. and Connor, J.A. (1991). A long-term depression of AMPA currents in cultured cerebellar Purkinje neurons. *Neuron.* **7,** 81-89.

Linden, D.J., Smeyne, M. and Connor, J.A. (1993). Induction of cerebellar long-term depression in culture requires postsynaptic action of sodium ions. *Neuron.* **11,** 1093-1100.

Linden, D.J., Smeyne, M. and Connor, J.A. (1994). Trans-ACPD, a metabotropic receptor agonist, produces calcium mobilization and an inward current in cultured cerebellar Purkinje neurons. *J. Neurophysiol.* **71,** 1992-1998.

Liu, Y.B., Disterhoft, J.F. and Slater, N.T. (1993). Activation of metabotropic glutamate receptors induces long-term depression of GABAergic inhibition in hippocampus. *J. Neurophysiol.* **69,** 1000-1004.

Livsey, C.T., Costa, E. and Vicini, S. (1993). Glutamate-activated currents in outside-out patches from spiny versus aspiny hilar neurons of rat hippocampal slices. *J. Neurosci.* **13,** 5324-5333.

Llano, I., Marty, A., Armstrong, C.M. and Konnerth, A. (1991). Synaptic- and agonist-induced excitatory currents of Purkinje cells in rat cerebellar slices. *J. Physiol. (Lond).* **434,** 183-213.

Lomeli, H., Wisden, W., Kohler, M., Keinanen, K., Sommer, B. and Seeburg, P.H. (1992). High-affinity kainate and domoate receptors in rat brain. *FEBS Lett.* **307,** 139-143.

Lovinger, D.M. and McCool, B.A. (1995). Metabotropic glutamate receptor-mediated presynaptic depression at corticostriatal synapses involves mGluR2 or 3. *J. Neurophysiol.* **73,** 1076-1083.

Lupica, C.R., Proctor, W.R. and Dunwiddie, T.V. (1992). Presynaptic inhibition of excitatory synaptic transmission by adenosine in rat hippocampus: analysis of unitary EPSP variance measured by whole-cell recording. *J. Neurosci.* **12,** 3753-3764.

Magleby, K.L. and Stevens, C.F. (1972). The effect of voltage on the time course of end-plate currents. *J. Physiol. (Lond).* **223,** 151-171.

Marr, D. (1969). A theory of cerebellar cortex. *J. Physiol. (Lond).* **202,** 437-470.

Martin, D., Bustos, G.A., Bowe, M.A., Bray, S.D. and Nadler, J.V. (1991). Autoreceptor regulation of glutamate and aspartate release from slices of the hippocampal CA1 area. *J. Neurochem.* **56,** 1647-1655.

Masu, M., Tanabe, Y., Tsuchida, K., Shigemoto, R. and Nakanishi, S. (1991). Sequence and expression of a metabotropic glutamate receptor. *Nature.* **349,** 760-765.

Mayer, M.L. and Westbrook, G.L. (1987). The physiology of excitatory amino acids in the vertebrate central nervous system. *Prog. Neurobiol.* **28,** 197-276.

McBain, C. and Dingledine, R. (1992). Dual-component miniature excitatory synaptic currents in rat hippocampal CA3 pyramidal neurons. *J. Neurophysiol.* **68,** 16-27.

McCormick, D.A. and Thompson, R.F. (1984). Cerebellum: essential involvement in the classically conditioned eyelid response. *Science.* **223,** 296-299.

McGlade McCulloh, E., Yamamoto, H., Tan, S.E., Brickey, D.A. and Soderling, T.R. (1993). Phosphorylation and regulation of glutamate receptors by calcium/calmodulin-dependent protein kinase II. *Nature.* **362,** 640-642.

Meguro, H., Mori, H., Araki, K., Kushiya, E., Kutsuwada, T., Yamazaki, M., Kumanishi, T., Arakawa, M., Sakimura, K. and Mishina, M. (1992). Functional characterization of a heteromeric NMDA receptor channel expressed from cloned cDNAs. *Nature.* **357,** 70-74.

Mennerick, S. and Zorumski, C.F. (1994a). Glial contributions to excitatory neurotransmission in cultured hippocampal cells. *Nature*. **368,** 59-62.

Mennerick, S. and Zorumski, C.F. (1994b). Presynaptic influences on the decay of excitatory synaptic currents. *Soc. Neurosci. Abstr.* **20,** 1336.

Momiyama, A., Feldmeyer, D. and Cull-Candy, S.G. (1996). Identification of a native low-conductance NMDA channel with reduced sensitivity to Mg^{2+} in rat central neurones. *J. Physiol.* **494,** 479-492.

Monaghan, D.T., Yao, D. and Cotman, C.W. (1984). Distribution of [^{3}H]AMPA binding sites in rat brain as determined by quantitative autoradiography. *Brain Res.* **324,** 160-164.

Monyer, H., Sprengel, R., Schoepfer, R., Herb, A., Higuchi, M., Lomeli, H., Burnashev, N., Sakmann, B. and Seeburg, P.H. (1992). Heteromeric NMDA receptors: molecular and functional distinction of subtypes. *Science*. **256,** 1217-1221.

Morita, T., Sakimura, K., Kushiya, E., Yamazaki, M., Meguro, H., Araki, K., Abe, T., Mori, K.J. and Mishina, M. (1992). Cloning and functional expression of a cDNA encoding the mouse beta 2 subunit of the kainate-selective glutamate receptor channel. *Brain Res. Mol. Brain Res.* **14,** 143-146.

Moriyoshi, K., Masu, M., Ishii, T., Shigemoto, R., Mizuno, N. and Nakanishi, S. (1991). Molecular cloning and characterization of the rat NMDA receptor. *Nature*. **354,** 31-37.

Mosbacher, J., Schoepfer, R., Monyer, H., Burnashev, N., Seeburg, P.H. and Ruppersberg, J.P. (1994). A molecular determinant for submillisecond desensitization in glutamate receptors. *Science*. **266,** 1059-1062.

Mosher, H.S. (1986). The chemistry of tetrodotoxin. *Ann. N.Y. Acad. Sci.* **479,** 32-43.

Moss, S.J., Blackstone, C.D. and Huganir, R.L. (1993). Phosphorylation of recombinant non-NMDA glutamate receptors on serine and tyrosine residues. *Neurochem. Res.* **18,** 105-110.

Motin, L. and Bennett, M.R. (1995). Effect of P_2-purinoceptor antagonists on glutamatergic transmission in the rat hippocampus. *Br. J. Pharmacol.* **115,** 1276-1280.

Murphy, S.N., Thayer, S.A. and Miller, R.J. (1987). The effects of excitatory amino acids on intracellular calcium in single mouse striatal neurons in vitro. *J. Neurosci.* **7,** 4145-4158.

Nakanishi, N., Axel, R. and Shneider, N.A. (1992). Alternative splicing generates functionally distinct N-methyl-D-aspartate receptors. *Proc. Natl. Acad. Sci. U.S.A.* **89,** 8552-8556.

Nakanishi, N., Shneider, N.A. and Axel, R. (1990). A family of glutamate receptor genes: evidence for the formation of heteromultimeric receptors with distinct channel properties. *Neuron.* **5,** 569-581.

Nakanishi, S. (1992). Molecular diversity of glutamate receptors and implications for brain function. *Science.* **258,** 597-603.

Nakazawa, K., Mikawa, S., Hashikawa, T. and Ito, M. (1995). Transient and persistent phosphorylation of AMPA-type glutamate receptor subunits in cerebellar Purkinje cells. *Neuron.* **15,** 697-709.

Nawy, S. and Copenhagen, D.R. (1987). Multiple classes of glutamate receptor on depolarizing bipolar cells in retina. *Nature.* **325,** 56-58.

Neher, E. (1995). Voltage offsets in patch-clamp experiments. *Single-channel recording.* Sakmann, B. and Neher, E. Eds. Plenum Press (New York), 147-153.

Nelson, P.J., Dean, G.E., Aronson, P.S. and Rudnick, G. (1983). Hydrogen ion cotransport by the renal brush border glutamate transporter. *Biochemistry.* **22,** 5459-5463.

Newman, E.A. (1985). Voltage-dependent calcium and potassium channels in retinal glial cells. *Nature.* **317,** 809-811.

Nicholson, C. and Phillips, J.M. (1981). Ion diffusion modified by tortuosity and volume fraction in the extracellular microenvironment of the rat cerebellum. *J. Physiol. (Lond).* **321,** 225-257.

Niggli, E. and Lederer, W.J. (1993). Activation of Na-Ca exchange current by photolysis of "caged calcium". *Biophys. J.* **65,** 882-891.

Nowak, L., Bregestovski, P., Ascher, P., Herbet, A. and Prochiantz, A. (1984). Magnesium gates glutamate-activated channels in mouse central neurones. *Nature.* **307,** 462-465.

Olney, J.W., Price, M.T., Samson, L. and Labruyere, J. (1986). The role of specific ions in glutamate neurotoxicity. *Neurosci. Lett.* **65,** 65-71.

Ortega, A., Eshhar, N. and Teichberg, V.I. (1991). Properties of kainate receptor/channels on cultured Bergmann glia. *Neuroscience.* **41,** 335-349.

Ottersen, O.P., Zhang, N. and Walberg, F. (1992). Metabolic compartmentation of glutamate and glutamine: morphological evidence obtained by quantitative immunocytochemistry in rat cerebellum. *Neuroscience.* **46,** 519-534.

Palay, S.L. and Chan-Palay, V. (1974). *Cerebellar cortex : cytology and organization.* Springer-Verlag (New York).

Palmer, E., Monaghan, D.T. and Cotman, C.W. (1989). Trans-ACPD, a selective agonist of the phosphoinositide-coupled excitatory amino acid receptor. *Eur. J. Pharmacol.* **166,** 585-587.

Patneau, D.K., Vyklicky, L., Jr. and Mayer, M.L. (1993). Hippocampal neurons exhibit cyclothiazide-sensitive rapidly desensitizing responses to kainate. *J. Neurosci.* **13,** 3496-3509.

Perkel, D.J., Hestrin, S., Sah, P. and Nicoll, R.A. (1990). Excitatory synaptic currents in Purkinje cells. *Proc. R. Soc. Lond. (Biol. Sci.).* **241,** 116-121.

Perkins, M.N. and Stone, T.W. (1985). Actions of kynurenic acid and quinolinic acid in the rat hippocampus in vivo. *Exp-Neurol.* **88,** 570-579.

Petralia, R.S., Yokotani, N. and Wenthold, R.J. (1994). Light and electron microscope distribution of the NMDA receptor subunit NMDAR1 in the rat nervous system using a selective anti-peptide antibody. *J. Neurosci.* **14,** 667-696.

Pfrieger, F.W., Gottmann, K. and Lux, H.D. (1994). Kinetics of $GABA_B$ receptor-mediated inhibition of calcium currents and excitatory synaptic transmission in hippocampal neurons in vitro. *Neuron.* **12,** 97-107.

Pin, J.P. and Duvoisin, R. (1995). The metabotropic glutamate receptors: structure and functions. *Neuropharmacology.* **34,** 1-26.

Pines, G., Danbolt, N.C., Bjoras, M., Zhang, Y., Bendahan, A., Eide, L., Koepsell, H., Storm Mathisen, J., Seeberg, E. and Kanner, B.I. (1992). Cloning and expression of a rat brain L-glutamate transporter. *Nature.* **360,** 464-467.

Pittaluga, A., Barbeito, L., Serval, V., Godeheu, G., Artaud, F., Glowinski, J. and Cheramy, A. (1988). Depolarization-evoked release of N-acetyl-L-aspartyl-L-glutamate from rat brain synaptosomes. *Eur. J. Pharmacol.* **158,** 263-266.

Plasman, P.O., Lebrun, P., Cragoe, E.J., Jr. and Herchuelz, A. (1991). Inhibition of Na/Ca exchange in pancreatic islet cells by 3',4'-dichlorobenzamil. *Biochem. Pharmacol.* **41,** 1759-1768.

Prezeau, L., Manzoni, O., Homburger, V., Sladeczek, F., Curry, K. and Bockaert, J. (1992). Characterization of a metabotropic glutamate receptor: direct negative coupling to adenylyl cyclase and involvement of a pertussis toxin-sensitive G protein. *Proc. Natl. Acad. Sci. U.S.A.* **89,** 8040-8044.

Prince, D.A. and Stevens, C.F. (1992). Adenosine decreases neurotransmitter release at central synapses. *Proc. Natl. Acad. Sci. U.S.A.* **89,** 8586-8590.

Quast, U. and Cook, N.S. (1989). In vitro and in vivo comparison of two K^+ channel openers, diazoxide and cromakalim, and their inhibition by glibenclamide. *J. Pharmacol. Exp. Ther.* **250,** 261-271.

Raman, I.M. and Trussell, L.O. (1992). The kinetics of the response to glutamate and kainate in neurons of the avian cochlear nucleus. *Neuron.* **9,** 173-186.

Raymond, L.A., Blackstone, C.D. and Huganir, R.L. (1993). Phosphorylation and modulation of recombinant GluR6 glutamate receptors by cAMP-dependent protein kinase. *Nature.* **361,** 637-641.

Renard, A. and Crépel, F. (1996). Origin of aspartate-induced responses in rat cerebellar Purkinje cells. *Eur. J. Neurosci.* **8,** 978-987.

Roche, K.W., Tingley, W.G. and Huganir, R.L. (1994). Glutamate receptor phosphorylation and synaptic plasticity. *Curr. Opin. Neurobiol.* **4,** 383-388.

Rogers, H. and Henderson, G. (1990). Activation of mu- and delta-opioid receptors present on the same nerve terminals depresses transmitter release in the mouse hypogastric ganglion. *Br. J. Pharmacol.* **101,** 505-512.

Rosenmund, C., Legendre, P. and Westbrook, G.L. (1992). Expression of NMDA channels on cerebellar Purkinje cells acutely dissociated from newborn rats. *J. Neurophysiol.* **68,** 1901-1905.

Rothman, S.M. (1985). The neurotoxicity of excitatory amino acids is produced by passive chloride influx. *J. Neurosci.* **5,** 1483-1489.

Rothman, S.M., Thurston, J.H. and Hauhart, R.E. (1987). Delayed neurotoxicity of excitatory amino acids in vitro. *Neuroscience.* **22,** 471-480.

Rothstein, J.D., DykesHoberg, M., Pardo, C.A., Bristol, L.A., Jin, L., Kuncl, R.W., Kanai, Y., Hediger, M.A., Wang, Y., Schielke, J.P. and Welty, D.F. (1996). Knockout of glutamate transporters reveals a major role for astroglial transport in excitotoxicity and clearance of glutamate. *Neuron.* **16,** 675-686.

Rothstein, J.D., Martin, L., Levey, A.I., Dykes Hoberg, M., Jin, L., Wu, D., Nash, N. and Kuncl, R.W. (1994). Localization of neuronal and glial glutamate transporters. *Neuron*. **13,** 713-725.

Rudolphi, K.A., Schubert, P., Parkinson, F.E. and Fredholm, B.B. (1992). Neuroprotective role of adenosine in cerebral ischaemia. *Trends Pharmacol. Sci.* **13,** 439-445.

Sagara, J., Miura, K. and Bannai, S. (1993). Cystine uptake and glutathione level in fetal brain cells in primary culture and in suspension. *J. Neurochem.* **61,** 1667-1671.

Sakimura, K., Bujo, H., Kushiya, E., Araki, K., Yamazaki, M., Yamazaki, M., Meguro, H., Warashina, A., Numa, S. and Mishina, M. (1990). Functional expression from cloned cDNAs of glutamate receptor species responsive to kainate and quisqualate. *FEBS Lett.* **272,** 73-80.

Sakimura, K., Morita, T., Kushiya, E. and Mishina, M. (1992). Primary structure and expression of the gamma 2 subunit of the glutamate receptor channel selective for kainate. *Neuron*. **8,** 267-274.

Sakurai, M. (1990). Calcium is an intracellular mediator of the climbing fiber in induction of cerebellar long-term depression. *Proc. Natl. Acad. Sci. U.S.A.* **87,** 3383-3385.

Sarantis, M., Ballerini, L., Miller, B., Silver, R.A., Edwards, M. and Attwell, D. (1993). Glutamate uptake from the synaptic cleft does not shape the decay of the non-NMDA component of the synaptic current. *Neuron*. **11,** 541-549.

Sarantis, M., Everett, K. and Attwell, D. (1988). A presynaptic action of glutamate at the cone output synapse. *Nature*. **332,** 451-453.

Sayer, R.J., Schwindt, P.C. and Crill, W.E. (1992). Metabotropic glutamate receptor-mediated suppression of L-type calcium current in acutely isolated neocortical neurons. *J. Neurophysiol.* **68,** 833-842.

Scanziani, M., Capogna, M., Gahwiler, B.H. and Thompson, S.M. (1992). Presynaptic inhibition of miniature excitatory synaptic currents by baclofen and adenosine in the hippocampus. *Neuron.* **9,** 919-927.

Scanziani, M., Gahwiler, B.H. and Thompson, S.M. (1995). Presynaptic inhibition of excitatory synaptic transmission by muscarinic and metabotropic glutamate receptor activation in the hippocampus: are Ca^{2+} channels involved? *Neuropharmacology.* **34,** 1549-1557.

Scharfman, H.E. and Schwartzkroin, P.A. (1989). Protection of dentate hilar cells from prolonged stimulation by intracellular calcium chelation. *Science.* **246,** 257-260.

Schoepp, D.D. and Johnson, B.G. (1993). Metabotropic glutamate receptor modulation of cAMP accumulation in the neonatal rat hippocampus. *Neuropharmacology.* **32,** 1359-1365.

Scholz, K.P. and Miller, R.J. (1991). Analysis of adenosine actions on Ca^{2+} currents and synaptic transmission in cultured rat hippocampal pyramidal neurones. *J. Physiol. (Lond).* **435,** 373-393.

Schousboe, A., Frandsen, A. and Drejer, J. (1989). Evidence for evoked release of adenosine and glutamate from cultured cerebellar granule cells. *Neurochem. Res.* **14,** 871-875.

Schuman, E.M. and Madison, D.V. (1994). Nitric oxide and synaptic function. *Annu. Rev. Neurosci.* **17,** 153-183.

Seeburg, P.H. (1993). The molecular biology of mammalian glutamate receptor channels. *Trends. Neurosci.* **16,** 359-365.

Sequier, J.M., Hunziker, W., Andressen, C. and Celio, M.R. (1990). Calbindin D-28k protein and mRNA localization in the rat brain. *Eur. J. Neurosci.* **2,** 1118-1126.

Sheng, M., Piser, T.M., Seybold, V.S. and Thayer, S.A. (1996). Cannabinoid receptor agonist inhibit glutamatergic synaptic transmission in rat hippocampal cultures. *J. Neurosci.* **16,** 4322-4334.

Shibuki, K. and Okada, D. (1991). Endogenous nitric oxide release required for long-term synaptic depression in the cerebellum. *Nature*. **349,** 326-328.

Shigemoto, R., Abe, T., Nomura, S., Nakanishi, S. and Hirano, T. (1994). Antibodies inactivating mGluR1 metabotropic glutamate receptor block long-term depression in cultured Purkinje cells. *Neuron*. **12,** 1245-1255.

Shigemoto, R., Ohishi, H., Nakanishi, S. and Mizuno, N. (1992). Expression of the mRNA for the rat NMDA receptor (NMDAR1) in the sensory and autonomic ganglion neurons. *Neurosci. Lett.* **144,** 229-232.

Silver, R.A., Colquhoun, D., Cull-Candy, S.G. and Edmonds, B. (1994). Mechanisms underlying decay of the fast component of EPSCs in rat cerebellar granule cells. *J. Physiol.* **476P,** 67P-68P.

Silver, R.A., Traynelis, S.F. and Cull Candy, S.G. (1992). Rapid-time-course miniature and evoked excitatory currents at cerebellar synapses in situ. *Nature*. **355,** 163-166.

Slaughter, M.M. and Miller, R.F. (1981). 2-amino-4-phosphonobutyric acid: a new pharmacological tool for retina research. *Science*. **211,** 182-185.

Slaughter, M.M. and Miller, R.F. (1985). Identification of a distinct synaptic glutamate receptor on horizontal cells in mudpuppy retina. *Nature*. **314,** 96-97.

Sommer, B., Burnashev, N., Verdoorn, T.A., Keinanen, K., Sakmann, B. and Seeburg, P.H. (1992). A glutamate receptor channel with high affinity for domoate and kainate. *EMBO J.* **11,** 1651-1656.

Sommer, B., Keinanen, K., Verdoorn, T.A., Wisden, W., Burnashev, N., Herb, A., Kohler, M., Takagi, T., Sakmann, B. and Seeburg, P.H. (1990). Flip and flop: a cell-

specific functional switch in glutamate-operated channels of the CNS. *Science*. **249,** 1580-1585.

Sommer, B., Kohler, M., Sprengel, R. and Seeburg, P.H. (1991). RNA editing in brain controls a determinant of ion flow in glutamate-gated channels. *Cell*. **67,** 11-19.

Stallcup, W.B., Bulloch, K. and Baetge, E.E. (1979). Coupled transport of glutamate and sodium in a cerebellar nerve cell line. *J. Neurochem*. **32,** 57-65.

Stanfield, P.R. (1983). Tetraethylammonium ions and the potassium permeability of excitable cells. *Rev. Physiol. Biochem. Pharmacol*. **97,** 1-67.

States, B. and Segal, S. (1990). Cystine and dibasic amino acid uptake by opossum kidney cells. *J. Cell Physiol*. **143,** 555-562.

Staub, C., Vranesic, I. and Knopfel, T. (1992). Responses to metabotropic glutamate receptor activation in cerebellar Purkinje cells: induction of an inward current. *Eur. J. Neurosci*. **4,** 832-839.

Stern, P., Behe, P., Schoepfer, R. and Colquhoun, D. (1992). Single-channel conductances of NMDA receptors expressed from cloned cDNAs: comparison with native receptors. *Proc. R. Soc. Lond. (Biol. Sci.)*. **250,** 271-277.

Stone, T.W. and Burton, N.R. (1988). NMDA receptors and ligands in the vertebrate CNS. *Prog. Neurobiol*. **30,** 333-368.

Storck, T., Schulte, S., Hofmann, K. and Stoffel, W. (1992). Structure, expression, and functional analysis of a Na^+-dependent glutamate/aspartate transporter from rat brain. *Proc. Natl. Acad. Sci. U.S.A*. **89,** 10955-10959.

Storm Mathisen, J. and Ottersen, O.P. (1990). Immunocytochemistry of glutamate at the synaptic level. *J. Histochem. Cytochem*. **38,** 1733-1743.

Stratton, K.R., Worley, P.F. and Baraban, J.M. (1990). Pharmacological characterization of phosphoinositide-linked glutamate receptor excitation of hippocampal neurons. *Eur. J. Pharmacol.* **186,** 357-361.

Swartz, K.J. and Bean, B.P. (1992). Inhibition of calcium channels in rat CA3 pyramidal neurons by a metabotropic glutamate receptor. *J. Neurosci.* **12,** 4358-4371.

Swartz, K.J., Merritt, A., Bean, B.P. and Lovinger, D.M. (1993). Protein kinase C modulates glutamate receptor inhibition of Ca^{2+} channels and synaptic transmission. *Nature*. **361,** 165-168.

Szatkowski, M. and Attwell, D. (1994). Triggering and execution of neuronal death in brain ischaemia: two phases of glutamate release by different mechanisms. *Trends Neurosci.* **17,** 359-365.

Szatkowski, M., Barbour, B. and Attwell, D. (1990). Non-vesicular release of glutamate from glial cells by reversed electrogenic glutamate uptake. *Nature*. **348,** 443-446.

Tan, S.E., Wenthold, R.J. and Soderling, T.R. (1994). Phosphorylation of AMPA-type glutamate receptors by calcium/calmodulin-dependent protein kinase II and protein kinase C in cultured hippocampal neurons. *J. Neurosci.* **14,** 1123-1129.

Tang, C.M., Dichter, M. and Morad, M. (1989). Quisqualate activates a rapidly inactivating high conductance ionic channel in hippocampal neurons. *Science*. **243,** 1474-1477.

Thompson, R.F. and Krupa, D.J. (1994). Organization of memory traces in the mammalian brain. *Annu. Rev. Neurosci.* **17,** 519-549.

Thompson, S.M. and Gahwiler, B.H. (1989). Activity-dependent disinhibition. III. Desensitization and $GABA_B$ receptor-mediated presynaptic inhibition in the hippocampus in vitro. *J. Neurophysiol.* **61,** 524-533.

Thompson, S.M. and Gahwiler, B.H. (1992). Effects of the GABA uptake inhibitor tiagabine on inhibitory synaptic potentials in rat hippocampal slice cultures. *J. Neurophysiol.* **67,** 1698-1701.

Thomsen, C., Boel, E. and Suzdak, P.D. (1994). Actions of phenylglycine analogs at subtypes of the metabotropic glutamate receptor family. *Eur. J. Pharmacol.* **267,** 77-84.

Tingley, W.G., Roche, K.W., Thompson, A.K. and Huganir, R.L. (1993). Regulation of NMDA receptor phosphorylation by alternative splicing of the C-terminal domain. *Nature*. **364,** 70-73.

Tong, G. and Jahr, C.E. (1994). Block of glutamate transporters potentiates postsynaptic excitation. *Neuron*. **13,** 1195-1203.

Trussell, L.O. and Fischbach, G.D. (1989). Glutamate receptor desensitization and its role in synaptic transmission. *Neuron*. **3,** 209-218.

Trussell, L.O., Zhang, S. and Raman, I.M. (1993). Desensitization of AMPA receptors upon multiquantal neurotransmitter release. *Neuron*. **10,** 1185-1196.

Turgeon, S.M. and Albin, R.L. (1993). Pharmacology, distribution, cellular localization, and development of $GABA_B$ binding in rodent cerebellum. *Neuroscience*. **55,** 311-323.

Ueda, H., Fukushima, N., Ge, M., Takagi, H. and Satoh, M. (1987). Presynaptic opioid kappa-receptor and regulation of the release of Met-enkephalin in the rat brainstem. *Neurosci. Lett.* **81,** 309-313.

Van Winkle, L.J., Mann, D.F., Wasserlauf, H.G. and Patel, M. (1992). Mediated Na^+-independent transport of L-glutamate and L-cystine in 1- and 2-cell mouse conceptuses. *Biochim Biophys Acta*. **1107,** 299-304.

Vignes, M., Clarke, V.R., Davies, C.H., Chambers, A., Jane, D.E., Watkins, J.C. and Collingridge, G.L. (1995). Pharmacological evidence for an involvement of group II and group III mGluRs in the presynaptic regulation of excitatory synaptic responses in the CA1 region of rat hippocampal slices. *Neuropharmacology*. **34,** 973-982.

Vranesic, I., Staub, C. and Knopfel, T. (1993). Activation of metabotropic glutamate receptors induces an outward current which is potentiated by methylxanthines in rat cerebellar Purkinje cells. *Neurosci. Res.* **16,** 209-215.

Wada, K., Dechesne, C.J., Shimasaki, S., King, R.G., Kusano, K., Buonanno, A., Hampson, D.R., Banner, C., Wenthold, R.J. and Nakatani, Y. (1989). Sequence and expression of a frog brain complementary DNA encoding a kainate-binding protein. *Nature*. **342,** 684-689.

Wadiche, J.I., Amara, S.G. and Kavanaugh, M.P. (1995a). Ion fluxes associated with excitatory amino acid transport. *Neuron*. **15,** 721-728.

Wadiche, J.I., Arriza, J.L., Amara, S.G. and Kavanaugh, M.P. (1995b). Kinetics of a human glutamate transporter. *Neuron*. **14,** 1019-1027.

Wahl, F., Obrenovitch, T.P., Hardy, A.M., Plotkine, M., Boulu, R. and Symon, L. (1994). Extracellular glutamate during focal cerebral ischaemia in rats: time course and calcium dependency. *J. Neurochem*. **63,** 1003-1011.

Waldmeier, P.C., Wicki, P., Feldtrauer, J.J. and Baumann, P.A. (1988). Potential involvement of a baclofen-sensitive autoreceptor in the modulation of the release of endogenous GABA from rat brain slices in vitro. *Naunyn. Schmiedebergs. Arch. Pharmacol*. **337,** 289-295.

Waniewski, R.A. and Martin, D.L. (1984). Characterization of L-glutamic acid transport by glioma cells in culture: evidence for sodium-independent, chloride-dependent high affinity influx. *J. Neurosci*. **4,** 2237-2246.

Watanabe, E. (1984). Neuronal events correlated with long-term adaptation of the horizontal vestibulo-ocular reflex in the primate flocculus. *Brain Res.* **297,** 169-174.

Watanabe, H. and Bannai, S. (1987). Induction of cystine transport activity in mouse peritoneal macrophages. *J. Exp. Med.* **165,** 628-640.

Watkins, J. and Collingridge, G. (1994). Phenylglycine derivatives as antagonists of metabotropic glutamate receptors. *Trends Pharmacol. Sci.* **15,** 333-342.

Werner, P., Voigt, M., Keinanen, K., Wisden, W. and Seeburg, P.H. (1991). Cloning of a putative high-affinity kainate receptor expressed predominantly in hippocampal CA3 cells. *Nature*. **351,** 742-744.

Wichmann, T. and Starke, K. (1988). Uptake, release, and modulation of release of noradrenaline in rabbit superior colliculus. *Neuroscience*. **26,** 621-634.

Wiklund, L., Toggenburger, G. and Cuénod, M. (1982). Aspartate: possible neurotransmitter in cerebellar climbing fibers. *Science*. **216,** 78-80.

Winder, D.G. and Conn, P.J. (1992). Activation of metabotropic glutamate receptors in the hippocampus increases cyclic AMP accumulation. *J. Neurochem*. **59,** 375-378.

Winder, D.G. and Conn, P.J. (1993). Activation of metabotropic glutamate receptors increases cAMP accumulation in hippocampus by potentiating responses to endogenous adenosine. *J. Neurosci*. **13,** 38-44.

Wu, L.G. and Saggau, P. (1995). $GABA_B$ receptor-mediated presynaptic inhibition in guinea-pig hippocampus is caused by reduction of presynaptic Ca^{2+} influx. *J. Physiol. (Lond)*. **485,** 649-657.

Wyllie, D.J., Mathie, A., Symonds, C.J. and Cull Candy, S.G. (1991). Activation of glutamate receptors and glutamate uptake in identified macroglial cells in rat cerebellar cultures. *J. Physiol. (Lond)*. **432,** 235-258.

Yamada, K.A. and Rothman, S.M. (1992). Diazoxide blocks glutamate desensitization and prolongs excitatory postsynaptic currents in rat hippocampal neurons. *J. Physiol. (Lond)*. **458,** 409-423.

Yamada, K.A. and Tang, C.M. (1993). Benzothiadiazides inhibit rapid glutamate receptor desensitization and enhance glutamatergic synaptic currents. *J. Neurosci*. **13,** 3904-3915.

Yamazaki, M., Mori, H., Araki, K., Mori, K.J. and Mishina, M. (1992). Cloning, expression and modulation of a mouse NMDA receptor subunit. *FEBS Lett.* **300,** 39-45.

Yawo, H. and Chuhma, N. (1993). Preferential inhibition of omega-conotoxin-sensitive presynaptic Ca^{2+} channels by adenosine autoreceptors. *Nature*. **365,** 256-258.

Yeo, C.H. and Hardiman, M.J. (1992). Cerebellar cortex and eyeblink conditioning: a reexamination. *Exp. Brain Res.* **88,** 623-638.

Yingst, D.R. (1988). Modulation of the Na,K-ATPase by Ca and intracellular proteins. *Annu. Rev. Physiol.* **50,** 291-303.

Yuzaki, M., Forrest, D., Curran, T. and Connor, J.A. (1996). Selective activation of calcium permeability by aspartate in Purkinje cells. *Science*. **273,** 1112-1114.

Yuzaki, M. and Mikoshiba, K. (1992). Pharmacological and immunocytochemical characterization of metabotropic glutamate receptors in cultured Purkinje cells. *J. Neurosci*. **12,** 4253-4263.

Zoltay, G. and Cooper, J.R. (1990). Ionic basis of inhibitory presynaptic modulation in rat cortical synaptosomes. *J. Neurochem*. **55,** 1008-1012.

~~p.15, l.21: "flip" → "flop"~~

p.72, $CaCl_2$ concentration for solutions B & C: 10 → 2.5

p.74: CaCl2 → $CaCl_2$

p.146, iontophoresis current labelling: +20pA &-40pA → +20nA & -40nA

p.192, l.4: $[glu]_{¥}$ → $[glu]_{\infty}$

p.199: interchange the labels for the panels C and D.